



Cape Peninsula
University of Technology

**DATA ACQUISITION AND DATA TRANSFER METHODS FOR REAL-TIME POWER
SYSTEM OPTIMISATION PROBLEMS SOLUTION**

by

GANESAN DEIVAKKANNU

Thesis submitted in fulfilment of the requirements for the degree

Master of Technology: Electrical Engineering

in the Faculty of Engineering

at the Cape Peninsula University of Technology

Supervisor: Mr. C. Kriger

Co-supervisor: Dr. S. Krishnamurthy

Bellville Campus

Date submitted: December 2014

CPUT copyright information

The dissertation/thesis may not be published either in part (in scholarly, scientific or technical journals), or as a whole (as a monograph), unless permission has been obtained from the University.

DECLARATION

I, Ganesan Deivakkannu, declare that the contents of this dissertation/thesis represent my own unaided work, and that the dissertation/thesis has not previously been submitted for academic examination towards any qualification. Furthermore, it represents my own opinions and not necessarily those of the Cape Peninsula University of Technology.

Signed

Date

ABSTRACT

The electric power utilities play a vital role in the generation, transmission and distribution of the electrical power to the end users. The power utilities face two major issues, i.e. i) power grids are expected to operate close to the maximum capacity, and ii) there is a need for accurate and better monitoring and control of the power system network using the modern technology and the available tools. These two issues are interconnected as better monitoring allows for better control of the power system. Development of the new standard-based power system technologies contributed to raising the ideas for building of a Smart grid. The challenges are that this process requires development of new control and operation architectures and methods for data acquisition, data transfer, and control computation. These methods require data for the full dynamic state of the power system in real-time, which leads to the introduction of the synchrophasor-based monitoring and control of the power system.

The thesis describes the research work and investigations for integration of the existing new power system technologies to build fully automated systems for real-time solution of power system energy management problems, incorporating data measurement and acquisition, data transfer and distribution through a communication network, and data storage and retrieval in one whole system.

The thesis developed methods, algorithms, procedures and software and hardware tools for implementation of lab-scale prototypes of the power system and its data acquisition and data transfer to the system control center in order to allow the solution of the optimal power dispatch problem in real-time using real-time data. Two data acquisition and data transfer systems, i.e. i) RTDS PB5 card analog output signals-based system (communication within the local PC), and ii) RTDS GTNET card PMU signals-based system (communication between the host and remote PC) are developed and implemented using suitable hardware platforms and software tools. The developed prototype systems are tested for two case studies of the five and eleven bus power system models, and the system operation test results are presented.

The developed data acquisition, data transfer, data retrieval and data storage system algorithms and software programs can be used for the power grid energy management system problem solutions in regional or national control centers, smart grid applications, educational courses and postgraduate research at universities.

ACKNOWLEDGEMENTS

I wish to thank:

- My family members, Father Deivakkannu and brother Kumar for their support, patience endurance and understanding during the study.
- My most sincere thanks go to CPUT staff members: Professor Raynitchka Tzoneva leader of CSAEMS and RTDS, Supervisor Mr Carl Kriger and Co-Supervisor Dr. Senthil Krishnamurthy. I thank them for introducing me to the wonders and frustrations of scientific research. I also thank them for their guidance, encouragement and support during the development of this project work.
- Adjunct Professor Alexander Apostolov Omicron USA, for his valuable suggestions on all phases of this project and for his seminars on the IEC61850 standard for Substation Automation Systems.
- The Centre for Real Time Distributed Systems and Substation Automation and Energy Management Systems at the Cape Peninsula University of Technology for their assistance in different areas of the research.
- I express my warm thanks to Professor S.C. Srivastava, and the postgraduate research scholar Mr. Param Banerjee for their support and guidance during my visit to the Centre for Advanced Power Systems Research, at the Indian Institute of Technology (IIT), Kanpur, from the 9th December 2013 to 3rd January 2014.
- The financial assistance of the National Research Foundation, CPUT center for postgraduate studies and ESKOM TESP towards this research project is acknowledged.

DEDICATION

For my Late Father Mr Deivakkannu and Family Members

TABLE OF CONTENTS

Declaration	ii
Abstract	iii
Acknowledgements	iv
Dedication	v
Table of contents	vi
Bibliography	xii
List of Figures	xiii
List of Tables	xix
List of Appendices	xxii
Glossary	xxiii
Mathematical Notations	xxv

CHAPTER ONE: INTRODUCTION

1	Introduction	1
1.1	Motivation and definition of the research problem	1
1.1.1	Motivation for research	1
1.1.2	Problem definition	5
1.2	Research aim and objectives	5
1.2.1	Research aim	5
1.2.2	Research Objective	5
1.3	Project assumptions, scope, delimitation and hypothesis	6
1.3.1	Project assumptions	6
1.3.2	Project scope	7
1.3.3	Project delimitation	7
1.3.4	Project hypothesis	8
1.4	The deliverables of the thesis	8
1.5	Chapter breakdown	10
1.6	Publications	11
1.7	Conclusion	11

CHAPTER TWO: REVIEW OF THE LITERATURE FOR REAL-TIME DATA ACQUISITION AND DATA TRANSFER METHODS FOR POWER SYSTEM APPLICATIONS

2.1	Introduction	13
2.2	Literature searching methodology	14
2.3	General structure of the communication systems	15

2.4	Type of the communication networks	16
2.4.1	Home Area Networks (HAN)	17
2.4.2	Field Area Networks (FAN)	18
2.4.3	Wide Area Networks (WAN)	19
2.5	Communication protocol	20
2.5.1	Ethernet protocol	21
2.5.2	TCP/IP and UDP protocol	22
2.5.3	Protocols in substations	23
2.5.4	The Modbus protocol	24
2.5.5	Distributed Networking Protocol 3 (DNP3)	25
2.5.5.1	Distributed networking protocol in SCADA communications	25
2.5.5.2	Advantages of using DNP3 protocol	26
2.5.6	IEC-870-5-101 protocol	26
2.5.7	IEC 61850 protocol and IEC 61850-90-5 standard based power system protection scheme using synchrophasor technology	27
2.5.8	IEEE standards	29
2.5.8.1	IEEE C37.1 standard	30
2.5.8.2	IEEE 1379 standard	30
2.5.8.3	IEEE 1547 standard	30
2.5.8.4	IEEE 1646 standard	31
2.5.9	Discussion and a legacy comparison of the different protocols used in the power systems	31
2.6	Power system communication network technologies	32
2.6.1	Power Line Carrier Communication (PLCC)	32
2.6.2	Microwave and radio wireless communication systems	33
2.6.3	Radio waves	34
2.6.4	Microwaves	34
2.6.5	Optical fiber communications	35
2.6.6	Satellite communications	36
2.6.7	Discussion on the communication media	37
2.7	Literature review on the communication architectures, protocols and media used in the power system applications	37
2.7.1	Power system control	38
2.7.2	Power system monitoring	40
2.7.3	Power system metering	41
2.7.4	Communication system for the smart grid	42
2.8	Review on the application of the DAQ cards, and synchrophasors for local or remote real-time simulation monitoring, and control using LabVIEW, MATLAB and RTDS software environments	44
2.8.1	Review on the application of the DAQ cards for local or remote real-time simulation, monitoring, and control using LabVIEW and MATLAB software environments	44
2.8.1.1	Discussion on the NI DAQ card used in the real-time monitoring and control using LabVIEW and MATLAB software environments	52

2.8.2	Power System applications using a Real-Time Digital Simulator	53
2.8.2.1	Discussion on the real-time monitoring and control of power systems using RTDS software environment	56
2.8.3	Application of the synchrophasor technology in power engineering	56
2.8.3.1	EMS applications using synchrophasor technology	57
2.8.3.2	Situational awareness and wide-area monitoring application using synchrophasor technology	57
2.8.3.3	Wide-Area Monitoring and Visualization (WAMV) application using synchrophasor technology	59
2.8.3.4	Power system stability assessment using synchrophasor technology	60
2.8.3.4	Discussion on the real-time monitoring and control of the power systems using synchrophasor technology	63
2.9	Conclusion	64

CHAPTER 3: DEFINITION, MEASUREMENT AND STANDARDIZATION OF THE PHASOR MEASUREMENT UNITS AND PHASOR DATA CONCENTRATORS

3.1	Introduction	65
3.2	Synchrophasor definition	65
3.3	Background, description, time synchronization and standards for phasor measurement unit	67
3.3.1	Historical background of the Phasor Measurement Unit (PMU)	67
3.3.2	Phasor measurement unit and its description	68
3.3.3	Phasor measurement unit time synchronization	69
3.3.4	Standards for phasor measurement unit	71
3.4	Phasor Data Concentrator (PDC): Description and protocols	72
3.4.1	Phasor Data Concentrator (PDC)	72
3.4.2	Protocols used to connect the PMU and the PDC	73
3.5	Synchrophasor measurement system and message format	74
3.5.1	Synchrophasor measurement message format	75
3.6	Conclusion	79

CHAPTER FOUR: HARDWARE AND SOFTWARE IMPLEMENTATION OF A LAB-SCALE REAL-TIME DATA ACQUISITION AND DATA TRANSFER SYSTEM

4.1	Introduction	81
4.2	Lab-scale data acquisition and data transfer system specifications	81
4.3	Hardware and software tools	83
4.3.1	Hardware tools	84
4.3.1.1	Real Time Digital Simulator (RTDS)	84
4.3.1.2	SEL-2407 satellite synchronized clock	85
4.3.1.3	National Instrument (NI) 6343 USB Data Acquisition (DAQ) card	86

4.3.1.4	Personal computer at remote end location	87
4.3.2.	Software tools	87
4.3.2.1	RSCAD software suite	87
4.3.2.2	National Instruments (NI) LabVIEW	89
4.3.2.3	NI DAQmx 9.8 driver	90
4.3.2.4	MATLAB software	90
4.3.2.5	MATLAB data acquisition toolbox	91
4.3.2.6	PMU connection tester	91
4.3.2.7	OpenPDC Software	91
4.3.2.8	MySQL workbench integrated development tool	92
4.4	Method One: Implementation of a lab scale data acquisition system using the PB5 card analog output channel	92
4.4.1	Assignment of the power system data to the RTDS front panel PB5 card	94
4.4.2	Configuration of the NI DAQ 6353 card in LabVIEW software to measure the RTDS output signal	95
4.4.3	NI DAQ card physical channel configuration for data acquisition	96
4.4.4	File saving option	97
4.5	Method Two: Implementation of a lab scale data acquisition system using RSCAD GTNET card Phasor Measurement Units (PMUs)	99
4.5.1	RSCAD GTNET card PMU Module	101
4.5.1.1	Common setting in the GTNET card PMU	101
4.5.1.2	User-defined RSCAD GTNET card PMU configuration setting	102
4.5.1.3	RSCAD GTNET card PMU AC source	103
4.5.1.4	RSCAD GTNET card PMU calibration	104
4.5.1.5	RSCAD GTNET card PMU card Analog/Digital source	104
4.5.2	Giga-Transceiver Synchronization Component (GTSYNC)	104
4.5.3	PMU connection tester	105
4.5.3.1	PMU connection tester parameter	106
4.5.3.2	Protocol and device ID	106
4.5.3.3	Configuration frame	106
4.5.3.4	Connection frame used in the PMU connection tester	107
4.5.4	OpenPDC software	108
4.5.4.1	OpenPDC manager	108
4.5.4.2	Real-Time monitoring GTNET card PMU devices in the OpenPDC manager	112
4.6	Conclusion	114

CHAPTER FIVE: POWER SYSTEM CASE STUDIES, FORMULATION AND ALGORITHM FOR SOLUTION OF THE OPTIMISATION DISPATCH PROBLEM

5.1	Introduction	115
5.2	Power system case studies and description	115

5.2.1	Case study one: Five bus power system network	115
5.2.1.1	Description of the five bus power system model and its data	115
5.2.1.2	RSCAD model of the five bus power system model	117
5.2.1.3	Simulation of the five bus power system model and load flow results	118
5.2.2	Case study two: Eleven bus power system network	119
5.2.2.1	Description of the eleven bus power system model and its data	119
5.2.2.2	RSCAD model of the eleven bus power system	121
5.2.2.3	Simulation of the eleven bus power system model and load flow results	122
5.3	Formulation and algorithm for solution of the dispatch problem	123
5.3.1	Formulation of the dispatch problem	123
5.3.2	Algorithm for solution of the dispatch problem	125
5.4	Conclusion	129

CHAPTER SIX: INVESTIGATION OF THE REAL-TIME OPERATION OF THE DEVELOPED DATA ACQUISITION SYSTEM AND RESULTS

6.1	Introduction	130
6.2	Investigation of the LabVIEW/MATLAB-based data acquisition and data transfer system using the RTDS front panel PB5 card analog output signals	131
6.2.1	LabVIEW-based data acquisition and data transfer system using the RTDS front panel PB5 card analog output signals for the five bus power system model	133
6.2.2	LabVIEW-based data acquisition and data transfer system using the RTDS front panel PB5 card analog signals for the eleven bus power system model	140
6.2.3	Discussion on the economic dispatch solution using the LabVIEW-based data acquisition and data transfer system	149
6.3	MATLAB-based data acquisition and data transfer system using the RTDS front panel PB5 card analog output signals	150
6.3.1	MATLAB-based data acquisition and data transfer system using the RTDS front panel PB5 card analog output signals for the five bus power system model	150
6.3.2	MATLAB-based data acquisition and data transfer system using the RTDS front panel PB5 card analog output signals for the eleven bus power system model	152
6.3.3	Discussion on the application of the MATLAB-based data acquisition and data transfer system using the RTDS front panel PB5 card analog output signals	155
6.4	Lab-scale data acquisition and data transfer system using the RTDS GTNET card Phasor Measurement Unit (PMU) signals	156
6.4.1	GTNET card PMU-based laboratory setup to solve the economic	157

	dispatch problem	
6.4.2	Real-time implementation of the algorithm for solution of the dispatch problem for the PMU-based data acquisition and transfer system	157
6.4.3	Implementation of the GTNET card PMU-based system for the five bus power system model	159
6.4.3.1	Power system model simulation and assignment of the load demand powers to the GTNET card PMU	159
6.4.3.2	Monitoring the RSCAD GTNET card PMU signals in the OpenPDC environment	162
6.4.3.3	Storing and retrieving the RTDS GTNET card PMU real-time data to and from the MySQL database	164
6.4.3.4	Solution of the dispatch problem using RTDS GTNET card PMU-based system	169
6.5	Discussion on the operation characteristics of the data acquisition and data transfer systems using the LabVIEW/MATLAB-based RTDS PB5 card output signals and the GTNET card PMU signals	170
6.6	Conclusion	171

CHAPTER SEVEN: CONCLUSION, DELIVERABLES AND FUTURE RECOMMENDATIONS

7.1	Introduction	172
7.2	Aim and objectives of the thesis	172
7.2.1	Objectives	172
7.3	Thesis deliverables	173
7.3.1	Investigation and a literature review of the real-time data acquisition and data transfer systems for power system applications	173
7.3.2	Development of power system models in RSCAD software environment and load flow simulations	173
7.3.3	Development of methods, algorithms and procedures for lab-scale implementation of the LabVIEW/MATLAB-based data acquisition and data transfer systems using the RTDS front panel PB5 card analog output signals	174
7.3.4	Development of software programs for the LabVIEW/MATLAB-based data acquisition, and transfer systems using the RTDS front panel PB5 card analog output signals	174
7.3.5	Development of the method, algorithm and procedures for the lab-scale implementation of the RTDS GTNET card PMU signal-based data acquisition and data transfer system	175
7.3.6	Development of the software program for the RTDS GTNET card PMU-based data acquisition and transfer system	175
7.4	Application of the thesis results	176
7.5	Future research	177

7.6	Publications	177
7.7	Conclusion	178
	Bibliography	179

LIST OF FIGURES

Figure 1.1	Lab-scale system functions	7
Figure 2.1	Total number of publications versus year of the publications	14
Figure 2.2	Block diagram of a communication system (Soni and Pareek, 2013)	16
Figure 2.3	The communication network architecture for electric system automation.(Gungor and Lambert, 2006)	17
Figure 2.4	Smart appliances are interconnected within a HAN (Balakrishnanan, 2012)	18
Figure 2.5	Field Area Network components(Baig et al., 2013)	19
Figure 2.6	Seven layers Open System Interconnection Model (Behrouz, 2006)	21
Figure 2.7	The structure of the Ethernet based communication system, (Behrouz, 2006)	22
Figure 2.8	TCP/IP four layer model (Li et al., 2011)	23
Figure 2.9	Typical communication protocols used in a power system (Mohagheghi et al., 2009)	24
Figure 2.10	Overview of DNP3 protocol (Bhattacharyya, 2008)	26
Figure 2.11	Substation automation topology based on IEC 61850 (Mohagheghi et al., 2009)	27
Figure 2.12a	Mapping of IEC61850 specific layer to OSI Model (Sidhu and Gangadharan, 2005)	28
Figure 2.12b	Overview of IEC TR 61850-90-5 (Madani et al., 2013)	29
Figure 2.13	Future communication system for power systems (Qiu, 2002)	37
Figure 2.14	Substation control communication network (Wang et al., 2011)	38
Figure 2.15	Communication Network for a Distribution System (Aravinthan et al., 2011)	39
Figure 2.16	The communication structure of wide-area control (Xiaoyang et al., 2005)	39
Figure 2.17	Communication architecture for the underground distribution feeder fault identification (Moghe et al., 2009)	40
Figure 2.18	Internet -Based Power Quality Monitoring System (Zhang and Li, 2009)	41
Figure 2.19	Smart metering communication systems (Toshiba Smart Meter, Manual, 2014)	42
Figure 2.20	Smart grid framework (Parikh et al., 2010)	43
Figure 2.21	Electrical capacitance tomography DAQ system (Rasmussen and Yang, 2008)	48
Figure 2.22	ICMS Measuring Setup (Cirstea et al., 2012)	49
Figure 2.23	Flow diagram of the brightness adjusting system (Huang et al., 2014).	49
Figure 2.24	Multi-point temperature remote monitoring system (Chen and Shen, 2012)	50

Figure 2.25	Measurement system for Ultra Wide Band (UWB) RF sensor (Jung et al., 2011)	51
Figure 2.26	Rapid Control Prototype System (Lee et al., 2013)	51
Figure 2.27	BCI system (Afdideh et al., 2012)	52
Figure 2.28	Interface JVC Study (Brandt et al, 1991)	53
Figure 2.29	RTDS protective relay interface (McLaren et al, 1991)	54
Figure 2.30	Control system design platform (Jackson et al, 2005)	55
Figure 2.31	Functional implementation of the laboratory set-up (Adewole and Tzoneva, 2014)	55
Figure 2.32	EMS integrated with synchrophasor technology (Giri, 2011)	57
Figure 2.33	PMU-based situational awareness system (Zhang et al., 2011)	58
Figure 2.34	RTDS-EPG synchrophasor applications deployment architecture at Southern California Edison (Chen et al., 2012)	60
Figure 2.35	Architecture of the smart grid test bed at SGDRIL (Biswas et al., 2013)	61
Figure 2.36	Block diagram of SCADA, data acquisition, transfer and state estimation (Tripathy, 2010)	62
Figure 2.37	Block diagram of Wide Area Monitoring Systems (Tripathy, 2010)	63
Figure 3.1a	Synchrophasor angle conventions (IEEE C57.18.10, 2008)	66
Figure 3.1b	Phasor representation of a sinusoidal signal (Singh et al., 2011)	67
Figure 3.2a	Block diagram of a Phasor Measurement Unit	69
Figure 3.2b	PMU utilization in a power system (Singh et al., 2011)	71
Figure 3.3	UDP/IP and TCP/IP data stream (Retty et al., 2013)	74
Figure 3.4	Synchrophasor data collection network (IEEE Std C37.118.2, 2011)	75
Figure 3.5	Message format (PAC World Magazine,2013)	76
Figure 4.1a	RTDS PB5 card LabVIEW/MATLAB-based lab-scale system functions	82
Figure 4.1b	RTDS GTNET card PMU-based lab-scale systems functions	82
Figure 4.2	Real-Time Digital Simulators (RTDS) in the Centre for Substation Automation and Energy Management Systems (CSAEMS)	85
Figure 4.3	SEL-2407 Satellite - Synchronized Clock (SEL, 2014)	86
Figure 4.4	The block and pin diagram for the NI 6343 DAQ card (National Instruments, 2014)	87
Figure 4.5	RSCAD architecture (RTDS Technologies, 2014)	88
Figure 4.6	MATLAB DAQ toolbox connection	91
Figure 4.7	Block diagram of the MySQL workbench (Guru, 2012)	92
Figure 4.8	Flow diagram of the lab-scale data acquisition system using the LabVIEW and MATLAB environments to acquire and transfer data and to solve the economic dispatch problem	93

Figure 4.9	Block diagram for the lab-scale data acquisition system in LabVIEW and MATLAB environment to solve the economic dispatch problem	94
Figure 4.10	RSCAD output components setting	94
Figure 4.11	LabVIEW Block diagram to capture the RTDS voltage output signal	95
Figure 4.12	LabVIEW front panel monitoring the RTDS voltage output signal	96
Figure 4.13	NI DAQ card channels and timing parameter setting in LabVIEW	96
Figure 4.14	LabVIEW block diagram of file saving setting in LabVIEW	97
Figure 4.15	LabVIEW block diagram of <i>While</i> loop program for DAQ	98
Figure 4.16	Flow diagram of the lab-scale data acquisition and data transfer system using the RTDS GTNET PMU technology to acquire and transfer data and to solve the economic dispatch problem	99
Figure 4.17	Block diagram for the lab-scale data acquisition system based on the RTDS GTNET card PMU to solve the economic dispatch problem	100
Figure 4.18	GTNET-PMU configurations setting	101
Figure 4.19	User-defined RSCAD GTNET PMU configuration	103
Figure 4.20	RSCAD GTNET PMU AC Source	103
Figure 4.21	GTSYNC card parameter setting	105
Figure 4.22	PMU connection tester	105
Figure 4.23	OpenPDC manager	108
Figure 4.24	OpenPDC historians window	109
Figure 4.25	OpenPDC connections file setting	110
Figure 4.26	OpenPDC configuration	111
Figure 4.27	OpenPDC device to configure	112
Figure 4.28	Real-Time monitoring of the GTNET card PMU device signal	112
Figure 4.29	OpenPDC Real-time archiving in MySQL database	113
Figure 5.1	Single line diagram of the five bus power system model (Kothari and Dhillon, 2006)	116
Figure 5.2	Five bus power system model in RSCAD environment	118
Figure 5.3	Single line diagram of the eleven bus power system model (Kothari and Dhillon, 2006)	120
Figure 5.4	The Eleven bus power system model in the RSCAD environment	122
Figure 5.5	The flow chart of the economic dispatch problem solution algorithm using the Lagrange's method (Krishnamurthy and Tzoneva, 2013)	128
Figure 6.1a	Block diagram for the lab-scale data acquisition system using the RTDS PB5 card analog outputs	131
Figure 6.1b	Real-time implementation of the algorithm for solution of the	133

	dispatch problem	
Figure 6.2	Five bus power system model in RSCAD environment including the NI DAQ 6343 card input channels	134
Figure 6.3	LabVIEW graphical diagram to connect the RTDS four channel PB5 card signals to the NI DAQ card 6343	135
Figure 6.4	Front panel design of the LabVIEW data acquisition system to monitor the four analog signals coming from the RTDS PB5 card	135
Figure 6.5	Initial values of the power demands (Sliders are at the bottom position) in the RSCAD run-time window	136
Figure 6.6	Final values of the four load power demands (Sliders are at the top position) in the RSCAD run-time window	137
Figure 6.7	RSCAD diagram to calculate the optimal fuel cost of the five bus power system in RSCAD environment	139
Figure 6.8	RCSAD diagram for the real power load signals assignment to the RTDS PB5 card for the eleven bus power system model	140
Figure 6.9	Initial values of the power demands of the eleven bus power system (Sliders are at the bottom position) in RSCAD run-time window	141
Figure 6.10	LabVIEW diagram to connect the RTDS eleven channel PB5 card signals to the NI DAQ 6343 card	142
Figure 6.11	LabVIEW front panel waveforms which show the RTDS PB5 card captured signals for the initial load conditions of the eleven bus power system	143
Figure 6.12	Captured by the LabVIEW front panel and transformed to MWs analog voltages of the initial power demands for the eleven bus power system	143
Figure 6.13	Final values of the power demands of the eleven bus power system (Sliders are at the top position) in RSCAD run-time window	144
Figure 6.14	LabVIEW front panel waveforms showing the RTDS PB5 card captured signals for the final load conditions of the eleven bus system	145
Figure 6.15	Captured by the LabVIEW front panel and transformed to MWs and analog voltages of the final power demands for the eleven bus power system	145
Figure 6.16	RCSAD diagram to calculate the fuel cost for the eleven bus power system	147
Figure 6.17	RCSAD diagram to calculate the emission value for the eleven bus power system	148
Figure 6.18	Amplitude of the analog signals captured from the RTDS PB5 card using the MATLAB-based data acquisition system for the final position of the load sliders	151
Figure 6.19	Comparison of the fuel cost and the generator real powers	152

	between the RSCAD load flow simulation and the MATLAB optimisation solution for the five bus power system model	
Figure 6.20	Power demand data at the analog outputs of the RTDS PB5 card	153
Figure 6.21a	RTDS GTNET card PMU-based laboratory setup to solve the dispatch optimisation problem in real-time	157
Figure 6.21b	Flow chart of the real-time solution of the dispatch problem using the GTNET card PMU-based data acquisition and transfer system	158
Figure 6.22	Five bus Power system network modelled in the RSCAD environment with additional components to implement data acquisition and data transfer using the GTNET card PMU signals	160
Figure 6.23	Monitoring the voltage and current magnitudes and the phase angles of the PMU 1 and PMU 2 signals in the RSCAD environment	161
Figure 6.24	Monitoring the voltage and current magnitudes and the phase angles of the PMU 3 and PMU 4 signals in the RSCAD environment	161
Figure 6.25	Monitoring the RSCAD GTNET card PMU 1 and PMU 2 signals in the OpenPDC environment	162
Figure 6.26	Monitoring the RSCAD GTNET card PMU 3 and PMU 4 signals in the OpenPDC environment	163
Figure 6.27	Economic dispatch problem solution in RSCAD environment for the power demand of 165 MW	169
Figure A1	RTDS processor card	189
Figure A2	Pin tip connections to front panel analogue outputs	190
Figure A3	Typical GTWIF card	191
Figure A4	IRC card connector and faceplate LEDs	192
Figure A5	GTNET card (100BaseTX Ethernet)	193
Figure B1	OpenPDC configuration setup	194
Figure B2	OpenPDC configuration setup to establish a new configuration	195
Figure B3	OpenPDC database configuration setup	195
Figure B4	OpenPDC database setup	196
Figure B5	OpenPDC MySQL database setup	196
Figure B6	OpenPDC windows authentication setup	197
Figure B7	Change the setup of the OpenPDC configuration	197
Figure B8	MySQL database for archive PMU measurement signals	198
Figure B9	OpenPDC confirmation setup utility	198
Figure B10	OpenPDC home screen window	199
Figure C1	MySQL workbench main window	200
Figure C2	MySQL workbench database connection setting window	201
Figure C3	MySQL server authentication window	201

Figure C4	SQL query in MySQL workbench	202
Figure D1	Five bus power system model in RSCAD environment	203
Figure D2	Eleven bus power system model in RSCAD environment	204
Figure D3	Five bus power system model of RSCAD environment, including the NI DAQ 6343 card input channels	205
Figure D4	RCSAD diagram for the real power load signal assignment to the RTDS PB5 card for the eleven bus power system model	206
Figure D5	Five bus power system network modelled in the RSCAD environment with components to implement data acquisition and data transfer using the GTNET card PMU	207
Figure E1	LabVIEW front panel diagram to connect the RTDS four channel PB5 card signals to the NI DAQ card 6343	208
Figure E2	Front panel design of the LabVIEW data acquisition system to monitor the four analog signals coming from the RTDS PB5 card	208
Figure E3	LabVIEW diagram to connect the RTDS eleven channel PB5 card signals to the NI DAQ 6343 card	209
Figure E4	LabVIEW front panel waveforms which show the RTDS PB5 card captured signals for the initial load conditions of the eleven bus power system	209

LIST OF TABLES

Table 2.1	Comparison between IEC 61850 and IEEE C37.118 (Herbert, 2012)	32
Table 2.2	Electromagnetic Spectrum for wireless communication system (Behrouz, 2006)	34
Table 2.3	Approximate coverage of wireless technology in smart grid applications	43
Table 2.4	Review on the architecture, the protocols and the communication media used in power system applications	45
Table 2.5	Comparison between the PMU-based and the SCADA-based systems (Tripathy, 2010)	59
Table 2.6	The definition of power system stabilities	61
Table 3.1	Configuration Frame Format 1 and 2 (IEEE Std C37.118.1, 2005)	76
Table 3.2	Configuration Frame Format 3 (IEEE Std C37.118.1, 2011)	77
Table 3.3	Header frame organization (IEEE Std C37.118.2, 2011)	79
Table 3.4	Command frame organization (IEEE Std C37.118.2, 2011)	79
Table 4.1	Specification values used in the lab-scale system functions	82
Table 4.2a	List of the hardware used	83
Table 4.2b	List of software used	83
Table 4.3	PB5 card specification	84
Table 4.4	PMU configuration parameter setting	102
Table 4.5	GTIO fiber port number, GTNET card PMU number and the processor card assignment	104
Table 4.6	OpenPDC historian connection string	109
Table 5.1	Five bus power system network transmission line data in per unit	116
Table 5.2	Five bus power system network transmission line B coefficients	117
Table 5.3	Load flow data for the five bus power system network	117
Table 5.4	Load flow simulation results of the five bus power system model in the RSCAD environment	119
Table 5.5	Transmission line data of the eleven bus power system	120
Table 5.6	Bus information and load data for the eleven bus power system	121
Table 5.7	Eleven bus system load flow results in RSCAD environment	123
Table 6.1	Five bus system power demand analog values from the RTDS front panel PB5 card outputs acquired using the developed LabVIEW front panel system and the NI DAQ 6343 card	138
Table 6.2	Fuel cost and generator limits of the five bus power system (Kothari and Dhillon, 2006)	138
Table 6.3	Economic dispatch optimal solution for the five bus system using the RTDS real-time data captured by the LabVIEW-based data acquisition system	139
Table 6.4a	Analog voltage measurement output from the RTDS PB5 card and their actual values for the eleven bus power system (Channels #1 to #6)	146

Table 6.4b	Analog voltage measurement output from the RTDS PB5 card and their actual values for analog output channels of the eleven bus power system (Channels #7 to #11)	146
Table 6.5	Fuel cost, emission coefficients and generator limits for the eleven bus power system	147
Table 6.6a	Economic dispatch problem solution for the eleven bus power system using the LabVIEW-based data acquisition system (generator powers)	148
Table 6.6b	Economic dispatch problem solution for the eleven bus power system using the LabVIEW-based data acquisition system (fuel cost and emission values)	149
Table 6.7	Five bus system analog values from the RTDS front panel PB5 card acquired using the MATLAB-based data acquisition system	151
Table 6.8	Economic dispatch solution for the five bus system using the RTDS real-time data captured by the MATLAB-based data acquisition system (Lagrange's algorithm)	151
Table 6.9a	Eleven bus power system analog values from the RTDS front panel PB5 card outputs and their actual values acquired using the MATLAB-based data acquisition system (Channels #1 to #6)	153
Table 6.9b	Eleven bus power system analog values from the RTDS front panel PB5 card outputs and their actual values acquired using the MATLAB-based data acquisition system	154
Table 6.10a	Economic dispatch problem optimal and load flow based solutions for the eleven bus power system using the RTDS real-time data captured by the MATLAB-based data acquisition system (generator powers)	154
Table 6.10b	Economic dispatch problem optimal and load flow based solutions for the eleven bus power system using the RTDS real-time data captured by the MATLAB-based data acquisition system (fuel cost and emission values)	155
Table 6.11	Signal ID Number and the name of the GTNET card PMU signals	164
Table 6.12	MySQL archived data and their signal names	164
Table 6.13	PMU signal monitored in the RSCAD and MySQL environment for the initial loading condition	165
Table: 6.14	PMU signals monitored in RSCAD and MySQL environment for the first loading condition	166
Table 6.15	PMU signals monitored in the RSCAD and MySQL environment for the second loading condition	166
Table: 6.16	PMU signals monitored in the RSCAD and MySQL environment for the third loading condition	167
Table 6.17	PMU signals monitored in the RSCAD and MySQL environment for the fourth loading condition	167
Table 6.18	Comparison of the measured load power demands in the RSCAD with the power demands calculated using the GTNET 170card PMU signals and OpenPDC software	169

Table 6.19	Economic dispatch problem solution using the GTNET card PMU signals	170
Table 6.20	Comparison of the economic dispatch problem solutions using the RTDS GTNET card PMU signals and the RTDS PB5 card front panel analog output signals	170
Table 7.1	The software programs for the data acquisition, and data transfer systems using the RTDS front panel PB5 card analog output signals and the RTDS GTNET card PMU output signals	176

APPENDICES

Appendix A	Structure of the Real-Time Digital Simulator (RTDS)	188
Appendix B	Open Phasor Data Concentrator (PDC) software installation	194
Appendix C	MySQL Workbench Installation	200
Appendix D	Development of RSCAD software for simulation of the five and eleven bus power systems	203
Appendix E	Development of DAQ/LabVIEW software for simulation of the five and eleven bus power systems	208
Appendix F	Software program to read the data saved by LabVIEW in the Excel file into the MATLAB environment and using them to solve the power dispatch optimisation problem for the five bus power system	210
Appendix G	Software program for the implementation of method one: MATLAB-based data acquisition and data transfer system using PB5 card analog output signals for the five bus power system	213
Appendix H	Software program used to read the data saved by LabVIEW in the Excel file into the MATLAB environment and using them to solve the power dispatch optimisation problem for the eleven bus power system	216
Appendix I	Software program for the implementation of method one: MATLAB-based data acquisition and data transfer using PB5 card analog output signals for the eleven bus power system	219
Appendix J	Software program used to acquire the saved data from the MySQL database into the MATLAB environment and using them to solve the power dispatch optimisation problem	223

GLOSSARY

BCI	Brain Computer Interface
CPS	Cyber-Physical Systems
CSAEMS	Center for Substations Automation and Energy Management Systems
CSMA/CD	Carrier-Sense Multiple Access/Collision Detection
CT/VTs	Current and Voltage Transformers
DAQ	Data acquisition system
DARPA	Defence Advanced Research Projects Agency
DAS	Distribution Automation System
DER	Distribution Energy Resources
DMS	Distribution Management System
DNP3	Distributed Network Protocol 3
ED	Economic Dispatch
EHF	Extremely High Frequency
EMI	Electromagnetic Interference
EPGs	Electric Power Group's
ESI	Energy Services Interface
FAN	Field Area Networks
FRACSEC	Fraction-of-Second
GOOSE	Generic Object Oriented and Substation Event
GPS	Global Positioning System
GSSE	Generic Substation Status Event
GUI	Graphical User Interface
HAN	Home Area Networks
HEMS	Home Energy Management Systems
HF	High Frequency
HIL	Hardware in the loop
HMI	Human Machine Interface
HVDC	High Voltage Direct Current
ICMS	Inductive Current Measurement System
IEC	International Electrotechnical Commission
IED	Intelligent Electronic Device
IP	Internet Protocol
IPHA	Current Phasor Angle
IPHM	Current Phasor Magnitude
IRC Card	Inter-Rack Communication card
IRIG-B	Inter Range Instrumentation Group time code format- B
ISO	International Organization for Standardization
JVC	Joint Var Controller
LabVIEW	Laboratory Virtual Instrument Engineering Workbench
LAN	Local Area Network
LF	Low Frequency
MDMS	Meter Data Management System

MF	Medium Frequency
NASPI	North American Synchrophasor Initiative
OSI	Open System Interconnection
PDC	Phasor Data Concentrators
PEVs	Plug-in Electric Vehicles
PLCC	Power Line Carrier Communication
PLCs	Programmable Logic Controllers
PMU	Phasor Measurement Units
PSTT	Performance and Standards Task Team
RCC	Regional Control Center
RCP	Rapid Control Prototyping
RF	Radio Frequency
RTDS	Real Time Digital Simulator
RTU	Remote Terminal Unit
SCADA	Supervisory Control and Data Acquisition
SCC	System Control Center
SCL	Substation Configuration Language
SE	State Estimation
SHF	Super High Frequency
SOC	Second of Century
SV	Sampled Values
TCP	Transmission Control Protocol
TCP/IP	Transmission Control Protocol /Internet Protocol
TVE	Total Vector Error
UC	Unit Commitment
UDP	User Datagram Protocol
UHF	Ultra High Frequency
USA	United States of America
UTC	Coordinated Universal Time
UWF	Ultra Wide Band
VHF	Very High Frequency
VLf	Very Low Frequency
VPHA	Voltage Phasor Angle
VPHM	Voltage Phasor Magnitude
WAMV	Wide-Area Monitoring and Visualization
WAN	Wide Area Networks
WASA	Wide Area Situation Awareness
WDM	Wave Division Multiplexing
WIF Card	Workstation Interface Card

MATHEMATICAL NOTATIONS

Symbols / letters	Definition/Explanation
α	Step size of the gradient procedure
δ_i	Phase angle of a bus i
ε	Tolerance value of the gradient procedure
λ	Lagrange's multiplier
$\Delta\lambda$	Gradient of the Lagrange's variable λ
Φ_1, Φ_2	Phase angle between the voltage and the current in degrees
a_i, b_i, c_i	Fuel coefficients of generation for the unit i
B_{ij}, B_{0i}, B_{00}	Transmission loss coefficients
d_i, e_i, f_i	Emission coefficients of the generating unit i
E, D	Matrices to calculate the real power of the generator for single area power system using Lagrange's method of optimisation
E_T	Total Emission value
F_C	Total Fuel cost
I_a, I_b, I_c	Branch currents in Amps
$Iter_{max}$	Maximum number of iterations
k	Current number of the iteration
n	Number of generating units
P	Vector of the real power produced in the whole power system
P_D	Total power demand in Watts
P_i	Real power generation of a generator unit i
$P_{i,min}, P_{i,max}$	Minimum and maximum value of the real power allowed at a generator i
P_L	Transmission line loss
$PA 1$ to $PA6$	PMU phasor angle of the three phase voltage and current signals respectively.
$PM1$ to $PM4$	PMU phasor magnitude of the three phase voltage and current signals respectively.
V_i	Bus voltage magnitude
YSh_{ij}	Transmission line Shunt admittance of line i to line j
$ZSER_{ij}$	Transmission line Series impedance of line i to line j

CHAPTER ONE

1. Introduction

The electric power utilities play a vital role in the generation, transmission and distribution of the electrical power to the end users. The power utilities face two major issues, i.e. i) power grids are expected to operate close to the maximum capacity, and ii) there is a need for accurate and better monitoring and control of the power system network using the modern technology and the available tools. These two issues are interconnected as better monitoring allows for better control of the power system.

The development of the new standard-based power system technologies contributed to raising the ideas for building of a Smart Grid. The challenges are that this process requires the development of new control and operation architectures and methods for data acquisition, data transfer, and control computation. These methods require data for the full dynamic state of the power system in real-time, which leads to the introduction of the synchrophasor-based monitoring and control of the power system.

The thesis describes the research work and investigations for integration of the existing new power system technologies to build fully automated systems for real-time solution of power system energy management problems, incorporating data measurement and acquisition, data transfer and distribution through a communication network, and data storage and retrieval in one whole system.

This chapter presents the motivation of the research problem and the problem definition in section 1.1. The research aim and objectives are presented in section 1.2, and the project assumptions, delimitation and hypothesis are given in the section 1.3. The deliverables of the thesis are described in section 1.4, with the chapter breakdown given in section 1.5. The publications on the research work results and chapter conclusion are presented in the sections 1.6 and 1.7 respectively.

1.1 Motivation and definition of the research problem

1.1.1 Motivation for research

One of the biggest challenges the world is facing at the present is how to solve the problem associated with the energy supply and demand, and how to achieve requirements such as sustainability, stability, environmental friendliness and accessibility to the produced energy.

Different solutions are proposed and are in the process of implementation as renewable generation, substation automation, distributed automation, deregulation market, and a smart grid (Kezunovic et al., 2009).

The U.S. Department of Energy, 2012, defines a smart grid as “a modern electrical grid” where use is made of both analogue and digital data together with the communication infrastructure to process the information using automation to benefit the consumer and to ensure that the production and distribution of electricity is improved reliable, efficient, economically viable and sustainable (<http://www.northwestleaf.com>, 2014).

The current technological developments to address the challenges of the introduction of a smarter grid include, sensing and measurement, integrated communication, improved control strategies, interfaces and knowledge-based decision making systems. (Thorp, 2008).

The need for further development of the above technologies requires an integrative approach and knowledge not only about the physical power system, but also about the communication and the control of the connected power components. In addition the requirements for the operation of the smart grid are that it acts as an autonomous, fully automated and optimized system.

The challenges brought about by these needs and requirements are: which existing methods, technologies, tools (hardware and software) are applicable and can be further developed, or which new ones can be investigated and implemented.

This means that there is a need for development of new interconnections between the power system elements, and understanding of the new approaches, methods, algorithms, hardware and software to achieve full integration of the operation of the smart grid.

These needs are addressed by the latest investigations and the development of a new type of system, known as Cyber-Physical Systems (CPS). A CPS is a system of collaborating elements controlling the physical world. They are designed as networks of interfacing elements with physical inputs and outputs.

Applications of the CPS are in aerospace, automotive, energy, manufacturing, and healthcare industries.

The latest developments in science and engineering make the link between the computational and physical elements of one system to be improved, possible. This tremendously increases its adaptability, safety, autonomy, usability, availability, efficiency, and functionality. On the basis of the above the CPS are a key area of research in the world and a lot of investigations at present are directed towards building of the smart grid technologies. (Paul et al., 2011)

The energy management systems are one of the main parts of the smart grid as they control and reduce the uncertainty into the daily operation of the power system, utilizing various methods and tools for monitoring, visualization, state estimation, real-time stability assessment, restoration, optimisation of power flow, optimal power dispatch, real-time control, etc.

At present the Energy Management System (EMS) operation are performed by existing SCADA systems, which supervise, control and manage the generation, transmission and distribution systems. The operation of the SCADA systems does not satisfy today's requirements for fast information in order to produce and implement real-time control in the power system. This situation is due to the fact that the SCADA system is designed and implemented using the principles of the old technology for measurement, communication and control, as follows:

- The 3-phase current and voltage signals from the CTs (Current Transformers) and PTs (Power Transformers) are sampled and sent to the energy management system only represented by their magnitude and the line active and reactive power.
- The measurement window is large which produces data that is not as accurate with the system changes. The assumptions that during the window period the load parameters will change and the system part will remain constant can appear not valid during the measurement window.
- The SCADA system does not allow measurement of the power system voltage and current angles and does not consider synchronised wide area measurement.
- Analysis of the system status is based on a multiple power flow approach, which creates a computation burden that is not fast enough for real-time implementation.

The existing situation is that critical data are required to monitor the system during transients and disturbances which require fast synchronised data in order to capture the system dynamics. Then, based on these data, creating a real-time situational awareness, fast real-time control is possible to be implemented. The need for high resolution synchronised data is addressed by the Phasor Measurement Units (PMUs), which are sophisticated digital recording devices capable of exporting GPS-synchronised data with a high sampling rate. This fact supported the approach to take decisions for power system operation based on steady state data from a local area to be shifted to paying attention to the system dynamic behavior in a global or wide area.

The use of the synchrophasor data requires a proper, fast, reliable, and safe communication network between the PMUs and the control center that supports both the existing functionalities and the future operational requirements to be developed. Using synchronized data at the control center requires restructuring of the available methods and software algorithms for solution (calculation) of the energy management problems and the transfer of the obtained control actions to the elements of the power systems.

On the basis of the above, it can be concluded that there is a need for interdisciplinary research to develop a close integrated framework of the latest achievements in the field of measurement, communication, optimisation and control of power systems. This thesis concentrates on research work in this field following the principles of the Cyber Physical Systems (CPSs), and aiming to produce real-time working prototypes implementing a real-time solution of the power dispatch optimisation problem for given power networks.

The prototypes are developed in the Laboratory of the Centre for Substation Automation and Energy Management Systems, at the Cape Peninsula University of Technology to demonstrate to the power utilities how such a measurement, communication and control optimisation framework can operate from one side, and to support the interdisciplinary education and research for graduate and postgraduate control and power system engineering students in the field of the new power system monitoring, protection, automation and control technologies, from the other side. At present the educational programs at universities are very narrow specialised programs, and the produced engineers are not capable to accept the challenges presented by the new smarter grid.

1.1.2 Problem definition

The existing problem in power systems is that there are not existing solutions for building a framework of fully automated smart systems for the real-time solution of the energy management problems, utilizing the new technologies for data measurement, data acquisition, data transfer and distribution. The research problem is how to apply the approach of the CPS to address this real-time problem.

The thesis proposes a solution to the above problems by emphasizing the interconnection of different engineering fields by interfacing the existing or newly developed respective methods, algorithms, and hardware and software tools to cope with the problem complexity by integration of these tools.

Implementation of the developed lab-scale prototypes is based on utilization of the Real-Time Digital Simulator (RTDS) as a source of power system data, software PMUs, Data Acquisition (DAQ) cards, Personal Computers (PCs), MATLAB, LabVIEW, MySQL, RSCAD software, and Ethernet communication, as described in the next chapters.

1.2 Research aim and objectives

1.2.1 Research aim

The aim of this thesis is to develop a framework which includes methods, algorithms, procedures, software and hardware tools for development and implementation of lab-scale prototypes of the power network and its data acquisition and data transfer and distribution system in order to allow the solution of the power dispatch optimisation problem in real-time, using real-time data.

1.2.2 Research Objective

In order to achieve the aforementioned aim, the following project objectives are proposed:

- To review the existing literature and investigate the communication systems, network technologies, media and protocols, and the power system application of

LabVIEW, Real-Time Digital Simulator (RTDS), and the synchrophasor technologies.

- To develop a framework which includes methods, algorithms, and procedures for implementation of two types of lab-scale data acquisition and transfer systems for application in power system monitoring and control, based on two types of data measurements: analog signals and synchrophasor signals.
- To identify suitable hardware platforms and software tools for implementation of the two lab-scale systems.
- To develop an algorithm and a procedure for capturing the RTDS PB5 card analogue output signals using the NI DAQ card in LabVIEW/MATLAB-based systems.
- To develop an algorithm and a procedure to transmit, store and retrieve the RTDS power system simulation model signals from the host PC to a remote PC using the RTDS GTNET card PMU-based synchrophasor output signals.
- To test the developed systems for two case studies of power systems.
- To apply the developed data acquisition and data transfer systems for the solution of the power dispatch optimisation problem.

1.3 Project assumptions, scope, delimitation and hypothesis

1.3.1 Project assumptions

The implementation of the project work is to be conducted on the basis of the assumptions used for the data acquisition, data transfer, distribution, storage and retrieval of the RTDS data to solve the economic emission dispatch problem in real-time; these are:

- For simplicity, the power demand of the power system is considered to be constant for the period of time in which the economic dispatch problem is solved. In reality the power demand is changing in real-time with respect to the load consumed by the consumer.
- The method of Lagrange produces a global solution of the optimisation problem.
- The initial values of the Lagrange's multiplier λ do not affect the final solution of the problem.

- The software-based PMU produces the same values of the data measurements as the hardware based ones.
- It is possible to build interfaces between the hardware and software elements of the system and to organise fast measurement and flow of data through the communication network.

1.3.2 Project scope

The real-time implementation of the lab-scale prototypes is based on using of the RTDS which simulates the power system model in real-time and in this way emulates the real power system. The power system model simulated outputs are measured in the RTDS simulation environment RSCAD, using the RTDS PB5 card analog output signals and RTDS GTNET card PMU signals. Two data acquisition and data transfer and distribution systems of the measured data are developed, i.e. i) RTDS PB5 card analog output signals-based NI DAQ system (communication within the local PC), and ii) RTDS GTNET card PMU signals-based (communication between the host and the remote PCs through Ethernet communication).

The main functions of the developed framework are given in Figure 1.1.

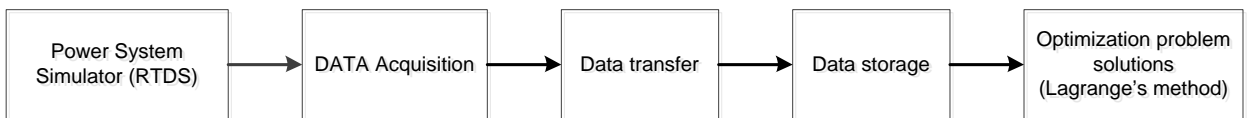


Figure 1.1: Lab-scale system functions

These functions are performed by corresponding hardware and software components of the above two prototypes.

1.3.3 Project delimitation

The investigation will not include a two-way communication system. The investigation will not include other existing power system management optimisation problems such as Unit Commitment (UC) problem; coordination of hydrothermal optimisation problem, optimisation problem for wind energy, and hydro power optimisation, etc., but the developed data acquisition and transfer methods will be capable to solve the other optimisation problems too. Other optimisation problems are not considered.

The following are implemented in the thesis:

- Implementation of the LabVIEW-based data acquisition and data transfer system using the RTDS PB5 card analogue output signals for five and eleven bus power system case studies.
- Implementation of the MATLAB-based data acquisition and data transfer system using the RTDS PB5 card analogue output signals for the five and eleven bus power systems case studies.
- Implementation of the RTDS GTNET card PMU-based synchrophasor data acquisition and data transfer system for the five bus power system case study
- Methods, algorithms and software are developed for the LabVIEW-based, MATLAB-based, PMU-based data acquisition and data transfer systems for the five and eleven bus power systems.

1.3.4 Project Hypothesis

The synchrophasor technology for measurement of the power system variables is capable to be used as a basis for the development of methods, algorithms, procedures, and software and hardware tools for implementation of real-time optimisation problem solution in the framework of a smart grid.

The proof of the hypothesis is done by implementation of the hardware and software structure of the lab-scale systems developed in the thesis.

1.4 The deliverables of the thesis

The main deliverables of the thesis can be summarized as follows:

- A literature review of the power system communication networks, protocols, and media used for data acquisition and transfer systems.
 - A literature review includes the power system communication architecture, media, protocols, synchrophasor applications, and data acquisition and transfer methods used in the power system applications.
- Development of the lab-scale data acquisition and data transfer systems. Two lab scale systems are developed, they are:
 - Lab-scale data acquisition and data transfer system using the RTDS PB5 card analogue output signals.

- Lab-scale data acquisition and data transfer system using the RTDS GTNET card PMU-based synchrophasor output signals.
- Implementation of the lab-scale data acquisition, and transfer systems: Case studies and their results
 - Development and implementation of the LabVIEW-based data acquisition and data transfer system using the RTDS PB5 card analogue output signals for the five bus power system model. The system operation test results are presented.
 - Development and implementation of the MATLAB-based data acquisition and data transfer system using the RTDS PB5 card analogue output signals for the five bus power system model. The system operation test results are presented.
 - Development and implementation of the LabVIEW-based data acquisition and data transfer system using the RTDS PB5 card analogue output signals for the eleven bus power system model. The system operation test results are presented.
 - Development and implementation of the MATLAB-based data acquisition and data transfer using the RTDS PB5 card analogue output signals for the eleven bus power system model. The system operation test results are presented.
 - Development and implementation of the RTDS GTNET card PMU-based data acquisition and data transfer system for the five bus power system model. The system operation test results are presented.
- Software developed and implemented for the LabVIEW-based, MATLAB-based and PMU-based data acquisition and data transfer systems for the economic dispatch problem solutions
 - Developed LabVIEW graphical software program for the data acquisition and data transfer using the RTDS PB5 card analogue output signals for the five bus power system model.
 - Developed software to acquire the saved by the LabVIEW data from the Excel file into the MATLAB environment and using them to solve the dispatch optimisation problem for the five bus power system model.

- Developed software program for the MATLAB-based data acquisition and data transfer using the RTDS PB5 card analogue output signals for the five bus power system model.
- Developed LabVIEW graphical software program for the data acquisition and data transfer using the RTDS PB5 card analogue output signals for the eleven bus power system model.
- Developed software to acquire the saved by the LabVIEW data from the Excel file into the MATLAB environment and using them to solve the dispatch optimisation problem for the eleven bus power system model.
- Developed software program for the MATLAB-based data acquisition and data transfer using the RTDS PB5 card analogue output signals for the eleven-bus power system model.
- Developed RSCAD GTNET card PMU configuration file for data acquisition, data transfer, and distribution system for the five bus power system model.
- Developed software program used to acquire and save data from the MySQL database into the MATLAB environment and using them to solve the power dispatch optimisation problem

A detailed description of the thesis deliverables is given in Chapter 7.

1.5 Chapter breakdown

This thesis has seven chapters, as follows:

Chapter 1 presents the motivation and definition of the research problem in the thesis. The research aim and objectives, hypothesis, research delimitation, and assumptions are described.

Chapter 2 reviews the power system communication architectures, media, protocols, synchrophasor applications, and data acquisition and data transfer methods used in power system applications.

Chapter 3 presents the definition of the synchrophasor, time synchronization, standards, protocols, and the Phasor Data Concentrator (PDC) which are the tools used in the lab-scale implementation and simulation.

Chapter 4 presents the methods, algorithms and procedures, hardware and software tools which are utilized to implement the real-time data acquisition and data transfer system framework.

Chapter 5 describes the case studies used to validate the developed lab-scale systems and the formulation of the algorithm to solve the economic dispatch problem. The investigations are done on the five and eleven bus power system models (Kothari and Dhillon, 2006). The power system simulation models are constructed in the RSCAD environment, the software suite of the RTDS.

Chapter 6 describes how to apply the developed two prototypes of data acquisition and data transfer systems (Chapter Four) and provides the results of these applications to the five and the eleven bus power system model case studies.

Chapter 7 presents the conclusion, and the deliverables of the thesis. The applications of the thesis results, the future work, and the author's publication are also included.

1.6 Publications

Based on the thesis outcomes, the following publications have been submitted as follows:

Deivakkannu, G., Krishnamurthy, S., Kriger, C., and Tzoneva, R. 2014. Development of a lab-scale data acquisition and data transfer system in the LabVIEW and MATLAB environment to solve the economic dispatch problem in real-time. Submitted to the International Journal of Computers, Communications and Control (IJCCC)

Deivakkannu, G., Krishnamurthy, S., Kriger, C., and Tzoneva, R. 2014. Development of a lab-scale data acquisition and data transfer system using the RTDS GTNET card PMU-based system to solve the economic dispatch problem in real-time. Submitted to the International Review of Electrical Engineering (IREE).

1.7 Conclusion

This chapter presents the motivation and definition of the research problem in the thesis. The research aim, objectives, and assumptions are described. Outline and deliverables of the thesis are stated.

In order to gain a deeper understanding of the communication systems used in power systems it is critical to review the literature - especially focusing on the papers that propose communication network architectures, media, and protocols used to acquire, transfer, store and retrieve the power system data in real-time at the remote end PC.

Chapter 2 reviews the power system communication architectures, media, protocols, synchrophasor applications, and data acquisition and data transfer methods used in power system applications.

CHAPTER TWO

REVIEW OF THE LITERATURE FOR REAL-TIME DATA ACQUISITION AND DATA TRANSFER METHODS FOR POWER SYSTEM APPLICATIONS

2.1 Introduction

The power system utilities face different difficulties such as the failure of equipment, lightning strikes, natural weather conditions and lightning strikes in their operation to provide a reliable power source to the consumers. Preventing or reacting rapidly to the above situations require large amount of real-time data for all levels of the power system. The existing control structures cannot perform well according to the requirements of the current power system. There is a need for monitoring and control of the power system using the new technology and the available tools. The drawbacks of the existing SCADA system are: i) the conventional methods use a SCADA system to monitor the power system variables based on the Root Mean Square (RMS) values, instead of using the phasor values of the voltage and current; ii) the measurement of the power system variables by the SCADA system is not synchronized with the GPS clock and these lead to the occurrence of power system instability, which can cause power blackouts; and iii) the SCADA system updates the state of the power system once every 15 minutes resulting in a longer sampling period for data acquisition which is not suitable for power system protection applications.

Due to the factors mentioned above, it is necessary to build a data acquisition and data transfer communication system to monitor and control the electrical power system and ensure that this newly developed communication system responds rapidly to real-time events. This motivated the author to investigate the different communication systems used in the power system from 1996 to 2014.

This chapter provides the results of the literature review and an investigation on the general structure of the communication systems in sections 2.2 and 2.3 respectively. Communication networks such as Home Area Networks (HAN), Field Area Networks (FAN), and Wide Area Networks (WAN) are described in section 2.4. Various communication protocols such as the Ethernet protocol, TCP/IP and UDP protocol, Modbus protocol, Distributed Networking Protocol (DNP3), IEC-870-5-101 protocol, IEC 61850 protocol, and the IEEE standards, which are used in the power systems, are

described in section 2.5. The review investigates the power system communication network technologies in section 2.6. Application of the synchrophasor technology in power engineering, and application of the DAQ cards for local or remote real-time simulation, monitoring and control using LabVIEW, MATLAB and Real-Time Digital Simulator (RTDS) software environments are described in the sections 2.7 and 2.8 respectively. The conclusion to the literature review is presented in section 2.9.

2.2 Literature searching methodology

The thesis focuses on the development of real-time data acquisition and data transfer methods for power system applications. In order to successfully achieve the aim of the thesis, it is therefore important to perform a thorough literature search based on some predefined objectives. The literature search presented in this chapter is articulated around the following goals:

1. Investigation of the communication architecture of the power systems.
2. Investigation of the communication media and supporting protocols for power system applications.
3. Investigation of the use of the Real Time Digital Simulator (RTDS) in the power engineering.
4. Investigation of the LabVIEW/MATLAB-based data acquisition and data transfer system in power engineering.

The literature search has been conducted according to five broad areas, which are:

- a. Communication system architecture type;
- b. History of the communication media and supporting protocols;
- c. Application of LabVIEW and their DAQ systems in the power system;
- d. Application of the RTDS in the power system;
- e. Application of the synchrophasor technology in the power system.

The literature survey is conducted from the year 1996 to the year 2014 for a period of 18 years. Forty-four papers were selected to be reviewed in the field of interest, namely - power system data acquisition and data transfer systems. The graph in Figure 2.1 shows the number of publications versus the year of the publications.

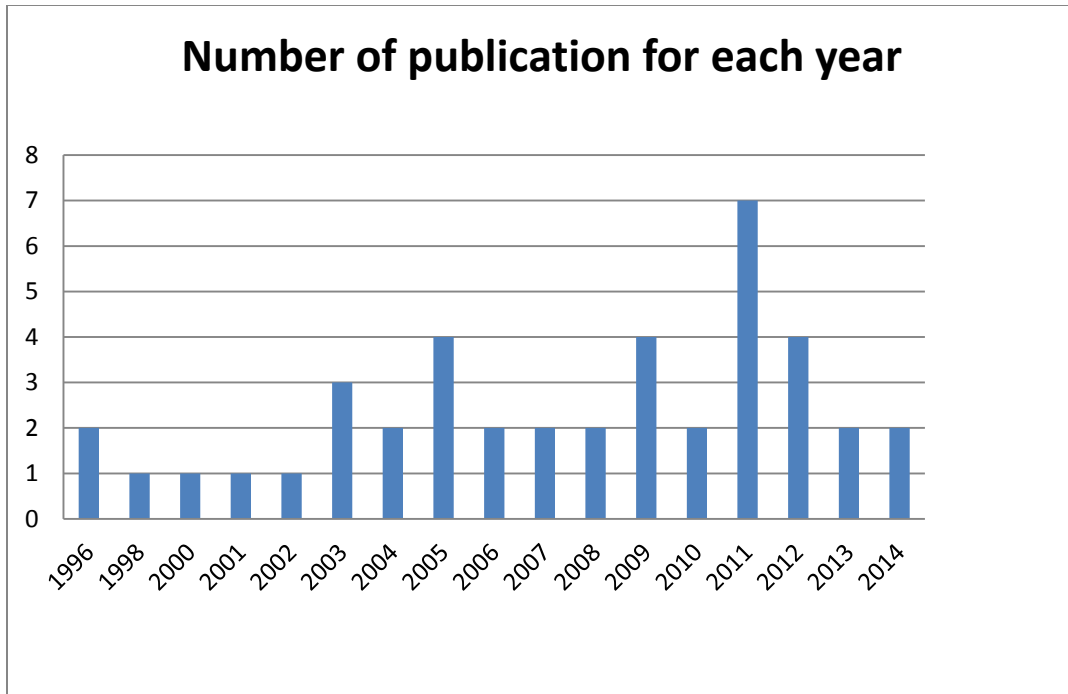


Figure 2.1: Total number of publications versus year of the publications

2.3 General structure of the communication systems

Communication networks can be broadly categorized to be either analog or digital. Analog systems have data signals that vary in frequency and amplitude that are added to carrier waves of a given frequency. Telephones and broadcast systems are examples of systems that utilize analog technology. Digital systems on the other hand generate, store, and process data in two possible states known as binary: where a zero represents one possible state and a 1 represents the other (Guha, 2011).

Figure 2.2 shows a typical communication system consisting of a microphone (transducer) that converts the input signal into a continuous time varying quantity that is transmitted over a communication media, and converted by a receiver into an output signal. An example of the output transducer for this system would be an amplified signal heard on a loudspeaker, which converts the input signal into an audible output.

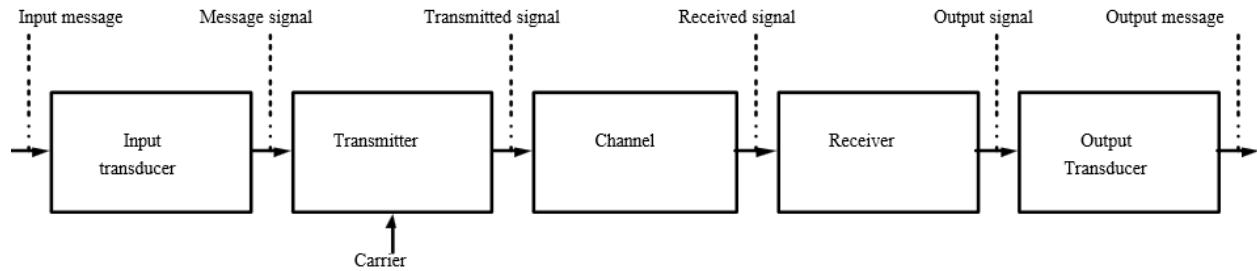


Figure 2.2: Block diagram of a communication system (Soni and Pareek, 2013)

All digital systems have to follow the requirements of the Nyquist theorem. The sampling theorem (Petraçovici and Rosenblatt, 2009) states that a band limited signal without spectral components are denoted as frequency f_m in Hertz and can be determined uniquely using the sampled values of the signal at uniform intervals of time T_s in seconds. The dependence between the signal frequency and the sampling interval is presented in Equations (2.1) to (2.3). The upper limit on T_s can be expressed in terms of the sampling rate.

$$f_s = 1/T_s \tag{2.1}$$

According to the Nyquist theorem it is required that

$$f_s \geq 2f_m \tag{2.2}$$

From here using the equation (2.1) it can be written

$$T_s \leq 1/(2f_m) \tag{2.3}$$

The Nyquist/sampling rate is the one, when $f_s = 2f_m$

The process of digitizing the original analogue signal is called quantization. It consists of mapping the amplitude of the signal into a number of discrete amplitude levels. These processes result in a loss of information, since it is not possible to recover the original analogue signal fully. The next section of this chapter describes the communication networks and their types.

2.4 Type of the communication networks

The communication infrastructure in a power system is expected to support the required application functionality and meet the performance requirements with regard to temporal behaviour. The system usually consists of many interconnected devices and the challenge

typically is the configuration and management of the device communications. The hierarchy is consists of with interconnected devices at different levels within the systems. This is depicted in Figure 2.3 where an example of the entire communication system is illustrated (Gungor and Lambert, 2006).

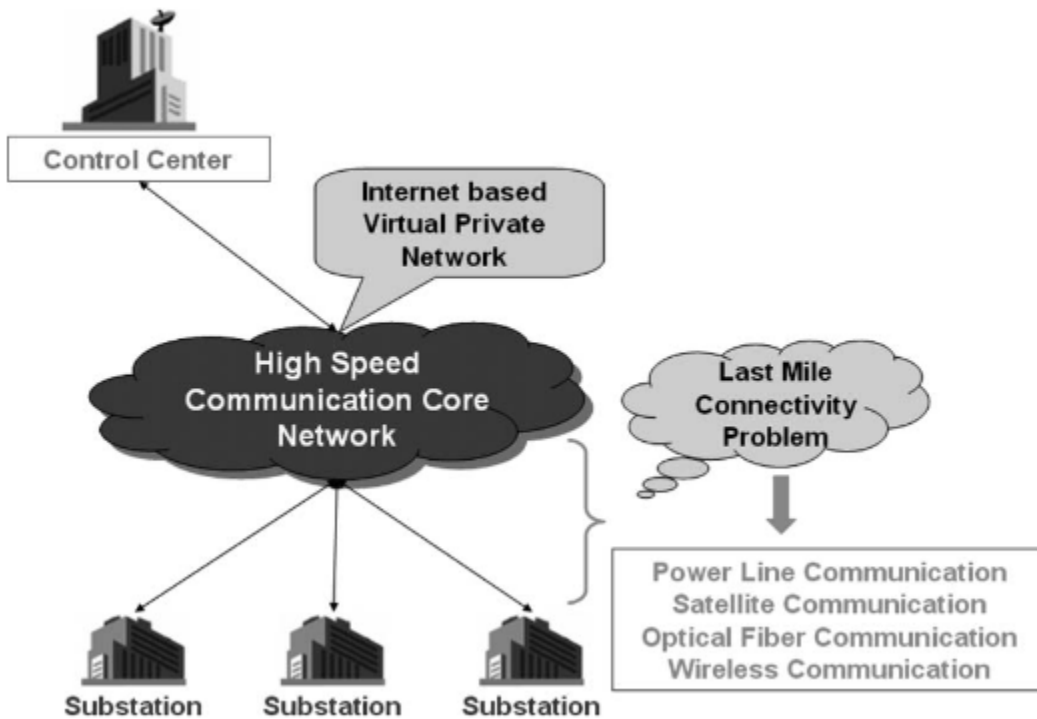


Figure 2.3: The communication network architecture for electric system automation (Gungor and Lambert, 2006).

Generally communication networks can be broadly categorized by three types of networks, such as (Wang et al., 2011): i) Home Area Networks; ii) Field Area Networks; and iii) Wide Area Networks. A short description of the three types of communication networks is given below.

2.4.1 Home Area Networks (HAN)

Home Area Networks (HAN) can be both wired and wireless, utilizing many standards. These systems are usually located in dedicated networks and they can be controlled and viewed remotely in a smart grid or wide area environment. Displays, automatic load control devices (e.g. hot water cylinders), and other technologically advanced appliances are integrated and can be used for smart metering and even automatic billing in future. This will ensure that the domestic power consumption can be monitored and controlled,

and that the power consumed by appliances such as heaters, air-conditioners, lights, washing machines, ovens, and tumble dryers can be reduced (Balakrishnanan, 2012).

To be able to fully appreciate the benefits offered by automation such as metering and automatic billing, the appliances in a HAN have to be able to communicate with other devices on the network and with the control center. In this environment, power utilities are better able to implement energy generation versus energy demand. One of the long-term benefits that a home automation network could offer would be the costs that would be minimized for owners and utilities alike. For this however to become a reality, the technology that already supports this paradigm, needs to be supplemented with the necessary legislation. Figure 2.4 gives an example of how these smart appliances are connected in a HAN (Balakrishnanan, 2012).

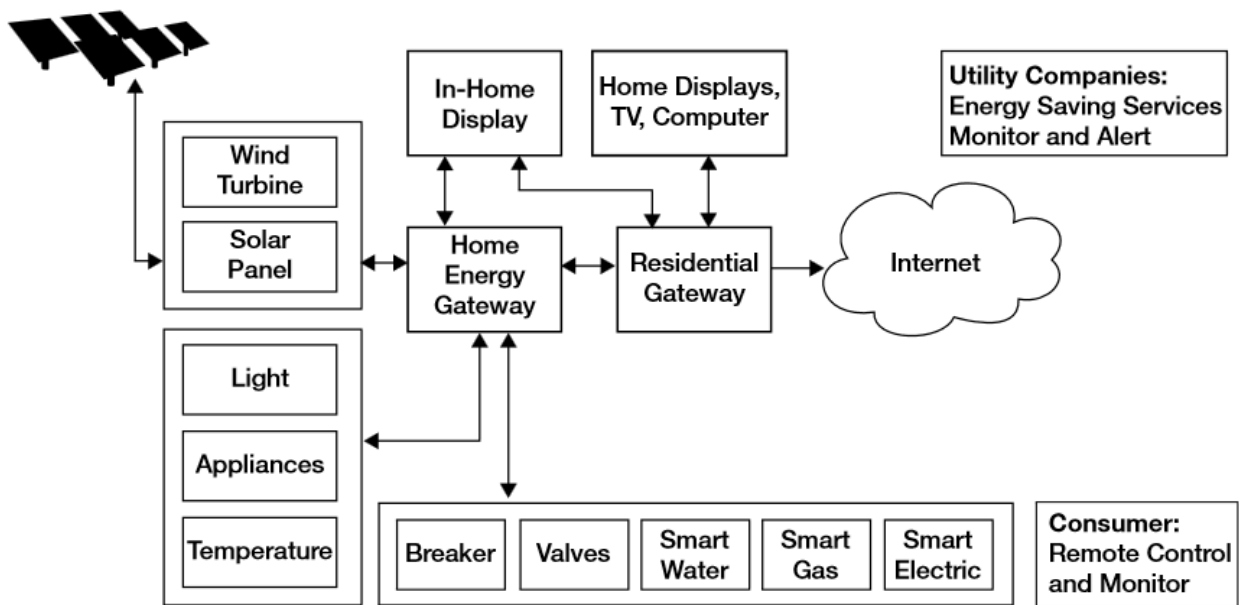


Figure 2.4: Smart appliances are interconnected within a HAN (Balakrishnanan, 2012)

2.4.2 Field Area Networks (FAN)

The communication network for electricity distribution systems are known as Field Area Networks (FANs) (Wang, 2011). Intelligent Electronic Devices (IEDs) carry out the control type of commands from the Distribution Management system (DMS) and the Distribution Energy Resource (DER) via the electrical sensors on the feeders and transformers in the

distribution network. The power system applications within the distribution network use the FANs to exchange information.

This application is categorized into two ways as presented by (Wang et al., 2011):

Field-based applications for example management systems for power outages, Supervisory Control and Data Acquisition (SCADA) applications, Distribution energy source monitoring and control.

Customer-based application such as automatic metering infrastructure, demand response, and load management systems.

Figure 2.5 shows the Field Area Network (FAN) components (Baig et al., 2013)

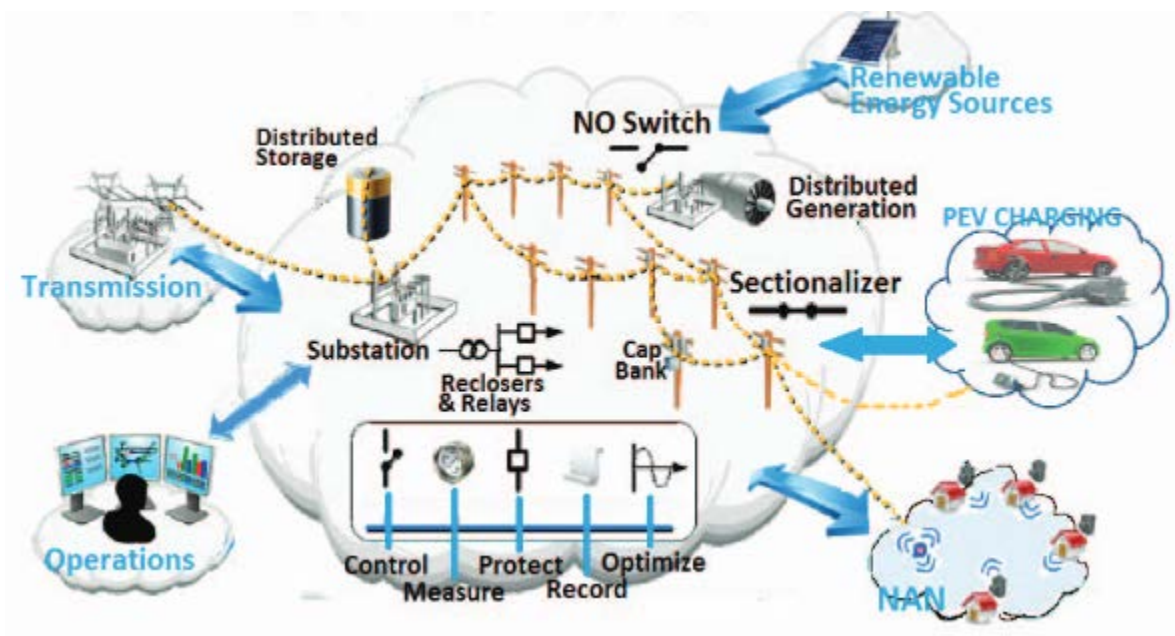


Figure 2.5 : Field Area Network components (Baig et al., 2013)

2.4.3 Wide Area Networks (WAN)

The distributed smaller area networks at various locations within the power system are known as Wide Area Networks (WANs) (Tholomier et al., 2009). The real-time data measurements are transferred from the substations to the control centers that are most of the time located far away from the substation, using the WANs. A WAN is able to transfer real-time, time-stamped information about the status of the system very quickly using specialized sensors located at the substations. The IEDs at the transmission level and

also at the distribution level in substations capture data from the plant and SCADA and respond to the control and protection commands from the control centers. Nowadays the communication between substations and control centers are facilitated with point-to-point telephone or microwave connections. (Hauser, 2005). New developments are needed in the WAN that can contribute to fast, interoperable and reliable communication as high speed networks are not in operation between substations and control centers as of yet..

The communication networks that transfer the data using appropriate communication protocols are described in the next section.

2.5 Communication protocol

A protocol is defining set of rules that have to implemented in order to ensure communication between two or more communication devices (Behrouz, 2006). In 1984, the International Organization for Standardization (ISO) developed the Open System Interconnection (OSI) reference model describing the transfer of information from devices on the same communication network. (Behrouz, 2006). The idea with this layered model is that a given layer offers data to the upper layers and receives data and information from the layer below it. The OSI model is not used so much these days, as the TCP/IP model is mainly used for designing protocols for today's Internet. The TCP/IP model has 4 or 5 layers depending on if the data link layer is divided into 2 layers or not. New protocols are usually hard to fit to the OSI model because they are designed for the TCP/IP model. Figure 2.6 shows two variant of the OSI models and how their layers correspond to each other (Behrouz, 2006).

The Physical Layer is the first layer of the OSI model and provides a description of the physical properties of the various communication media, including the electrical properties and an interpretation of the signals. This layer for example, gives a definition of the Ethernet coaxial cable size.

The second layer of the OSI model is known as the Data Link Layer. The logical organization of data bits transmitted on a particular medium is defined. This layer for example, describes the structure of the Ethernet frame and address.

The following layer is the Network Layer that defines how data is delivered between any two nodes in a network over different data links. One of the main tasks performed by this layer includes the addressing and routing structure of the Internet.

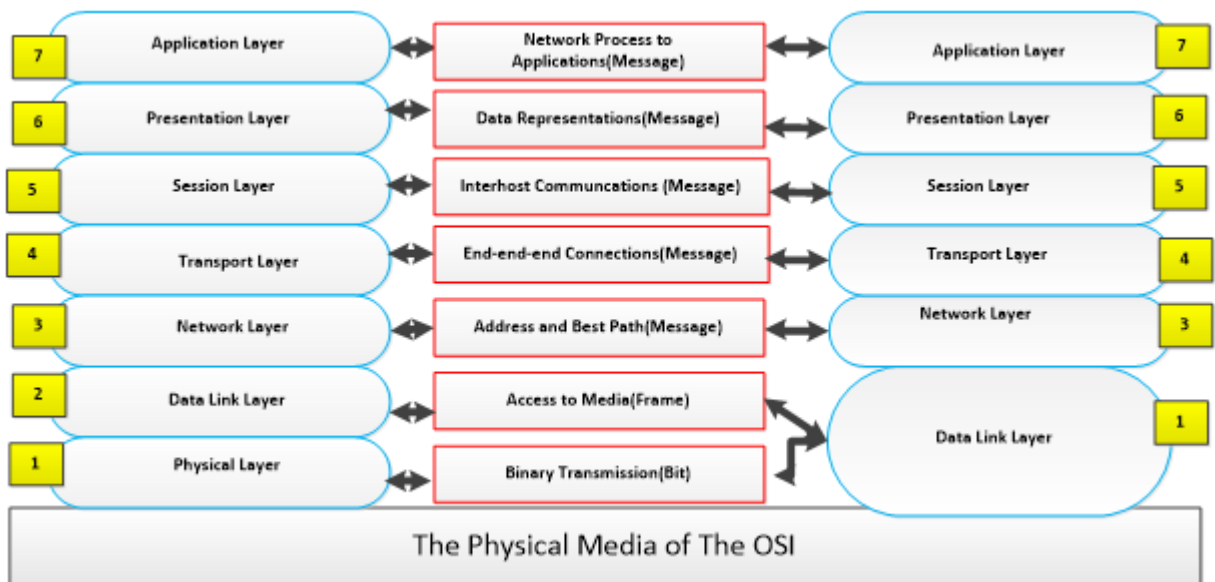


Figure 2.6: Seven layers Open System Interconnection Model (Behrouz, 2006)

The fourth layer is the Transport Layer that defines the quality and how data is to be delivered. If and how retransmissions are used to guarantee the delivery of data, are described here.

The fifth layer is the Session Layer that defines how data sequences with larger packet sizes than those handles at the lower layers, are organized. This layer specifies how to pair a request and reply packet in a remote procedure call, as an example.

The sixth layer is the presentation layer that provides the functions for encoding and encryption that are applied to the application layer data (final layer). The functions ensure that information sent from the application layers of different systems are readable by each other, as is presented in (Kabir, 2012).

2.5.1 Ethernet protocol

The Ethernet protocol is described in the IEEE 802.3 standard and refers to the medium for communication as the Local Area Network (LAN) (Saka, 2001). The Ethernet uses the basic principle of Carrier-Sense Multiple Access/Collision Detection (CSMA/CD) procedure from Aloha technology. This standard specific is that the data transfer speed is 10-Mbps. Figure 2.7 illustrates the structure of the Ethernet-based communication system (Behrouz, 2006)

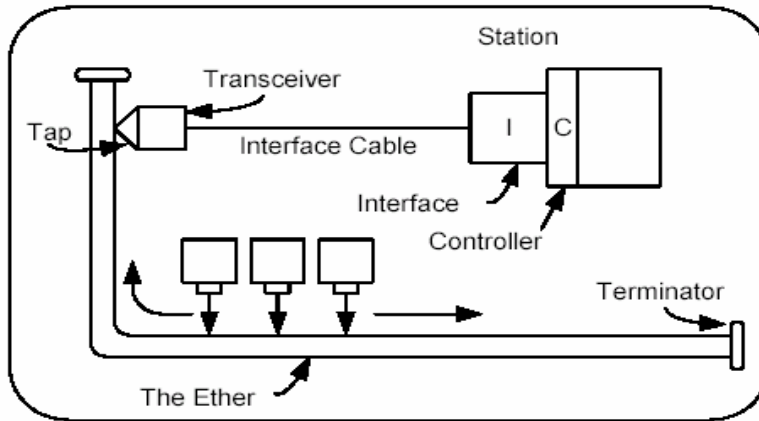


Figure 2.7: The structure of the Ethernet based communication system, (Behrouz, 2006)

Collisions occur when two devices transmit at the same time – this can affect the total throughput. Once a collision has occurred, the devices are forced to wait a certain amount of time before attempting to re-transmit the data. The delay caused by retransmitting the data is very small and does not affect the speed of other transmissions on the network (Behrouz, 2006). Ethernet cables using four data rates with either fiber-optical or twisted-pair cables being typically used. These are:

- 10 Mbps - 10Base-T Ethernet (IEEE 802.3)
- 100 Mbps - Fast Ethernet (IEEE 802.3u)
- 1000 Mbps - Gigabit Ethernet (IEEE 802.3z)
- 10-Gigabit - 10 Gbps Ethernet (IEEE 802.3ae)

2.5.2 TCP/IP and UDP protocol

The TCP/IP protocol suite, known as the Internet Protocol (IP), is a set of communication protocols that implement the protocol stack on which the Internet and most commercial networks are based. The IP is a network layer protocol which uses moving packets of data (datagram) over the network. It provides datagram services for the transport layer using the Transmission Control Protocol (TCP) and the User Datagram Protocol (UDP). The main protocol is the Transmission Control Protocol (TCP). It provides connectionless, delivery of the datagram through an Internet network. The original TCP/IP Protocol suite only had four layers and was known as the Defence Advanced Research Projects Agency (DARPA) model. It is shown in Figure 2.8 (Li et al., 2011).

For communication to occur using the TCP/IP protocol it is required that all computers on the network have a unique IP address to enable them to connect to the Internet, and therefore each IP packet has an address that enables communication to other computers on the network. (Prabhaker, 2007).

TCP is a protocol, which supports flow control; error control (to guarantee that the segments arrive at the destination without error, and resending of corrupted packets), and congestion control (reduces the loss of a segment due to congestion in the network). UDP is a connection-less protocol which does not support the provision of flow, error or congestion control. This means that a small overhead is attached to an application program that needs to send short messages and it cannot afford to retransmit the packet involved in the TCP, when the packet is corrupted or lost.

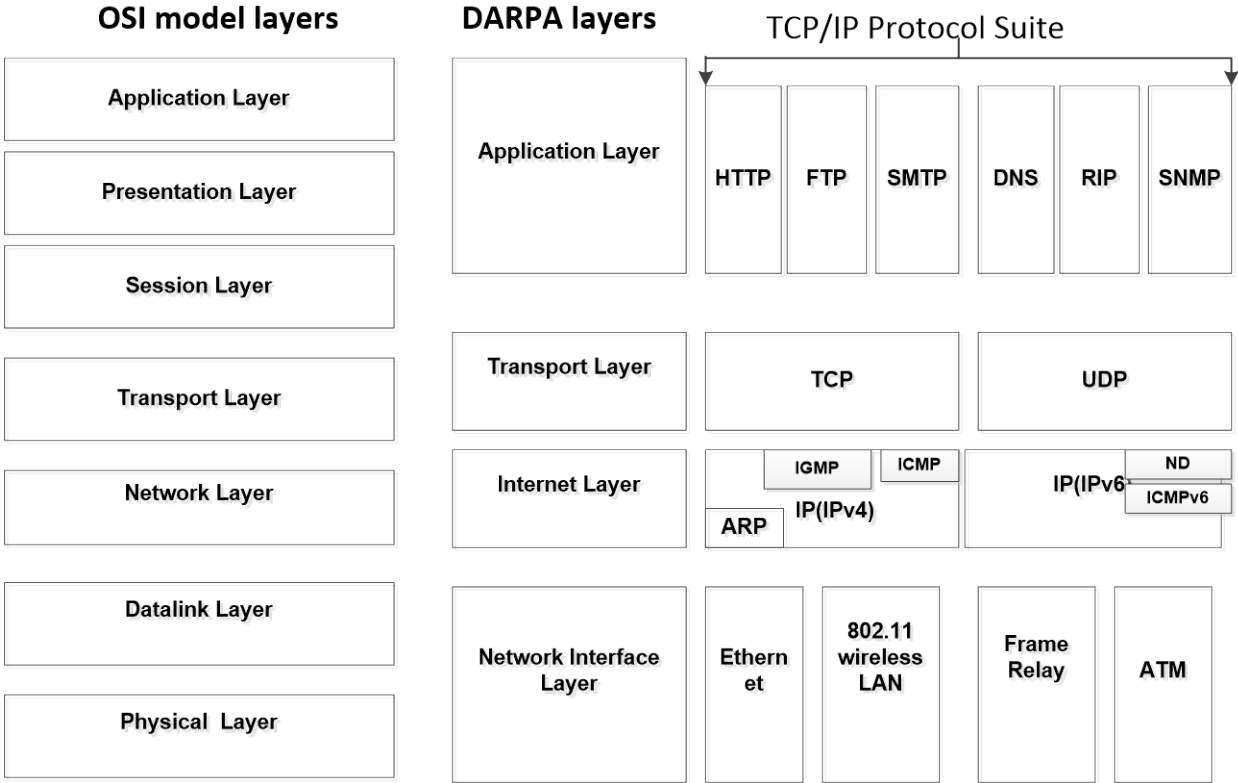


Figure 2.8: TCP/IP four layer model (Li et al., 2011)

2.5.3 Protocols in substations

The power system comprises of generation, transmission and distribution. The generated power must be transmitted to the distribution network via transmission lines. In an ideal scenario, all levels of the power system network should be able to communicate with each

other and transfer data between them. At present, the power system network has several communication protocols, covering certain application areas each having different data types. Figure 2.9 shows examples of some communication protocols typically used in power system networks (Mohagheghi et al., 2009).

Substations generally have switching, protection and different types of control equipment and transformers, sometimes from different vendors. Various protocols such as DNP3, IEC 61850, Modbus and wireless protocol are used to co-ordinate and share information between these devices. This data is usually transferred to a higher level within the hierarchy, known as the control center. Additionally, distribution substations also have to monitor the data from feeders and load points to improve the protection and control functions currently implemented. The main protocols that are established in the substation environment are Modbus, DNP3 and IEC61850 (Mohagheghi et al., 2009).

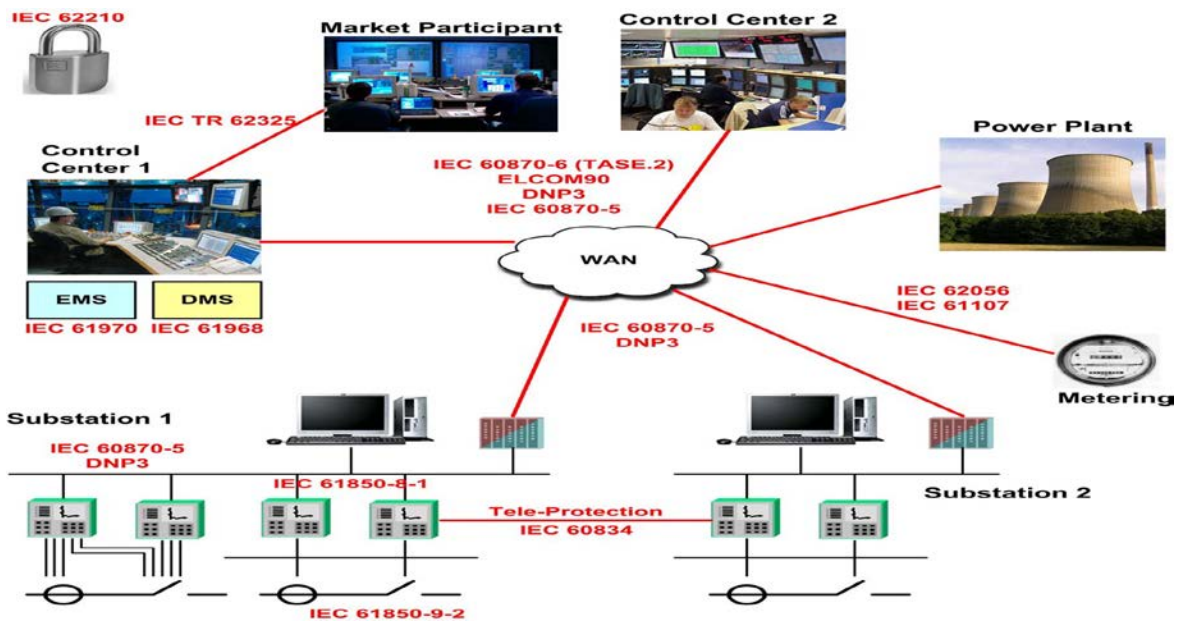


Figure 2.9: Typical communication protocols used in a power system (Mohagheghi et al., 2009)

2.5.4 The Modbus protocol

The Modbus Protocol is a master-slave/client-server messaging structure that was introduced by Modicon in 1979 (Sena, 2014). It is extensively used in specifically manufacturing industries. This allows devices such as PLCs (Programmable Logic Controllers) to communicate with sensors, meters and instruments. The Modbus message structure similar to HTTP consists of a request that the client initiates and a response by

the server. The slave devices for example, transducers, valves, network devices, input-output devices, etc. supply the data requested by the master, or take the appropriate action requested by the master. The master device can send a request to an individual slave, or a broadcast message can be sent to all slave devices. The slave device cannot respond to a broadcast message.

2.5.5 Distributed Networking Protocol 3 (DNP3)

The Distributed Networking Protocol (DNP) was proposed by GE Harris in 1990 (DNP3, 2011). In 1993, the “DNP 3.0 Basic 4” specification document was publically released and was intended specifically to be used in electric utilities for control system applications. DNP3 defines communications between the client station, Remote Terminal Unit (RTU) and other IEDs. The DNP3 is an open protocol that is intelligent, robust and modern for use with SCADA systems. One of the functions of DNP3 is the handling of different data types. To reduce the rate at which errors occur, the message is apportioned into data frames, and data requests are dealt with in accordance with the priority afforded it. DNP 3 can respond to peer-to-peer requests and to the transfer of files (Bhattacharyya, 2008).

2.5.5.1 Distributed networking protocol in SCADA communications

DNP3 supports client/server type of architecture, and the client is known as the master and the server is known as the outstation. An example of a master might be a Human Machine Interface (HMI) or real-time server. An example of an outstation includes a Programmable Logic Controller, RTU, IED or a controller communicating with actuators, sensors and other instrumentation devices. DNP3 is used in different SCADA system communications that incorporate the SCADA Human Machine Interface (HMI) or master, IEDs, and RTUs, (DNP3, 2011).

Figure 2.10 shows an overview of the DNP3 protocol (Bhattacharyya, 2008).

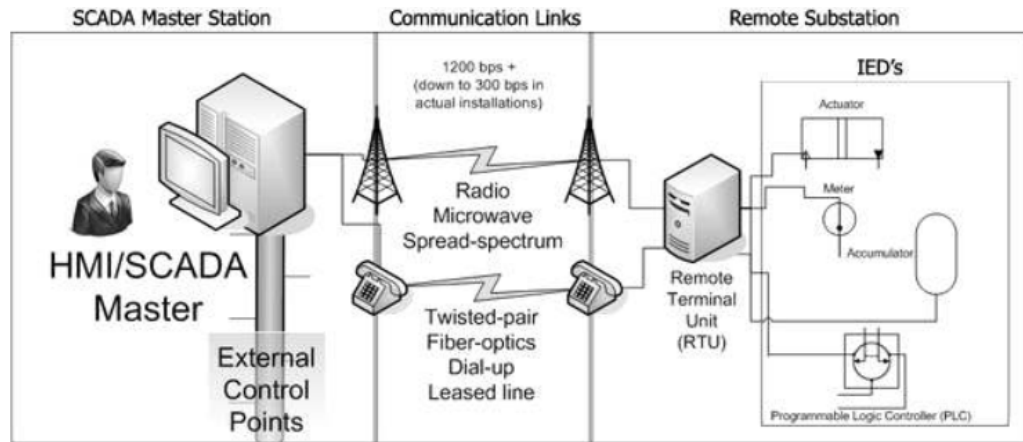


Figure 2.10: Overview of DNP3 protocol (Bhattacharyya, 2008)

2.5.5.2 Advantages of using DNP3 protocol

DNP3 was initially proposed for SCADA system applications, and was not deemed to be as useful as those on the Internet for the transmission of emails, SQL queries, hypertext and multimedia (DNP3, 2011).

The advantages of DNP3 as presented by (Bhattacharyya, 2008), are as follows:

- It is an open protocol, allowing end users to use a common protocol across many hardware platforms.
- It is improved for SCADA communications
- It gives interoperability between different vendor's equipment
- It is supported by a substantial number of SCADA equipment manufacturers
- It will give immediate and long-term benefits to users.

2.5.6 IEC-870-5-101 protocol

The IEC 870-5-101 protocol is regarded as the European counterpart of the DNP3 protocol. It is different from DNP3 and has a slightly different structure to the message and is also able to request object information from an IED. IEC 870-5-101 is mostly applied with slower transmissions on an asynchronous V.24 interface. Baud rates of up to 9600 bit/s are allowed, but baud rates higher than 115200 bit/s are used in reality (Cen and Fang, 2007).

2.5.7 IEC 61850 Protocol and IEC61850-90-5 standard-based power system protection scheme using synchrophasor technology

The IEC 61850 standard was proposed by the International Electrotechnical Commission (IEC) for communications within substations specifically between devices from different vendors. There are three levels within the topology typically referred to: process level (for the I/O devices, sensors and actuators); bay/unit level (protection and control IEDs); and the control center level (control center computer) (see Figure 2.11). Edition 1 of the IEC 61850 standard does not address the exchange of protection-type data between bay level and remote protection. The standard also does not include the exchange of control-type data between the substation and the control center. This standard is however widely accepted for the communication developments within the modern substation automation systems.

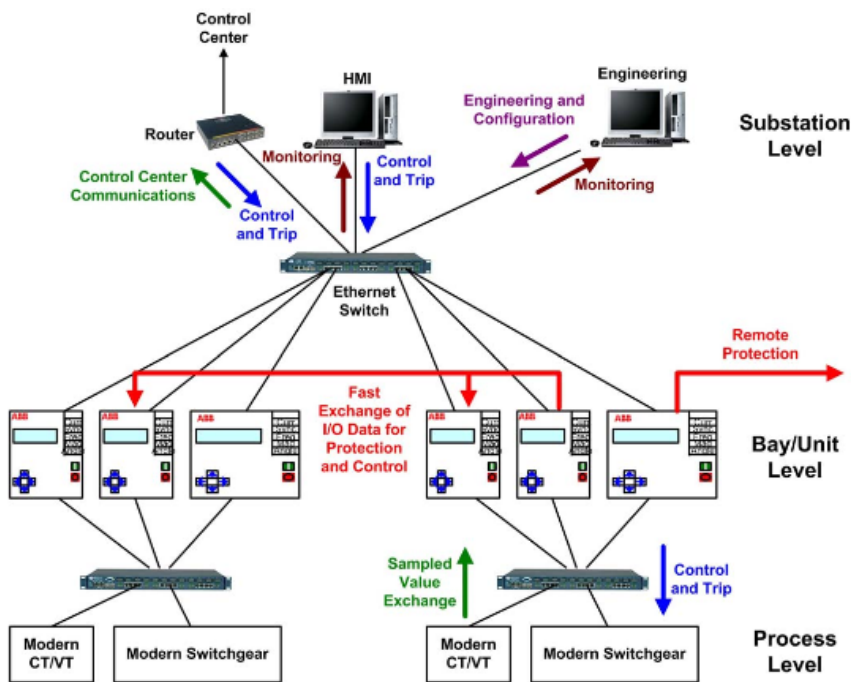


Figure 2.11: Substation automation topology based on IEC 61850 (Mohagheghi et al., 2009)

The IEC61850 standard supports the standard seven-layer Open Systems Interconnection (OSI) model. The data services and applications related to the power system substation are built at the application layer of the OSI model. Figure 2.12a (Sidhu and Gangadharan, 2005) shows the mapping structure for IEC 61850, which specifies the seven layers on the OSI model.

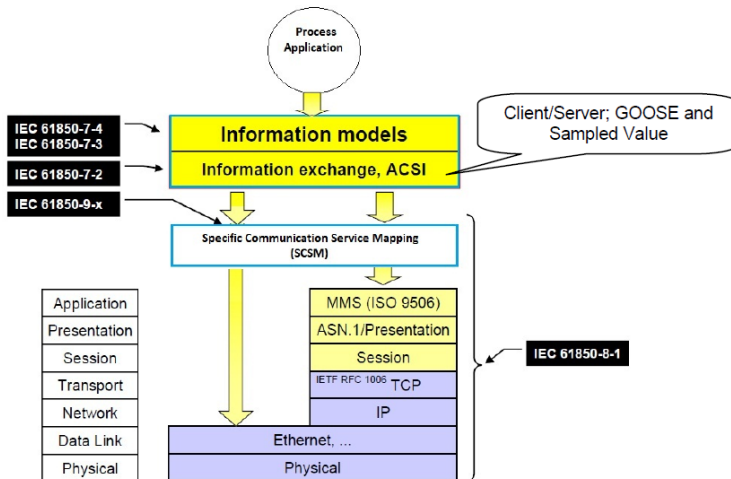


Figure 2.12a: Mapping of IEC61850 specific layer to OSI Model (Sidhu and Gangadharan, 2005)

The IEC 61850 standard, allows for interoperability between IEDs from different vendors. Power system utilities sometimes require IED interchange-ability, where a device supplied by one vendor can be replaced with a device supplied by another vendor, without changing any other elements in the system (Apostolov and Muschlitz, 2003).

The main features of the IEC 61850 standard presented by (Sidhu and Gangadharan, 2005) include:

- Data Modelling - Object oriented platform-independent modelling of all the functions.
- Fast Transfer of Events and Messages- Generic Object Oriented Substation Event (GOOSE) messages and Generic Substation Status Event (GSSE) messages for peer-to-peer communications.
- Setting Groups - Control blocks allow the user to switch from any active group of setting values to another.
- Sampled Value - Transfer of sampled values from the modern switchgear and nonconventional CT/VTs (Current and Voltage Transformers) to the IEDs
- Data Storage and Representation - Configured data of the substation is stored in the XML format using the Substation Configuration Language (SCL).

The IEC 61850-90-5 is a Technical Report covering transmission of digital and time-synchronized power data over WANs, which require the application of Wide Area

Measurement, Protection and Control (WAMPAC) systems that also support GOOSE and SV messages. Figure 2.12b shows an overview of the IEC 61850-90-5 Technical Report.

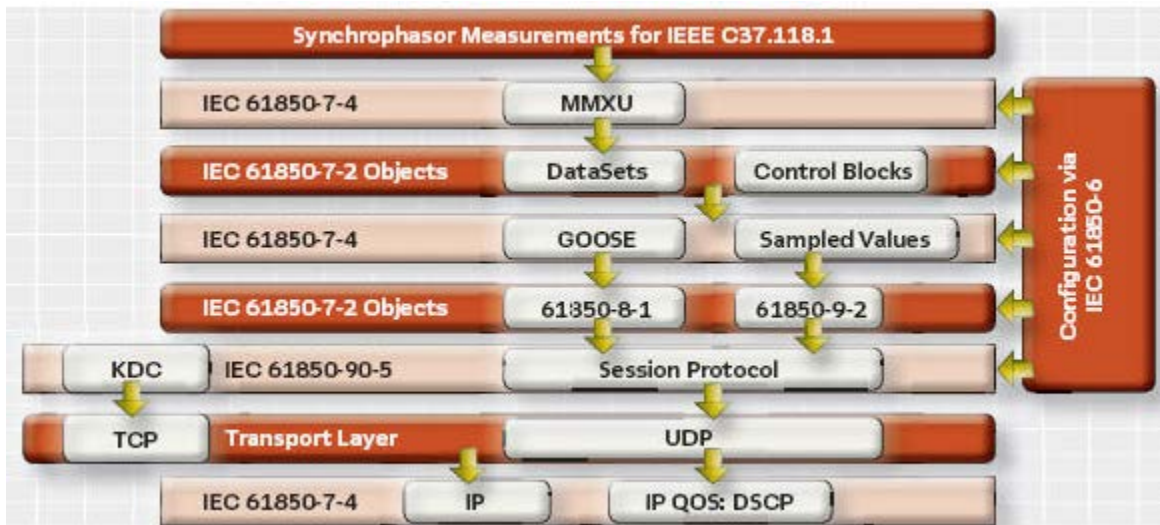


Figure 2.12b: Overview of IEC TR 61850-90-5 (Madani et al., 2013)

The requirements of the IEC TR 61850-90-5 protocol are shown below (PAC world Magazine, 2013):

- The functional performance requirements for the GOOSE message were changed from the initial 4 mS to 3 mS with the release of IEC 61850-5 in 2003.
- The introduction of SV messages, for sampled voltage and current measurements from the CTs and VTs to be distributed to multiple IEDs.
- Security standard development for IEC 61850, covering GOOSE and SVs completed in 2007.
- Substation-to-substation and substation-to-control center communications initiated in 2005, however the GOOSE messages were still not routable.

2.5.8 IEEE standards

The IEEE has proposed several standards relating to power system communications, including the C37.1, 1547, 1379, and 164 standards. These standards are described in the following sections.

2.5.8.1 IEEE C37.1 standard

The IEEE C37.1 standard (McClung and Hill, 2010) defines the practical requirements, application and performance analysis for SCADA and automation systems. It characterizes the architecture of the systems and capacities in a substation including which protocol to select, HMI and implementation requirements. This standard also defines the requirements to ensure viability, security, dependability, availability, expandability and changeability of the network performance (Wang et al., 2011).

2.5.8.2 IEEE 1379 standard

The IEEE 1379 standard (IEEE Power Engineering, 2004) prescribes implementation rules and requirements to ensure IED and RTU communications and interoperability of these devices. This standard defines the mapping of the communication protocol for devices sharing information from within the substation environment to DNP3 and IEC 60870-5 compliant devices. To enhance the functions that are supported by the network, certain processes are discussed to extend the data elements and objects used.

2.5.8.3 IEEE 1547 standard

The IEEE 1547 standard defines the interconnection of distributed resources within the electric power system. It comprises of three sections: the electric power system (McClung and Hill, 2010), the information exchange (IEEE Guide Monitoring, 2007), and the compliance test (IEE Standard P1547.4, 2011). The power system section, defines the prerequisites for interconnection and requirements for power conversion from various technological platforms. Issues such as power quality, different irregular power system situations, and the forming of subsystem islands are addressed. The information exchange section details the prerequisites for monitoring and control of the power system using the data networks. Different network situations and architectures are described, which include interoperation of devices, execution and how to extend their functionality. Security and various protocols are discussed in this portion of the standard. The conformance test section describes the methodology for checking compliance when interconnecting different systems. The standard discusses the testing methodology to guarantee that systems perform as expected due to the complex nature of the power system and its functions and components in general (Wang et al., 2011).

2.5.8.4 IEEE 1646 standard

The IEEE 1646 standard (IEEE Committee, 1998) defines the temporal behaviour for the on communication system inside and outside of the substation. Due to the various types of communications, the standard groups, classifies and characterizes the communication delay requirements for each classification. This ensures that the time for the processing of network packets is considered in the communication delay and that combining of the time for processing and transmission does not exceed the defined system delay. The standard also discusses the requirements of the communication system to transfer real-time data timeously, data prioritisation, together with the system interfacing (Wang et al., 2011).

2.5.9 Discussion and a legacy comparison of the different protocols used in the power systems

Although the IEC 61850 and IEEE C37 standards are often regarded as more developed communication protocols, that support object-oriented modelling and communication interfaces, they are more than simply protocols as is traditionally known. These standards are much more versatile and extensible than traditional protocols, such as Modbus, DNP3 and IEC 60870-5-101/104. As an example, the IEC 61850 standard defines fast and dependable communication between IEDs in a substation environment where peer-to-peer communication for GSE is required. An example of a GSE service message is the Generic Object Oriented Substation Event (GOOSE) message. A detailed description and structure of the GOOSE message together with simulation and practical case studies, is described as a motivation for the development of IEC 61850-compliant hardware (Kriger et al., 2013).

IEC 61850 Sampled Values (SV) is used to evaluate the acquiring, merging, integration and distribution of the data between the various devices and components in a smart grid environment (Herbert, 2012).

To implement an IEEE C37.118-compliant system which is more suited for power system wide area monitoring, is more complex than for an IEC 61850, Modbus, DNP3 or IEC 60870-5 compliant system; hence the slower pace for adoption of these systems within industry.

Table 2.2 shows the functions performed by the IEEE C37.118 and IEC 61850 standards.

Table 2.1: Comparison between IEC 61850 and IEEE C37.118 (Herbert, 2012)

Function	IEEE C37.118	IEC 61850 (GOOSE and Sample Values)
Streaming protocol	Yes	Sampled Value message
Rate of measurement /reporting	10-60 sample/sec.	80-256 samples/cycle (4800-15360 sample/sec)
Natively routable using IP	Yes	Does not use bridged –routing
Application focus	Situational awareness	Control
Standard address security	No	Yes
Communication profile fully specified	No	Yes
Measurement specification for synchrophasors	Yes	No
Even driven capability	No	GOOSE messages
Protocol semantically driven	No	Yes
Standard configuration language	No	Yes

2.6 Power system communication network technologies

In a power system, different communication technologies are used to send the measured data from one end to the other end of the system. Which technologies are used depends on the requirements and the technology feasibility. The most commonly used technologies for power system communication are (Qiu, 2002) :

- Power Line Carrier Communication (PLCC);
- Radio and microwave communication;
- Fiber optic communication;
- Satellite communication.

2.6.1 Power Line Carrier Communication (PLCC)

PLCC media is used globally for the implementation of protection functions. This approach is used to utilize the existing power lines to transmit data. In 1922, a carrier frequency system was operated over high-tension lines with frequencies ranging from 15 to 500 kHz

for telemetry applications. In 1924, a transmitting and receiving communication signal system over three-phase power lines was developed. PLCC communication is used in either a broadband or a narrowband network. Narrowband networks have the capability of signal transmission ranging between 3 kHz to 148 kHz over the low voltage public and private grids (Qiu, 2002). Broadband networks provide two-way communication where the signals range from 1MHz to 34MHz. The advantages and disadvantages of the PLCC as presented in (Gunger, 2006) are given below.

Advantages of the PLCC

- Extensive Coverage: Due to the fact that there are already power lines installed almost anywhere, PLCC provides a broad coverage area.
- Cost Effective: This type of communication network can be established quickly and at a significantly lower cost as existing signal cables are the communication medium. This is regarded as one of the cheaper methods used to remotely monitor power usage.

Disadvantages of the PLCC

- Electromagnetic interference over power lines: This is a noisy environment for data communications as there is considerable electromagnetic noise and interference from devices such as electric motors, power supplies, lights and radio signals.
- Open circuit problem: Data communication using power lines is not preferred as data loss can be attributed to the open circuit between devices during a fault condition.
- High Attenuation: A loss in data over the power lines may occur due to distortion and a high signal attenuation, which would compromise data reliability when responding to an event.

2.6.2 Microwave and radio wireless communication systems

A Wireless communication system is used to transport the electromagnetic waves without using a physical layer (Behrouz, 2006). The Electromagnetic spectrum for use in wireless communication ranges between 3 kHz to 900 kHz. Wireless signals travel from the source to destination via ground, sky, or line-of-sight. The Electromagnetic spectrum is divided in to eight bands. The bands start from Very Low Frequency (VLF) to Extremely High Frequency (EHF). Table 2.1 shows the Electromagnetic Spectrum for wireless

communication system including the type of band and its range, propagation, and application area.

Table 2.2: Electromagnetic Spectrum for wireless communication system (Behrouz, 2006)

S.NO	BAND	RANGE	PROPAGATION	APPLICATIONS
1	Very Low Frequency (VLF)	3 -30 kHz	Ground	Long-rang radio
2	Low Frequency (LF)	3-300 kHz	Ground	A radio station that broadcasts a directional signal for navigational purposes
3	Medium Frequency (MF)	300 kHz-3 MHz	Sky	Amplitude Modulation Radio
4	High Frequency (HF)	3-30 MHz	Sky	Citizen Band (CB), ship/aircraft communication.
5	Very High Frequency (VHF)	30-30 MHz	Sky and line-of-sight	Very High Frequency TV, Frequency Modulation radio
6	Ultra High Frequency (UHF)	300 MHz-3 GHz	Line-of-sight	UHF TV, Cellular phones, paging, satellite.
7	Super High Frequency (SHF)	3-30 GHz	Line-of-sight	Satellite communications
8	Extremely High Frequency (EHF)	30-300 GHz	Line-of-sight	Radar-satellite

2.6.3 Radio waves

The radio wave frequencies range from 3 kHz to 1GHz. Antennas that transmit radio waves to be propagated in all directions are called omnidirectional (Behrouz, 2006). There is therefore not a requirement for the transmitting and receiving antennas to be aligned. Radio waves propagate through the air and are capable of travelling over long distances.

2.6.4 Microwaves

Microwave frequencies range from 1 to 300 GHz and are unidirectional. The transmitted microwave signal has a very narrowly polar pattern and this implies that for optimal signal transmission the antenna at both ends have to be aligned. Microwaves travel in space and any object in the path can obstruct communications. Microwaves are also known as Line-of-sight communication systems. Dish antennas mounted on high towers where signals

are transmitted to other dish antennae located in the line-of-sight is an example of microwave communications. The advantages and disadvantages of the microwave communication system are given below (Qiu, 2002).

Advantages of microwave communication systems:

- **Efficiency:** Microwave up to 299 GHz technologies are used to improve data communications for faster transfer of information from one end to the other end.
- **Rapid Installation:** Microwave networks are configured and installed rapidly in comparison to the wired network. It is cheaper and easier to install.
- **Cost:** The running cost for the maintenance of a microwave-based communication system is lower as there are no cabling costs associated with microwave technology as the operator and user of these systems can communicate while on the move.

Disadvantages of the microwave communication system:

- **Line-of-Sight:** Microwave communication system is a line-of-sight type of technology because signals cannot pass through objects such as mountains and buildings. This limitation requires a line-of-sight communication system between transmitting and receiving antenna.
- **Interference problem:** Electromagnetic Interference (EMI) affects microwave signals. EMI is defined to be anything that interferes with the communication and causes signal degradation, is an obstruction or causes an interruption in the communication of these signals.

2.6.5 Optical fiber communications

Optical fiber communications were introduced in the year 1960 (Behrouz, 2006). There are many advantages to using fiber-optic over copper-based communications systems. A fiber optic-based system is more suitable as the transmission medium for the power system control, protection and monitoring data. The properties of fiber-optic communications which make it attractive are low attenuation, high bandwidth, electromagnetic interference immunity and security. Fiber-optic communication systems that span longer distances require less repeaters compared to existing wireless networks. This leads to reduction in infrastructure costs for communication over longer distance for applications such as substation monitoring and control. Fiber optic cables are made up of

super-thin filaments of glass or plastic and it transmits signals in the form of light. As these communication media is optic-based, data can be transmitted and received at the speed of light. It uses a laser transmitter that encodes frequency signals into pulses of light, as 1's and 0's that are transmitted via the cable. At the receiving end, the light signals are translated back into data and they can be read by a computer. The advantages and disadvantages of the fiber optic communication system are given below (Qiu, 2002).

Advantages of the fiber-optic communications:

- High bandwidth and it is relatively easy to increase the bandwidth.
- Early detection of the cable damage guarantees secure transmission.
- High immunity to electromagnetic interference.
- No electromagnetic radiation and no crosstalk between the cables.

Disadvantages of the fiber optic communications:

- Installation cost is high.
- Need for more expensive optical transmitters and receivers.
- More difficult and expensive to splice than copper wires.

2.6.6 Satellite communications

Satellite communication is especially useful for remote control and monitoring of remote substations where telephone networks and other traditional communication methods cannot be implemented (Forouzan, 2012). Use is made of the Global Positioning System (GPS) for time synchronization with microsecond accuracy for applications such as substation automation. The advantages and disadvantages of the satellite communication systems are given below (Qiu, 2002).

Advantages of the Satellite communications:

- **Geographical Coverage:** Satellite communication is more cost-effective for applications and systems covering wider areas with longer distances for transmission of data.
- **Higher Bandwidth:** This type of communication supports the streaming of video information as it has a very large bandwidth.

Disadvantages of Satellite communications:

- Long Delay: The delay from transmission to acknowledgement of the reception of a message from a remote location is comparatively higher than is the case in a wired network.
- Satellite Channel Characteristics: Changes in climatic conditions degrade the performance and efficiency of the entire satellite system.

2.6.7 Discussion on the communication media

Wired technologies such as, Power Line Carrier Communication (PLCC), fiber-optical communications, and copper wires are used in existing Wide Area Networks (WANs). Among the wired technologies, PLCC could be a promising communication technology for Multi Agent Systems (MAS) communications. Due to the noisy environment and the low capacity of the narrow-band PLCC, its viability is questionable (Ghorbani et al., 2013).

In conclusion, PLCC and the fiber-optical communications (wired technology) cost more to implement for wide area applications, but the communication capacity, reliability and security capacity is increased. However, wireless systems are cheaper to install, but the bandwidth and security consider are limited .

2.7 Literature review on the communication architectures, protocols and media used in the power system applications

Power system communications require fast, real-time and broad data acquisition and transmission. The real-time data can be used for power system data acquisitions, control, protection, monitoring and optimisation. This section highlights some typical communication scenarios in power systems. Figure 2.13 shows the future communication system for power systems, (Qiu, 2002).

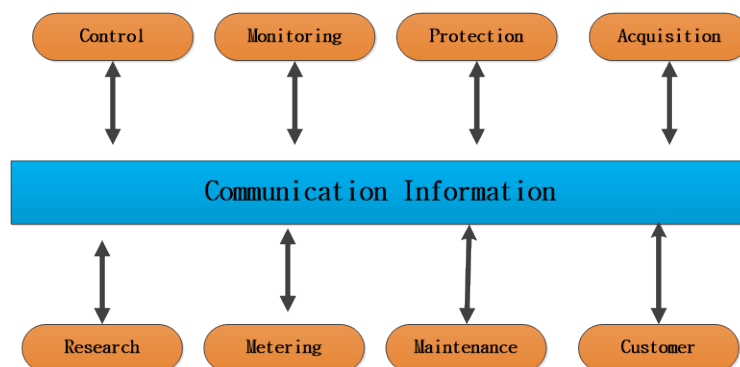


Figure 2.13 : Future communication system for power systems (Qiu, 2002)

2.7.1 Power system control

The electrical substation is an integral system within the power system. Here the voltages from the transmission lines are stepped down and the power flow within transmission is controlled. The substation is a very complex system consisting of transformers, circuit breakers, capacitors and voltage regulators. The data communication network technologies utilized here includes Ethernet and wireless LAN systems. The devices in a substation are interconnected with sensors on the primary plant equipment for their current status information. The data from the sensors are sampled, digitized and transmitted using the LAN to the control center. Figure 2.14 shows communication network in a substation (Wang et al., 2011).

The data communication network consists of various subnets connected using network switches. The data are continuously transmitted as network packets, at a rate that depends on the specific application. For example, when a network packet is received by the control station, a configuration message might be transmitted to the plant equipment. The communication bandwidth is shared by the various types of primary and secondary plant equipment that are monitored and controlled.

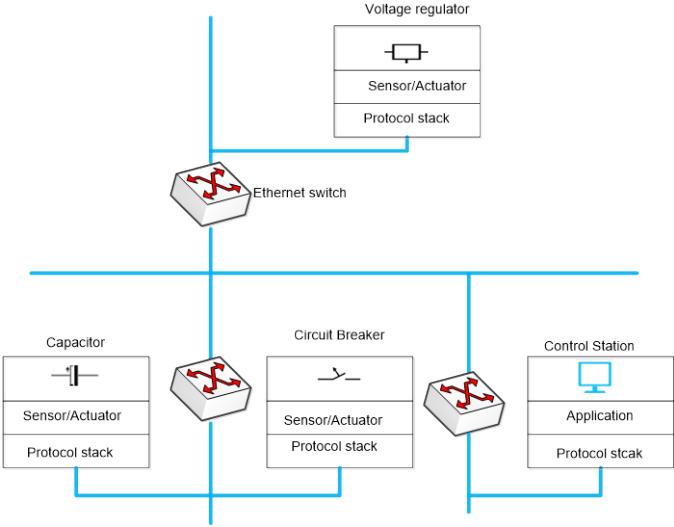


Figure 2.14 : Substation control communication network (Wang et al., 2011)

Aravinthan et al., 2011 investigate distribution feeder level communications, where there is a large number of distribution components connected. An example for this type of system application is a wireless communication network. Communications are prioritized where irregular events and control operations are assigned a higher priority, and asset management applications have a lower communication priority. The proposed communication network is shown in Figure 2.15 (Aravinthan et al., 2011).

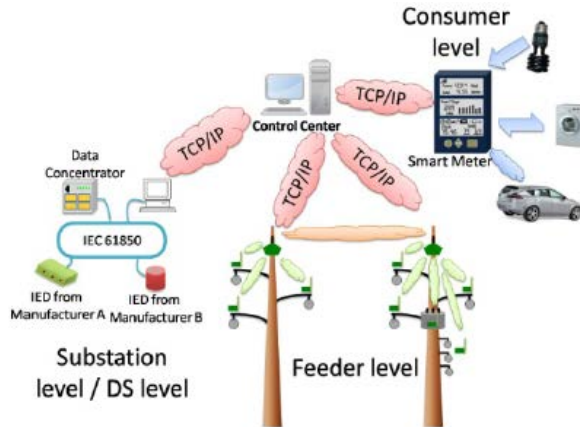


Figure 2.15: Communication Network for a Distribution System (Aravinthan et al., 2011)

The communication structure of the wide-area control system described in (Xiaoyang et al., 2005) is shown in Figure 2.16, where 10 Mbps or 100 Mbps Ethernet are used in the power system and substation environment, The Regional Control Center (RCC), and the System Control Center (SCC). These LANs are interconnected to the Internet Protocol using the Wave Division Multiplexing (WDM) and a backbone network via a 1 Gbps Ethernet bridge. The Energy Management of SCC and the Distribution Management System of RCC are connected via the IP addressing mechanism on the WDM network.

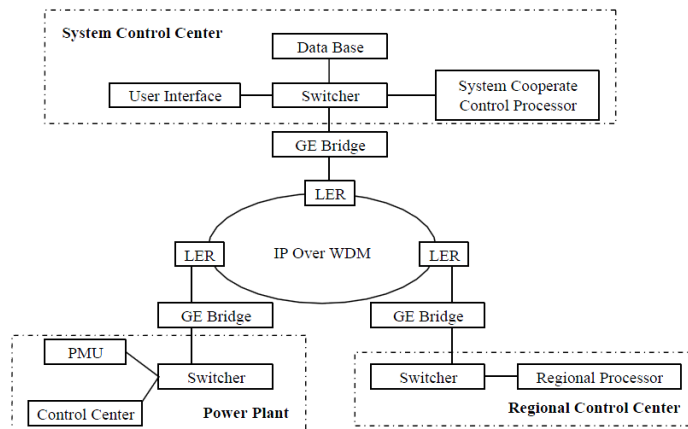


Figure 2.16: The communication structure of wide-area control (Xiaoyang et al., 2005)

The substation control communication network allows for network delays of up to 1s. When the message conveys real-time control data, the network delay is 10ms. In the case where the messages carry fault information from the equipment, the delivery time to the control station is typically 3ms.

2.7.2 Power system monitoring

Electricity is transmitted and distributed from the power generation plants to end-users via transmission lines. These transmission lines stretch over long distances through sparsely populated areas, yet it is imperative that any fault conditions be detected and corrected to guarantee power quality and service. Sensors are typically installed along the transmission lines to gather real-time data measurements. These sensors exchange data using wireless communication in real-time to the control center.

(Moghe et al., 2009) described faults in underground distribution systems. The information acquired by IEDs is stored at regular intervals on a computer located within the substation; the data is downloaded afterwards to a local database over a secure communication network. The communication architecture for the underground distribution feeder fault identification is shown in Figure 2.17 (Moghe et al., 2009).

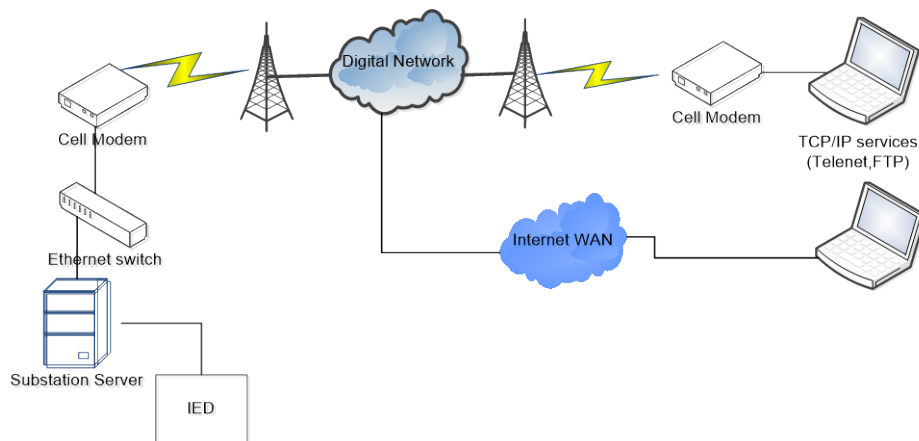


Figure 2.17: Communication architecture for the underground distribution feeder fault identification (Moghe et al., 2009)

The authors (Louie et al, 2006) present an analysis of the marketing and the technical aspects of the Power Line Carrier Communication (PLCC) developments and applications.

(Zhang and Li, 2009) developed an Internet-based system for monitoring of the power quality using ASP.NET technology as shown in Figure 2.18. This low-cost power quality monitoring solution uses the Internet for interactive diagnostics and supports remote monitoring and analysis of the power quality over a globally-wide area network.

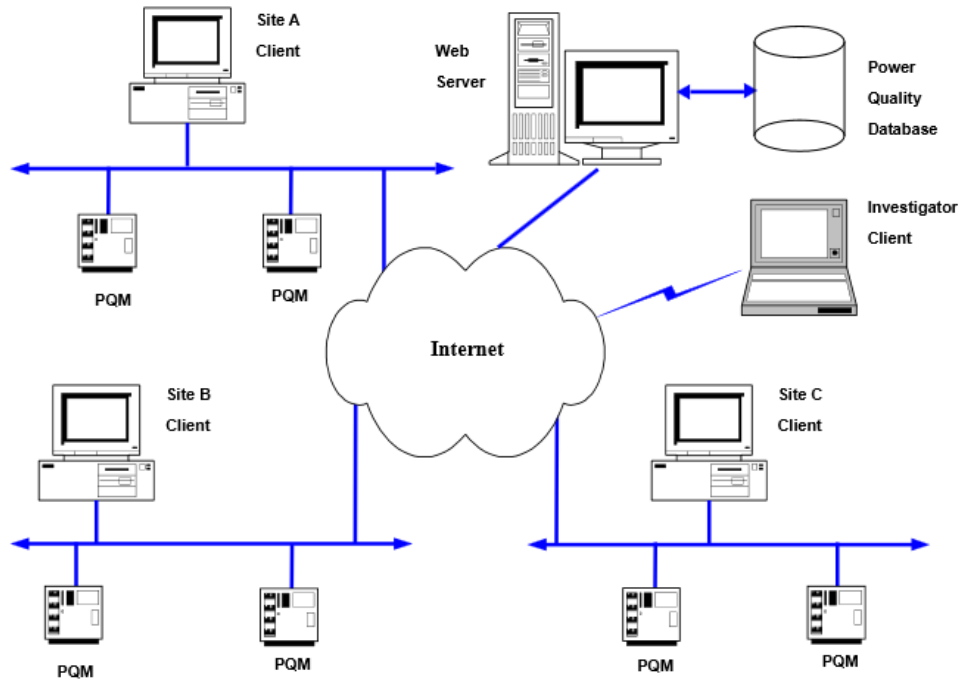


Figure 2.18: Internet -Based Power Quality Monitoring System (Zhang and Li, 2009)

2.7.3 Power system metering

The power metering system consists of the display measurements such as voltages and power consumption with the required accuracy for in-plant metering. There is no longer a requirement for individual meters, thus the costs are significantly lowered and the wiring is reduced. The applications for power system metering are presented by (Duncan and Bailey, 2003):

- Information for commissioning and testing are available;
- Profiles of the load data may be displayed;
- A status of the energy consumption that is allocated for different applications;
- Real-time display of all measurements.

Nowadays a two-way flow of information between the electricity producers and consumers is used. The biggest smart metering communication system would hoop up tens of millions of smart meters through various communication protocols to collect meter data and control communication flow. The acquired data is fed into a Meter Data Management System (MDMS), which serves as a foundation to create common services; including demand response management, remote meter reading, and linkage with the Home

Energy Management Systems (HEMS). Figure 2.19 shows a smart metering communication system (Toshiba Smart Meter, Manual, 2014).

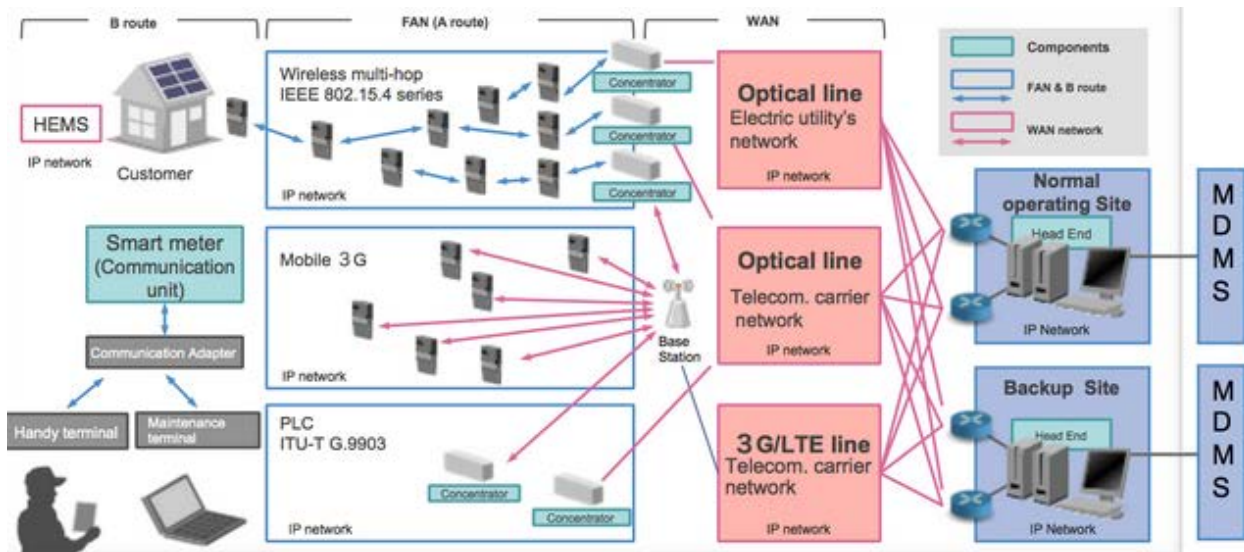


Figure 2.19: Smart metering communication systems (Toshiba Smart Meter, Manual, 2014)

2.7.4 Communication system for the smart grid

The power generation plant information is distributed to the regional control centers, and operators. When a generation event occurs or when there is a generator failure, a rapid response is required by the system operators.

The transmission system is also monitored by the system operators within the control center. It is an advantage if both generation and transmission systems support a Wide Area Situation Awareness (WASA) system together with an advanced Energy Management System (EMS).

As the trend is now towards more renewable and “environmentally friendly” sources of energy, application such as plug-in electric vehicles and other distributed energy resources could be supported in a Distribution Automation System (DAS) using a Distribution Management System (DMS). Figure 2.20 illustrates the Smart grid framework (Parikh et al., 2010).

Some of challenges in the implementation of a smart grid communication system include:

The system integration of equipment from different vendors that exchange information in a multi-disciplinary environment with multiple protocols.

The identification of relevant communication media and system architecture for the smart grid implementation.

The security of the information to maintain data integrity across the entire smart grid system.

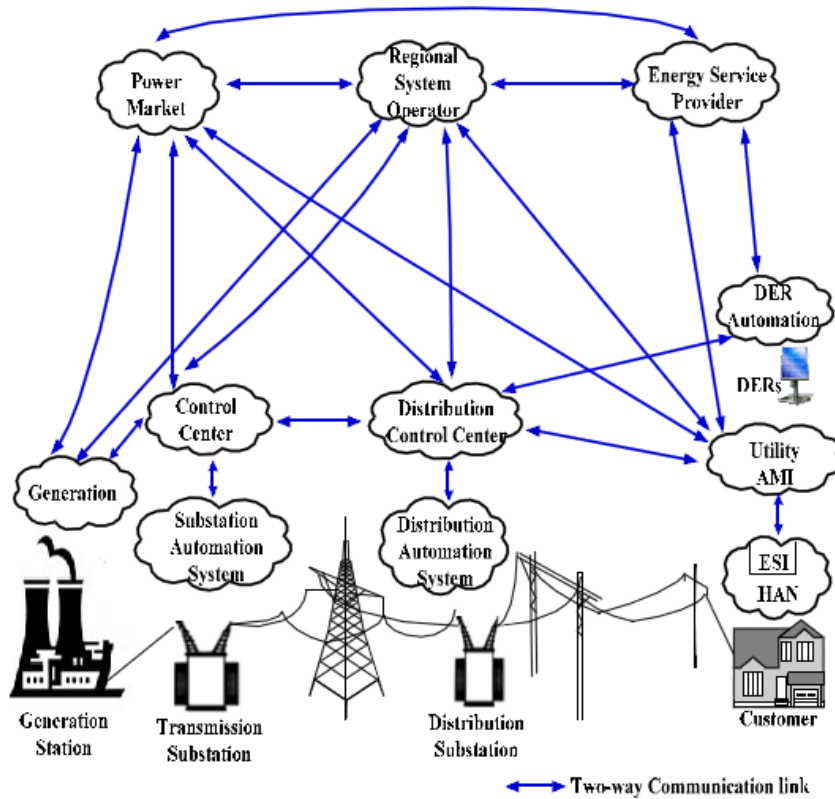


Figure 2.20 : Smart grid framework (Parikh et al., 2010)

Table 2.3 shows the wireless technology coverage and applications in power systems.

Table 2.3: Approximate coverage of wireless technology in smart grid applications

Wireless Technology	Approximate coverage	Potential Smart Grid Applications
Wireless LAN	100m	Distribution protection and automation
WiMAX	48Km	Wireless Automatic Meter Reading (WMAR)
Cellular	10-50km	SCADA and monitoring for remote distribution
ZigBee	10-100m	Direct load control of home appliances
MobileFi	Vehicular	Communication for Plug-in Electric

	Standard	Vehicles(PEVs) and remote monitoring
Digital Microwave	60 km	Transfer trip (point-to-point) communication
Bluetooth	1-100m	Local online monitoring applications

Table 2.4 shows the architecture, the protocols and the communication media used in the power system applications.

From Table 2.4, it is observed that most of the literature review considered in this chapter is focused on power system monitoring, control, and uses the communication architectures WAN or HAN, the protocols IEC61850, TCP/IP, and IEEE 802.11 and the wireless communication media.

2.8 Review on the application of the DAQ cards, and synchrophasors for local or remote real-time simulation, monitoring, and control using LabVIEW, MATLAB and RTDS software environments

This section provides a review on the application of the DAQ cards and synchrophasors used for real-time monitoring and control using LabVIEW, MATLAB, and RTDS software environment.

2.8.1 Review on the application of the DAQ cards for local or remote real-time simulation, monitoring, and control using LabVIEW and MATLAB software environments

A modular approach towards a communication system structure would show that it comprises of blocks which take input from the preceding blocks, process the signals and send their output for further processing (Kramer, 2005). These blocks could be code modulators, channel filters, detectors, or decoders. If these different blocks could be modelled separately and somehow combined to represent a complete communication system, then the communication system could be completely simulated.

Table 2.4: Review on the architecture, the protocols and the communication media used in power system applications

Author and year	Aim of the paper	Communication Architecture	Communication Protocol	Communication Media	Field of applications
(Moghe et al., 2009)	Field Investigation and Analysis of Incipient Faults Leading to a Catastrophic Failure in an Underground Distribution Feeder	Wide Area Network(WAN)	IEEE 802.11	Wireless	Electrical -Power distributions systems monitoring
(Russell et al., 2009)	Reliability Improvement of Distribution Feeders through Real-Time, Intelligent Monitoring	Wide Area Network(WAN)	IEEE 802.11	3G cellular	Electrical-Substation Feeder monitoring
(Xiaoyang et al., 2005)	The Analysis of Communication Architecture and Control Mode of Wide Area Power Systems Control	Wide Area Network(WAN)	TCP/IP	Optical Network	Wide Area Power Systems Control
(Hyun and Lee, 2008)	Compound communication network over the high voltage power line for Distribution Automation System	Home Area Network(HAN) and Wide Area Network(WAN)	Master and Slave	Power Line Carrier Communication	Distribution Automation System monitoring
(Adebisi et al., 2011)	Narrowband Power Line Carrier Communication (PLCCC) for Smart Grid Applications	Wide area network	IPV4 and IPV6	Power Line Carrier Communication	Smart grid
(Shwehdi & Khan, 1996)	Power line data communication interface using spectrum technology in home automation	Home Area Network	Master and Slave	Power Line Carrier Communication and spectrum technology	Smart house control
(Aravinthan et al., 2011)	Wireless Communication for Smart Grid Applications at Distribution Level	Wide Area Network(WAN)	Substation protocol (IEC 61850)	Wireless technology	Smart grid control
(Mak & Holland, 2002)	Electrical power network SCADA systems	Home Area Network	TCP/IP	Wireless-PABX (private automatic	Electrical power

	using TCP/IP and Ethernet networking			branch exchange)	network monitoring
(Bauer et al., 2009)	Packet-Oriented Communication Protocols for Smart Grid Services over Low-Speed PLC	Home Area Network	Master and Slave	Power Line Carrier	Smart Grid control
(Huertas et al., 2010)	Wireless Data Transmission from Inside Electromagnetic Fields	Home Area Network	TCP/IP	Wireless	Power system Electromagnetic Fields monitoring
(Jiang, 2008)	Distribution Power Automation Communication Systems Based On Mobitex Technology	Wide Area Network	TCP/IP	Mobitex-wireless	Distribution Power Automation Systems control
(Lin et al., 2011)	Power System and Communication Network Co-Simulation for Smart Grid Applications	Wide Area Network	TCP/IP	Wireless (Interent)	Smart Grid Applications
(Mak and Radford, 1996)	Implementation of a large scale demand side management and distribution automation	Home Area Network	File Transfer Protocol	Cellular- wireless	Large scale demand side management and distribution automation
(Zhang and Li, 2009)	Power Quality Monitoring System over the Internet	Wide Area Network	TCP/IP	Wireless-Internet	Power quality monitoring in the Control center
(Rodrigues et al., 2004)	Web-based monitoring & control system in plastic rotational modelling machine	Wide Area Network	HTTP	Wireless-Internet	Plastic rotational modelling machine monitoring and control
(Bucci et al., 2005)	A Low Cost Embedded Web Services for Measurements on Power System	Wide Area Network	SOAP	Wireless-Internet	Power system monitoring
(Branch & Bradley, 2006)	Real-time web-based system monitoring	Wide Area Network	TCP IP,MODEBUS	Wireless-Internet	Power system monitoring

In a simulation-based approach, a computer is used to acquire data or simulate waveforms that flow through the model of the communication system, involving generating of sampled values of the signal and noise processing. These sampled values are processed through the discrete time models of the function blocks in the model of the communication system.

Digital simulation can provide useful and effective analytical performance evaluation or direct hardware evaluation of the communication system. It is a computationally demanding task due to the large number of repetitive signal processing operations that must be performed in order to obtain statistically valid measurements of the system performance. Various computer languages have been used in the past such as Simula, FORTRAN, PASCAL, and C to simulate the communication systems. Due to the technological advancement today, LabVIEW and MATLAB software allow such analysis and simulation.

The data acquired from the primary plant equipment are generally analog that is converted into digital data that is processed, transmitted, displayed and stored. Typically these systems use sensors to acquire the signals that are amplified or attenuated to the appropriate voltage levels.

Generally, in the papers that were reviewed, the DAQ cards are used with two types of software environments: LabVIEW and MATLAB. The first one is used more for industrial applications; the second one is used more for development and research work in research organizations and at universities. The review is done first for LabVIEW and then for MATLAB applications.

Laboratory Virtual Instrument Workbench (LabVIEW) is a software programming development language. Programming languages such as C are text-based, but LabVIEW is a graphical programming language (Kramer, 2005) developing algorithms in a block diagram form.

(Rasmussen and Yang, 2008) developed the Electrical Capacitance Tomography System (ECT) that measures the capacitor signal using a NI USB DAQ device where six signals are displayed on a laptop. The ECT hardware system contains six channels of the capacitor charge and discharge measurement by a circuit placed on a printed circuit board (PCB). The channels are labelled from A to F on the PCB as shown in Figure 2.21. The

six channels operate in parallel. They are configured by the PC via the NI USB-6008 DAQ card using the LabVIEW software environment. The DAQ card has a resolution of 12 bits and its inputs and outputs work with a signal range of $\pm 10V$.

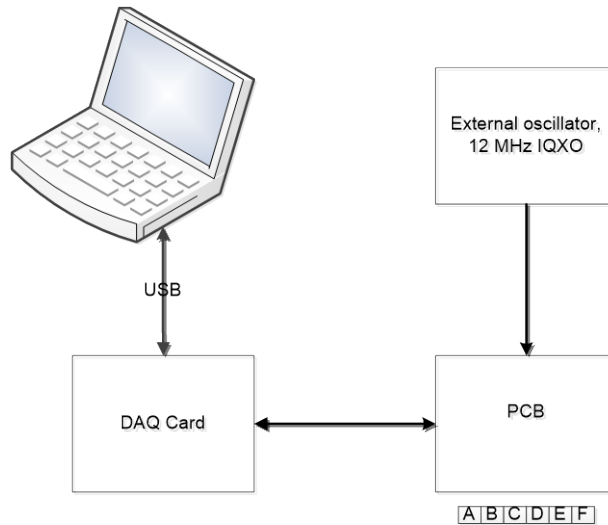


Figure 2.21: Electrical capacitance tomography DAQ system (Rasmussen and Yang, 2008)

(Nishikido et al., 2013) proposed a real-time monitoring distribution system for IVR (Interventional radiology). The system has three X-ray detectors. They consist of square shape plastic scintillators, optical fiber, and photo detectors. Each photodiode output independently is fed to a current/voltage conversion amplifier. The output voltages are measured using the NI USB DAQ 6351 card and are displayed in real-time by the LabVIEW software. The 6351 DAQ card supports 16 analog input channels with, 16-bit resolution and a channel range of $\pm 10V$.

(Cirstea et al., 2012) describes a system design known as the Inductive Current Measurement System (ICMS), where use is made of the P2110 radio frequency energy harvesting hardware platform. The current is read from the output of the hardware platform when a load is connected to the power system. The outputs of both transducers are sent to passive filters and are input to the AD8230 rail-to-rail instrumentation. The output of the AD8230 is passed to the analog input of the National Instruments USB 6251 data acquisition card. In the LabVIEW environment, the software program reads the current value. Figure 2.22 shows block diagram of ICMS system measuring setup (Cirstea et al., 2012).

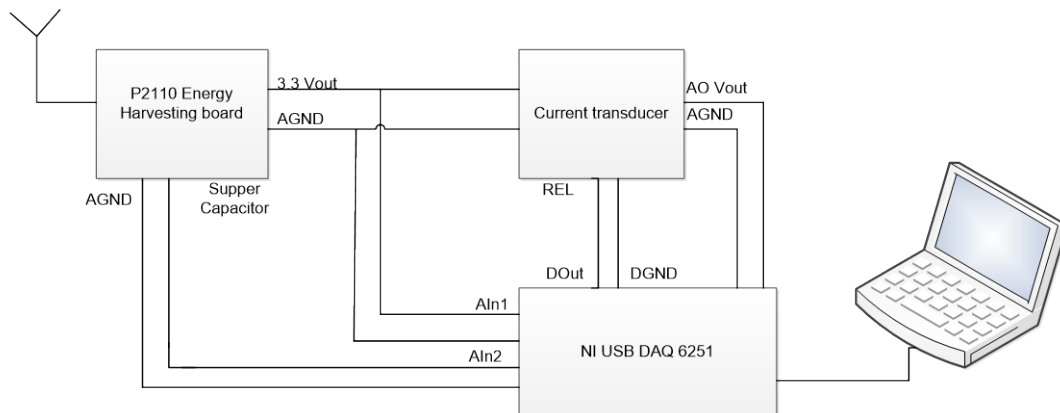


Figure 2.22 : ICMS Measuring Setup (Cirstea et al., 2012)

An Intelligent house lightning control system using a ZigBee wireless network and the NIUSB DAQ-6009 card is developed by (Huang et al., 2014). The control system developed using LabVIEW can decide if the blinds need to be opened or closed according to the brightness of the indoors/outdoors. The controller was constructed using the auxiliary LabVIEW Fuzzy logic Toolbox. The Fuzzy logic method is used to design the operations of the controllers and as such, they are different from the conventional types. The illumination intensities for both indoor and outdoor use is obtained from the system interface developed using the LabVIEW programming software. Figure 2.23 shows the flow diagram of the brightness adjusting system (Huang et al., 2014).

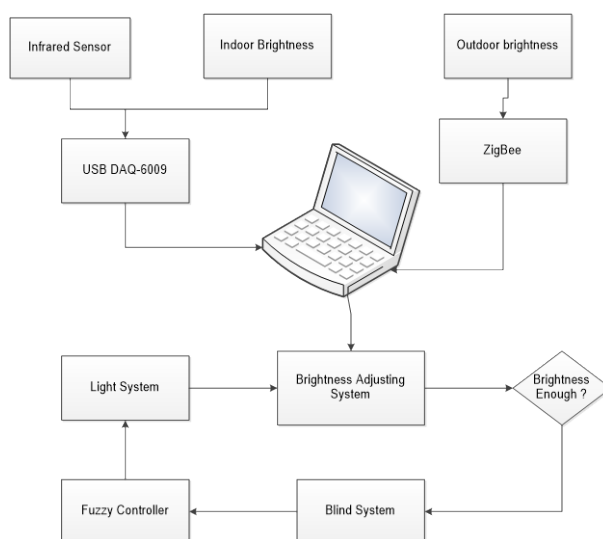


Figure 2.23 : Flow diagram of the brightness adjusting system (Huang et al., 2014).

(Hasim et al., 2012) developed a water bath temperature control system, using the MATLAB fuzzy logic toolbox. The input to the system is taken from the thermal transducer to the Fuzzy Logic Controller (FLC) that is the controller for the water temperature. The NI USB DAQ card is used to together with the MATLAB software for the real-time application.

(Chen and Shen, 2012) describe a remote monitoring system of a multi-point temperature plant based on the Client/Server (C/S) network developed using LabVIEW software. This system uses the integrated temperature sensors SMT16030 and a data acquisition (DAQ) card NI USB-6251. The card provides two 32-bit counters and $\pm 5V$ DC voltage source. The SMT16030 temperature sensor, the USB-6251 and two multiplexers on the server-side are used to acquire the positive and the negative pulse widths of Pulse Width Modulation (PWM) waves from the multiple sensors outputs. These signals are transmitted to the client through the LAN. Figure 2.24 shows the multi-point remote temperature monitoring system (Chen and Shen, 2012).

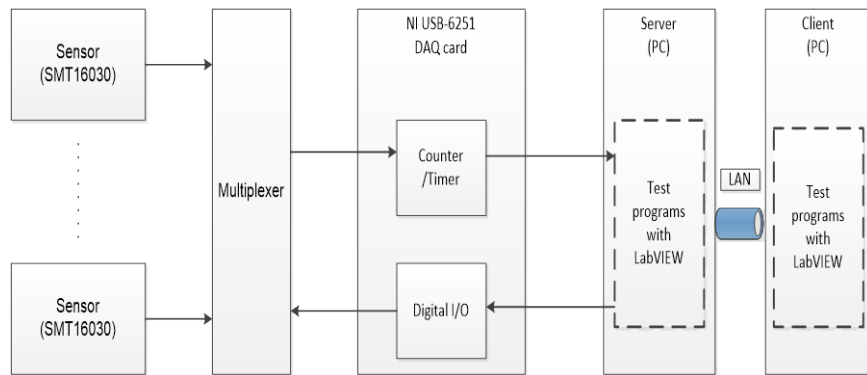


Figure 2.24: Multi-point temperature remote monitoring system (Chen and Shen, 2012)

(Jung et al., 2011) designed a measurement system for Ultra Wide Band (UWB) RF sensor integrated circuit. This system detects UWB radar waveform pulse and processes the waveform with an algorithm to convert it to a baseband signal. The NI DAQ collects the baseband signal from the RF chip and saves the collected signal to a file. MATLAB software is used to save and generates the resulting waveforms. Figure 2.25 shows the block diagram of system.

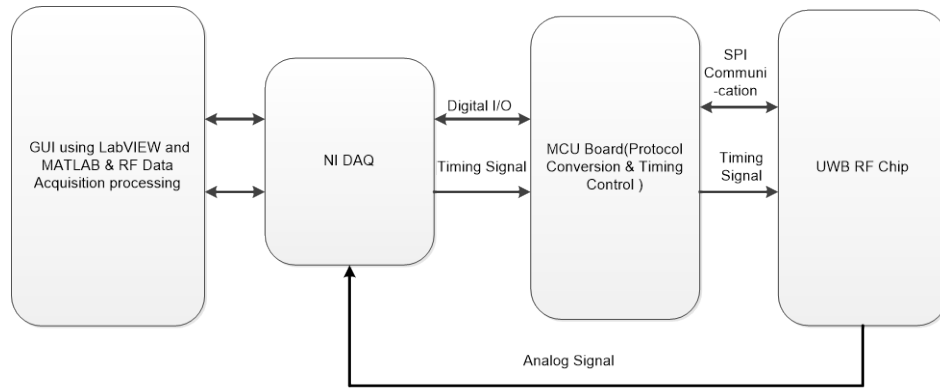


Figure 2.25: Measurement system for Ultra Wide Band (UWB) RF sensor (Jung et al., 2011)

(Lee et al., 2013) describes a Rapid Control Prototyping (RCP) system based on MATLAB/Simulink and a DAQ (Data Acquisition) unit. The block diagram of the RCP is shown in Figure 2.26.

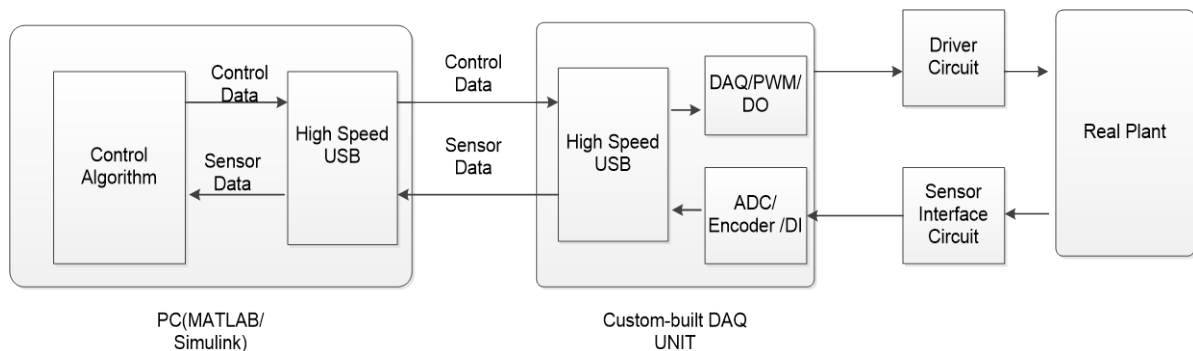


Figure 2.26: Rapid Control Prototype System (Lee et al., 2013)

The RCP system consists of two subsystems. In the first subsystem, a PC-based MATLAB/Simulink model of the control is running using data received from the real plant. In the second subsystem, the controller designed in MATLAB/Simulink is converted to C-code using an automated code generator. It is compiled, and then downloaded to an embedded control hardware platform.

(Afdideh et al., 2012) describes a MATLAB GUI based Brain Computer Interface (BCI) system. The system uses two networked computers; - the one computer to acquire and process the electroencephalographic (EEG) signal, and the other for the processing of the

virtual reality environment. Both computers are connected using the TCP/IP protocol. Figure 2.27 shows the proposed BCI system.

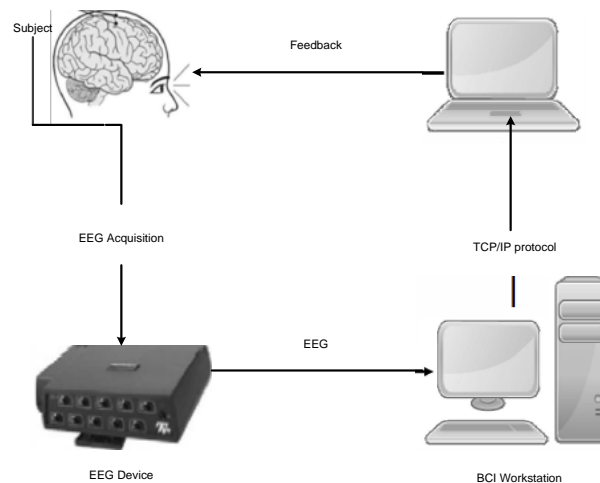


Figure 2.27: BCI system (Afdideh et al., 2012)

2.8.1.1 Discussion on the NI DAQ card used in the real-time monitoring and control using LabVIEW and MATLAB software environments

MATLAB is basically a scripted language, while LabVIEW is a graphical programming environment. LabVIEW uses a data-driven programming paradigm where code is executed in a parallel manner, whereas MATLAB uses a more traditional "sequential" type of programming paradigm, where each line of code is executed sequentially. However, both programming environments enable one to interface to hardware devices and provide the necessary analytical tools for the analysis of data. Selecting either LabVIEW or MATLAB for real-time monitoring and control of the power system depends on the application. If a MATLAB algorithm is needed in the loop in an automated way, then the MATLAB Instrument Control Toolbox (ICT) is used to control the instrument programmatically. MATLAB software is used to connect one or more instruments, capture data, transfer the captured data into MATLAB environment and perform some analysis on the data. The Real-time Target data acquisition toolbox in MATLAB and Simulink environment support DAQ functions from the physical devices. MATLAB is not as good as LabVIEW for control of instruments or user interface. LabVIEW handles multitasking easier compared to MATLAB and also supports real-time applications.

2.8.2 Power System applications using a Real-Time Digital Simulator

The Real-Time Digital Simulator (RTDS) allows accurate and reliable simulations of three-phase electromagnetic and electromechanical transient phenomenon in electric networks both for closed loop equipment testing and offline simulation studies. The RTDS works in continuous real-time to provide solutions to power system equations fast enough, with a typical time step of 50 μ secs to accurately represent conditions in the actual power system. The real-time features facilitate interfacing of physical devices such as controllers and protective relays to the simulator and operate it under 'real life' conditions.

(Brandt et al, 1991) developed the first Hardware-In- the- Loop (HIL) system between the Real Time Digital Simulator (RTDS) and a Joint Var Controller (JVC). The system is installed at the Hydro Dorsey Converter station in Manitoba. The RTDS model simulates a portion of the Nelson River High Voltage Direct Current (HVDC) system with emphasis placed on the inverter station's Alternating Current (AC) system. The JVC monitors the reactive power supplied by the simulated models representing synchronous condensers. The JVCs main function is to ensure the reactive load is shared equally amongst the different machines. Figure 2.28 shows the setup used in JVC system (Brandt et al, 1991).

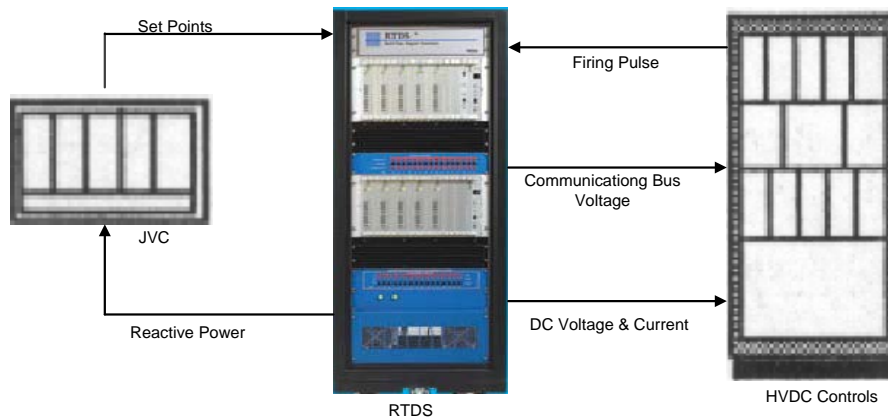


Figure 2.28: Interface JVC Study (Brandt et al, 1991)

The input quantities to the HVDC system produced by the RTDS monitored by the JVC include the communicating bus RMS voltage and machine reactive power outputs. The JVC provides set points to raise or lower pulses, which are used by the machine exciter models simulated by the RTDS.

(McLaren et al, 1991) are the first to test a protective relay performance when the protected line includes series capacitors which are protected by metal oxide varistors

(MOVs). The protection of a series commutated line presents significant challenges to relay designers since the series capacitor combined with the protection device may show wide variations in impedance during a fault condition. By using the RTDS to model the line, the relays can be tested to ensure proper operation under the various fault conditions. Figure 2.29 (McLaren et al, 1991) shows the protective relay under test connected to the RTDS via voltage and current amplifiers. The RTDS's operation continues in real-time, and the relay tripping signal can be fed back to the RTDS and used to operate actual circuit breakers. On-site testing of protection relays with RTDS has demonstrated an advantage in time expediency over the off-line playback test methods.

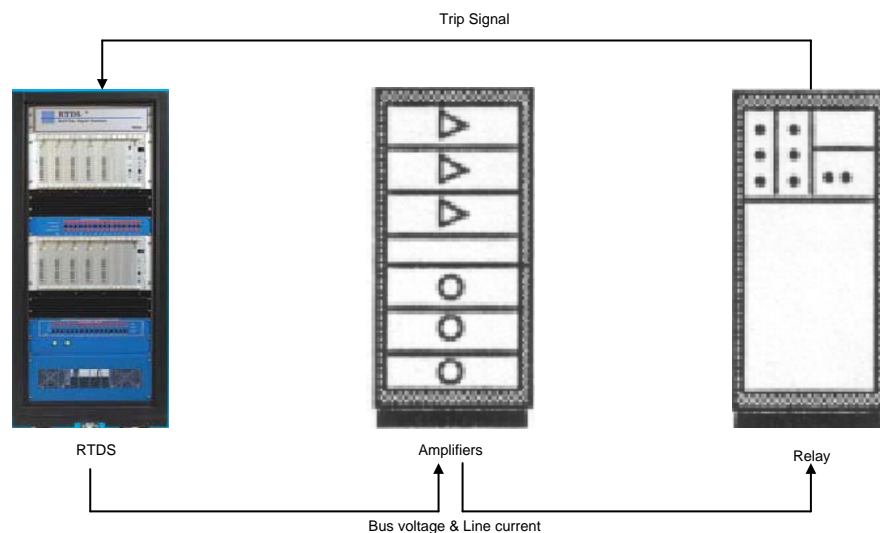


Figure 2.29: RTDS protective relay interface (McLaren et al, 1991)

(Jackson et al, 2005) developed a rapid controller-prototyping platform known as dSPACE. This platform is connected to the real-time power system simulator (RTDS). It is used for educational purposes as a platform for teaching of design principles for power system controllers (see Figure 2.30). The RTDS is useful to quickly build a detailed and realistic simplified simulation model of any power system. The simplified model is linearized and finally a feasible controller is designed. Now it is possible to implement a physical controller where use is made of the dSPACE platform to implement it. The control signals from the dSPACE platform can be viewed within the RSCAD environment as plots (Jackson et al, 2005).

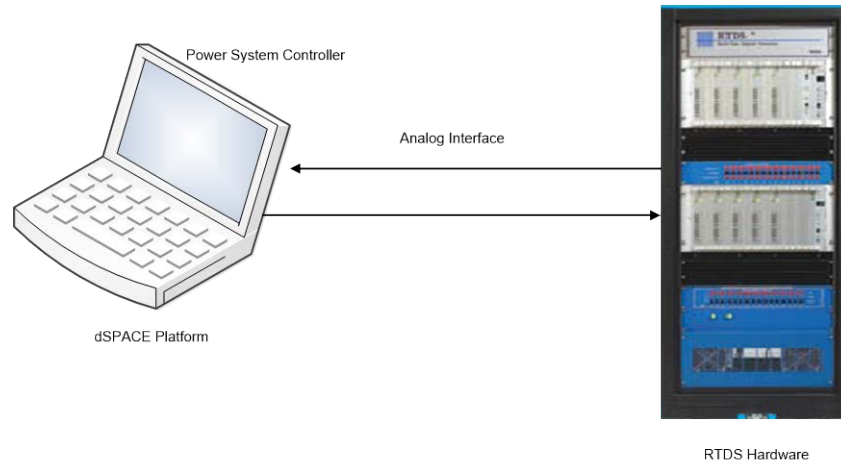


Figure 2.30: Control system design platform (Jackson et al, 2005)

(Adewole and Tzoneva, 2014), investigates the impact of the IEC 61850-9-2 part of the standard where sampled value messages are exchanged between IEDs an operating performance in terms of dependability, security and operating speed is reported on. The lab-scale setup includes the use of the Real-Time Digital Simulator (RTDS), IEDs supporting sampled value (SV) messages, conventional hardwired IEDs, a GPS satellite clock for time synchronization, and industrial network switches are used in a hardware-in-the-loop practical implementation. Figure 2.31 shows the laboratory set-up of the implementation (Adewole and Tzoneva, 2014).

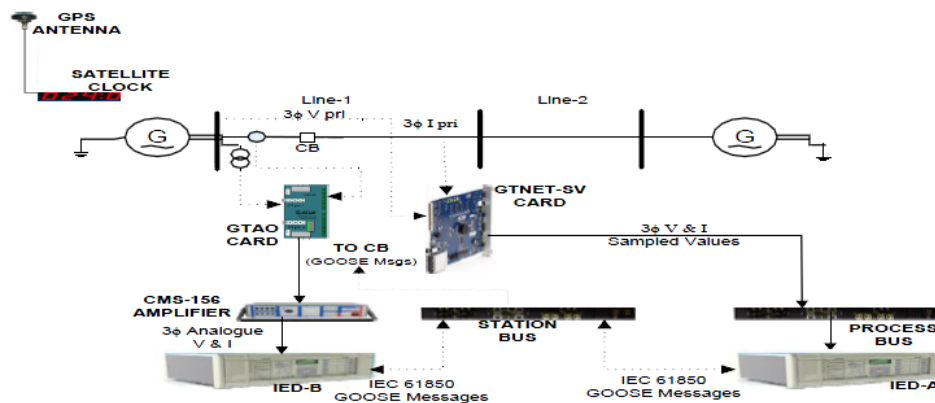


Figure 2.31: Functional implementation of the laboratory set-up (Adewole and Tzoneva, 2014)

2.8.2.1 Discussion on the real-time monitoring and control of power systems using RTDS software environment

The real-time monitoring and control of the power systems using RTDS plays a wide role in various applications such as: general AC and DC systems operations, interactions of AC and DC systems, integrated protection and control systems, control system for synchronous machines, HVDC, SVC, FACTS and custom power devices, protective relaying schemes, and advanced education and training.

The real-time monitoring and control of the power systems using the RTDS provides the benefits such as increased system reliability, security, stability and efficiency of equipment and communication network, to improve system understanding, knowledge and insight, to minimize the equipment system failure, and to reduce project/equipment commissioning time.

2.8.3 Application of the synchrophasor technology in power engineering

Synchrophasor measurement technology can assist with the implementation of many power system control functions, including the Energy Management System (EMS), Wide-Area Monitoring (WAM), situational awareness, advanced warning systems, protection and control applications. Synchrophasor technology is useful for daily monitoring of the system operation and asset performance. The state estimation (SE) functions, supported by SCADA systems, provide magnitude measurements and phasors through state estimation algorithms that is time extensive. More frequent and precise power system measurements are required for real-time solution of the energy management problems (Madani et al., 2013).

The addition of synchrophasor technology provides magnitude measurement speed of 60 or 120 measurements per second as opposed to SCADA system measurement of once every 4 to 8 seconds. It can also help to identify and capture higher speed phenomena in the power system. Additionally, time synchronization to one microsecond allows for accurate comparison of phase angles across the grid and identification of major disturbances, for example voltage instability and islanding. The synchrophasor technology is identified as the key technology to help detect and prevent wide-spread blackouts across the power system (Madani et al., 2013).

2.8.3.1 EMS applications using synchrophasor technology

The control center uses many technologies for the solution of the EMS applications. Synchrophasor measurements enable readings of voltages and currents across the power system and provide a more accurate state estimation than the existing Energy Management System (EMS). A synchrophasor system covering a large footprint coupled with fast sampling rates may be best served by a distributed architecture to process data for new advanced algorithms and for historical analysis. Figure 2.32 shows EMS integrated with synchrophasor technology (Giri, 2011).

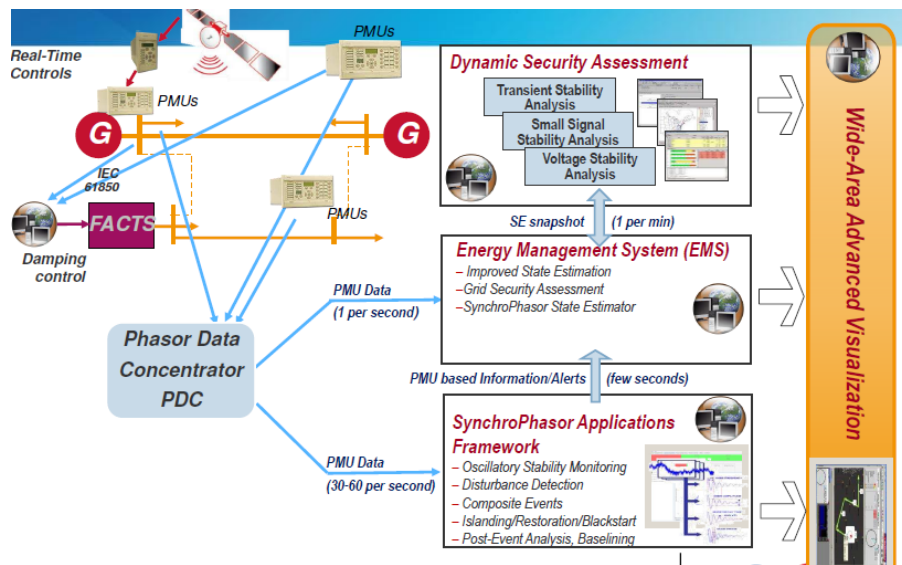


Figure 2.32: EMS integrated with synchrophasor technology (Giri, 2011)

2.8.3.2 Situational awareness and wide-area monitoring application using synchrophasor technology

The data from the entire power system including generation, transmission and distribution substations is usually transferred to the national or regional control center. Operators in control centers need to have a very good idea of the current status of the power system. This awareness (situational awareness) of the system state needs to cover a wide geographical area. As the coverage area is geographically widely distributed it is assumed that there many systems that are interconnected. If a fault occurs in one segment of the power system it might spread to the rest of the network and cause a system-wide power outage if not attended to timeously. Once an event of this magnitude occurs where an

entire power system is brought down, it might take some time (weeks or months) to perform the fault analysis by sifting through large amounts of data. (Zhang et al., 2011).

The problem of performing post-fault diagnosis within a reasonable amount of time can be resolved by installing a number of Phasor Measurement Units (PMUs) at strategic locations within the power system network. Events that might have contributed to the system shutdown can now be identified within a very short space of time when using the PMUs. The playback of events can also be performed in near real-time.

Table 2.5 shows the comparison between the PMU-based and the SCADA-based systems.

(Zhang et al., 2011) developed a PMU-based situational awareness application shown in Figure 2.33, which provides the following modules:

1. Online event detection.
2. Location of disturbances.
3. Real-time reliability monitoring.
4. Near real-time event replay or tracking.
5. Early warning of potential stability problems.
6. Post event analysis.

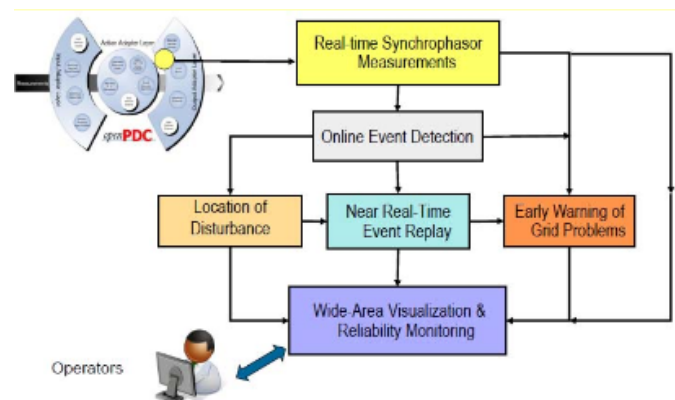


Figure 2.33: PMU-based situational awareness system (Zhang et al., 2011)

Table 2.5: Comparison between the PMU-based and the SCADA-based systems (Tripathy, 2010)

Attribute	PMUs	SCADA
Measurement	Digital	Analog
Resolution	Up to 60 samples per cycle	2-4 samples per cycle
Observability	Dynamic/Transient	Steady State
Monitoring	Wide-Area	Local
Phasor Angle Measurement	Yes	No

2.8.3.3 Wide-Area Monitoring and Visualization (WAMV) application using synchrophasor technology

Several Recovery Act projects are deploying synchrophasor data-based WAMV systems. These systems gather phasor data across a wide area which could be 100's of miles in size, and present them to the operators in real-time. Digital displays provide alerts to indicate possible levels of stress in the grid such as areas of low voltage, frequency oscillations, or rapidly changing phase angles between two locations (such as substations) on the grid. Many WAMV applications have indicative capacities that identify grid stress (measured by the changing phase angles of synchrophasors at different substation locations; termed phase-angle separation), grid robustness in terms of system events (oscillations, damping and trends), instability (frequency and voltage instability), or reliability margins (which describes how close the system is to the edge of its stability boundary). These systems provide context-appropriate graphics and visualizations, basic data archiving, the ability to drill-down into specific locations or conditions on the grid (e.g., voltage or a frequency oscillation), and playback capabilities (US Magazine, 2013).

(Chen et al., 2012) described the Real Time Digital Simulator (RTDS) integration with Electric Power Group's (EPG) synchrophasor engineering applications for information synchronization, visualization, and furthermore investigation. The authors use different software such as ePDC for data synchronization, RTDMS for visualization, and PGDA for data analytics, and RTDS for simulation. Figure 2.34 shows RTDS EPG deployment architecture.

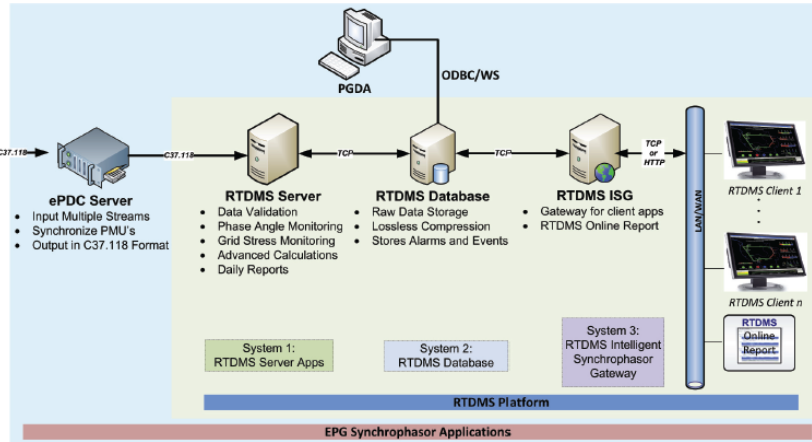


Figure 2.34 : RTDS-EPG Synchrophasor applications deployment architecture at Southern California Edison (Chen et al., 2012)

2.8.3.4 Power system stability assessment using synchrophasor technology

(P.Kundur et al., 2004) defined power system stability as “the ability of an electric power system for a given initial operating condition, to regain a state of operating equilibrium after being subjected to a physical disturbance, with most system variables bounded so that practically the entire system remains intact”.

The authors proposed classification of the power system types of stability which determined by the following conditions:

- Physical nature of the resulting mode of instability,
- Size of the disturbance, and
- The duration for which the stability phenomena is observed.

In light of these criteria, the power system stability is chiefly ordered into three types: and is given in Table 2.6. They are: rotor angle stability, frequency stability and voltage stability.

Assessment of the voltage and frequency stability of wide area power system is very important in order to prevent blackouts.

Table 2.6: The definition of power system stabilities

Rotor angle stability	Frequency stability	Voltage stability
The ability of synchronous machines of an interconnected power system to remain in synchronism after being subjected to a disturbance	The ability of a power system to maintain steady frequency following a severe upset resulting in a significant imbalance between generation and load	The ability of a power system to maintain steady voltage at all buses in the system after being subjected to a disturbance from a given initial operating condition

Biswas et al., 2013 examine the limitations of few existing online voltage stability algorithms and presents a new real-time algorithm for voltage stability monitoring based on local measurements using the RTDS GTNET PMU, PDC and NS3 software. Figure 2.35 shows detailed setup of the implementations. (Biswas et al., 2013)

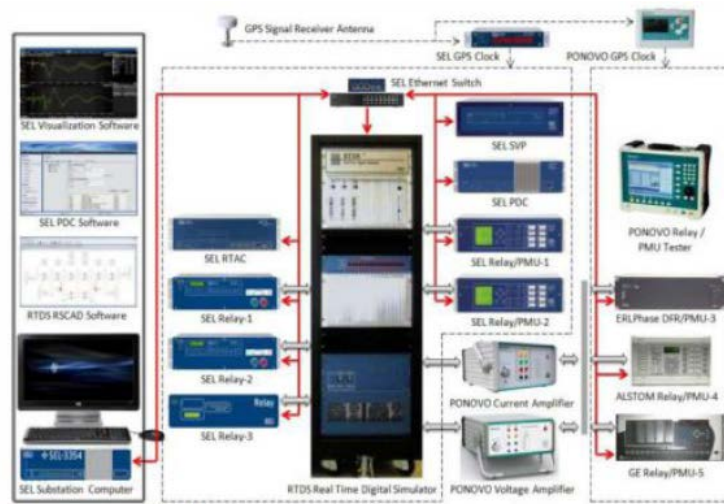
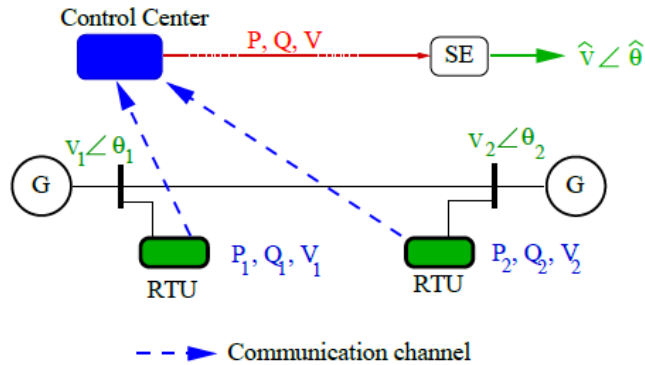


Figure 2.35 : Architecture of the smart grid test bed at SGDRIL (Biswas et al., 2013)

The SCADA/EMS system shown in Figure 2.36 uses the Remote Terminal Units (RTUs) for measuring the voltage and current magnitudes. It measures the power flows in the transmission lines. Normally, the RTU provides the measurement with the update rate of 2-10 seconds. The pre-processing of the information gathered from the RTUs is completed at the control center, which incorporate the handling of bad information, and completing the nonlinear state estimation. These capacities bring about the estimation of the states, at an ordinary time intervals of 5-10 minutes. Hence, the SCADA/EMS is

useful for monitoring the system under the steady state, but is not useful for observing the system under transients (Tripathy, 2010).



SE -means State Estimation

RTU -means Remote Terminal Unit

Figure 2.36: Block diagram of SCADA, data acquisition, transfer and state estimation (Tripathy, 2010)

With the improvement of the Phasor Measurement Unit, a (PMU)-based Wide Area Monitoring System (WAMS), as demonstrated in Figure. 2.37, uses the time-synchronizing pulse (with a one microsecond accuracy) from the Global Positioning System (GPS). It is possible to quantify both the magnitude and the phase angle of the bus voltages in the power system. The PMU regularly supplies the phasor data once every one or two cycles. This rapid refresh rate of the PMUs enables them to capture the system states during transient conditions. The information measured from the PMU is sent to the Phasor Data Concentrator (PDC) by using the suitable communication media such as phone line, microwave communication or fiber-optics. Among the different communication media, fiber-optic communications have the lowest connection delay. These measurements can further be utilized to take some rapid control action, to ensure the stable operation of the power system (Tripathy, 2010).

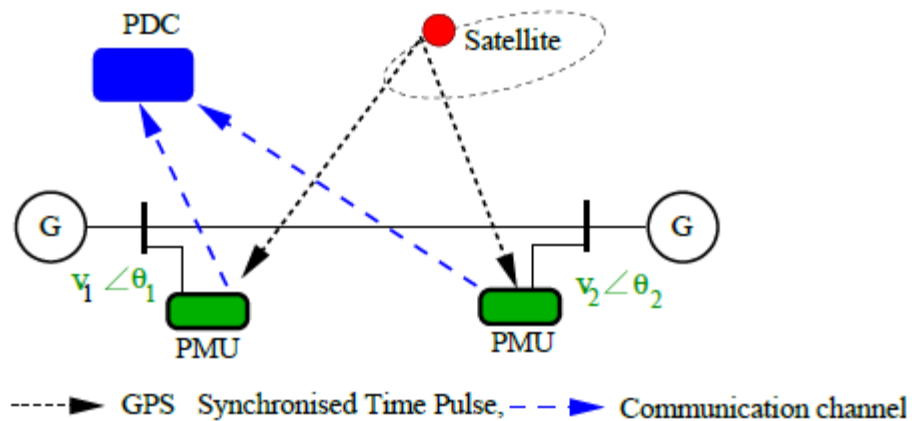


Figure 2.37 : Block diagram of Wide Area Monitoring Systems (Tripathy, 2010)

2.8.3.4 Discussion on the real-time monitoring and control of the power systems using synchrophasor technology

Synchrophasors are phasor measurements that are synchronized to a clock source. The clock is synchronized to a satellite and the measured values are time-stamped so the measurements are referenced to a time source. This provides an accurate and comprehensive view of the power system. Traditional SCADA systems use state estimation to calculate the system state based on unsynchronized data points collected at a central location every 2-4 seconds. The advantage of synchrophasors is that they allow the dynamic measurement of the system state in real-time. This enables a snap-shot view of the power system as a whole.

The benefits offered by synchrophasor technology include (PAC World Magazine, DEC 2013):

- The reliability of the power system as a whole is improved as the down-time of the network as a result of power failure is reduced which lessens the impact to end-users and problems in the power grid are detected early using knowledge-based software systems;
- Operational, maintenance energy ancillary costs are reduced as a result of efficient operation and an improvement in the utilization of assets.; and
- Distributed energy resources can be integrated into the national power grid – synchrophasor data can be used to monitor the grid and operations from generation,

transmission and distribution levels can be optimized using renewable or non-renewable sources of energy.

On the basis of the above it can be concluded that the synchrophasor technology for use in the monitoring and control of greater geographically located areas quickly transition will the existing grid into an even “smarter grid”.

2.9 Conclusion

This chapter investigates the communication networks, protocols, media and power system applications of LabVIEW, DAQ, RTDS and Synchrophasor technologies. The review provides an overview of the communication systems used in the power industry. Future power systems have new challenges and requirements for the next generation infrastructure and communication networks. These include:

- Supporting high-speed, real time communication links needed in power system protection, monitoring and control applications.
- Supporting high bandwidth and the highest data rate required by the new power system services between the control centers.
- Accessing all locations to support real time monitoring and control functions.
- Continual operation even if part of the network is damaged

The next chapter presents the definition, measurement and standardization of the Phasor Measurement Units.

CHAPTER 3

DEFINITION, MEASUREMENT AND STANDARDIZATION OF THE PHASOR MEASUREMENT UNITS AND PHASOR DATA CONCENTRATORS

3.1 Introduction

Power utilities face an increasing number of threats of security of operation due to overstressed power networks in a competitive market scenario. This leads to an increase of the need for the application of new technologies for monitoring and control of these complex power systems. One of the recent widely used technologies to fulfill the above need is based on application of the Phasor Measurement Units (PMU). The PMU provides the voltage phasor of the power system bus where it is installed and current phasors of the entire set of branches connected to that bus. Direct measurement of all the system states is possible by placing PMUs in all buses of the power network. The aim of the power system operator is to provide electric power continuously and reliably to the end users. In order to achieve these goals, the system state needs to be monitored; this can be done by using PMUs. As this thesis uses software-based PMUs supported by the Real-Time Digital Simulator (RTDS) to develop and implement a lab-scale system for PMU data acquisition and data transfer, a deeper understanding of the phasor measurement units in the power system is needed. The aim of this chapter is to investigate the definition of the synchrophasor, time synchronization, standards, protocols, and Phasor Data Concentrators (PDC) which are the tools used in the lab-scale implementation.

This chapter provides the Introduction in section 3.1. The definition of synchrophasors is given in section 3.2. The background, description, time synchronization and synchrophasor standards are presented in section 3.3. The Phasor Data Concentrator (PDC) description and protocols used are described in section 3.4. Industrial applications of the synchrophasor technology are discussed in section 3.5 and the conclusion is presented in section 3.6.

3.2 Synchrophasor definition

The idea of a phasor is more than a century old and dates back to (Steinmetz,1893) who proposed complex numbers for investigation of the linear electrical systems with sinusoidal sources under unfaltering stated conditions. A sinusoidal signal, $x(t)$, of a

known recurrence, can be completely presented by its magnitude size X_m and its angular position ϕ , for an arbitrary time reference t as (IEEE C57.18.10, 2008)

$$x(t) = X_m \cos(2\pi ft + \phi) \quad (3.1)$$

The phasor representation \bar{X} of the signal $x(t)$ is given by the following equation (IEEE C57.18.10, 2008).

$$\bar{X} = (X_m / \sqrt{2}) e^{j\phi} \quad (3.2)$$

where \bar{X} is the RMS value of the sinusoidal signal. It is important to note that the frequency does not appear expressly in the phasor representation; however it is an intimated property of the phasor. The synchrophasor is a phasor with the angle referenced to GPS-driven time reference. Figure 3.1a and 3.1b clarifies the stage plot reference given in the IEEE standard C37.118 and (Singh et al., 2011). A PMU is obliged to have a time-tag that refers to the time. The angle is 0° when the most extreme value of $x(t)$ is synchronized to the 1 pulse per second (PPS) signal, and -90° when positive zero intersection occurs with the 1 PPS signal. This implies that each one inspecting moment in the information window must correspond with the absolute time given by the GPS clock.

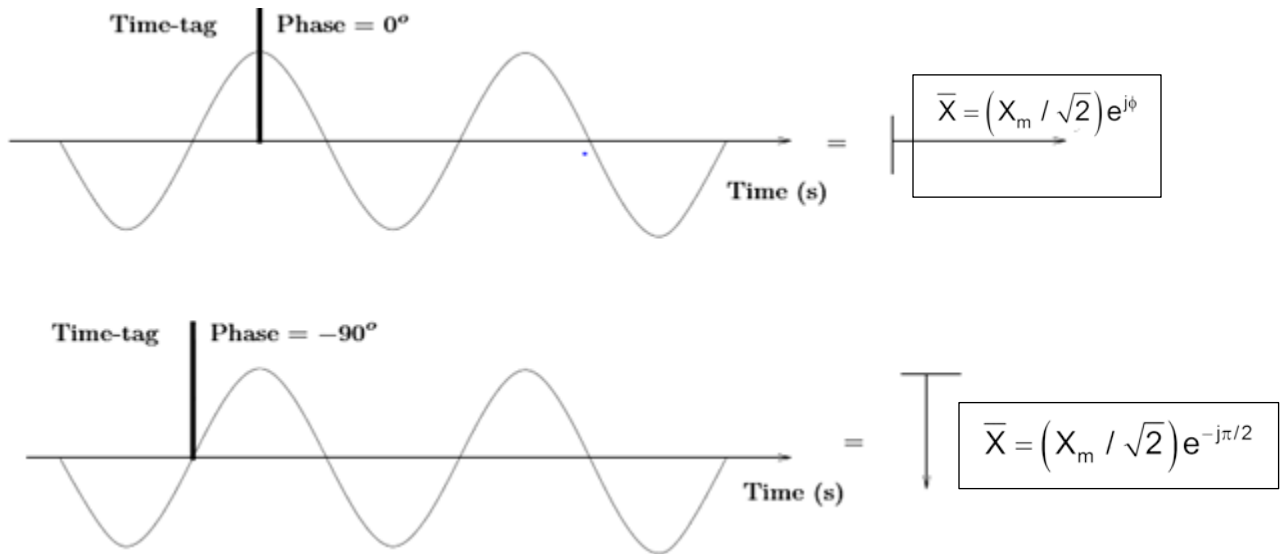


Figure 3.1a : Synchrophasor angle conventions (IEEE C57.18.10, 2008)

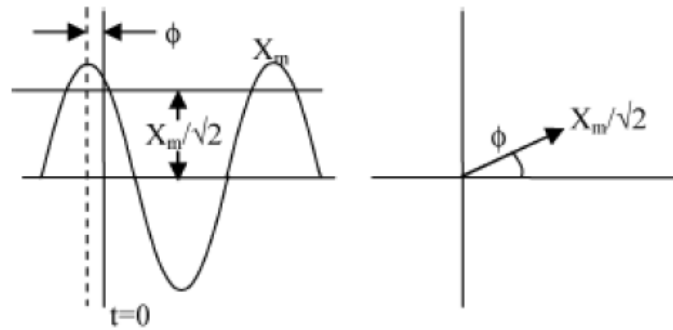


Figure 3.1b : Phasor representation of a sinusoidal signal (Singh et al., 2011)

3.3 Background, description, time synchronization and standards for phasor measurement unit

This section provides the historical background, time synchronization and standards for the phasor measurement unit.

3.3.1 Historical background of the Phasor Measurement Unit (PMU)

In 1965, the North-eastern power grid in the United States of America (USA) experienced a blackout that revealed the need to monitor the power system as a whole in real-time. With the limited capabilities of the technology available at that time, a method was devised that used a sequential measurement scan with a non-linear state estimation scheme to obtain a snapshot of the power system state as described in (Philip, 2012). This method advanced the awareness of the state of the power system, but the information provided was not sufficient to significantly reduce the probability of blackouts.

In most power systems, the techniques for state estimation, which were developed in the 1970's, involved measuring active and reactive power at substations and sending that information to a central location to process all of the data. Because of the fact that the scan time for all of the measurements taken varied from seconds to minutes, the estimates of the system state had limitations due to the large scanning window (Philip, 2012).

The state estimation setup assumes that all of the measurements are taken at the exact same time and are sent to the centralized location instantaneously. In the 1970's, there was no way to determine precisely when a measurement was recorded so the central

processing would have to assume the measurements were taken at the same time even if they were taken seconds apart.

As the technology developed, Intelligent Electronic Devices (IEDs) were introduced in substations to ensure faster communications, and the size of the scanning window was reduced. This resulted in faster updates from the state estimators, but it has not eliminated the limitation as a result of the size of the scanning window. The solution to this problem is to have a way to time-synchronize all substations so that a device can acquire a measurement and time-stamp the data additionally. If the devices are time-synchronized, it becomes desirable to decrease the sampling window and the communication channels then allow for fast data transfer (Philip, 2012).

The phasor measurement units are the next generation technology that ensures fast acquisition measurement and time-stamping of the data of the whole power system.

3.3.2 Phasor measurement unit and its description

According to the Performance and Standards Task Team (PSTT) of the North American Synchrophasor Initiative (NASPI) a PMU can be characterized as, "a device that gives, as a minimum, synchrophasor measurements for one or more periods of an AC voltage and/or current waveform. The synchrophasor can be single phase or symmetrical segment values" (NASPI, 2014).

Figure 3.2a; presents the block diagram of a Phasor Measurement Unit (PMU). The Global Positioning System (GPS) gives two signals, every millisecond (1kPPS), and the Inter Range Instrumentation Group time code format B (IRIG-B) signal, which is at a rate of one time mark for every second. The 1kpps (pulse per second) signal is used by the sampling clock for synchronization with the Global Positioning System (GPS) clock, while, the IRIG-B signal gives the time tag to the estimated phasors. The voltage and current signals acquired from the auxiliary side of the power transformers and the current transformers are pre-processed separately by an anti-aliasing filter to prevent aliasing of the signals from the reconstructed signal. The analog to digital converter samples the pre-processed analog data, which are utilized by the microprocessor-based phasor estimator. The estimated phasors are finally sent to the Phasor Data Concentrator (PDC) which conforms to the IEEE C37.118 standard (Best et al., 2010).

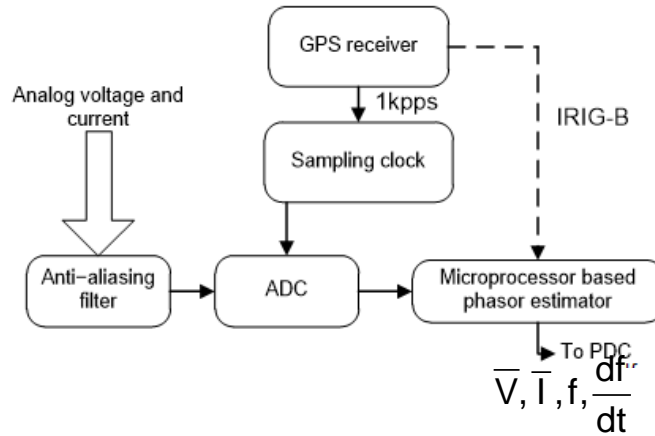


Figure 3.2a: Block diagram of a Phasor Measurement Unit

With reference to Figure 3.2, \bar{V} is the phasor of the voltage and \bar{I} is the phasor of the current; f is the frequency, $\frac{df}{dt}$ is the change in frequency with respect to time.

3.3.3 Phasor measurement unit time synchronization

In the early 1980's, communication engineering enhanced and the first GPS satellites were dispatched into space, which made it possible to have precise time-synchronized devices with GPS receivers. At the point when the first PMUs were produced, there were very few GPS satellites in orbit so a GPS collector would lose synchronization with a satellite regularly. If the PMU lost synchronization with the GPS clock, a bit would be set to indicate that the GPS clock is out of synchronization, which would imply that the measurements are incorrect.

All Synchrophasor measurements are time-labelled with the Universal Time Coordinated (UTC), through the GPS. All GPS receivers are exceptionally accurate (+100 nanoseconds) and PMUs are synchronized to the GPS receivers to ensure very accurate time-stamping. PMUs provide a more accurate system status because the samples are taken and time-stamped in a microsecond sampling window. The standard that governs synchrophasor data transfer is the IEEE C37.118.2-2011 standard and this is the main guideline for Phasor Data Concentrator (PDC) communication. This standard characterizes the reporting rate of the approaching PMU data frames as sub-products of the system frequency, for example, 10, 25 and 50 for a 50 Hz system and 10, 12, 15, 20, 30 and 60 for a 60 Hz system. The PDC must send the time-adjusted frame at an

equivalent, lower or higher data rate utilizing down-sampling or up-sampling systems. The measurement time tag of the synchrophasor comprises of three numbers. They are:

- ❖ Second-of-Century (SOC),
- ❖ Fraction-of-Second (FRACSEC) and
- ❖ Time quality flag.

The SOC is a parallel check of seconds from UTC midnight (00:00:00) of January 1, 1970 to the current second. Every device has a Time_BASE number and the actual fraction of the second check is a number represented to the FRACSEC divided by the Time_BASE of the device, so each one frame is equally divided. Both parts integrate to a structure where the actual time is indicated in Equation (3.3). The FRACSEC is constantly zero at the turn of a second (IEEE-SA Standards Board, 2011)

$$Time = SOC + FRACSEC/TIME_BASE \quad (3.3)$$

The time quality flag shows the greatest vulnerability in the time stamp at the time of measurement. This value is focused around the time source and incorporates the instabilities in the PMU measuring methodology. The synchrophasors must be synchronized to UTC time to meet the precision prerequisites of the IEEE Standard C37.118.1. The maximum steady-state error allowed by the standard can cause up to 1% Total Vector Error (TVE) which is equivalent to a phase error of 0.01 radians. This corresponds to a time error of ± 26 microseconds for a 60Hz system and ± 31 microseconds for a 50 Hz system. These limits require a highly reliable time source to be connected to the synchrophasor devices and GPS clocks are used to provide the required time accuracy (IEEE-SA Standards Board, 2011). Figure 3.2b shows the PMU utilization in a power system.

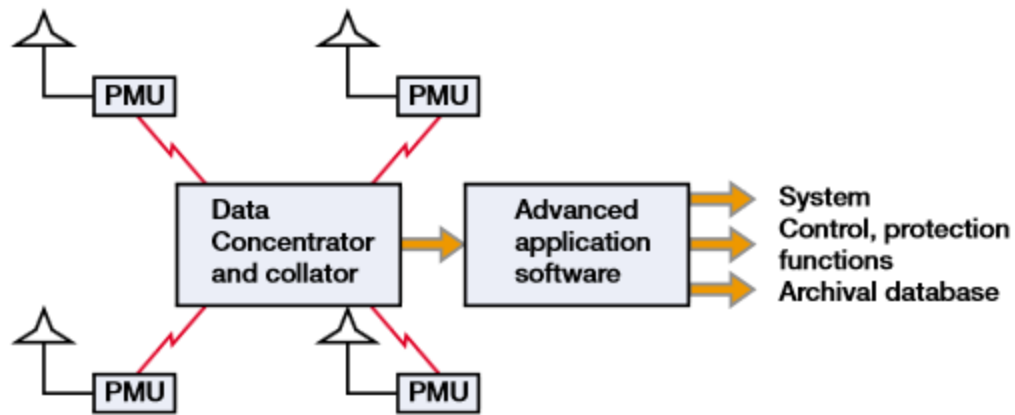


Figure 3.2b: PMU utilization in a power system (Singh et al., 2011)

3.3.4 Standards for phasor measurement unit

To have the capability to transfer phasor measurements between various devices from different vendors with different communication protocols, standards need to be set up which ought to be implemented by all the vendors. The standard which PMUs typically conform to is called the "Synchrophasor Standard for Power Systems". Two synchrophasor standards are typically used. They are the IEEE Standard 1344-1995 known as the, "Standard for Synchrophasor Measurements for Power Systems," and its substitute known as the IEEE standard C37.118. These standards provide the definition for synchronized phasors; discuss time synchronization and application of time labels; provide a procedure to check measurement compliance with the standard, and provides the message structure for the transmitted data e and procedures for the transmission and reception of real-time data.

PMUs utilize a standard for synchrophasor measurements known as the IEEE C37.118.2-2011, which was a successor to the previous, IEEE C37.118-2005 standard. The IEEE C37.118-2005 standard was an amendment of the IEEE 1334-1995 standard that was the first push to guarantee PMUs from different vendors could be utilized in a typical application. The C37.118.1-2011 presents the best approach to test the accuracy of the existing PMUs. The C37.118.2 standard defines how the PMU information is communicated.

3.4 Phasor Data Concentrator (PDC) : Description and protocols

A Phasor Data Concentrator (PDC) combines and time-aligns information from several PMUs. This section provides the description of the PDC and the protocol used to connect the PMU and the PDC.

3.4.1 Phasor Data Concentrator (PDC)

PMUs use data to compute the phasors of the sinusoidal voltage and current measurements and time-label them with the UTC time given by the GPS receiver. Phasor information are processed and transmitted once every second. PMU information is sent to a central location to be handled. At this location, a receiver known as Phasor Data Concentrator (PDC) acknowledges and time aligns information from a several PMUs. After the PMU's information is adjusted, the PDC sends the information stream to an alternate PDC or computer to be examined. As more PMUs are added to the power system, the number of PDCs increase proportionately.

The Phasor Data Concentrator (PDC) is a node in the system where phasor data from a number of PMUs are correlated and fed out as a single stream to other applications. The PDC processes real-time streamed time-series data. The measured values synchronized with the Global Positioning System (GPS) time from hundreds of input sources are time-sorted. The PDC correlates data according to the time tag and then broadcasts the combined data for processing within an organizational unit. It verifies the integrity and completeness of the data stream from the PMUs and ensures delivery of the data to local data consumers, including Phasor Gateways. PDCs are expected to either be the main system on which the historical archive is kept, or from which the historical archive is managed. The PDC handles the temporary capture of data to the unspecified time duration, it acts as the principal buffer between data sources and data sink (Phadke and Thorp, 2008).

In view of their improvement, PDCs are separated into two classifications; those devices that only have PDC functions, and those devices that include the PDC functions with others. The PDC-only devices are intended to work just with the PMU information. The devices support PDC functions and other functions are useful for acquiring information about the devices and other utility applications where the PDC capacity has been added

to the current capacities. Because of the constraints set by the different applications and their existing standards, this research focuses on PDC-only devices. Based on their implementation, PDC-only devices can be divided into hardware and software PDC types. A Hardware PDC is a physical device with a set number of inputs and it typically used in applications with a number of PMUs. The hardware size and structure are dictated by the size of the wide area network system (For example: Substations). A Software PDC is a software bundle executed in proposed business fittings (top of the line PCs and Servers). This type of device can likewise be utilized at a substation with various PMUs.

3.4.2 Protocols used to connect the PMU and the PDC

PMUs are joined with a single PDC through an Ethernet cable, which has a downlink speed of up to 1 Gigabit. The information is transmitted utilizing standard protocols, such as the User Datagram Protocol (UDP)/Internet Protocol (IP) or Transmission Control Protocol (TCP)/IP. Figure 3.3 shows the communication differences between the two protocols where the TCP/IP communication has an acknowledgment of reception of a data packet, but UDP does not. At the point when UDP/IP is utilized, the source shows the data to the destination IP address without handshaking and recognizing the transmission channel. Therefore there is no real way to check whether the data was received at the designation, so it is possible for the packet to be dropped with the UDP/IP protocol utilization. If TCP/IP is utilized for communication, there is handshaking between the source and destination node and packets are only sent once a data path has been determined and acknowledged. If a packet is not received at the destination, then it will be retransmitted from the origin. This provides error checking and correction over the data frames but makes TCP/IP significantly slower than the UDP/IP (Retty et al., 2013).

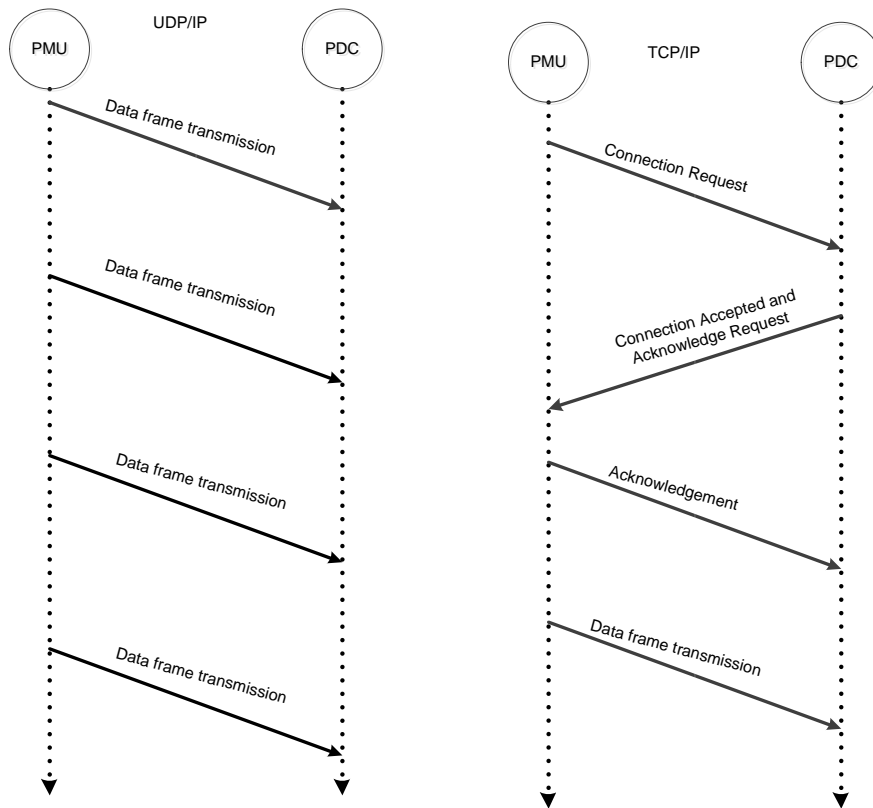


Figure 3.3: UDP/IP and TCP/IP data stream (Retty et al., 2013)

3.5 Synchrophasor measurement system and message format

The synchrophasor measurement includes the steady state and dynamic performance requirements for synchrophasors, frequency, and a measure of the rate of change of frequency. Additionally the rate at which data is transferred is also specified. A simple synchrophasor network comprises of several Phasor Measurement Units (PMUs) and a Phasor Data Concentrator (PDC) as shown in Figure 3.4. The PMUs located at different key substations gather data and send it in real-time to a PDC at a location where the data is aggregated and analyzed. If multiple Intelligent Electronic Devices (IEDs) in a substation support synchrophasor measurements, a PDC may be installed at the substation. The data gathered by PDCs may be used to support many applications, ranging from visualization of information and alarms for situational awareness, to ones that provide sophisticated analytical, control, or protection functionality.

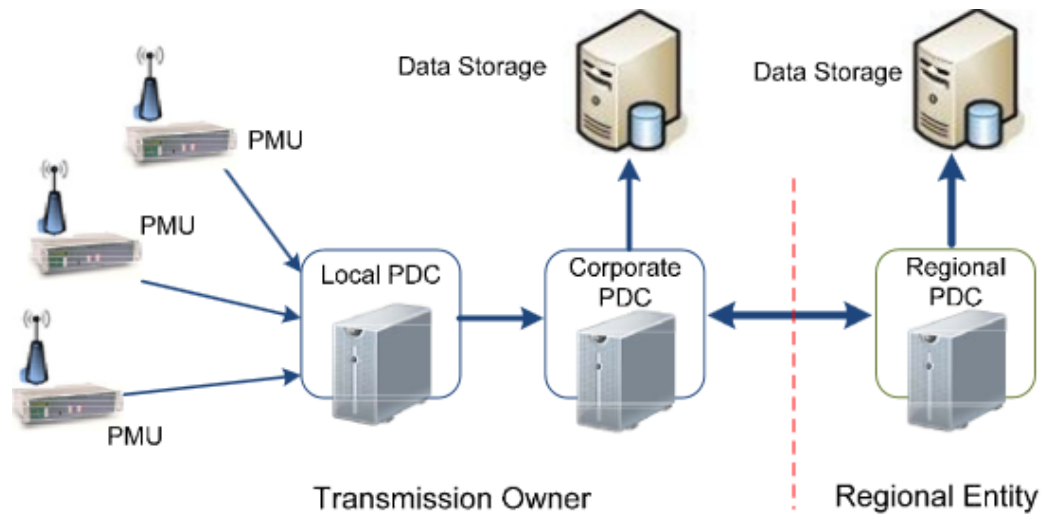


Figure 3.4 : Synchrophasor data collection network (IEEE Std C37.118.2, 2011)

3.5.1 Synchrophasor measurement message format

The C37.118.2 standards describe four types of messages to be transferred from a PMU or PDC. These are data, configuration, header and command. The first three message types are transmitted from the PMU/PDC that serves as the data source, and the last (command) is received by the PMU/PDC.

A. Data Frame

The data frame contains the real-time data measured or calculated by the PMU/PDC. The message incorporates a recognizable header, message length, the source ID of the message, a period stamp, detailed status information regarding the data and its source and quality; and, the 'data.' The 'data' includes phasors (in rectangular or polar format), frequency, rate of change of frequency and analog and digital quantities. All information except digital (Boolean) quantities may be in fixed or floating-point format. The status word in the message demonstrates data validity, time source quality, particular data conditions (trigger types for example) and is intended to be translated by a receiving device or application that uses the data. The data frame may contain the data from a single PMU or several PMUs (PAC World Magazine,2013). The data from every PMU is organized as a block of data headed with the status of that block of data as shown in Figure 3.5.

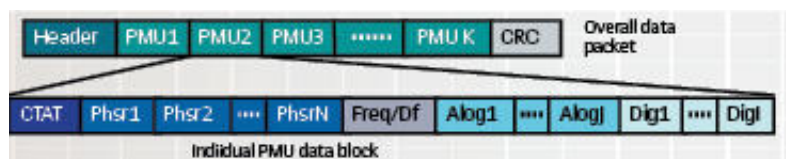


Figure 3.5 : Message format (PAC World Magazine,2013)

B. Configuration Frame

A configuration frame is a BINARY data set that contains information and also the processing parameters for a synchrophasor data stream. Three configuration frame types are specified CFG-1 and CFG-2 are part of the version 1 (IEEE Std C37.118-2005) message set, and optional CFG-3 is introduced with version 2 (IEEE Std C37.118.2-2011).

CFG-1 refers the PMU/PDC capability, demonstrating all the data that the PMU/PDC is capable of reporting. CFG-2 indicates measurements currently being reported (transmitted) in the data frame. This may be only a subset of the available data. Both frames have identical structures with 19 fields, and with fields 8–19 repeated as necessary. In these frames, all fields are with fixed length as described and no delimiters may be used (PAC world Magazine, 2013). The frame contents are shown in Table 3.1.

Table 3.1: Configuration Frame Format 1 and 2 (IEEE Std C37.118.1, 2005)

S.No	Field	Size in bytes	Short description
1	SYNC	2	Sync byte followed by frame type and version number
2	FRAME SIZE	2	Number of byte frame
3	IDCODE	2	PMU/DC ID number
4	SOC	4	SOC time stamp
5	FRACSEC	4	Fraction of second and Time quality
6	TIME_BASE	4	Resolution of fraction-of-second time loop
7	NUM_PMU	2	The number of PMUs include in the data frame
8	STN	16	Station name -16 bytes in ASCII format
9	IDCODE	2	PMU ID number as above, identifiers source of each data block
10	FORMAT	2	Data format with in data frame
11	PHNMR	2	Number of phasors- 2 byte integer(0 to 32767)
12	ANNMR	2	Number analog values – 2 byte integer
13	DGNMR	2	Number of digital status words – 2 byte integer

14	CHNAM	16x(PHNMR +ANNMR +16x DGNMR)	Phasors and channel names – 16 bytes each phasor, analog and each digital channel (16 channels in each word) in ASCII format in same order as they transmitted. For digital channel the channel names order from the least significant the most significant.
15	PHUNIT	4 x PHNMR	Conversion factor for phasor channels.
16	ANUNIT	4 x ANNMNR	Conversion factor for analog channels.
17	DIGUNIT	4 x DGNMR	Mask words for digital status words.
18	FNOM	2	Nominal line frequency code and flags
19	CFGCNT	2	Configuration change count
	Repeat 8-19		Fields 8 – 18 repeated for many PMUs as in field 7(NUM_PMU)
20+	DATA_RATE	2	Rate of data transmission
21+	CHK	2	CRC – CCITT

CFG-3 is similar to the other configuration frames and contains the same data but with flexible framing information included. CFG-3 shows measurements presently being reported in the data frame (the same as CFG-2). CFG-3 has variable length fields, a PMU included, signal information, and extendable frame. The frame contents are given in Table 3.2. Note CFG-3 is optional; a synchrophasor device does not have to implement this message to be considered compliant with this standard(PAC world Magazine, 2013).

Table 3.2 : Configuration Frame Format 3 (IEEE Std C37.118.1, 2011)

S.No	Field	Size in bytes	Short description
1	SYNC	2	Sync byte followed by frame type and version number
2	FRAME SIZE	2	Number of byte frame
3	IDCODE	2	PMU/DC ID number
4	SOC	4	SOC time stamp
5	FRACSEC	4	Fraction of second and Time quality
6	CONT_IDX	2	The number of PMUs included in the data frame
7	TIME_BASE	4	Resolution of fraction of-second time loop
8	NUM_PMU	2	The number of PMUs included in the data frame
9	STN	1-256	Station name -16 bytes in ASCII format
10	IDCODE	2	PMU ID number as above, identifiers source of each data block
11	G_PMU_ID	16	Global PMU ID
12	FORMAT	2	Data format with in data frame
13	PHNMR	2	Number of phasors- 2 byte integer(0 to 32767)

14	ANNMR	2	Number analog values – 2 byte integer
15	DGNMR	2	Number of digital status words – 2 byte integer
16	CHNAM	1–256 per name)	Phasors and channel names – Minimum of 1 byte for each phasor, analog, and digital channel. Names are in the same order as they are transmitted: all phasors, all analog s, and all digitals. For digital channels, the channel name order will be from the least significant to the most significant
17	HSCALE	12×PHNMR	Conversion factor for phasor channels with flags.
18	ANSCALE	8 × ANNMR	Conversion factor for analog channels.
19	DIGUNIT	4 x DGNMR	Mask words for digital status words.
20	PMU_LAT	4	PMU Latitude in degrees, 32-bit floating point, WGS84 datum.
21	PMU_LON	4	PMU Longitude in degrees, 32-bit floating point, WGS84 datum.
22	PMU_ELEV	4	PMU Elevation in meters, 32-bit floating point, WGS84 datum.
23	SVC_CLASS	1	Service class, as defined in IEEE Std C37.118.1, a single ASCII character that is M or P for IEEE Std C37.118.1.
24	WINDOW	4	Phasor measurement window length including all filters and estimation windows in effect. Value is in microseconds, 4-byte integer value (to nearest microsecond)
25	GRP_DLY	4	Phasor measurement group delay including all filters and estimation windows in effect. Value is in microseconds, 4-byte integer value (to nearest microsecond).
26	FNOM	2	Nominal line frequency code and flags
27	CFGCNT	2	Configuration change count
	Repeat 9-27		Fields 9–27, repeated for as many PMUs as in field 8 (NUM_PMU).
28+	DATA_RATE	2	Rate of data transmission
29+	CHK	2	CRC – CCITT

C. Header Frame

The Header Frame is sent from the PMU/PDC to the host (PDC) system. It contains information about the sender (PMU/PDC) in plain ASCII format. There is no change in the format of header frame as compared to C37.118-2005 standard (PAC world Magazine, 2013). The frame has the same SYNC, FRAMESIZE, SOC, FRACSEC, and CHK as the other frames, and is identified by bits 4–6 of the SYNC word as shown in Table 3.3.

Table 3.3 : Header frame organization (IEEE Std C37.118.2, 2011)

S.No	Field	Size(bytes)	Comment
1	SYNC	2	Sync byte followed by frame type and version number (AA11 hex).
2	FRAMESIZE	2	Number of bytes in frame
3	IDCODE	2	MU/PDC data stream ID number, 16-bit integer
4	SOC	4	SOC time stamp
5	FRACSEC	4	Fraction of Second and Time Quality
6	DATA 1	1	ASCII character, 1st byte.
K+6	DATA k	1	ASCII character, K_{th} byte, $K>0$ is an integer.
K+7	CHK	2	CRC-CCITT

D. Command Frame

A data sending device (PMU or PDC) should have the capacity receive commands and take appropriate actions. The Command Frame uses the same SYNC, FRAMESIZE, SOC, FRACSEC, and CHK words. The command message frame is shown in Table 3.4 IDCODE should be a 2-byte identification code assigned to a PMU/PDC data stream output and is the same as field 3 in the configuration frame. Before any command can be accepted or executed, the PMU/PDC should have the same IDCODE as the internally stored one. The IDCODE for each output stream is user configurable. The PMU/PDC shall match the command code with that of a configured output stream and execute the command for the indicated data stream output, leaving other streams, if there are any, unchanged. CMD might be a 2-byte command code as defined in (IEEE Std C37.118.2, 2011).

Table 3.4 : Command frame organization (IEEE Std C37.118.2, 2011)

S.No	Field	Size(bytes)	Comment
1	SYNC	2	Sync byte followed by frame type and version number (AA11 hex).
2	FRAMESIZE	2	Number of bytes in frame
3	IDCODE	2	MU/PDC data stream ID number, 16-bit integer
4	SOC	4	SOC time stamp
5	FRACSEC	4	Fraction of Second and Time Quality
6	CMD	2	Command being sent to the PMU/PDC (0).
7	EXTFRAME	0–65518	Extended frame data, 16-bit words.
8	CHK	2	CRC-CCITT

3.6 Conclusion

This chapter provides the overview of the Synchrophasor, standards and protocols. In addition to that, time synchronization description and how the data is transferred from PMU to PDC using UDP/IP and TCP/IP is described. The industrial applications of the

Synchrophasor for wide area power system monitoring and IEC61850-90-5 standard-based power system protection scheme using Synchrophasor is given.

The next chapter provides the description of the lab-scale implementation of two methods: Data acquisition and data transfer method one, based on the PB5 card analog output signals and method two, based on the GTNET PMU card from the RTDS. The detailed explanation of the experimental set-up and the hardware and software tools used in the developed lab-scale system are described.

CHAPTER FOUR

HARDWARE AND SOFTWARE IMPLEMENTATION OF A LAB-SCALE REAL-TIME DATA ACQUISITION AND DATA TRANSFER SYSTEM

4.1 Introduction

This chapter presents the hardware and software tools and the lab-procedures which are developed to implement the real-time data acquisition and data transfer system. Two methods are developed for implementation of lab-scale data acquisition and data transfer systems in the laboratory of the Center for Substations Automation and Energy Management Systems (CSAEMS). i.e., i) DAQ card LabVIEW and MATLAB-based system using the RTDS PB5 card front panel analog signals (Method One), and ii) RTDS GTNET card PMU-based system using the software PMU measurement (Method Two) for data acquisition and data transfer from the simulated power system to the PC at the control center.

This chapter provides an introduction in section 4.1. The lab-scale data acquisition and transfer system specifications are given in section 4.2. The hardware and software tools used are described in section 4.3. The implementation of the lab-scale data acquisition system using the RTDS PB5 card front panel analog signals (Method One) and RTDS GTNET PMU-based system (Method Two) are presented in sections 4.4 and 4.5 respectively, and the conclusion is given in section 4.6.

4.2 Lab-scale data acquisition and data transfer system specifications

This section describes the functions and the specifications for the operation of the two lab-scale systems. The aim of this thesis is to develop methods, algorithms and procedures for implementation of two lab-scale systems for data acquisition of the simulation model data produced by the power system simulation in the RSCAD software environment (at the local end PC) and to transfer and distribute these data to a remote end (control center) for further utilization in the optimisation problem solution.

The data acquisition is implemented using the NI DAQ 6343 card, which acquires the data from the RTDS PB5 card analog output signals in the first case and using the RTDS GTNET card PMU signals in the second case. The data storage has been implemented at the local end by saving the data in the MS (Microsoft) Excel file format,

and at the remote end the data is stored in the MySQL database. The data from MS Excel or MySQL database are transferred to the PC with the MATLAB algorithm for the solution of the optimisation problem.

The functions of the LabVIEW and MATLAB-based lab-scale systems as given in Figure 4.1a are:

- ❖ Simulation;
- ❖ Data acquisition;
- ❖ Data storage;
- ❖ Optimisation problem solution.

This system does not include transfer of data from the remote end back to the local PC.

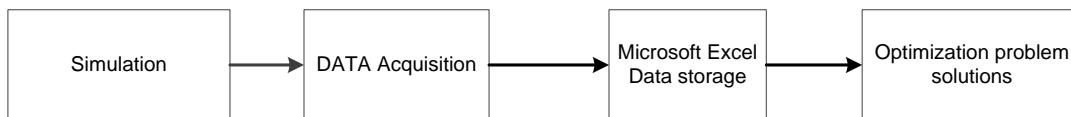


Figure 4.1a: RTDS PB5 card LabVIEW/MATLAB-based lab-scale system functions

The functions of the RTDS PMU-based system are described below together with the data transfer to the remote end, which is regarded as the power system control center (see Figure 4.1b).

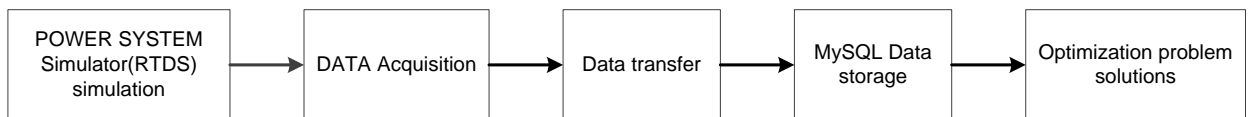


Figure 4.1b: RTDS GTNET card PMU-based lab-scale systems functions

The specification for the two lab-scale systems are determined according to number of simulation outputs, time for data acquisition, time for data transfer, type of synchronization, and time for the solution of the optimal dispatch problem.

The specifications determined for the two lab-scale systems are given in Table 4.1.

Table 4.1: Specification values used in the lab-scale system functions

Type of specification	Specification value	
	LabVIEW/MATLAB-based system	GTNET PMU-based system for the five bus power system model
Number of simulation outputs	<ul style="list-style-type: none"> ❖ Five bus power system model has 4 loads, hence 4 output signals are measured using the RTDS PB5 card ❖ Eleven bus power system model has 11 loads, hence 11 output 	48 outputs (one PMU capture 3phase voltage and current magnitudes and phase angles [12

	signals are measured using the RTDS PB5 card	outputs) 4PMUX12=48 outputs
Maximum Time for data acquisition	<ul style="list-style-type: none"> ❖ For the LabVIEW-based system maximum 50 seconds for data acquisition ❖ For the MATLAB-based system maximum 5 minutes for data acquisition 	To maximum milliseconds for data acquisition
Maximum Time for data transfer	From 5 seconds to 5 minutes	Maximum 10 milliseconds
Type of synchronism	LabVIEW/MATLAB-based system is not time synchronized	GPS using IRIG-B time synchronized clock
Type of data storage	Microsoft Excel file storage	MySQL database
Maximum Time for solution of the optimisation problem	10 seconds	10 seconds

All developments in this thesis and presented in this chapter are done according to the specifications described in Table 4.1 above.

4.3 Hardware and software tools

This section briefly describes the different software and hardware modules used in the process of implementation of the data acquisition and data transfer systems. In the next section, the integration of these tools to achieve the desired objectives is presented. The list of hardware and software used for every one of the systems is shown in Table 4.2(a) and 4.2(b).

Table 4.2a: List of the hardware used

List of hardware	
LabVIEW MATLAB-based data acquisition	RTDS GTNET card PMU-based data acquisition
Real Time Digital Simulator (includes PB5 Card)	Real Time Digital Simulator (includes GTNET)
NI 6343 USB DAQ	SEL 2407 Satellite Synchronized Clock
PC at the Local end	PC at the remote end

Table 4.2b: List of software used

List of software	
LabVIEW/MATLAB-based data acquisition	RTDS GTNET card PMU-based data acquisition
RSCAD	RSCAD
NI LabVIEW 2011	OpenPDC
NI DAQmx 9.8 Driver	PMU connection tester
MATLAB Data Acquisition Toolbox	MySQL database
MATLAB for optimisation problem solution	MATLAB for optimisation problem solution
Microsoft Excel	

4.3.1. Hardware tools

The hardware tools used in the thesis for data generation, data capturing, and data storage in real-time are shown in Table 4.2(a). Some important development characteristics and specification of these tools for the lab-scale system are shortly described below:

4.3.1.1 Real Time Digital Simulator (RTDS)

The RTDS (Real-Time Digital Simulator) is a digital simulator, performs real-time simulations with a 2 microsecond time step. This platform was developed by RTDS Technologies Incorporated located in Manitoba. The ability to simulate models in real-time with the RTDS, allows the user to develop and test protection and control models for power systems (RTDS Technologies, 2014).

The RTDS also supports hardware cards and some of these include: an Inter-Rack Communication (IRC) Card, a Workstation Interface (WIF) Card, a Digital Input and Output card. All communication between the RTDS and the Personal computer (PC) is facilitated by the WIF card. The IRC card deals with the communication between the different racks of the simulator. The RTDS at the Centre for Substation Automation and Energy Management Systems (CSAEMS) within the Electrical Engineering Department at the Cape Peninsula University of Technology consists of two cubicles with two processor racks in each one (as shown in Figure 4.2). These two contain two processor cards as known as PB5 cards. The PB5 card is the processor card for solving equations that represent the mathematical models of the power system components and the control system components modelled within the RSCAD environment. Each PB5 card contains two Freescale MC7448 RISC processors, which operate at a maximum clock speed of 1.7 GHz. These cards contain 12 loading units, which allow a number of components to be included on one card. Each card can handle 72 single-phase nodes or 24 three-phase nodes. If the cards are properly configured it is possible to simulate networks up to a maximum of 72 nodes. Table 4.3 shows the specifications of the PB5 processor card.

Table 4.3: PB5 card specification

Card Type	PB5
Year	2015
Processor type	Freescale MC7448 RISC
Clock speed	1.7 GHz

No. of processors per card	2
Load units per processor	12
Network solution (max nodes)	$72 \times 2 = 144$
Number of I/O fiber ports	2
Number of Communication Ports	6
Number of 12 bit d/a's	24



Figure 4.2: Real-Time Digital Simulators (RTDS) in the Centre for Substation Automation and Energy Management Systems (CSAEMS)

Real-time power system data acquisition and data transfer is carried out using the analog output of the PB5 card of the RTDS (local end) and the GTNET PMU-based system is used for the remote end.

4.3.1.2 SEL-2407 satellite synchronized clock

The SEL-2407 (SEL, 2014) is a satellite synchronized clock shown in Figure 4.3 and is used in this thesis for time-stamping that supports the Inter-Range Instrumentation Group B (IRIG-B) time code output for the synchrophasor devices with the RSCAD simulation model. Since there is a requirement for time-stamped Phasor Measurement Unit (PMU) measurements from different parts of the power network, the PMUs need to be synchronized to a basic time-source. The time-source that is chosen is the facilitated Universal Time (UTC) as described in Chapter 3. The PMUs and RTDS are

synchronized using the SEL-2407clock. The device is connected with a BNC (Baynet Neill-Concelman) connector to a Global Positioning System (GPS) antenna that receives the UTC signal from the satellites. The GPS signal is converted to the IRIG-B type time format to the PMUs and the Giga Transceiver Synchronization Card (GTSYNC) card of the RTDS. With the UTC as time reference the actual PMUs and software PMUs (within the RTDS) can time-stamp their measurements, so that the PDC can time-adjust the received data and give an accurate perspective of the power system operation (Diakos et al., 2012).



Figure 4.3: SEL-2407 Satellite - Synchronized Clock (SEL, 2014)

4.3.1.3 National Instrument (NI) 6343 USB Data Acquisition (DAQ) card

The Data Acquisition (DAQ) card samples the real world signals to produce data that can be interpreted by a computer. The components of the DAQ system incorporate sensors that change any measurement parameter to an electrical signal, which is obtained from the DAQ hardware. In the considered case the measurements are acquired from the RTDS PB5 card front panel analog outputs.

The NI USB DAQ 6343 card supports 16 differential or 32 single ended channels, 16-bit resolution and sampling rate of 500 KS/s for the signal input range of $\pm 10V$. The pin diagram for the NI DAQ card 6343, is given in Figure 4.4.



Figure 4.4:The block and pin diagram for the NI 6343 DAQ card (National Instruments, 2014)

4.3.1.4 Personal computer at the remote end location

The personal computer is used in the two developed data acquisition and data transfer systems. The PC at the local end is configured with the RSCAD, LabVIEW, and MATLAB software for system one and with the PMU connection tester, OpenPDC, MySQL and MATLAB software for system two at the remote end.

4.3.2 Software tools

The software tools used in the thesis for data acquisition, processing and transfer in real-time are shown in Table 4.2(b)

4.3.2.1 RSCAD software suite

The RSCAD software for use with the RTDS is equipped with a library of accurate models of the power system components, which can be used to build simulation models of the power system network. In addition, a Graphical User Interface (GUI) is provided and can be used to design and analyze power system network models (Monali, 2002). The existing analogue simulators are used to compute voltage and current values continuously; which limit their speed and capability. Digital simulators perform computations when the state changes at discrete instants in time. This allows the simulator to perform faster. It is easy to make changes in the digital simulation schemes. Evaluation and test of network designs or upgrades can be accurately performed using RTDS (Monali, 2002; Povh et al., 2004).

The RSCAD software is the graphical user interface where the models are created, simulated, modified and executed. In this environment results can be analyzed and data can be acquired. All interactions between the user and the RTDS Simulator occur with the use of the graphical user interface within the RSCAD environment. The most frequently used modules of RSCAD are Filemanager, Draft and Runtime. Figure 4.5 shows the architecture of the RSCAD software suite.

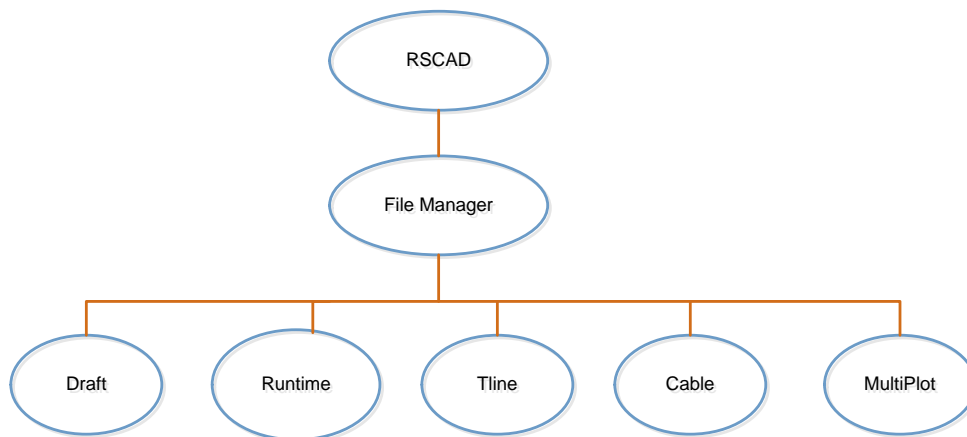


Figure 4.5 : RSCAD architecture (RTDS Technologies, 2014)

1. File Manager

The file manager module is the first module in the development of the simulation models. The rest of the supported modules within this environment are accessible using the File manager module.

2. Draft

The Draft module allows the user to design and develop the simulation module with the required parameters being input. The entire model is developed graphically and is not text-based. The Draft module supports power system and control system libraries with their associated components. Upon completion of the model design, it can be saved for compilation and finally simulation. The power system model can be viewed in either 3-phase or Single Line Diagram (SLD) format. Draft also has the ability to include a hierarchy so that circuit detail can be hidden from view in higher levels.

3. Runtime

The Runtime module allows one to execute of the model with the RTDS Simulator. A user-interface is created which can be simulated, downloaded and controlled. Meters, plots and sliders can be viewed and adjusted while the simulation is being executed. Text can be added for clarity and data can be saved for further processing.

4. Compiler

The compiler is the bridge between the user interface software and code that is executed on the RTDS platform. The parameters from the draft module together with the model are used to provide the processor code using the compiler. The assignment of each processor during the simulation is performed by the compiler – this can be manually done or is automatically performed. The “MAP file” for use by the operator contains the complete input/output information, and is also produced by the compiler.

5. Component Model Libraries

The compiler uses a predefined library of power system and control system components for the production of the code required by the processors. The simulation time step is proportional to the size of the model; therefore the component models within the libraries are optimized. The component models are developed in Assembler language; however the user is not required to develop any models using this language. Using the Component Builder module, the user can also develop custom user-defined components to use in the model development.

In this thesis, the RSCAD software is used to build the power system model and to analyse the system performance in real-time. The power system variables are transported from the RTDS hardware structure in real-time to solve the economic dispatch problem using the developed data acquisition and data transfer systems.

4.3.2.2 National Instruments (NI) LabVIEW

LabVIEW (Laboratory Virtual Instrument Engineering Workbench), created by National Instruments (NI), is a graphical programming language that is easy to use and is utilized to create complex measurement and control applications rapidly and effortlessly.

LabVIEW utilizes dataflow graphical programming language, where the execution is dictated by the structure of a graphical block diagram. LabVIEW projects/sub - subroutine are called Virtual Instruments (VIs) as a result of their appearance and their imitation of actual instruments. A LabVIEW VI fundamentally comprises of three sections. These are block diagram, front panel, and a connector board. Essentially the front panel is a client interactive interface which permits inputting or concentrating information. The real executable code inherent to represent the VI is utilizing the predefined and user-defined blocks. A subVI can be utilized to represent the VI, that it must be utilized as a subroutine. Ordinarily, a VI inside an alternate VI is known as sub VI.

4.3.2.3 NI DAQmx 9.8 driver

The NI DAQ driver software interfaces the LabVIEW VIs with the DAQ hardware devices and helps in developing complete instrumentation acquisition and control application. Analogue or digital signals can be given as input parameters to LabVIEW for processing and output parameters can be interfaced to other hardware devices. Real-time signals can be processed and analyzed using these DAQ interfaces. The NI driver is interfaced with LabVIEW graphical software to capture the real-time RTDS data using the NI6343 card analog output signals for development of the LabVIEW/MATLAB-based data acquisition systems

4.3.2.4 MATLAB software

MATLAB is one of the most widely used tools in scientific and technical computing (Text Mining with MATLAB®, 2013). It began in 1970 as an intelligent interface to LINPACK and EISPACK, a set of Eigen value and linear system solution routines. It has since developed to a feature rich item using advanced numerical libraries, for example, FFTW and ATLAS and with toolboxes in number of uses for example financial mathematics, neural networks and control theory. It has implicit translated language that is similar to FORTRAN. MATLAB gained popularity as a result of its ease of use. It has been broadly used in classrooms as an educating instrument. Its solid graphical abilities make it a great data analysis tool. Additionally, researchers have been known to construct exceptionally very complex systems utilizing MATLAB script and toolboxes (Choy and Edelman, 2005).

The software for the Lagranges algorithm described in Section 5.5 (Chapter 5) is

programed in the MATLAB environment to solve the economic dispatch problem.

4.3.2.5 MATLAB data acquisition toolbox

The Data Acquisition Toolbox (MATLAB DAQ, 2005) supports a few commands to configure the equipment including the command for detecting the hardware, configuring them for use with MATLAB, sending signals to the output and acquiring the signal from the input. The one of the objectives of this thesis is to develop MATLAB data acquisition software code that controls modal test from the earliest starting point to the end. This code is the bridge between the National Instruments (NI) equipment, the test structure and the computer. Figure 4.6 shows a connection between the DAQ toolbox, MATLAB and the hardware.

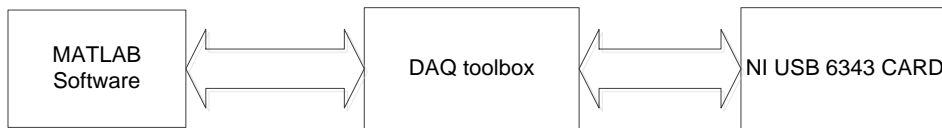


Figure 4.6: MATLAB DAQ toolbox connection

4.3.2.6 PMU connection tester

The PMU Connection Tester is an open source tool made available by the Grid Protection Alliance (<http://Pmuconnectiontester.com>, 2014). It can be used to test the data stream from any known phasor measurement device

4.3.2.7 OpenPDC software

The OpenPDC (so named as it is open-sourced) runs as a Windows service where the data concentrator parser responds to changes in the streaming data. The OpenPDC can process any data such as temperature, voltage, current, vibration, location, luminosity and phasor data; as long as it is time-stamped. It is important to note that the Real-time Digital simulator (RTDS) phasor measurement unit supports only voltage and current signals. (www.openpdc.com, 2014).

This thesis uses the real-time GTNET phasor measurement unit signals, which are transferred and are monitored at the remote end using the OpenPDC software and the remote connection between the host and remote end PC is tested using the PMU connection tester.

4.3.2.8 MySQL workbench integrated development tool

The MySQL workbench provides a graphical tool for the MySQL database interactions. It is used for database design and modeling Structure Query Language (SQL) development and server administration as shown in Figure 4.7.

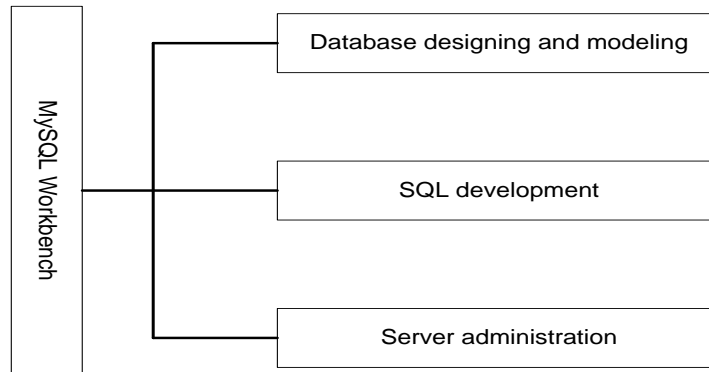


Figure 4.7: Block diagram of the MySQL workbench (Guru, 2012)

- MySQL workbench IDE (Integrated Development Tool) allows programmers and database administrators to create database design models that can be easily translated into MySQL database.
- MySQL workbench supports and creates multiple database models in the same environment.
- MySQL workbench supports all objects to view, store and trigger the data from the MySQL database.

This thesis uses the MySQL database to store the GTNET card PMU real-time data from the OpenPDC software using the MySQL query in the MATLAB environment.

4.4 Method One: Implementation of a lab scale data acquisition system using the PB5 card analog output channel

To implement all requirements for the design and implementation of the lab-scale data acquisition system, a flowchart representing the sequence of the functions to be performed and the hardware and software needed to implement these functions is designed. The proposed flowchart is shown in Figure 4.8

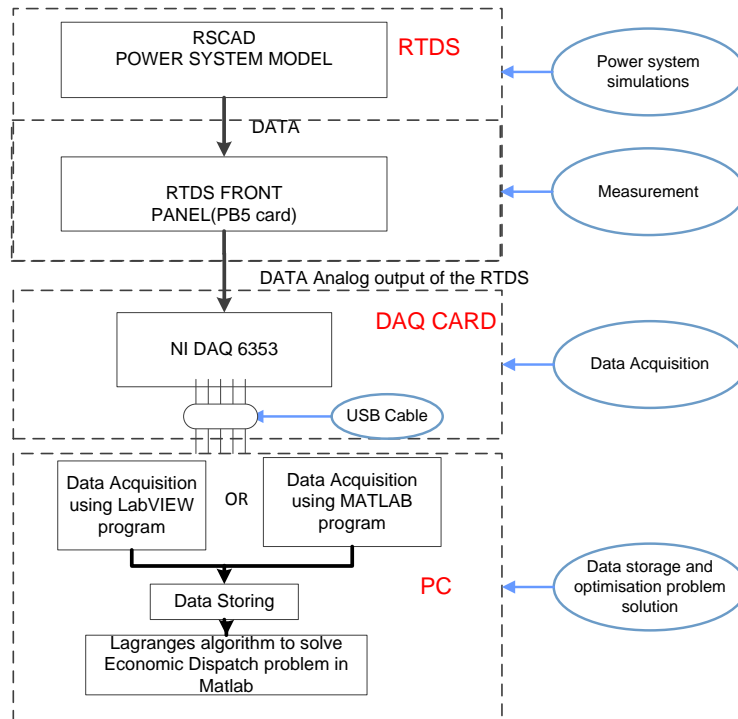


Figure 4.8: Flow diagram of the lab-scale data acquisition system using the LabVIEW and MATLAB environments to acquire and transfer data and to solve the economic dispatch problem

This thesis considers two cases of power system models: the five and eleven bus power system models for the lab-scale data acquisition and data transfer system. The power system models are simulated in the RSCAD environment in order to produce data needed for the dispatch problem solution. The implementation of the flowchart in Figure 4.8 is done through the integration of the hardware and software components by physical wiring, determination of the parameters, and software configuration for use with the given hardware. The structure of the integrated data acquisition systems using the RTDS front panel PB5 card system is shown in a block diagram in Figure 4.9. The results from the simulations of the power system models are sent from the RSCAD environment to the RTDS front panel analog output channels. LabVIEW/MATLAB programs are used to measure the output signal from the RTDS front panel by the NI DAQ 6343 card. The acquired data is then sent by an USB cable to the local control center PC and is saved in Microsoft Excel files formats. Finally, the data retrieval from the MS Excel file is carried out by a MATLAB program which uses this data to solve the economic dispatch problem in real-time. The next section discusses the implementation

and setting of all components of the RTDS PB5 card analog output signals-based lab-scale system.

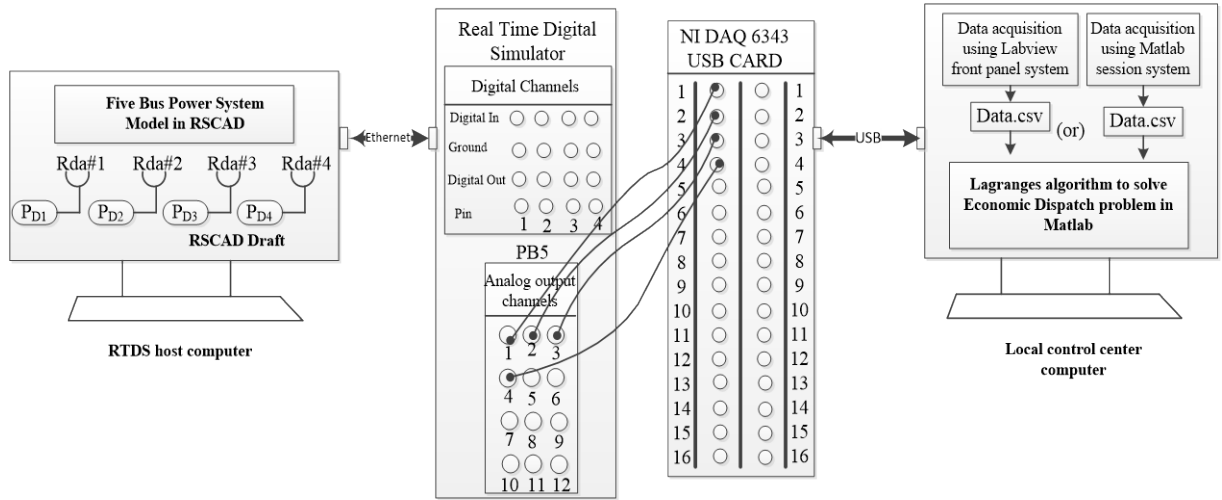


Figure 4.9: Block diagram for the lab-scale data acquisition system in LabVIEW and MATLAB environment to solve the Economic Dispatch problem

4.4.1 Assignment of the power system data to the RTDS front panel PB5 card

The five-bus power system is modelled in the RSCAD software suite of RTDS. The power system consists of three generators, four loads and seven transmission lines (Kothari and Dhillon, 2006). The real powers of the four loads (power demands) are sent to the RTDS PB5 card front panel analog output channels using the RSCAD analog output module. The common setting of the analog output component provides an analog output channel number, scaling factor, card type and assigned control processor. The RSCAD output component “load 1” (power demand P_{D1}) is shown in Figure 4.10.

rtds_sharc_ctl_AOUT					
Parameters					
Name	Description	Value	Unit	Min	Max
DA	Analogue Output Channel	1		1	12
SC	Floating Point Value <--> 5 volts	20		1.0e-6	
SL	Include dynamic scale & offset sliders?	No		1	0
Icon	Show component icons as	Large			
prtyp	Solve Model on card type:	GPC/PB5		0	1
Proc	Assigned Controls Processor	3		1	54
Pri	Priority Level	2		1	999

Figure 4.10: RSCAD output components setting

In the setting of the analog output module, the scaling factor is set according to the range of the measured load power. In the five bus power system, the real power of load1 (P_{D1}) is determined to be 20 MW, to optimize the range of the analog output module of the RTDS, that has a maximum operating voltage range of [0-10]. The NI –DAQ card’s range is ± 10 Volt, therefore the appropriate scaling factor is 5 Volts for 1 Unit. Therefore if the real power load (P_{D1}) is 20 MW, the voltmeter will read 5 Volts at the input to the DAQ card.

4.4.2 Configuration of the NI DAQ 6353 card in LabVIEW software to measure the RTDS output signal

The main function of the LabVIEW program is to ensure the correct measurement of the output signal from the RTDS front panel. This signal is an input signal for the data acquisition system.

The LabVIEW program was created by making use of the front panel components (within the software environment) and the LabVIEW graphical programming tools. The graphical program provides the logical control and manipulation of the front panel parameters in order to achieve the desired functionality.

The graphical program (block diagram) is illustrated in Figure 4.11 below. The explanation of the LabVIEW program alternatively describes the corresponding components from the LabVIEW front panel and those from the LabVIEW graphical program to maintain clarity. To start off the complete LabVIEW graphical and front panel programs are presented in Figures 4.11 and 4.12 respectively.

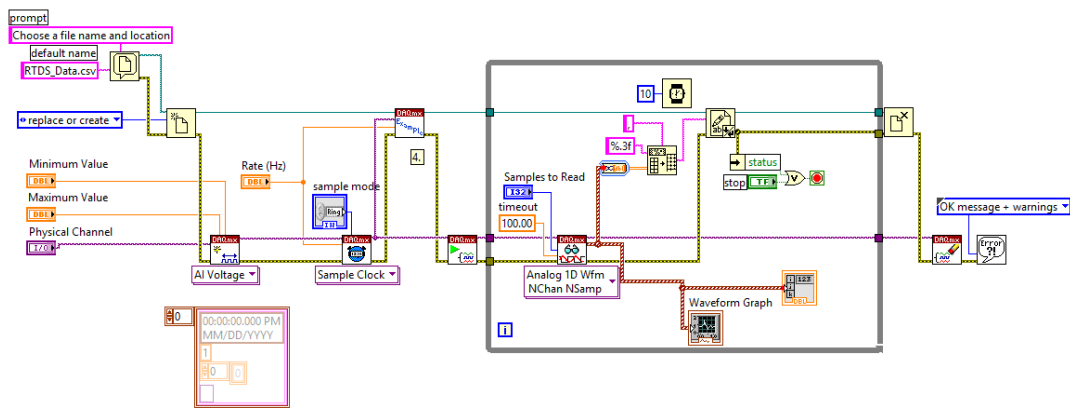


Figure 4.11: LabVIEW Block diagram to capture the RTDS voltage output signal

The separate parts of the block diagram in Figure 4.11 are explained below for the NI DAQ configuration, saving the acquired data in files, and the functions to manipulate the acquired data (while loop).

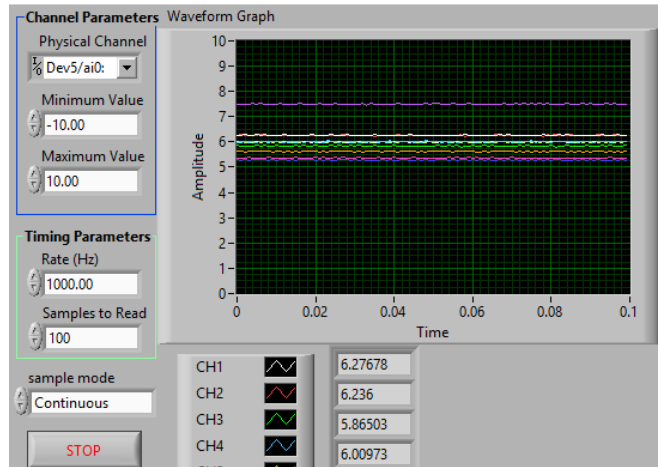


Figure 4.12: LabVIEW front panel monitoring the RTDS voltage output signal

4.4.3 NI DAQ card physical channel configuration for data acquisition

Before acquiring data from a specific channel on the NI-DAQ card, the channel has to be configured first. The configuration of the channel is facilitated by the NI-DAQmx graphical programming blocks, which allow different channel parameters to be set so that the data is acquired as desired. The parameters for this particular analog channel used for the test are set up as shown in Figure 4.13 below:

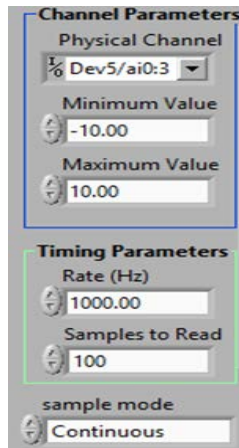


Figure 4.13: NI DAQ card channels and timing parameter setting in LabVIEW

As shown above the analogue input (ai0) was chosen for the “load 1”. In the same manner the channels ai1, ai2 and ai3 are selected for “load 2”, “load 3” and “load 4”

respectively. The voltage ranges are set to ± 10 Volts. A continuous sampling mode was chosen with a sampling frequency of 1000 Hz for real-time data acquiring. A maximum of 100 samples are read in a single acquisition cycle.

4.4.4 File saving option

Since the acquired data is to be saved in the MS Excel file format, a directory for saving has to be specified. The filename is also specified and this is done through the File Dialog Express VI LabVIEW. The LabVIEW graphical diagram for this is illustrated in Figure 4.14.

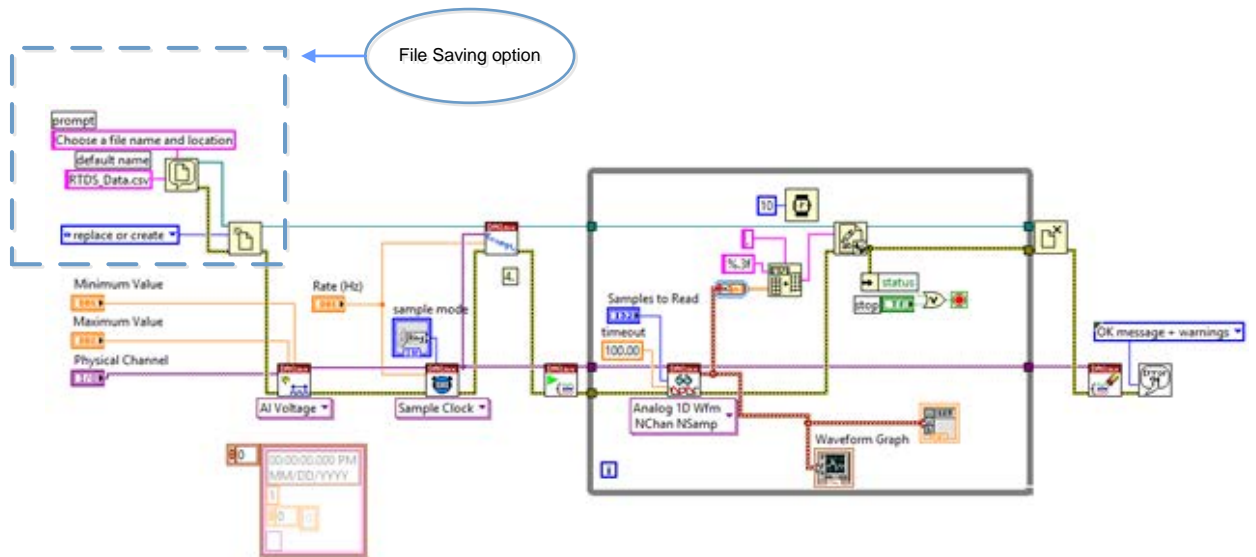


Figure 4.14: LabVIEW block diagram of file saving setting in LabVIEW

Once the filename and directory for file saving are specified, the data obtained from the analog channels is retrieved using a *While loop* which incorporates logical commands and graphical functions to manipulate the acquired data as arrays before the file logging. Figure 4.15 below shows the *While loop*.

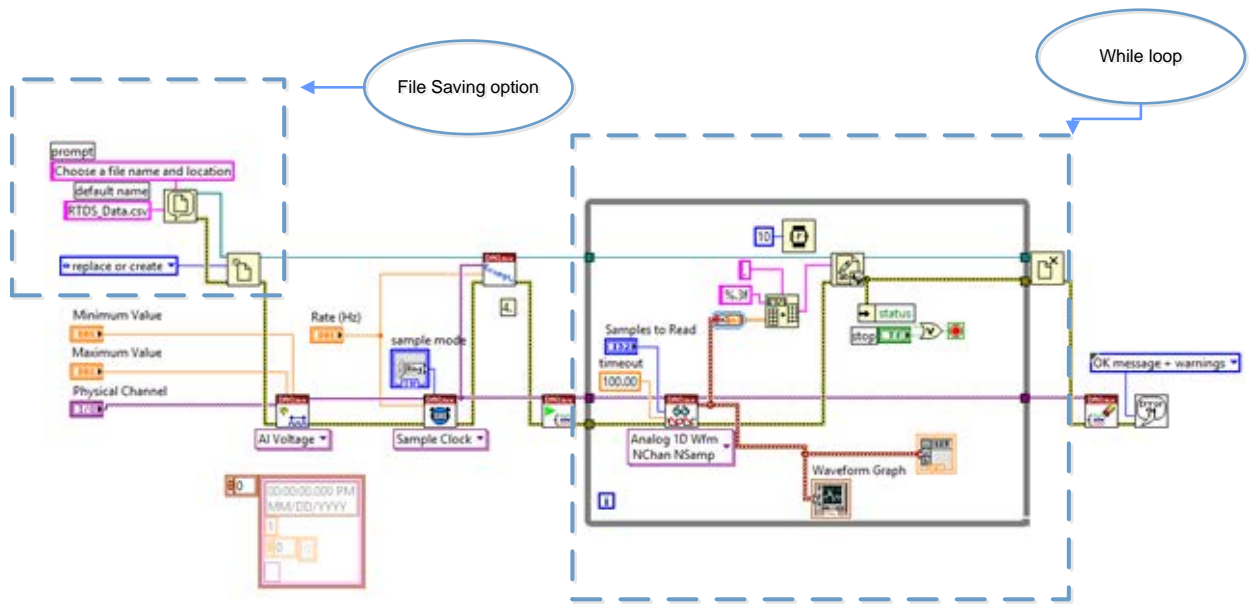


Figure 4.15: LabVIEW block diagram of *While* loop program for DAQ

Firstly, the *While loop* executes the logical instructions within iterations that are separated by a time period of 10ms. The program structure is better understood from the left hand side of Figure 4.15. Three signals are passed into the *While loop*. The top-most signal passes the file name and properties through to the *Write to Text File* Function. These file properties are passed within each iteration of the loop, so that data is continuously saved to the specified file.

The second signal (from the top) which is passed into the loop via the *DAQmx Start Task* (VI) is the channel number. This signal carries the identification parameter for the signal which is being logged at a particular time to all the VIs which is involved in the data acquisition and file saving processes.

Within the loop, the signal first passes through the *DAQmx Read* (VI), which records data from the analog channel. The *DAQmx Read* (VI) also has the sampling information (settings) and an error signal passed to it as an input. The data from the *DAQmx Read* (VI) is then saved as an array and also viewed graphically by using the *Waveform* VI. The acquired data is then converted from dynamic data into array by the *Convert function* from the *Dynamic Data Express* VI. Finally, the array conversion is carried out by the *Array to Spreadsheet String* Function. This step allows the saving of the data into

spreadsheet files in the form of tab separated strings. The *Write to Text File* Function then completes the file writing process. The file is then closed and a notification for an error or successful logging is then issued.

The saved analog data which represent the different load values in MS Excel is then used by the MATLAB Lagrange's algorithm to solve the economic dispatch problem in real-time.

4.5 Method Two: Implementation of a lab scale data acquisition system using RSCAD GTNET card Phasor Measurement Units (PMUs)

The fundamental concepts governing synchrophasor technology-based data acquisition and data transfer for power system economic dispatch problem solutions is explained in this section, the following subsections are aimed at giving the technical steps taken in development of the lab-scale system based on the RSCAD GTNET-PMU card, the PMU connection tester and the OpenPDC software. The data from the OpenPDC is then archived in a database using MySQL database and Microsoft Database tools shown in Figure 4.16.

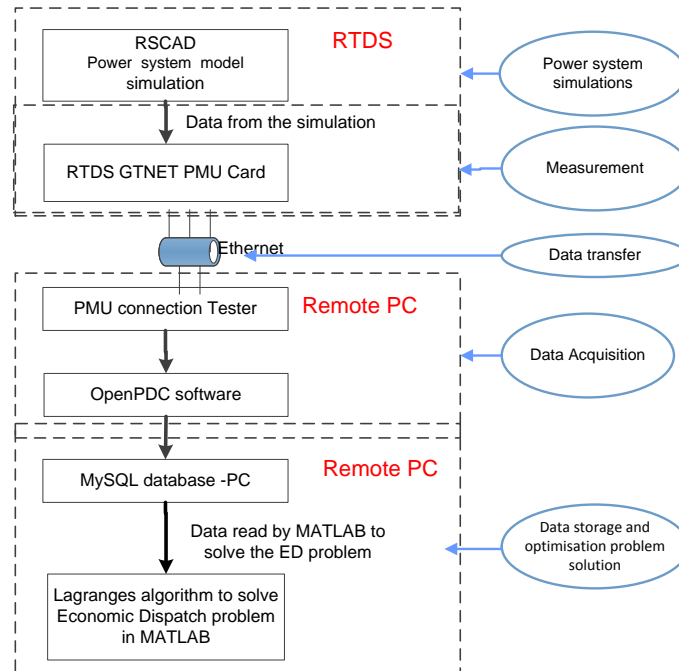


Figure 4.16: Flow diagram of the lab-scale data acquisition and data transfer system using the RTDS GTNET PMU technology to acquire and transfer data and to solve the economic dispatch problem

The structure of the developed RTDS GTNET card PMU-based laboratory scale system to solve the economic dispatch problem in real-time is shown in Figure 4.17, where the RTDS generates the voltages and currents within the RSCAD software environment. These signals are then fed to the software-based PMUs (GTNET-PMUs). The measured data from the GTNET-PMU are transferred to the Phasor Data Concentrator (PDC) using Ethernet communication. The GTNET card PMU used is configured within the RSCAD library and is synchronized to the GPS using a SEL-2407 satellite clock with an antenna. The RTDS GTNET PMU card allows one to use a maximum of 8 independent PMUs to provide symmetrical component information related to the 3-phase sets of voltages and currents, conforming to the IEEE-C37.118 standard. A single PMU can provide a total of 12 phasors (3 phase voltage and current magnitudes and phase angles), the measured frequency, the rate of change of frequency as well as 4 analogue values and a 1 to 16 bit digital value (http://www.pacw.org/september_2013.htm). The described RTDS output signals with the desired parameters are generated from the RTDS using a GTNET card. From the GTNET card fixed in the rack-1 of the RTDS, voltage and current signals are sent to the remote end via Ethernet. On the remote end, the OpenPDC software is used to capture the RTDS signals in real-time. These signals are archived in the MySQL database. Every five minutes, the data is retrieved from the MySQL database to the MATLAB environment. The Lagranges algorithm developed by (Krishnamurthy and Tzoneva, 2013) is used to solve the Economic Dispatch (ED) problem using the real-time data which is retrieved from the MySQL database. Implementation of the separate modules of the lab-scale data acquisition and transfer system is described below:

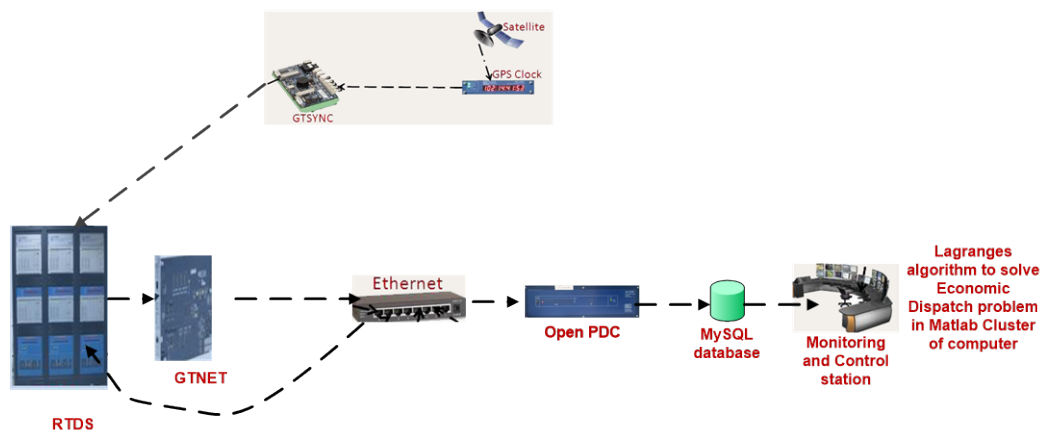


Figure 4.17: Block diagram for the lab-scale data acquisition system based on the RTDS GTNET card PMU to solve the economic dispatch problem

4.5.1 RSCAD GTNET card PMU module

The GTNET configuration tab provides a means of identifying the GTNET hardware of the RTDS, external output of the C37.118 data stream, the PMU performance class, configuration frame format, nominal frequency and some other parameters. The GTNET card PMU in the RSCAD software has the following menus for configuration: PMU configuration, PMU AC source, PMU Calibration and PMU Analog/Digital source.

4.5.1.1 Common setting in the GTNET card PMU

The common configuration setting in the GTNET card PMU provides the PMU model type, configuration frame format, base frequency, maximum number of PMUs, options to enable the angle difference meter, Giga Transceiver Input and Output (GTIO) fiber port number, GTNET PMU card number, order of the phase rotations either ABC or ACB, and assigned control processor number. The GTNET card PMU configuration is shown in Figure 4.18

The PMU configuration parameters are given in Table 4.4, this setting is used in the laboratory set-up, and the rest of the parameters in the GTNET configuration window are used at their default values.

The screenshot shows a configuration window titled 'rtds_GTNET_PMU_v4.def'. It has several tabs: 'PMU1-8 ANALOG/DIGITAL SOURCE', 'PMU4 CONFIG', 'PMU1-8 CALIBRATION', 'PMU1-8 AC SOURCE', 'CONFIGURATION', 'PMU1 CONFIG', 'PMU2 CONFIG', and 'PMU3 CONFIG'. The 'CONFIGURATION' tab is active, displaying a table of parameters.

Name	Description	Value	Unit	Min	Max
eC37data	Enable output of C37.118 data using GTNET	Yes		0	1
Name	GTNET Component Name	RTDSPMU			
pmutype	PMU Model Type	Anne...		0	2
cfgtype	Configuration frame format	Confi...		0	1
freq	Base Frequency (Hz)	50.0		0	1
nPMU	Number of PMUs (maximum 8)	4		0	8
adv	Delay Input Signal to align V & I	None		0	1
eAngM	Enable Angle Difference Meter	NO		0	1
nAngDiff	Angle Difference Meter Name (PMUx-PMUy)	angdiff		0	0
sfx	Plot Signal Suffix				
calib_const	Common offset applied to all PMU inputs	0	degre...	-360.0	360.0
dt_adj	Time-step adjustment to all input signals	-1	dt	-500	500
ePri	Enable Primary Signals	YES		0	1
GT_SOC	GTSYNC advance TIME signal name	ADVSECD		0	0
GT_STAT	GTSYNC advance STAT signal name	ADVSTAT		0	0
phs_rot	Phase Rotation	ABC		0	1
Port	GTIO Fiber Port Number	1		1	8
Card	GTNET_PMU Card Number	1		1	8
Proc	Assigned Controls Processor	1		1	40
Pri	Priority Level	1		1	

At the bottom of the window are three buttons: 'Update', 'Cancel', and 'Cancel All'.

Figure 4.18: GTNET-PMU configurations setting

Table 4.4: PMU configuration parameter setting

Description	Value
Enable output of C37.118 data using GTNET	Yes
GTNET component name	RTDSPMU
Configuration frame format	Config 2
Base frequency	50.0
Number of PMUs	4
GTIO fiber port number	1
GTNET_PMU Card Number	1
Assigned control processor	1
Priority level	1

4.5.1.2 User-defined RSCAD GTNET card PMU configuration setting

The GTNET card PMU provides a user-defined action to select any number of PMUs from the available eight maximum PMUs per one GTNET card. This thesis uses four PMUs based on the IEEE C37-118 standard to transfer the three-phase current and voltage signals from the power system model simulation measurements to the remote end. Each PMU configuration has user-defined signal frame rates at either 50 or 60 Hz.

The RSCAD GTNET card PMU configuration has user-defined station name, hardware ID code, Transmission Commission Protocol (TCP) number options to select the number of phasor signals (maximum six signals: three-phase voltages and currents), and an option to select the phasor number format either in real or integer ones. The Phasor Number Format is defined in the IEEE C37.118.2-2011 standard depending on the communication bandwidth available. If 'Real' is chosen as the phasor number format, the phasor would have 32-bit floating-point values. The 'Integer' Phasor number format would support 16-bits.

There is option to select the phasor output format either in magnitude and phase angle (or) real and complex formats. In addition to that, it has an option to select the frequency signal number format, number of analog values, analog signal number format, user-defined names for the six phasor signals (VA,VB,VC,IA,IB,IC), and an option to monitor either all the six or a specific signals in runtime. If there is a need to transfer the digital signals, there are some options available in the PMU configuration, but this thesis uses only analog signals. The GTNET card PMU configuration is shown in Figure 4.19

rtds_GTNET_PMU v4.def					
PMU1-8 ANALOG/DIGITAL SOURCE					
PMU1-8 AC SOURCE					
PMU3 CONFIG		PMU4 CONFIG		PMU1-8 CALIBRATION	
CONFIGURATION		PMU1 CONFIG		PMU2 CONFIG	
Name	Description	Value	Unit	Min	Max
p1FPSa	Reporting Rate (frames)	50		0	10
p1FPSb	Reporting Rate (frames)	50		0	6
p1deci...	Decimate PMU runtime	YES		0	1
p1STN	Station Name	PMU1			
p1IDC	Hardware ID Code	10		1	65534
p1TCP	Output TCP/IP or UDP	1000		1	65535
p1CFG	Configuration Change	0		0	32767
p1PH...	Number of Phasors	6		0	12
p1lorFp	Phasor Number Format	REAL		0	1
p1OUTF	Phasor Output Format	Cn & phi		0	1
p1lorFf	Frequency Number Fo...	REAL		0	1
p1IAout	Number of Analog valu...	0		0	4
p1lorFa	Analog Number Format	REAL		0	1
p1IDout	Number of 16 bit Digit...	0		0	1
p1LAT	PMU1 Latitude in degr.	49.88619		-90.0	90.0
p1LON	PMU1 Longitude in de...	-97.153191		-180.0	180.0
p1ELEV	PMU1 Elevation in met...	4294		0	4294
p1ePH...	Phasor 1 PMU Output	VA		0	0
p1ePH...	Phasor 2 PMU Output	VB		0	0
p1ePH...	Phasor 3 PMU Output	VC		0	0
p1ePH...	Phasor 4 PMU Output	IA		0	0
p1ePH...	Phasor 5 PMU Output	IB		0	0
p1ePH...	Phasor 6 PMU Output	IC		0	0

Figure 4.19: User-defined RSCAD GTNET PMU configuration

4.5.1.3 RSCAD GTNET card PMU AC source

The instrument transformer's (PTs and CTs) turns ratios are defined in the RSCAD GTNET card PMU AC source. Figure 4.20 shows the four PMUs with the user-defined input signal names for the three-phase voltage and current signals. The default turns ratio setting used in the PTs and CTs are 2000:1 and 600:1 turns respectively.

rtds_GTNET_PMU v4.def					
PMU1-8 ANALOG/DIGITAL SOURCE					
PMU4 CONFIG		PMU1-8 CALIBRATION		PMU1-8 AC SOURCE	
CONFIGURATION		PMU1 CONFIG		PMU2 CONFIG	
PMU3 CONFIG		PMU2 CONFIG		PMU3 CONFIG	
Name	Description	Value	Unit	Min	Max
rVT1	PMU1_Turns Ratio : 1	2000.0		1.0	10000.0
rVTA1	PMU1_A phase Input Signal Name	V2A			
rVTB1	PMU1_B phase Input Signal Name	V2B			
rVTC1	PMU1_C phase Input Signal Name	V2C		0	0
rCT1	PMU1_Turns Ratio : 1	600.0		1.0	5000.0
rCTA1	PMU1_A phase Input Signal Name	I2A		0	0
rCTB1	PMU1_B phase Input Signal Name	I2B		0	0
rCTC1	PMU1_C phase Input Signal Name	I2C		0	0
rVT2	PMU2_Turns Ratio : 1	2000.0		1.0	10000.0
rVTA2	PMU2_A phase Input Signal Name	V3A			
rVTB2	PMU2_B phase Input Signal Name	V3B			
rVTC2	PMU2_C phase Input Signal Name	V3C		0	0
rCT2	PMU2_Turns Ratio : 1	600.0		1.0	5000.0
rCTA2	PMU2_A phase Input Signal Name	I3A		0	0
rCTB2	PMU2_B phase Input Signal Name	I3B		0	0
rCTC2	PMU2_C phase Input Signal Name	I3C		0	0
rVT3	PMU3_Turns Ratio : 1	2000.0		1.0	10000.0
rVTA3	PMU3_A phase Input Signal Name	V4A			
rVTB3	PMU3_B phase Input Signal Name	V4B			
rVTC3	PMU3_C phase Input Signal Name	V4C		0	0
rCT3	PMU3_Turns Ratio : 1	600.0		1.0	5000.0
rCTA3	PMU3_A phase Input Signal Name	I4A		0	0
rCTB3	PMU3_B phase Input Signal Name	I4B		0	0
rCTC3	PMU3_C phase Input Signal Name	I4C		0	0
rVT4	PMU4_Turns Ratio : 1	2000.0		1.0	10000.0
rVTA4	PMU4_A phase Input Signal Name	V5A			
rVTB4	PMU4_B phase Input Signal Name	V5B			
rVTC4	PMU4_C phase Input Signal Name	V5C		0	0
rCT4	PMU4_Turns Ratio : 1	600.0		1.0	5000.0
rCTA4	PMU4_A phase Input Signal Name	I5A		0	0
rCTB4	PMU4_B phase Input Signal Name	I5B		0	0
rCTC4	PMU4_C phase Input Signal Name	I5C		0	0

Figure 4.20: RSCAD GTNET PMU AC Source

4.5.1.4 RSCAD GTNET card PMU calibration

The RSCAD GTNET card PMU anti-alias filter component has a group delay that is related to the coefficients that are generated at the power system models compilation process, with the specified simulation time-step. A change in the time-step results in a change to the group filter delay. During the compilation time, the RSCAD GTNET card PMU does a frequency scan in the framework of variation of ± 10 Hz from the nominal one and measures the time delay and frequency magnitude variations (RTDS, 2013). This information is used to calculate the group filters delay using the simulation time-step and to compensate for the group of delay time in the phasor output. A common angle offset can be applied to all signals using the “calibration” parameter found in the configuration. Each PMU has independent angle offsets that can be applied to each voltage and current input (RTDS, 2013).

4.5.1.5 RSCAD GTNET card PMU Analog/Digital source

The user-defined signal names for the analog and digital sources are specified in the PMU Analog/Digital source tab. Table 4.5 shows the GTIO fiber port and GTNET_PMU card number assigned for the RTDS.

Table 4.5: GTIO fiber port number, GTNET card PMU number and the processor card assignment

Rack	GTIO Fiber port number	GTNET card PMU number	Assigned control processor card
Rack1	1	1	3
Rack 2	2	1	2

The GTIO fiber port is used to interface the RTDS with the Intelligent Electronic devices (IEDs) for power system protection applications.

4.5.2 Giga-Transceiver Synchronization Component (GTSYNC)

The GTSYNC card Figure 4.21 has an option to enable both advanced and the GTSYNC card with current time set using the satellite synchronization clock. The GTSYNC component works in conjunction with the GTSYNC card and a source of time synchronization is required for the power system model to run the RTDS *Draft Case*. This thesis uses the time synchronization source as IRIG-B from the SEL-2407 Satellite Synchronization Clock. Figure 4.21 shows the Giga-Transceiver Synchronization card parameter setting.

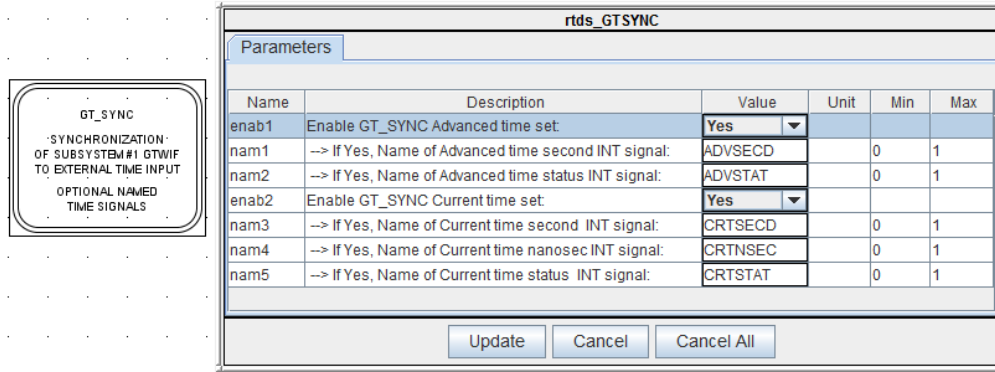


Figure 4.21: GTSYNC card parameter setting

4.5.3 PMU connection tester

The PMU Connection Tester is used to test the data stream from any known Phasor Measurement Device. The main window of the PMU connection tester is shown in Figure 4.22

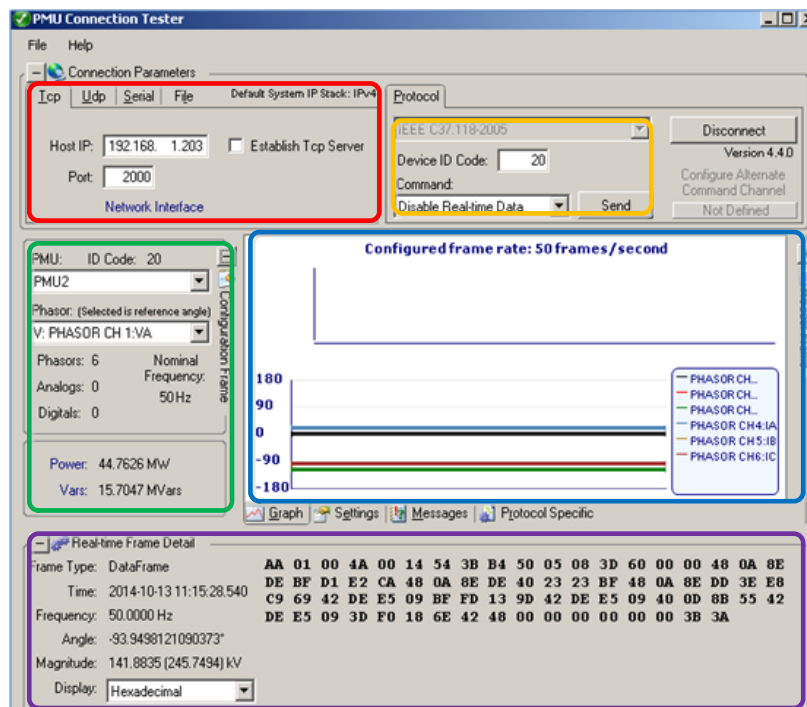


Figure 4.22: PMU connection tester

Configuration of the PMU connection tester for the various parts of main window is described below.

4.5.3.1 PMU connection tester parameter

The host device IP and port number are defined in the PMU connection tester and shown in Figure 4.22 (Red color box)

The Host IP and port number used in the laboratory setup are given below

1. The TCP/IP address of the RTDS rack, is defined in the Host IP : **192.168.1.203**
2. The port number through which the PMU connection tester is connected to and receives data from the RSCAD GTNET PMU device is defined, **2000**

4.5.3.2 Protocol and device ID

PMU connection tester protocol and ID setting are shown in Figure 4.22 (orange color box)

1. The PMU connection tester supports many protocols. This thesis uses IEEE C37.118 -2011 protocol to transfer data from the host to the remote end PC
2. The RSCAD GTNET card PMU Figure 4.19 has a device ID of 20 when is used to establish the connection between the RSCAD GTNET card PMU and the PMU connection tester.

4.5.3.3 Configuration frame

The PMU connection tester configuration frame displays the relevant information from the configured elements in the connected RSCAD GTNET card PMU 2 shown in Figure 4.22. It consists of

1. **PMU:** It shows the configured GTNET PMU which is labelled in the RSCAD software as PMU2
2. **ID Code:** It displays the unique identified code of the GTNET card PMU. This is populated from the device ID code entered on the connection parameter section. in Figure 4.22 (Green color box)
3. **Phasor:** It shows the labels of all phasor signals selected by the GTNET card PMU
4. **Phasors:** It display the total number of phasors in selected GTNET card PMU

5. **Digital:** It shows total number of digital values in the selected GTNET card PMU
6. **Nominal Frequency:** It shows the power system nominal frequency
7. **Power (Megawatts):** It shows the calculated megawatts, based on the voltage and current phasor signals.
8. **Vars (Mvars):** It displays calculated megavars, based on the voltage and current phasor signals.

4.5.3.4 Connection frame used in the PMU connection tester

This section describes the connection frame of the PMU connection tester as given in Figure 4.22 (purple color box). The frame type, system frequency and phasor signal magnitude and phase angle are defined in the connection frame of the PMU connection tester which is described in detail in this section.

Frame type: It displays the received phasor protocol frame type of the frame received from the RSCAD GTNET card PMU2

1. **Frequency:** It displays the measured system frequency received from the RSCAD GTNET card PMU
2. **Angle:** It shows the measured phase angle of the received phasor signal.
3. **Magnitude:** It shows the measured magnitude of the received phasor signal.

To verify the RSCAD GTNET card PMU signal received at the remote end, the following steps have to be followed:

Step 1: Model the power system model in the RSCAD software suite of the RTDS.

Step 2: The simulation results of the RSCAD software measured by the PMUs must be transferred to the remote end location using the TCP port of the GTNET card PMU configuration settings.

Step 3: The PMU connection tester tool is used to verify whether the host end PMU signal is received at the remote end without any data loss.

Once the connection configuration is tested using the PMU connection tester, the corresponding configuration and connection files for each PMU are saved on the remote Personal-Computer (PC) where the OpenPDC software is running. The saved

PMU configuration and the connection files are exported to the OpenPDC software environment.

4.5.4 OpenPDC software

The OpenPDC software runs as a Windows service. The phasor data concentrator parser responds to changes in the streaming data. The OpenPDC software processes measured values that are time-stamped. A description of the configuration of the OpenPDC software is done below.

4.5.4.1 OpenPDC manager

Once the OpenPDC software setup within the wizard is completed the OpenPDC manager home screen appears, as shown in Figure 4.23

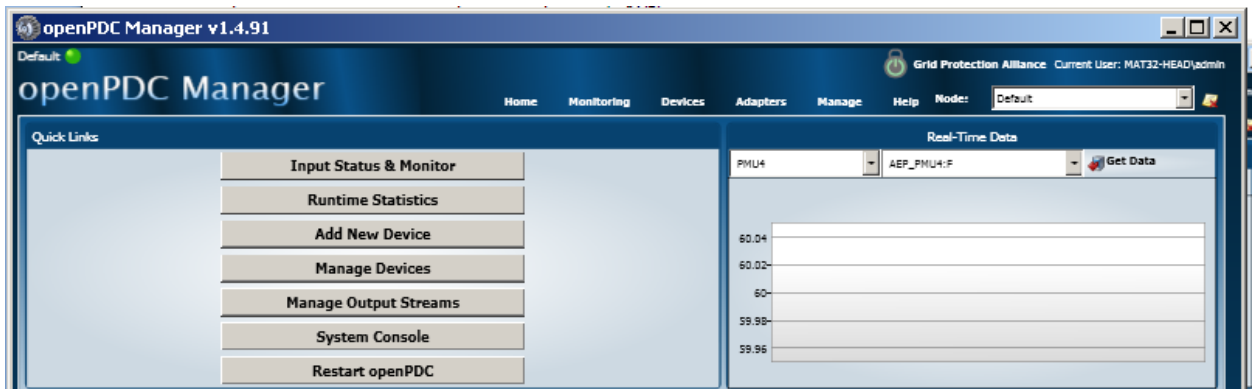


Figure 4.23: OpenPDC manager

This section describes how to use the OpenPDC manager to configure the OpenPDC to receive data from the RSCAD GTNET card PMU devices.

Step 1: Create historian

Figure 4.24 shows how to create a historian that archive the data received by the OpenPDC.

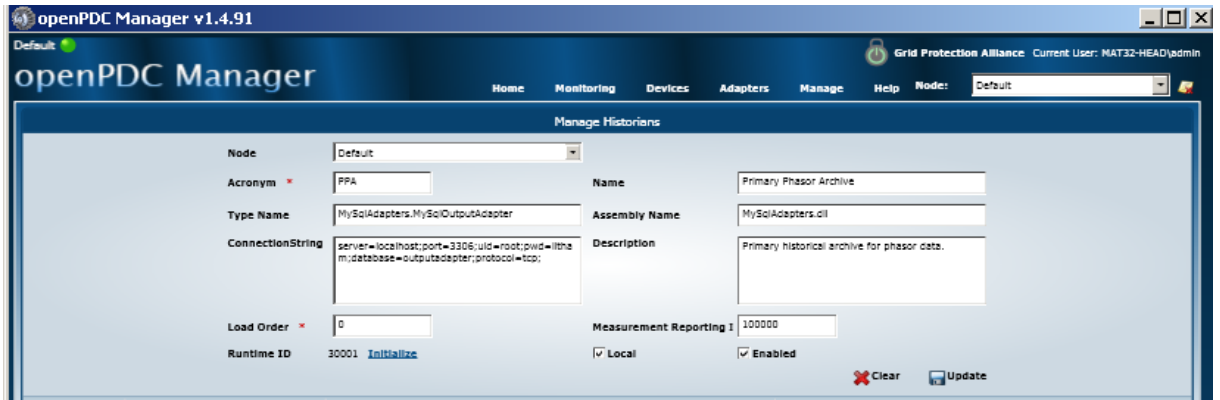


Figure 4.24: OpenPDC historians window

The elements of the windows in Figure 4.24 are given below:

Node: The user-defined selected node type using the historian to archive data.

Acronym and Name: It is used to identify historian data.

Type name and assembly name: It contains Dynamic Link Data (DLL) of the .NET class extending Outputadapter database.

Connection String: It is used to connect the historian to the MySQL database

OpenPDC historian connection string shown in Figure 4.24, is described in Table 4.6.

Table 4.6: OpenPDC historian connection string

Key	Description
Server=localhost	The host name MySQL database
port=3306	The port number of MySQL database for listing connection
uid=root	The user id for the MySQL account
pwd=litham	The password for the MySQL account
database=outputadapter	The name of database to use to store historian data
Protocol=tcp	Specifies type of connection to make server

Measurement reporting: It is used to determined how many measurement should be process before reporting.

Runtime ID: The identification number is used to send commands to the historian and initialize a link used to initialize a command to the adapter from the historian management system.

Step 2: Creating GTNET card PMU devices connection setting.

How to configure the connection setting in the OpenPDC manager is described in this section. The connection file, connection string, device ID and device must be defined in the configuration connection setting window of the OpenPDC manager. The OpenPDC

connection setting is shown in Figure 4.25:

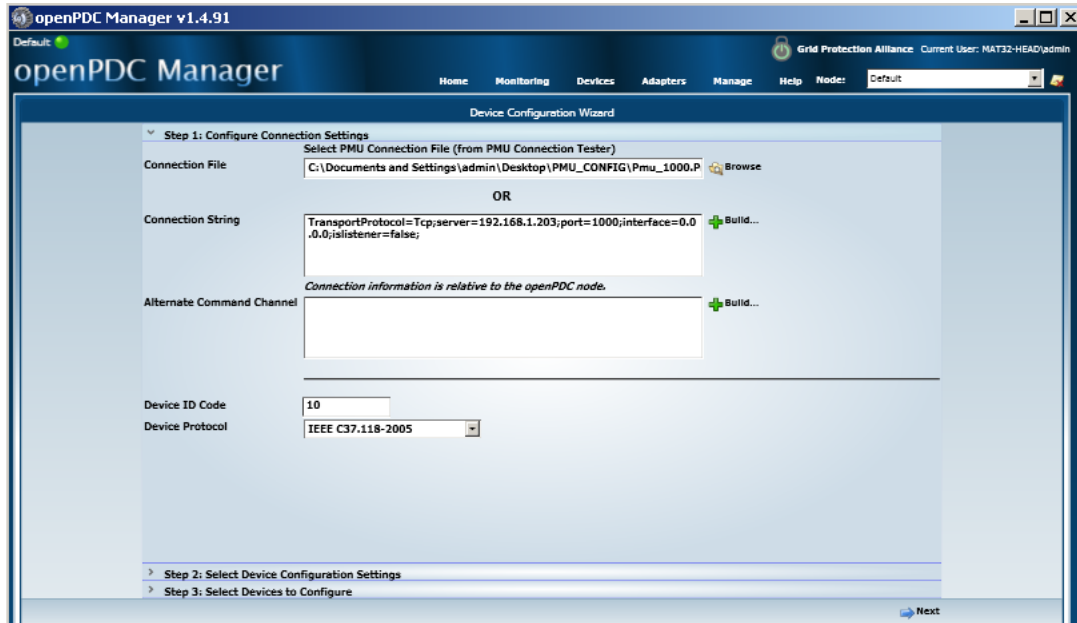


Figure 4.25: OpenPDC connections file setting

Connection File: The connection file of the GTNET card PMUs that is generated by the PMU connection tester described in section 4.5.3. The connection file automatically connects the GTNET card PMU and build the connection string and phasor protocol.

Connection String: The connection string is automatically configured and is specified in the GTNET card PMU connection file.

Device ID Code: The device ID code of the GTNET card PMU is used to connect the OpenPDC by using the PMU connection tester.

Device Protocol: The phasor protocol used by the GTNET card PMU devices is specified in the connection file of the OpenPDC manager.

Once all necessary information is entered click “Next”.

Step 3: Creating GTNET card PMU devices configuration setting.

The OpenPDC configuration setting is shown in Figure 4.26.

Configuration File: Configuration file of GTNET PMU devices are generated by the PMU connection tester and are described in Appendix B. The configuration file automatically configures the GTNET card PMU devices, connection string and phasor protocol.

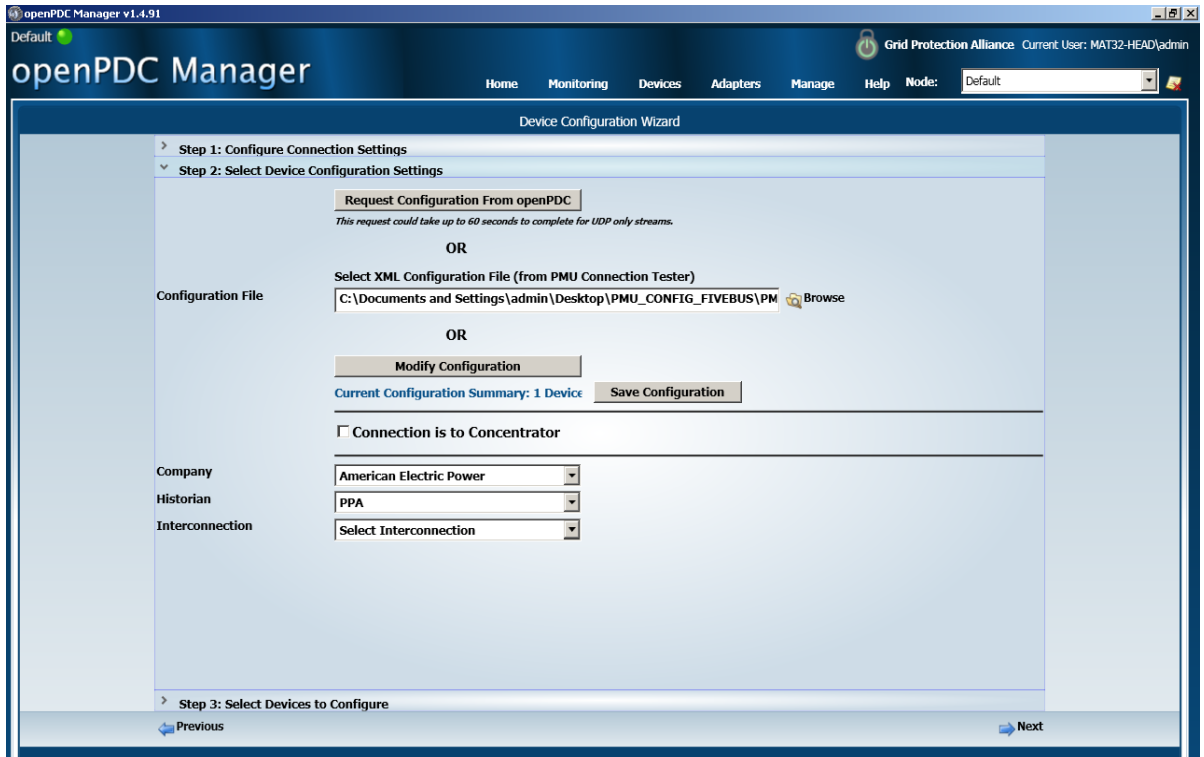


Figure 4.26: OpenPDC configuration

Step 4: Select GTNET PMU (device) to be configured.

In this step, the check box allows one to choose which GTNET card PMU and phasors are to be added in the OpenPDC manager as shown in Figure 4.27. The detailed description of the selected device to be configured is explained in this section, as follows:

Acronym and Name: The acronym and name of the GTNET card PMU device is defined in RSCAD.

Longitude and latitude: It describes the physical location of GTNET card PMU device

Label, Type and phase: It describes the GTNET card PMU name, signal type and phase sequence.

Once entered all necessary information is entered click “Finish”.

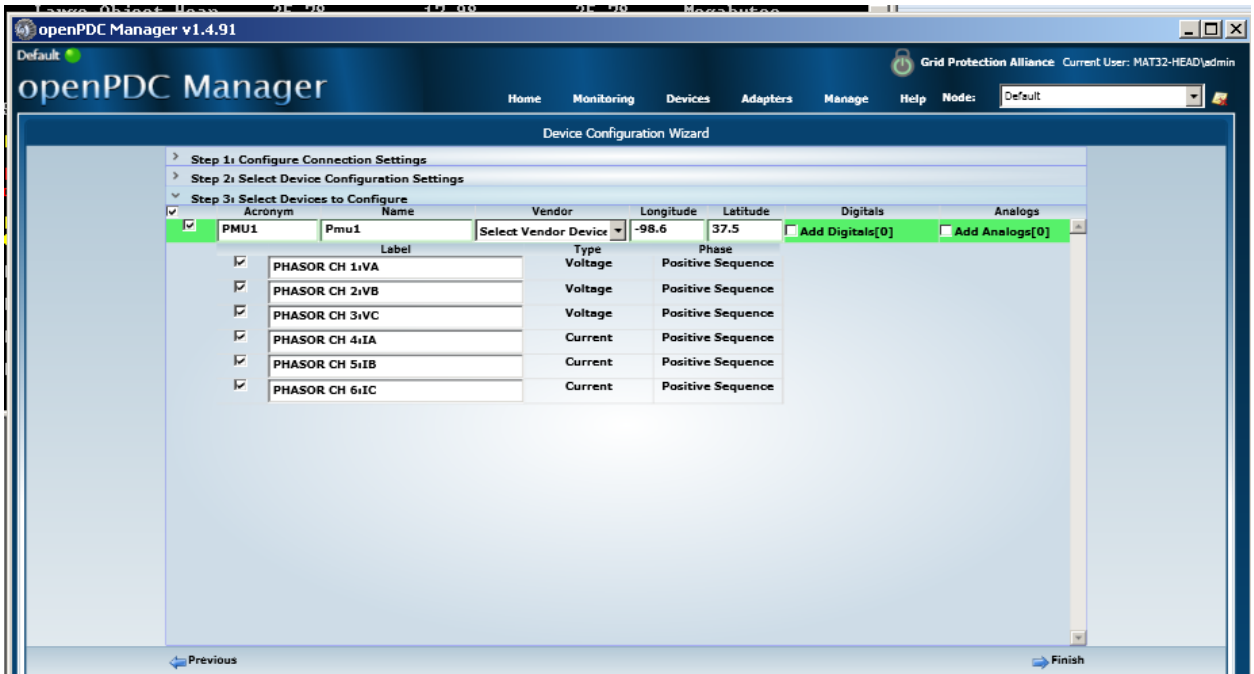


Figure 4.27: OpenPDC device to configure

4.5.4.2 Real-Time monitoring GTNET card PMU devices in the OpenPDC manager

The real-time measurement shows all information about the GTNET card PMU devices defined within the active node. Besides each GTNET PMU device has a list of all measurements, recent values and time stamp values as shown in Figure 4.28. Each measurement signal is updated once every 10 seconds.

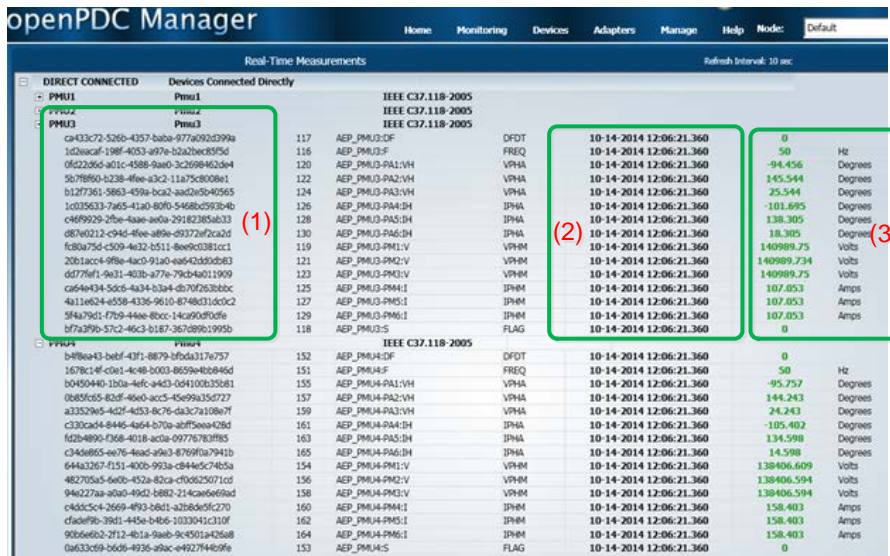


Figure 4.28: Real-Time monitoring of the GTNET card PMU device signal

Figure 4.28 presents a snippet of an active window's real-time measurements from the GTNET card PMU. On the left pane as highlighted by the rectangle are the values of the GTNET card PMU3 signals (current and voltage signals). The next highlighted set of values (2), represents the time stamps of when these measurements are actually taken. Lastly, marked with (3) are the numerical values of the measured data (voltage and current signals) of the GTNET card PMU3.

Now, having retrieved the data set from the OpenPDC software, it is necessary to log this data to a suitable database. This thesis uses the MySQL data base application software.

Figure 4.29, shows data sets are stored in a "measurement (1)" table and output "adaptor database (2)" using MySQL Integrated Development Environment (IDE). The MySQL IDE is a versatile and important tool for managing databases. However, for clarity Figure 4.29 is directly presented below to illustrate the transferred data from the OpenPDC to the MySQL database. The data is conveniently presented in a similar manner to the OpenPDC by keeping the original signal IDs, Time stamps and Values.

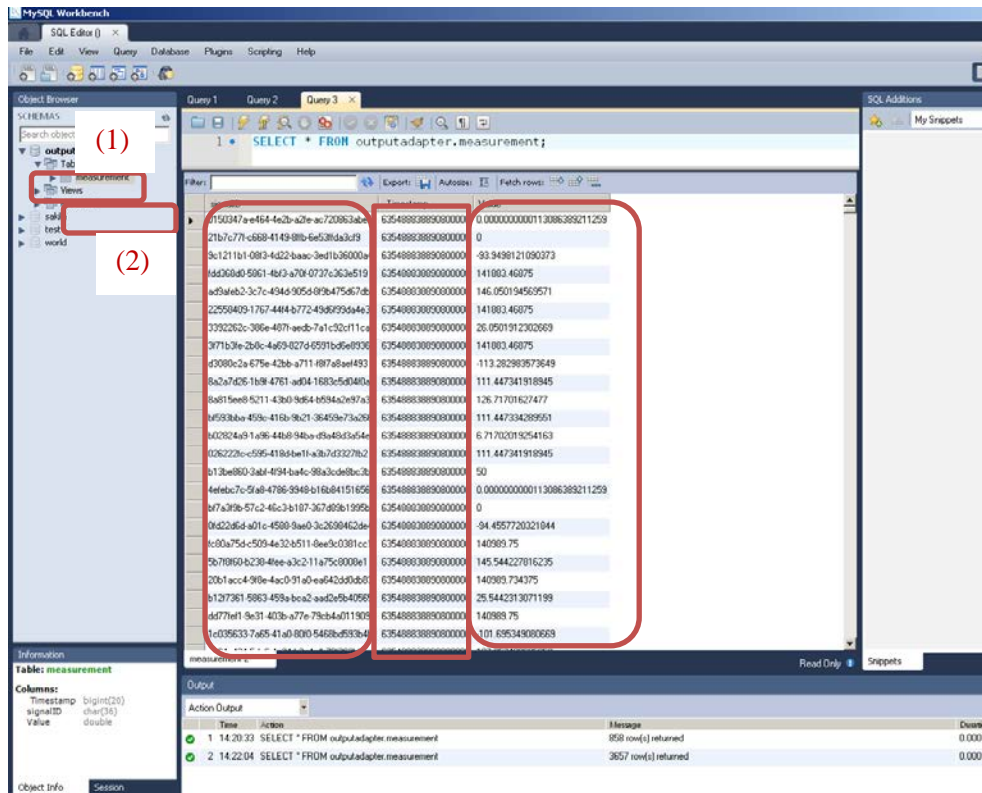


Figure 4.29: OpenPDC Real-time archiving in MySQL database

4.6 Conclusion

This chapter describes the developed methods, algorithms and procedure for hardware and software implementation of two lab scale real-time data acquisition and data transfer systems. Verification of the operation of these systems for the solution of the dispatch problem optimisation is presented. In Chapter 6, the results from the operation of the developed data acquisition and data transfer systems are presented.

The next chapter introduces the considered two cases of power systems to be simulated in the RTDS and the formulation and algorithm for solution of the dispatch optimisation problem.

CHAPTER FIVE

POWER SYSTEM CASE STUDIES, FORMULATION AND ALGORITHM FOR SOLUTION OF THE OPTIMISATION DISPATCH PROBLEM

5.1 Introduction

This chapter describes firstly, the case studies used to validate the developed lab-scale data acquisition and data transfer systems and secondly, the formulation of the algorithm used to solve the economic dispatch problem. The investigations are done on the five and eleven bus power system models (Kothari and Dhillon, 2006) which are constructed in RSCAD, the software suite of the Real-Time Digital Simulator (RTDS). The load flow simulation is invoked to initialize the generators, sources and dynamic loads within the circuit. The formulation of the optimisation problem and the algorithm to solve it are described further in this chapter. The algorithm is derived on the basis of the Lagrange's method for optimisation. This chapter provides the introduction in section 5.1. The power system case studies and their description are given in section 5.2. The formulation and the algorithm for the solution of the dispatch problem is explained in section 5.3, and the conclusion is presented in section 5.4.

5.2 Power system case studies and description

This research work considers the five and eleven bus power system models to validate the data acquisition and data transfer capability of the developed Lab-scale system. The data of the five and eleven bus power system models are given in (Kothari and Dhillon, 2006). The description of the two power system models together with their data are provided in this section. The development of the RSCAD models for the five and eleven bus power systems are presented and the load flow simulation is invoked to validate the off-line study of the power system models in the RSCAD environment.

5.2.1 Case study one: Five bus power system network

This section provides the description of the five bus power system model and its data and the RSCAD model of the five bus system together with the load flow results.

5.2.1.1 Description of the five bus power system model and its data

The single line diagram of the five bus power system model is given in Figure 5.1. It has three generators which are connected to the buses 1, 2 and 3 respectively. Bus one is

considered as the slack bus. The power system model has four pure resistive loads which are connected to buses 2, 3, 4 and 5 respectively. The power system model is connected with the help of the transmission lines. The five bus power system model has seven transmission lines which are interlinked between the buses as shown in the single line diagram in Figure 5.1 (Kothari and Dhillon, 2006).

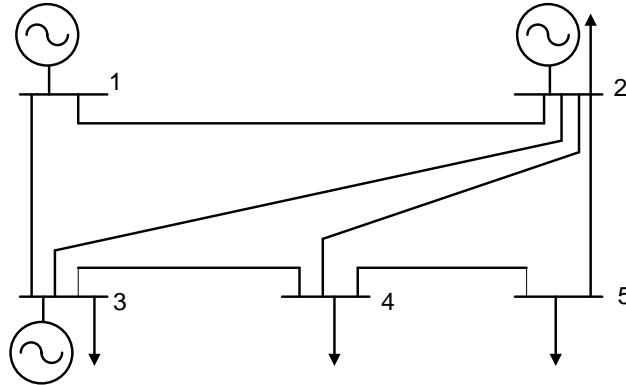


Figure 5.1: Single line diagram of the five bus power system model (Kothari and Dhillon, 2006)

The power flow for the transmission line depends on the series impedance and shunt capacitance values as given in Table 5.1. The transmission loss is calculated using the Boron's Equation (5.4), and the B coefficients to calculate the transmission loss are given in Table 5.2. The power system data such as the type of the bus, real and reactive power and the bus voltage magnitude and phase angle are given in Table 5.3, which is used to calculate the load flow solution.

Table 5.1: Five bus power system network transmission line data in per unit

Line Number	Sending end bus	Receiving end bus	$Y_{sh_{ij}}$	$ZSER_{ij}$
1	1	2	$j0.06$	$0.02+j0.06$
2	1	3	$j0.05$	$0.08+j0.24$
3	2	3	$j0.04$	$0.06+j0.18$
4	2	4	$j0.04$	$0.06+j0.18$
5	2	5	$j0.03$	$0.04+j0.12$
6	3	4	$j0.02$	$0.01+j0.03$
7	4	5	$j0.05$	$0.08+j0.24$

Table 5.2: Five bus power system network transmission line B coefficients

B_{ij} , where $i = \overline{1,5}, j = \overline{1,5}$,	1	2	3	4	5
1	0.02423	0.00033	-0.00500	-0.00374	-0.00339
2	0.00033	0.00469	-0.00315	-0.00342	-0.00132
3	-0.00500	-0.00315	0.00868	0.00380	-0.00390
4	-0.00374	-0.00342	0.00380	-0.00806	-0.00298
5	-0.00339	-0.00132	-0.00390	-0.00298	0.01969

Table 5.3: Load flow data for the five bus power system network

Bus Number	Type of Bus	P_i (p.u)	Q_i (p.u)	V_i (p.u)	δ_i (rad)
1	Slack bus	-----	-----	1.00	0.0000
2	PV bus	0.6867	-----	1.07	-----
3	PV bus	0.5215	-----	1.06	-----
4	PQ bus	0.4000	0.0500	-----	-----
5	PQ bus	0.6000	0.1000	-----	-----

5.2.1.2 RSCAD model of the five bus power system model

The single line diagram of the five bus power system model given in Figure 5.1 and it is constructed in the RSCAD software, which is the user interface provided with the RTDS hardware as shown in Figure 5.2. For simplicity this thesis considers only the resistive loads. The RSCAD software allows the user to select either a constant source models or synchronous machine model with an excitation and a governor. This work uses a constant source model as a generator and this is implemented in the RSCAD environment.

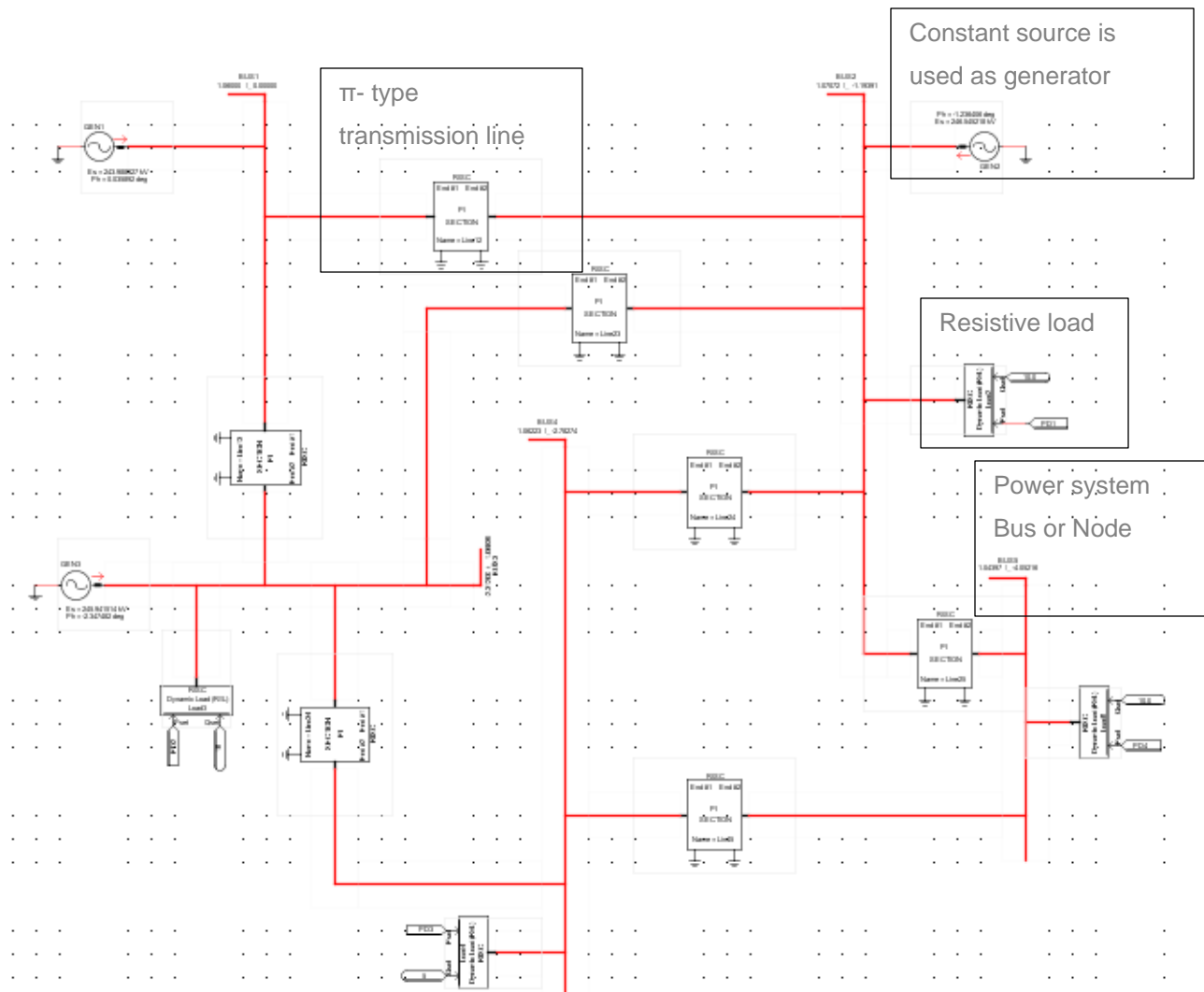


Figure 5.2: Five bus power system model in RSCAD environment

5.2.1.3 Simulation of the five bus power system model and load flow results

The simulation model is developed in the RSCAD software suite of the RTDS. The actual bus voltage magnitude and phase angle are identified by invoking the load flow analysis. The load flow analysis computes the real and reactive power for the generators according to the considered power demand. The load flow simulation result for the five bus power system model is given in Table 5.4. It is observed that the voltage profile of the five bus power system model lies within ± 5 percent deviation from the nominal voltage as per the (IEEE standard 399, 1997).

Table 5.4: Load flow simulation results of the five bus power system model in the RSCAD environment

Bus number	P_G [MW]	Q_G [MW]	P_D [MW]	Q_D [MW]	V (p.u)	δ [Degree]
1	46.04	-37.25	0.0	0.0	1.06000	0.0000000
2	68.78	45.11	20.0	10.0	1.04836	-0.8102600
3	52.22	37.48	45.0	15.0	1.03725	-1.8173700
4	0.0	0.0	40.0	05.0	1.03266	-2.3478100
5	0.0	0.0	60.0	10.0	1.01858	-3.7639500

5.2.2 Case study two: Eleven bus power system network

The eleven bus power system model given in (Kothari and Dhillon, 2006) is considered as the second case study to validate the developed lab-scale data acquisition and data transfer systems. This section provides the description of the eleven bus power system model and its data, the RSCAD simulation model of the eleven bus system, and the load flow results.

5.2.2.1 Description of the eleven bus power system model and its data

The power system consists of 11 buses, 5 generators, 11 loads, and 17 transmission lines and is shown in the single line diagram in Figure 5.3. A constant power source is used for the generator model. The PI-type medium transmission lines and a resistive load are used to build the eleven bus power system model in the RSCAD environment. The power system is operating at a frequency of 50 Hz and a base of 100MVA, 230kV.

The eleven bus power system model has five generators which are connected to the buses 1 to 5 respectively and eleven loads which are connected between the buses 1 to 11 respectively. The power system network contains short transmission lines and hence the PI-type transmission line model is chosen in the RSCAD environment.

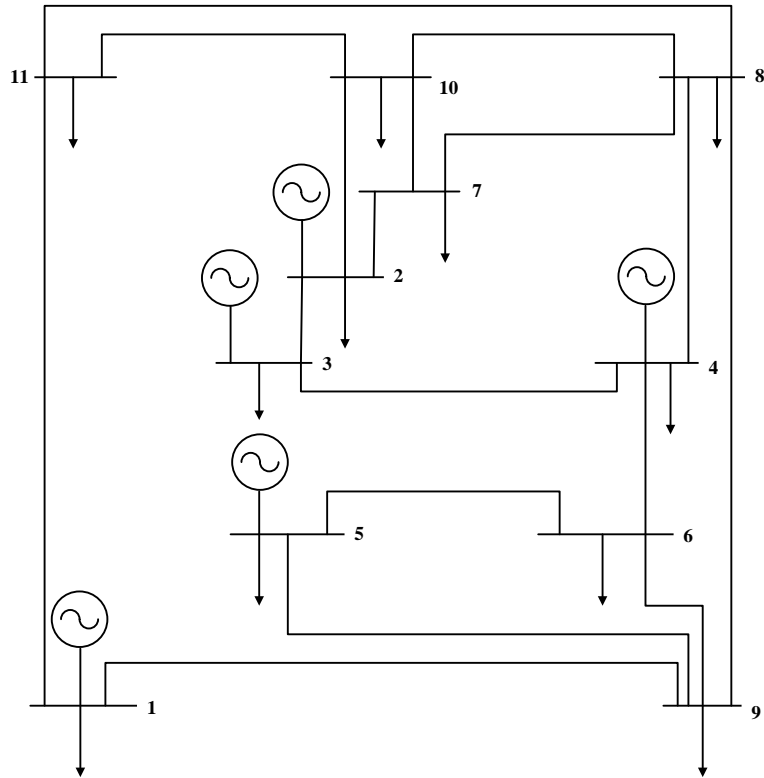


Figure 5.3: Single line diagram of the eleven bus power system model (Kothari and Dhillon, 2006)

The transmission line data and the bus information of the eleven bus power system model are given in Table 5.5 and 5.6 respectively. The line resistance, reactance and the charging capacitance of the transmission lines are given in Table 5.5.

Table 5.5: Transmission line data of the eleven bus power system

Line No	Bus		Resistance (p.u)	Reactance (p.u)	Line charging (p.u)
	From	To			
1	1	9	0.15	0.50	0.030
2	1	11	0.05	0.16	0.100
3	2	3	0.15	0.50	0.030
4	2	7	0.10	0.28	0.020
5	2	10	0.05	0.16	0.010
6	3	4	0.08	0.24	0.015
7	4	6	0.10	0.28	0.020
8	4	8	0.10	0.28	0.020
9	4	9	0.15	0.50	0.030
10	5	6	0.12	0.36	0.025

11	5	9	0.05	0.16	0.010
12	7	8	0.05	0.16	0.010
13	7	10	0.08	0.24	0.015
14	8	9	0.12	0.36	0.025
15	8	10	0.08	0.24	0.015
16	8	11	0.10	0.28	0.020
17	10	11	0.12	0.36	0.025

The real and reactive power of the loads, bus voltages and their phase angles are also given in Table 5.6. This information is used as input data to model the power system network and to conduct the load flow analysis in the RSCAD environment.

Table 5.6: Bus information and load data for the eleven bus power system

Bus data				Load data	
Bus No	Bus Type	V_i p.u	δ_i rad	P_D [MW]	Q_D [Mvar]
1	Slack	1.070	0.0	20	05
2	PV	1.088	0.0	20	05
3	PV	1.095	0.0	30	10
4	PV	1.062	0.0	25	05
5	PV	1.046	0.0	25	05
6	PQ	1.0	0.0	10	002
7	PQ	1.0	0.0	40	10
8	PQ	1.0	0.0	90	45
9	PQ	1.0	0.0	70	35
10	PQ	1.0	0.0	25	05
11	PQ	1.0	0.0	25	05

5.2.2.2 RSCAD model of the eleven bus power system

The eleven bus power system network is implemented in the RSCAD software suite of the RTDS and is given in Figure 5.4.

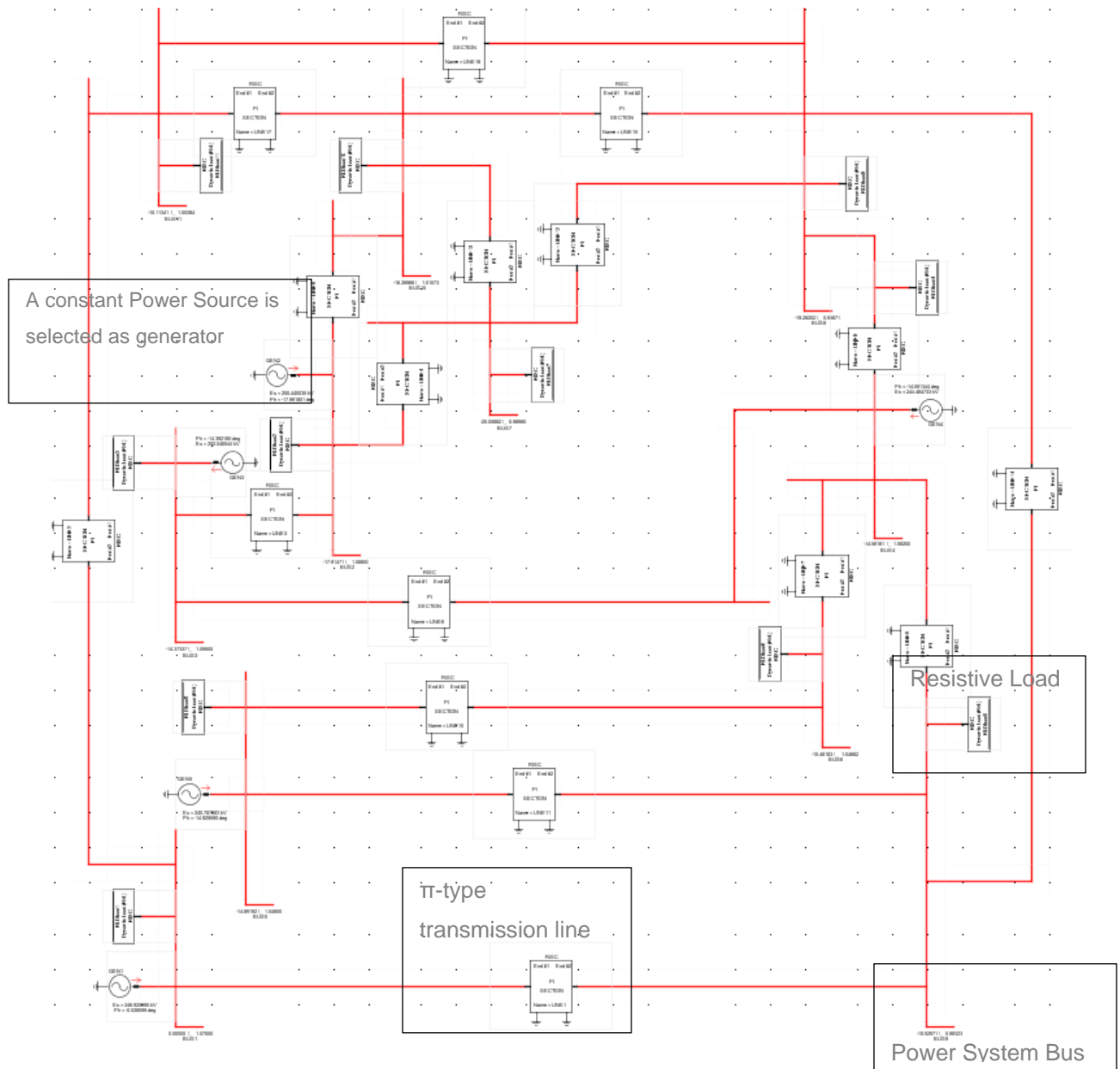


Figure 5.4: The Eleven bus power system model in the RSCAD environment

5.2.2.3 Simulation of the eleven bus power system model and load flow results

The load flow simulations are carried out using the RSCAD software. The actual bus voltage magnitudes, phase angles, real and reactive powers are identified by invoking the load flow analysis. The load flow simulation result for the eleven bus power system model is given in Table 5.7. It is observed that the voltage profile V_i of the eleven bus power system model lies within ± 5 percent deviation from the nominal voltage magnitude as per the (IEEE standard 399, 1997).

Table 5.7: Eleven bus system load flow results in RSCAD environment

Bus No	P _i [MW]	Q _i [Mvar]	P _D [MW]	Q _D [Mvar]	V _i p.u	δ _i [degree]
1	203.20	29.80	20	05	1.07000	0.000000
2	50	84.317	20	05	1.08800	-17.9147
3	50	20.842	30	10	1.09500	-14.37337
4	50	30.990	25	05	1.06200	-14.56161
5	50	38.090	25	05	1.04600	-14.89192
6	-----	-----	10	02	1.04662	-15.46183
7	-----	-----	40	10	0.98960	-20.05882
8	-----	-----	90	45	0.95871	-19.26202
9	-----	-----	70	35	0.98323	-15.92971
10	-----	-----	25	05	1.01073	-18.26968
11	-----	-----	25	05	1.00384	-10.11341

5.3 Formulation and algorithm for solution of the dispatch problem

The objective of the economic dispatch is to simultaneously minimize the generation cost rate and to meet the load demand of the power system over an appropriate period of time, while satisfying various operating constraints. The formulation of the economic dispatch problem is given in section 5.3.1 and the algorithm for the solution of the economic dispatch problem is described in section 5.3.2. The real power optimisation problem is for the minimization of the fuel cost or for minimization of the pollutant emission, and is solved using the Lagranges algorithm in the MATLAB software.

5.3.1 Formulation of the dispatch problem

The objective function of the economic dispatch problem is to minimize the fuel cost or the emission criterion function of the thermal power plant as given in Equations (5.1) and (5.2) respectively.

$$\text{Minimize } F_C = \sum_{i=1}^n F_i(P_i) = \sum_{i=1}^n (a_i P_i^2 + b_i P_i + c_i) [\$/hr] \quad (5.1)$$

$$\text{Minimize } E_C = \sum_{i=1}^n E_i(P_i) = \sum_{i=1}^n (d_i P_i^2 + e_i P_i + f_i) [kg/hr] \quad (5.2)$$

Where:

F_C is the total Fuel Cost

E_C is the total emission value

$F_i(P_i)$ is the fuel cost of the i^{th} generator

$E_i(P_i)$ is the emission value of the i^{th} generator

P_i is the real power generation of unit i

a_i, b_i, c_i are the fuel cost coefficients of generating for unit i

d_i, e_i, f_i are the emission value coefficients of generating for unit i

n is the number of generating units

Under the constraints determined by the power balance, transmission loss, and generator limits, as given below.

1) Power balance constraint

$$\sum_{i=1}^n P_i = P_G = P_D + P_L [MW] \quad (5.3)$$

Where:

P_G is the total power generation of the system

P_D is the total demand of the system and

P_L is the total transmission loss of the system

2) The transmission loss constraint can be expressed as

$$P_L = \sum_{i=1}^n \sum_{j=1}^n P_i B_{ij} P_j + \sum_{i=1}^n B_{0i} P_i + B_{00} [MW] \quad (5.4)$$

Where

B_{ij}, B_{0i}, B_{00} are the transmission loss coefficients

3) Generator operational constraints

$$P_{i,\min} \leq P_i \leq P_{i,\max}, i = \overline{1, n} \quad (5.5)$$

Where

$P_{i,min}$ is the minimum value of the real power allowed to be produced by the generator i

$P_{i,max}$ is the maximum value of the real power allowed to be produced by the generator i .

Two optimisation dispatch problems are formulated on the basis of the criteria (5.1) or (5.2) and the constraints given in Equations (5.3) to (5.5) as follows: Find the values of

the active power $P_i, i = \overline{1, n}$ in such a way that the criteria Equations (5.1) or (5.2) are minimized under the constraints (5.3) to (5.5). The algorithm for solution of both optimisation dispatch problems are the same. They are described in the next section using the criterion given in Equation (5.1).

5.3.2 Algorithm for solution of the dispatch problem

A method for the Lagrange's solution of the economic dispatch optimisation problem Equation (5.1), subject to the constraints given in the Equations (5.3), (5.4) and (5.5) is developed on the basis of the function of Lagrange (L) by introduction of Lagrange's multiplier λ (Krishnamurthy and Tzoneva, 2013).

$$L = \left[\sum_{i=1}^n [a_i P_i^2 + b_i P_i + c_i] + \lambda \left(P_D + \sum_{i=1}^n \sum_{j=1}^n P_i B_{ij} P_j + \sum_{i=1}^n B_{0i} P_i + B_{00} - \sum_{i=1}^n P_i \right) \right] \quad (5.6)$$

The optimisation problem in Equation (5.1), subject to the constraints given in Equations (5.3), (5.4) and (5.5) is transferred to the problem for minimization of L according to $P_i, i = \overline{1, n}$, and maximization of L according to λ , under the constraints given in Equation (5.5). The conditions for optimality are derived for the solution of the problem presented by Equations (5.5) and (5.6) as follows:

$$\text{According to } P_i, \quad \frac{\partial L}{\partial P_i} = 0, i = \overline{1, n} \quad (5.7)$$

$$\text{According to } \lambda, \quad \frac{\partial L}{\partial \lambda} = 0 \quad (5.8)$$

The derivation of the condition presented in Equation (5.7) is as follows:

$$\frac{\partial L}{\partial P_i} = 2a_i P_i + b_i + \lambda \left(2 \sum_{j=1}^n B_{ij} P_j + B_{0i} - 1 \right) = 0, i = \overline{1, n} \quad (5.9)$$

Equation (5.9) can be written in a matrix–vector form as follows:

$$\begin{bmatrix} \frac{a_1}{\lambda} + B_{11} & B_{12} & B_{1n} \\ B_{21} & \frac{a_2}{\lambda} + B_{22} & B_{2n} \\ B_{n1} & B_{n2} & \frac{a_{1n}}{\lambda} + B_{nn} \end{bmatrix} \begin{bmatrix} P_1 \\ P_2 \\ \vdots \\ P_n \end{bmatrix} = \frac{1}{2} \begin{bmatrix} 1 - \left(\frac{b_1}{\lambda}\right) - B_{01} \\ 1 - \left(\frac{b_1}{\lambda}\right) - B_{02} \\ 1 - \left(\frac{b_1}{\lambda}\right) - B_{0n} \end{bmatrix} \quad (5.10)$$

If the value of the Lagrange's multiplier λ is known, Equation (5.10) can be solved according to the unknown vector P , using the MATLAB command:

$$P = E \setminus D \quad (5.11)$$

Where

$$E = \begin{bmatrix} 1 - \left(\frac{b_1}{\lambda}\right) - B_{01} \\ 1 - \left(\frac{b_1}{\lambda}\right) - B_{02} \\ 1 - \left(\frac{b_1}{\lambda}\right) - B_{0n} \end{bmatrix} \text{ and } D = \begin{bmatrix} \frac{a_1}{\lambda} + B_{11} & B_{12} & B_{1n} \\ B_{21} & \frac{a_2}{\lambda} + B_{22} & B_{2n} \\ B_{n1} & B_{n2} & \frac{a_{1n}}{\lambda} + B_{nn} \end{bmatrix}$$

The value of λ is unknown and has to be calculated using the necessary condition for optimality as defined by Equation (5.11):

$$\frac{\partial L}{\partial \lambda} = \left(P_D + \sum_{i=1}^n \sum_{j=1}^n P_i B_{ij} P_j + \sum_{i=1}^n B_{0i} P_i + B_{00} - \sum_{i=1}^n P_i \right) = 0 = \Delta \lambda \quad (5.12)$$

Equation (5.12) is not a function of λ , but represents the gradient of L according to λ . At the optimal solution this gradient has to be equal to zero. An analytical solution for λ is not possible and a gradient procedure for calculation of λ is developed as follows:

$$\lambda^{(k+1)} = \lambda^k + \alpha \Delta \lambda^{(k)}, \lambda \neq 0 \quad (5.13)$$

Where $\Delta \lambda^{(k)}$ is determined by the equation (5.12), k is the index of the gradient procedure, and α is the step of the gradient procedure that starts with some given initial value of the Lagrange's variable $\lambda^{(0)}$. When $\Delta \lambda = 0$, during the iterations the optimal

solution for the Lagrange's variable is obtained. It determines the optimal solution for the energy that has to be produced by the generators as a solution of Equation (5.10).

The obtained solutions for $P_i, i = \overline{1, n}$ have to belong to the constraint domain determined by Equation (5.5). That is why for every index k of the gradient procedure, the obtained solution is fit to the constraint domain following the procedure:

$$P_i^{(k)} = \begin{pmatrix} P_{i,\min}, & \text{if } P_i^{(k)} < P_{i,\min} \\ P_i^{(k)}, & \text{if } P_{i,\min} \leq P_i^{(k)} < P_{i,\max} \\ P_{i,\max}, & \text{if } P_i^{(k)} > P_{i,\max} \end{pmatrix} \quad (5.14)$$

The condition for the end of the iterations is:

$$\Delta\lambda^{(k)} \leq \varepsilon, \text{ or } k = m \quad (5.15)$$

Where $\varepsilon > 0$ is a small number and m is the given maximum number of iterations.

The algorithm of the method is developed by (Krishnamurthy and Tzoneva, 2013), and is presented as follows:

- 1) The initial value of the Lagrange's multiplier is guessed: $\lambda^{(0)}$, and the value of the condition for optimality ε is given.
- 2) In Equation (5.10) matrix $E^{(0)}$ and $D^{(0)}$ are formed.
- 3) Equation (5.11) is solved and $P^{(0)} = E^{(0)} \setminus D^{(0)}$ is determined.
- 4) The obtained vector $P^{(0)}$ is fit to the constraint domain (5.14).
- 5) $\Delta\lambda^{(0)}$ is calculated using Equation (5.12) where $P^{(0)}$ is substituted.
- 6) The condition (5.15) is checked. If it is fulfilled the calculations stop, if not, improved value of $\lambda \rightarrow \lambda^{(1)}$ is calculated using Equation (5.13).
- 7) Calculations of the improved values of $P_i \rightarrow P_i^{(1)}$ are done as in Equation (5.14) and so on. Iterations continue until condition (5.15) is satisfied or the maximum number of iterations is reached.
- 8) The optimal solution is used to calculate the total fuel cost and emission using Equation (5.1) and (5.2) respectively.

The flowchart of the algorithm is shown in Figure 5.5.

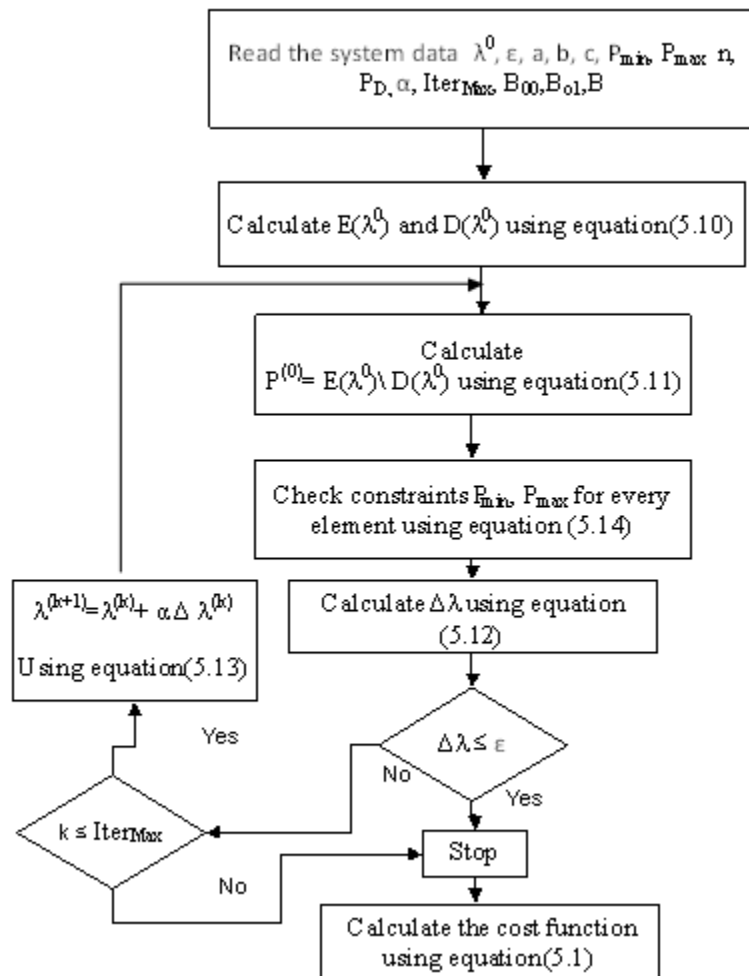


Figure 5.5: The flow chart of the economic dispatch problem solution algorithm using the Lagrange’s method (Krishnamurthy and Tzoneva, 2013)

The MATLAB software that has been developed for the economic dispatch problem is given in Appendix D to G for the RTDS PB5 card analogue output signals and in Appendix H for the RTDS PMU-based synchrophasor systems. It can be seen that the values of the matrices E and D influence the power demand given in Equation (5.12) and in this way the components of the optimal vector P of the active power received by each generator are different for each power demand.

The algorithm given in Figure 5.5 is the same for the case of emission optimisation problem. The only differences are the coefficients for the criterion function.

5.4 Conclusion

This chapter presented the two power system case studies used to validate the developed lab-scale data acquisition and data transfer system. The case studies include the five and eleven bus power system models together with their RSCAD simulation models. The transmission line coefficients, bus and load data are presented. This chapter also provides the formulation and the algorithm for solution of the optimisation dispatch problem using the Lagrange's algorithm.

Chapter Six presents an investigation of the real-time operation of the developed data acquisition and data transfer systems, together with the acquired results.

CHAPTER SIX

INVESTIGATION OF THE REAL-TIME OPERATION OF THE DEVELOPED DATA ACQUISITION SYSTEMS AND RESULTS

6.1 Introduction

The Energy management system plays a vital role in power systems to perform the dispatch operation of the generators in the system control centre with coordination of the power demand required at a specific period of time. In the control centre, the dispatch problem usually has to be solved once every 15 minutes. It is a challenging job for the power system engineers to take the appropriate control action to coordinate the power generation for the power demand required. At present, there is a lack of real-time data in the control centres and the solution of the economic dispatch problem is delayed.

The economic dispatch problem is solved using the Lagrange's algorithm in (Krishnamurthy and Tzoneva, 2013). Most of the Economic Dispatch (ED) research papers use IEEE models and data to solve the economic dispatch problem in non-real time software environments, such as MATLAB or C programming. Their research aims are mostly focused on the development of new classical or heuristics algorithms to optimize the generators real power subjected to certain constraints, and to minimize the fuel cost.

A few papers solve the problem for dispatch of power for a real system and using real-time data and optimisation. The required changes to the power production are also not communicated in real-time to the power producers. The reason for these problems are that communication systems for data acquisition, data transfer, data storage, and data retrieving in real-time have not been developed yet. The aim of this thesis is the development of lab-scale variants of the power system and of real-time data acquisition and data transfer systems using the available modern technology to demonstrate the possibilities for real-time solution of the optimal power dispatch problem using real-time data.

Two lab-scale systems for data acquisition and data transfer using the RTDS PB5 front panel analogue output data and the GTNET card PMU synchrophasor data are developed to investigate different possibilities for capturing the power system data from the RTDS simulation model and to transfer these data to a local or remote control

centre. The investigations are done for the five and eleven bus power system models (Kothari and Dhillon, 2006) which are constructed in the RSCAD environment, which is the software suite of the RTDS. The load flow is invoked to initialize the generators, sources and dynamic loads within the simulation model as described in Chapter five. This chapter describes how to apply the developed two variants of data acquisition and data transfer systems (Chapter Four) and provides the results of these applications for the five and eleven bus case studies.

This chapter provides the introduction in section 6.1. The lab-scale data acquisition and data transfer system using the RTDS Front Panel PB5 card analogue outputs in the LabVIEW/MATLAB software environments are presented in sections 6.2 and 6.3 respectively. The acquisition system using the GTNET card PMU synchrophasor output applications are described in sections 6.4. Section 6.5 discusses the operation characteristics of the developed system, and the conclusion is presented in section 6.6.

6.2 Investigation of the LabVIEW/MATLAB-based data acquisition and data transfer system using the RTDS front panel PB5 card analog output signals

The structure of the developed lab scale system to solve the economic dispatch problem in real-time using the PB5 card analogue outputs is given in Figure 6.1.

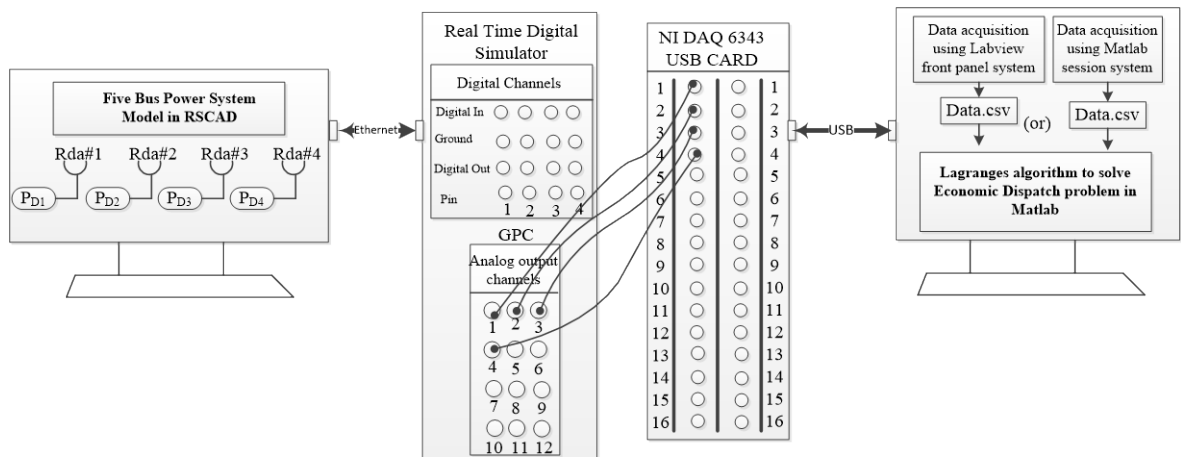


Figure 6.1a: Block diagram for the lab-scale data acquisition system using the RTDS PB5 card analog outputs

The hardware data acquisition system is developed using two software platforms:

- i) LabVIEW-based system and
- ii) MATLAB-based system

Each of these platforms is used to acquire, transfer and store data, and solve the optimisation dispatch problem in real-time for the five and eleven bus power system cases.

The aim of the solution of the optimisation problem in real-time is to recalculate the values of the real-power that have to be produced by the generating units for a previously determined period of time, on the basis of measurement of the power demand generated by the loads in the system at a selected instant in time.

The major steps of the real-time dispatch problem solution are: The power system model is simulated in RSCAD (RTDS); changing of the power demand during the simulation is done through changing the values of the loads in the simulated systems. The produced power demand values are measured and are sent to the analogue outputs of the PB5 card. From these outputs the values are captured by the NI DAQ card, transferred and stored in an Excel file in the local personal computer.

The optimisation algorithm in Figure 5.5, described in Chapter 5 is run. The new values of the power demands are read and the optimisation problem is solved. The obtained solution is used by the operator to control the generation production.

The algorithm for real-time solution of the problem is given in Figure 6.1b. This algorithm is implemented as per the structure in Figure 6.1a. The thesis investigation considers only the real-time solution of the optimisation problem based on real-time acquired and transferred data. It does not solve the problem for control of the generators. This problem can be solved by future research work.

In Figure 6.1b, $P_D = \sum_{i=1}^m P_{D_i}$ is the total power demand and $P = \sum_{i=1}^n P_i$ is the total real power produced by the generators to correspond to the required power demand, m is the number of the power demands, and n is the number of the generators in the power system.

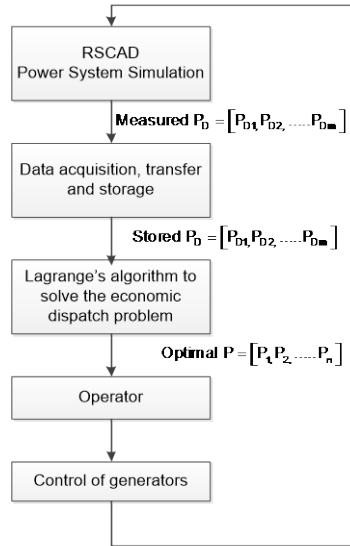


Figure 6.1b: Real-time implementation of the algorithm for solution of the dispatch problem

The implementation of the algorithm from Figure 6.1b and the obtained results are described for every data acquisition method, every platforms and every case study developed in the thesis.

6.2.1 LabVIEW-based data acquisition and data transfer system using the RTDS front panel PB5 card analog output signals for the five bus power system model

The power system model is simulated in the RSCAD environment. The real-time data for the power demand is generated and sent to the analogue outputs of the PB5 card. The NI USB DAQ 6343 is used to capture the analog output voltages from the RTDS PB5 card. The user can configure the NI-DAQ analog inputs according to their own requirements. The test system for the five bus power system model uses four analog input channels to capture the signals of the four real power demands (P_{D1} to P_{D4}) from the RTDS PB5 card analog outputs. Four sliders are designed in the RSCAD run-time window to vary the real power of the four loads (P_{D1} to P_{D4}). The simulation is started and the NI USB DAQ 6343 card acquires and transmits the data with the help of the developed LabVIEW data acquisition system to a local computer where the Lagranges algorithm is programmed in MATLAB software to solve the economic dispatch problem.

The RSCAD software model of the five bus power system is given in Figure 6.2 in which the PB5 card analog output channels 1 to 4 are assigned to the NI DAQ 6343 card input channels 1 to 4 respectively (Rda#1 to Rda#4).

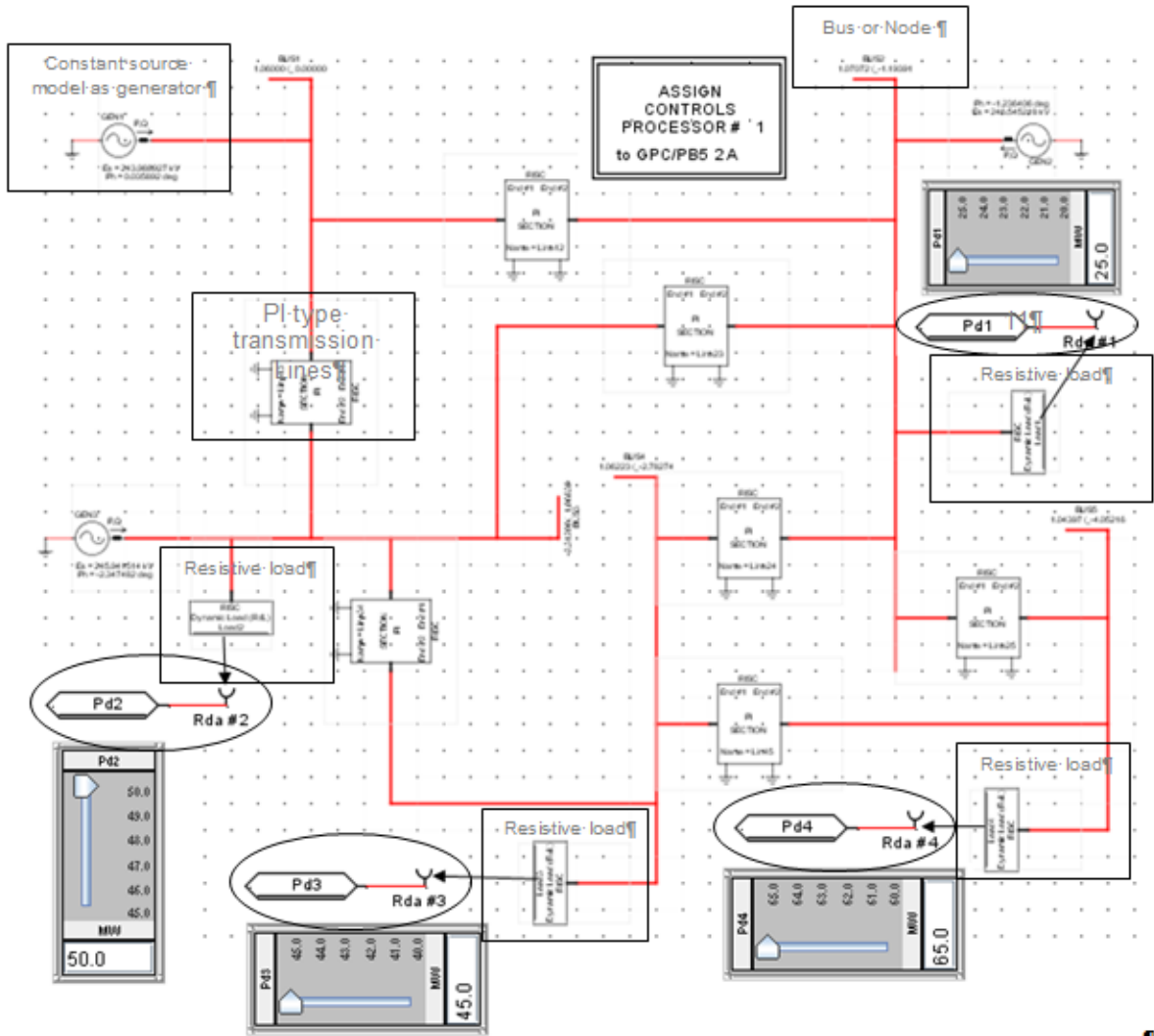


Figure 6.2: Five bus power system model in RSCAD environment including the NI DAQ 6343 card input channels

The data acquisition system is developed using the LabVIEW software. The LabVIEW block diagram to capture the four P_D signals from the four channels of the PB5 card using the NI DAQ 6343 card is given in Figure 6.3.

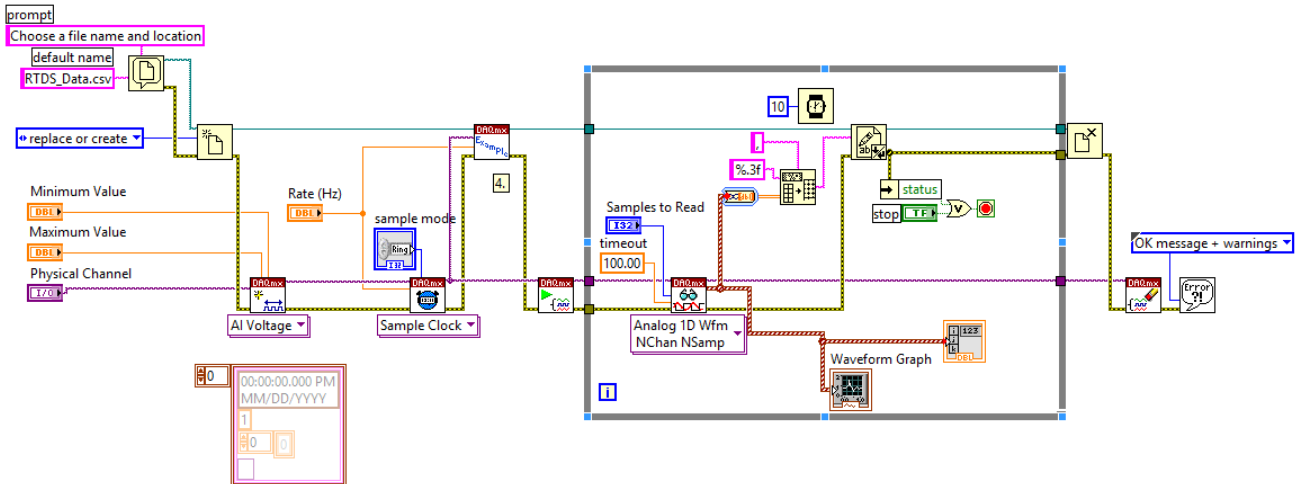


Figure 6.3: LabVIEW graphical diagram to connect the RTDS four channel PB5 card signals to the NI DAQ card 6343

The corresponding front panel diagram in Figure 6.3 of the LabVIEW data acquisition system has the channels windows in which the physical variable and its minimum and maximum values are assigned. It also has timing windows in which the sampling rate and number of samples are assigned (See Figure 6.4). The sampling mode is set to continuous. The analog output voltages from the RTDS PB5 card representing the real power demands of P_{D1} to P_{D4} are also displayed.

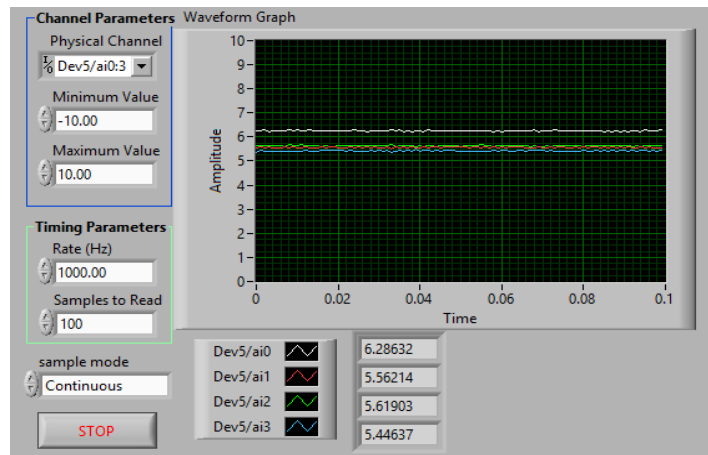


Figure 6.4: Front panel design of the LabVIEW data acquisition system to monitor the four analog signals coming from the RTDS PB5 card

The test of the developed system according to the flow chart in Figure 6.1b is performed in the following steps:

- The power demands of the four loads are initially set to 20, 45, 40 and 60 MWs respectively. The power demand of the first load, P_{D1} is increased from 20 to 25MW by increasing the slider 1 as shown in Figure 6.2. This procedure is repeated for the other loads P_{D2} , P_{D3} , and P_{D4} by varying the corresponding sliders. The analog voltage measurement from the RTDS PB5 card and the calculated actual values in MW are given in Table 6.1. The RSCAD simulation graphs of the real powers of the loads are plotted in the RTDS run-time window for the initial and the final values of the power demands and are shown in Figures 6.5 and 6.6 respectively.

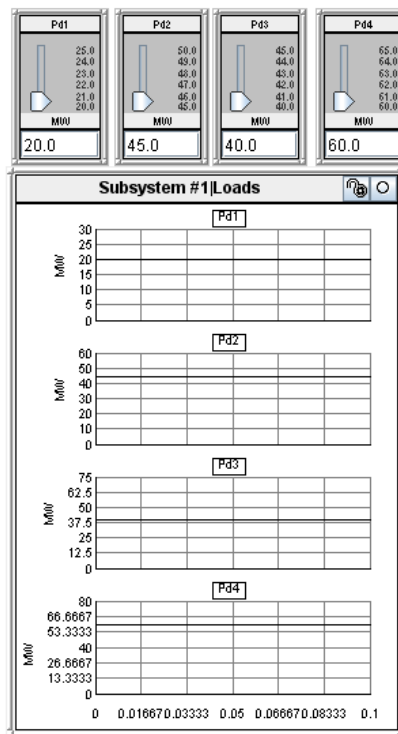


Figure 6.5: Initial values of the power demands (Sliders are at the bottom position) in the RSCAD run-time window

- The real powers of the four loads (power demands) are sent to the RTDS PB5 card front panel analog output channels Rda#1 to Rda#4 respectively with a suitable scaling factor. The PB5 card front panel Digital to Analog Conversion (DACs) uses the DAC7802 IC for the D/A conversion, an OP470G OpAmp to provide the output voltage, and a REF102CU precision reference for calibration (RTDS, manual). The four analog outputs of the PB5 card are captured using the NI DAQ 6343 at a sampling rate of 10 kHz. Table 6.1 summarizes the settings of

the scaling factors for the output channels of the PB5 card. For the analog output channels, the scaling factor is set in accordance with the range of the measured load power.

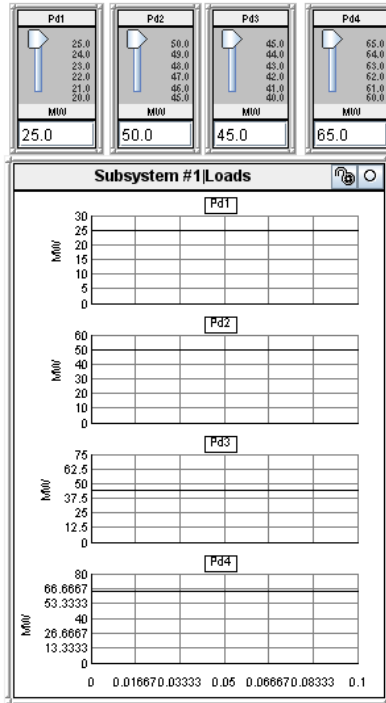


Figure 6.6: Final values of the four load power demands (Sliders are at the top position) in the RSCAD run-time window

For the five bus power system, the real power of the load (P_{D1}) is determined to be 20 MW, to optimize the range of the analog output module of the PB5 card that has a maximum output voltage of 10 V, therefore the appropriate scaling factor is 5 Volts for 1 Unit. Therefore if the real power load (P_{D1}) is 20 MW, the voltmeter will read 5 Volts. This scaling factor should be factored in when using the Lagrange's algorithm in the MATLAB environment to convert the acquired analog voltage back into its actual value in MW in order to solve the economic dispatch problem. The average value of the first 1000 samples of the RTDS real-time data (P_{D1} to P_{D4}) is accepted as the total power demand P_D for the given period of the data acquisition and is used to solve the economic dispatch problem.

Table 6.1: Five bus system power demand analog values from the RTDS front panel PB5 card outputs acquired using the developed LabVIEW front panel system and the NI DAQ 6343 card

Channel #1 (P _{D1})		Channel #2 (P _{D2})		Channel #3 (P _{D3})		Channel #4 (P _{D4})	
Scaling factor =4 $\frac{MW}{V}$		Scaling factor =9 $\frac{MW}{V}$		Scaling factor =8 $\frac{MW}{V}$		Scaling factor =15 $\frac{MW}{V}$	
Analog values in Volt	Actual Values in MW	Analog values in Volt	Actual Values in MW	Analog values in Volt	Actual Values in MW	Analog values in Volt	Actual Values in MW
5.0008	20.0032	5.0072	45.0649	4.9997	39.9975	4.9969	59.9629
5.2503	25.0011	5.0069	45.0620	5.0001	40.0011	4.9972	59.9662
6.2504	25.0015	5.5592	50.0338	4.9999	39.9991	4.9971	59.9656
6.2509	25.0037	5.5590	50.0313	5.6251	45.0009	4.9972	59.9665
6.2504	25.0015	5.5593	50.0338	5.6253	45.0025	5.4920	64.9446

- The transformation from volts to MW is done at the beginning of the optimisation algorithm. The next step is to solve the dispatch problem. The analog values from the RTDS front panel PB5 card is given in Table 6.1 are converted into their equivalent real power in MW using the scaling factors specified in Table 6.1. These real powers represent the load power of the four resistive loads of the five bus power system modelled in the RSCAD, Figure 6.2.
- The algorithm described in section 5.5 of Chapter 5, based on the function of Lagrange is used to solve the optimisation dispatch problem. The economic dispatch problem optimal solution $P = [P_1, P_2, P_3]$ based on the real-time load demands (Table 6.1) is given in Table 6.3. The fuel cost for the thermal power plant is calculated using Equation 5.1, Chapter 5 and the fuel cost coefficients and the limits for the produced power are given in Table 6.2 (Kothari and Dhillon, 2006).

Table 6.2: Fuel cost and generator limits of the five bus power system (Kothari and Dhillon, 2006)

Fuel Cost coefficients			Generator Limits	
a _i	b _i	c _i	P _{min}	P _{max}
60	200	140	20	55
75	150	120	20	80
70	180	80	20	65

The fuel cost for the total power demand of 165 MW (Table 6.3) is 695.89 Rs/hr as given in (Kothari and Dhillon, 2006). The Lagrange's method in MATLAB calculates a fuel cost of 709.6 Rs/hr. Another possibility for calculation of the power system network fuel cost, under the measured power demand is directly in the RSCAD environment through the proposed diagram given in Figure 6.7 based on the load flow results. The RSCAD software uses the Newton-Raphson method to solve the load flow problem. The five bus power system model has three generator and four loads. The total power demand of the power system is 160 MW. By solving the power flow problem the real power of the three generators are known and they are used to calculate the fuel cost of the power system as given in Table 6.3.

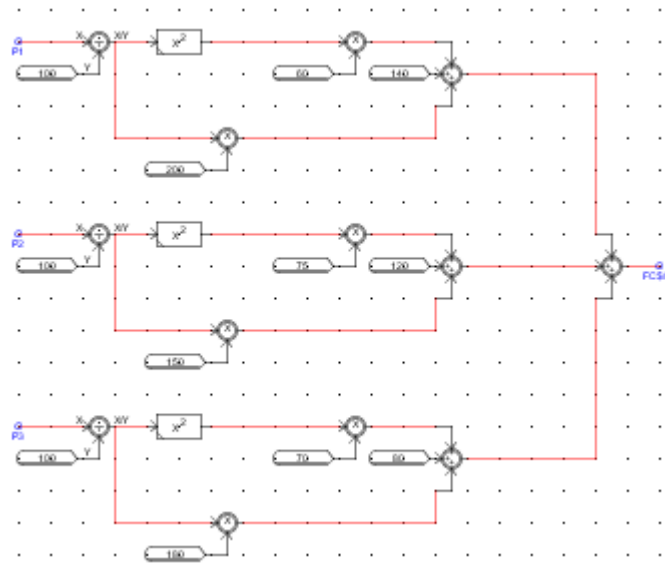


Figure 6.7: RSCAD diagram to calculate the optimal fuel cost of the five bus power system in RSCAD environment

- The values P_1, P_2, P_3 from Table 6.3 provide the optimum set points for the real power production of the three generators in the five bus power system model. These values can be sent by the operator to the power producer in order to control the generation process. It is noted that the optimal generator real power in MATLAB (Lagrange's method) and RSCAD (Newton Raphson method) simulations are different since the two methods do not use the same constraints. RSCAD uses bus voltage and reactive power constraints in addition to the generator limits and power balance constraints which are considered in the

Lagrange's method. These additional constraints provide a variation in the fuel cost for the five bus power system as given in Table 6.3.

Table 6.3: Economic dispatch optimal solution for the five bus system using the RTDS real-time data captured by the LabVIEW-based data acquisition system

Total P_D in MW	Optimal generator real powers in MW			Generator real powers in MW (RSCAD simulation)			P_L in MW	Lagrange's algorithm		Fuel cost in Rs/hr	
	P1	P2	P3	P1	P2	P3		Number of iterations to obtain solution	Computation time in sec	MATLAB (Optimal)	RSCAD (Simulation)
165.02	40.30	53.65	75.98	46.05	68.81	52.22	4.80	701	1.27	709.60	696.7
170.03	41.47	55.41	78.34	46.10	73.70	52.26	5.10	703	1.25	723.40	709.60
174.99	42.63	57.16	80.69	46.11	73.74	57.22	5.40	705	1.34	737.28	722.40
180.00	43.80	58.94	83.06	46.13	74.77	61.23	5.71	706	1.41	751.42	735.70
184.98	44.96	60.71	85.42	46.16	78.52	62.63	6.03	708	1.26	765.65	749.50

6.2.2 LabVIEW-based data acquisition and data transfer system using the RTDS front panel PB5 card analog signals for the eleven bus power system model

The second test system is an eleven bus system in which eleven sliders are designed in the RSCAD run-time window to vary the real power of the eleven loads (PD1 to PD11), which are assigned to the PB5 card analog output channels Rda#1 to Rda#11 as is given in Figure 6.8. The RSCAD diagram for the eleven bus power system model is given in Figure 5.4, Chapter 5. The power demands of the eleven loads are initially set to [20, 20, 30, 25, 25, 10, 40, 90, 70, 25 and 25] MWs respectively, Figure 6.9

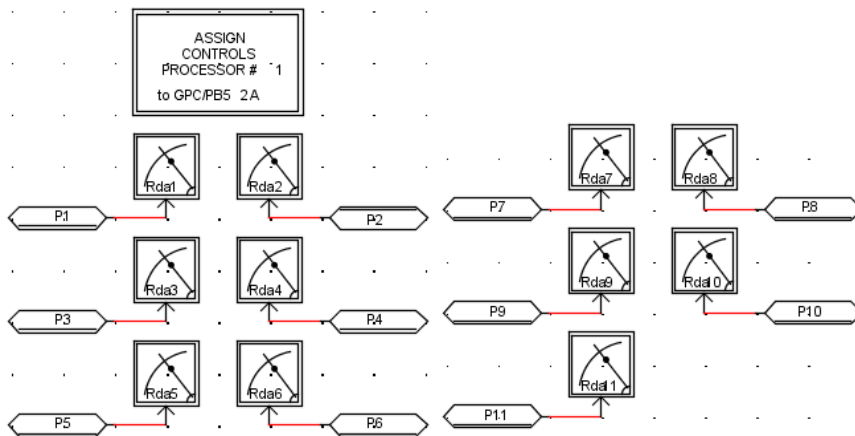


Figure 6.8: RSCAD diagram for the real power load signals assignment to the RTDS PB5 card for the eleven bus power system model

The PB5 analog output channels 1 to 11 are assigned to the NI DAQ 6343 input channels 1 to 11 respectively. The analog output voltages from the RTDS PB5 card represent the real power demands from P_{D1} to P_{D11} . The LabVIEW design diagram to capture the RTDS eleven channel PB5 card signals, using the NI DAQ 6343 card, is given in Figure 6.10.

The test for the second case of power system model is done in the same way as the first one, as follows:

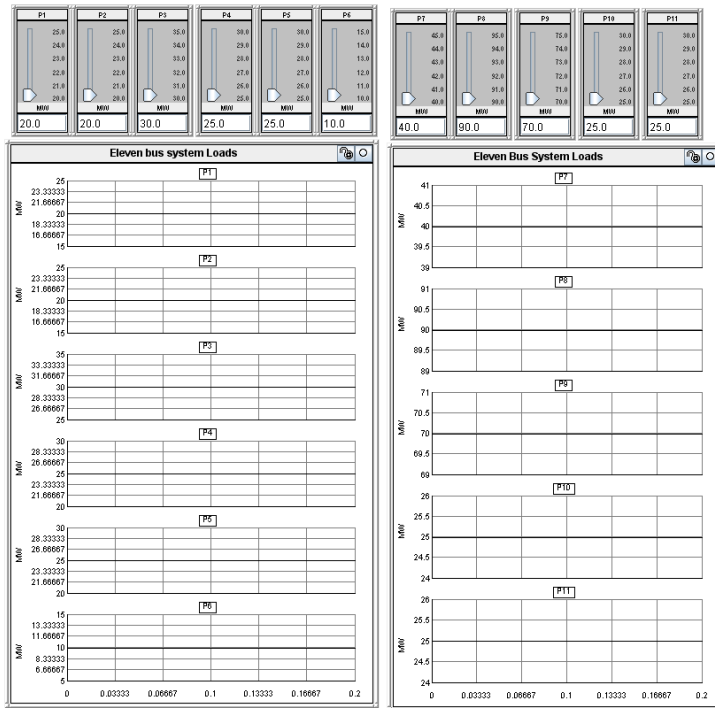


Figure 6.9: Initial values of the power demands of the eleven bus power system (Sliders are at the bottom position) in RSCAD run-time window

The LabVIEW front panel waveforms (Figure 6.11) show the RTDS PB5 card captured signals for the initial real power values of the eleven loads [20 20 30 25 25 10 40 90 70 25 25] MWs. The signals are captured at a sampling rate of 1000 Hz for 100 samples cycle. The analog voltage limits of the NI DAQ 6343 card are $\pm 10V$ which are the minimum and maximum values of the waveforms. The sampling mode is chosen to be continuous. The analog voltage amplitude is plotted versus time in Figure 6.11.

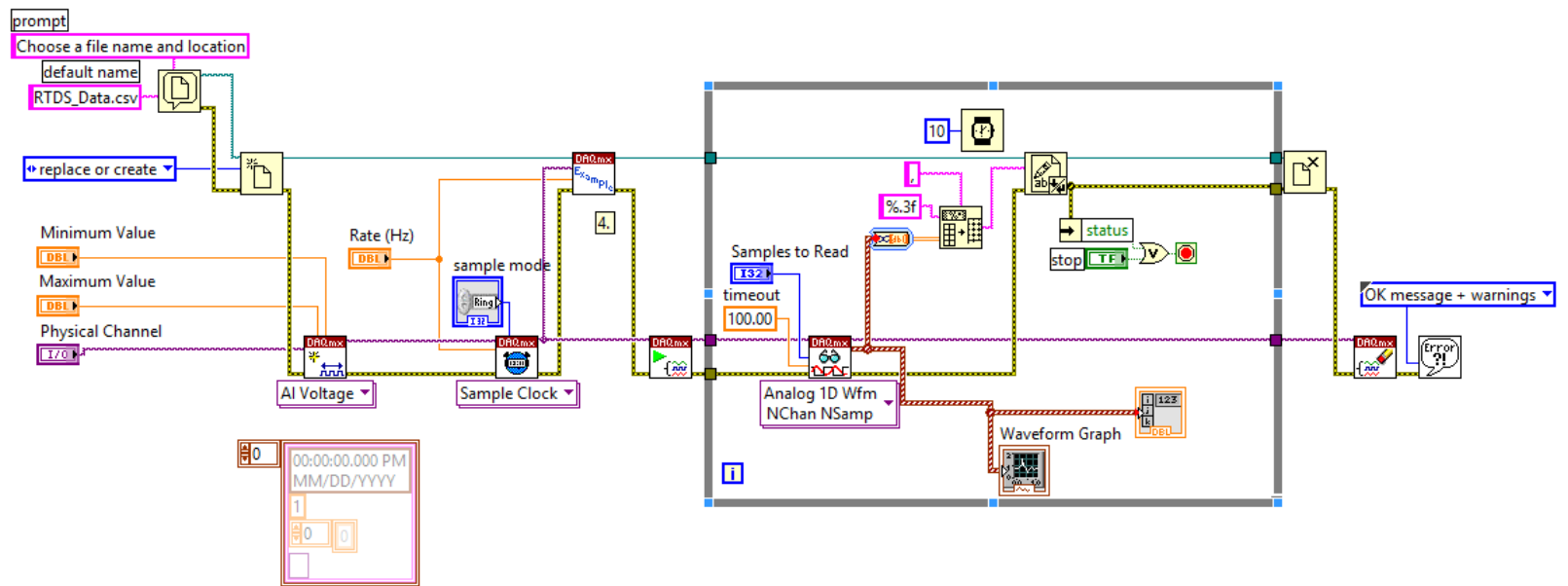


Figure 6.10: LabVIEW diagram to connect the RTDS eleven channel PB5 card signals to the NI DAQ 6343 card

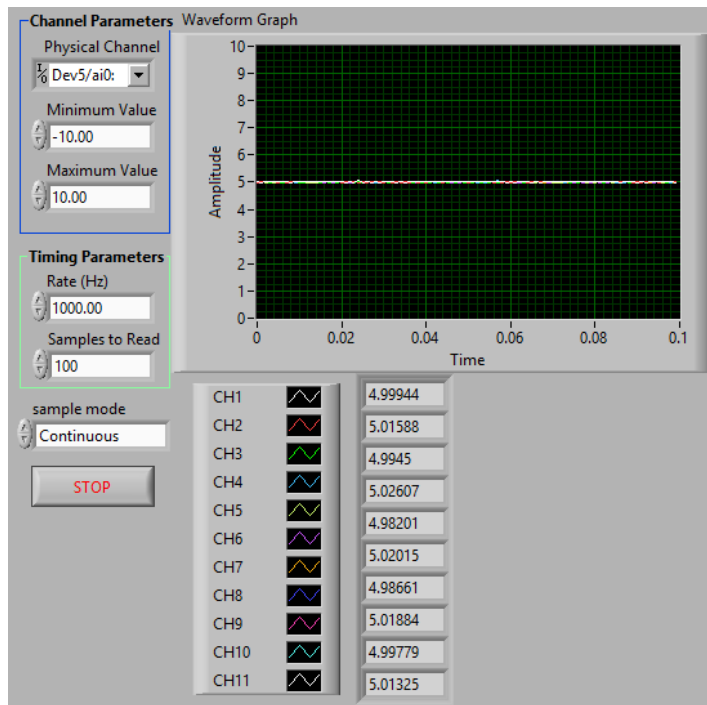


Figure 6.11: LabVIEW front panel waveforms which show the RTDS PB5 card captured signals for the initial load conditions of the eleven bus power system

These analog voltages are converted back into real power in the optimisation software by multiplying with the suitable scaling factors assigned to each channel as given in Table 6.4. The real power values of the power demands for the initial values of the loads are plotted in the MATLAB environment, Figure 6.12 and these for the final power demand are shown in Figure 6.15.

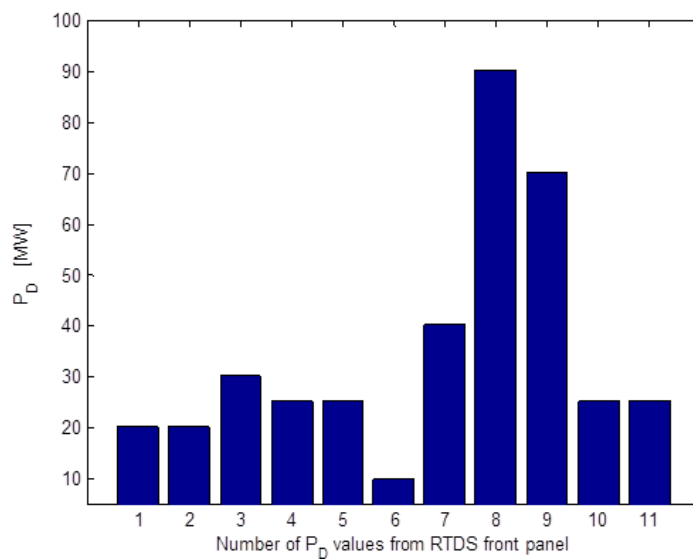


Figure 6.12: Captured by the LabVIEW front panel and transformed to MWs analog voltages of the initial power demands for the eleven bus power system

- The power demand of the first load, P_{D1} is increased from 20 to 25MW by increasing the slider one as shown in Figure 6.13. This procedure is repeated for the other loads P_{D2} to P_{D11} by varying the corresponding load sliders. The final values of the power demands of the eleven bus power system (Sliders are at the top position) in the RSCAD run-time window are shown in Figure 6.13.

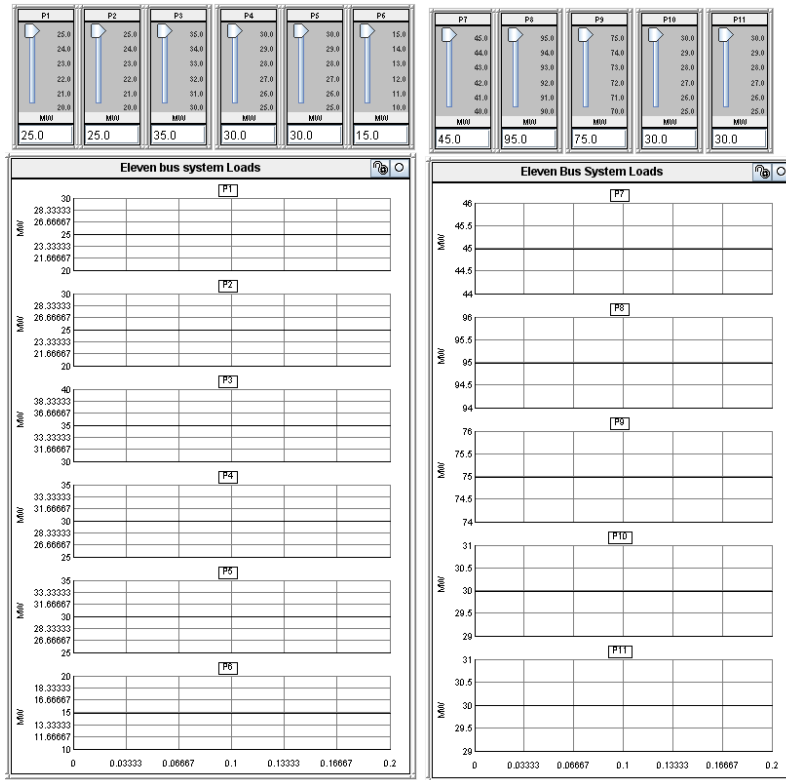


Figure 6.13: Final values of the power demands of the eleven bus power system (Sliders are at the top position) in RSCAD run-time window

- The LabVIEW front panel waveforms (Figure 6.14) show the RTDS PB5 card captured signals for the eleven channels which represent the final real power values of the eleven loads [25 25 35 30 30 15 45 95 75 30 30] MWs of the eleven bus power system. The scaling factors for all the eleven channels are set according to the real power value of the loads. They are given in Table 6.4

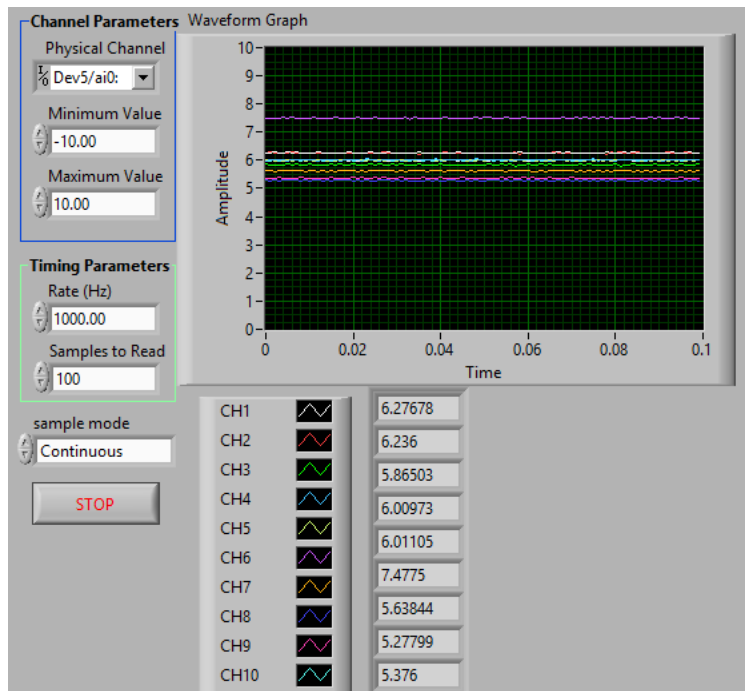


Figure 6.14: LabVIEW front panel waveforms showing the RTDS PB5 card captured signals for the final load conditions of the eleven bus system

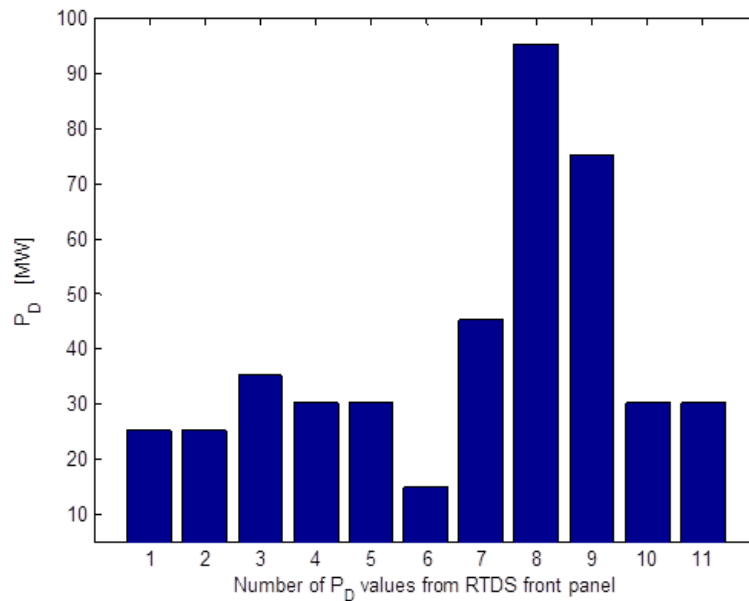


Figure 6.15: Captured by the LabVIEW front panel and transformed to MWs and analog voltages of the final power demands for the eleven bus power system

Table 6.4a: Analog voltage measurement output from the RTDS PB5 card and their actual values for the eleven bus power system (Channels #1 to #6)

Channel #1 (P _{D1})		Channel #2 (P _{D2})		Channel #3 (P _{D3})		Channel #4 (P _{D4})		Channel #5 (P _{D5})		Channel #6 (P _{D6})	
Scaling factor = $4 \frac{MW}{V}$		Scaling factor = $4 \frac{MW}{V}$		Scaling factor = $6 \frac{MW}{V}$		Scaling factor = $5 \frac{MW}{V}$		Scaling factor = $5 \frac{MW}{V}$		Scaling factor = $2 \frac{MW}{V}$	
Analog values in Volt	Actual Values in MW	Analog values in Volt	Actual Values in MW	Analog values in Volt	Actual Values in MW	Analog values in Volt	Actual Values in MW	Analog values in Volt	Actual Values in MW	Analog values in Volt	Actual Values in MW
5	20	5	20	5	30	5	25	5	25	5	10
6.268	25	5	20	5	30	5	25	5	25	5	10
6.268	25	6.264	25	5	30	5	25	5	25	5	10
6.268	25	6.264	25	5.84	35	5	25	5	25	5	10
6.268	25	6.264	25	5.84	35	6.02	30	5	25	5	10
6.268	25	6.264	25	5.84	35	6.02	30	6.005	30	5	10
6.268	25	6.264	25	5.84	35	6.02	30	6.005	30	7.505	15
6.268	25	6.264	25	5.84	35	6.02	30	6.005	30	7.505	15
6.268	25	6.264	25	5.84	35	6.02	30	6.005	30	7.505	15
6.268	25	6.264	25	5.84	35	6.02	30	6.005	30	7.505	15
6.268	25	6.264	25	5.84	35	6.02	30	6.005	30	7.505	15
6.268	25	6.264	25	5.84	35	6.02	30	6.005	30	7.505	15
6.268	25	6.264	25	5.84	35	6.02	30	6.005	30	7.505	15

Table 6.4b: Analog voltage measurement output from the RTDS PB5 card and their actual values for analog output channels of the eleven bus power system (Channels #7 to #11)

Channel #7 (P _{D7})		Channel #8 (P _{D8})		Channel #9 (P _{D9})		Channel #10 (P _{D10})		Channel #11 (P _{D11})	
Scaling factor = $8 \frac{MW}{V}$		Scaling factor = $9 \frac{MW}{V}$		Scaling factor = $14 \frac{MW}{V}$		Scaling factor = $5 \frac{MW}{V}$		Scaling factor = $5 \frac{MW}{V}$	
Analog values in Volt	Actual Values in MW	Analog values in Volt	Actual Values in MW	Analog values in Volt	Actual Values in MW	Analog values in Volt	Actual Values in MW	Analog values in Volt	Actual Values in MW
5	40	5	90	5	70	5	25	5	25
5	40	5	90	5	70	5	25	5	25
5	40	5	90	5	70	5	25	5	25
5	40	5	90	5	70	5	25	5	25
5	40	5	90	5	70	5	25	5	25
5	40	5	90	5	70	5	25	5	25
5	40	5	90	5	70	5	25	5	25
5.629	45	5	90	5	70	5	25	5	25
5.629	45	5.288	95	5	70	5	25	5	25
5.629	45	5.288	95	5.369	75	5	25	5	25
5.629	45	5.288	95	5.369	75	6.010	30	5	25
5.629	45	5.288	95	5.369	75	6.010	30	6.014	30

- Analog voltages measured from the RTDS PB5 card for the eleven bus power system are converted into their equivalent real power values using the respective scaling factor at the beginning of the optimisation problem solution,

Table 6.4. These real power values are used to solve the economic dispatch problem in order to find the set/operating points of the five generators of the eleven bus power system. The fuel cost and the emission function of the dispatch problem are calculated using Equations (5.1) and (5.2), Chapter 5, respectively, using the fuel cost and emission coefficients given in Table 6.5. The diagrams to calculate the fuel cost and emission values for the eleven bus power system as a result of the load flow simulation in the RSCAD environment are given in Figures 6.16 and 6.17 respectively.

Table 6.5: Fuel cost, emission coefficients and generator limits for the eleven bus power system

Gen. No.	Fuel cost coefficients			Emission coefficients			Generator limits in p.u			
	a_i	b_i	c_i	d_i	e_i	f_i	$P_{i,min}$	$P_{i,max}$	$Q_{i,min}$	$Q_{i,max}$
1	0.0015	1.80	40	0.0120	-0.555	30	0.5	3.0	-0.25	1.5
2	0.0030	1.80	60	0.0150	-0.555	50	0.2	1.3	-0.45	1.0
3	0.0012	2.10	100	0.0105	-1.355	60	0.3	1.8	-0.30	1.0
4	0.0080	2.00	25	0.0180	-0.805	80	0.1	1.0	-0.50	1.0
5	0.0010	2.00	120	0.0080	-0.600	45	0.4	2.5	-0.50	0.5

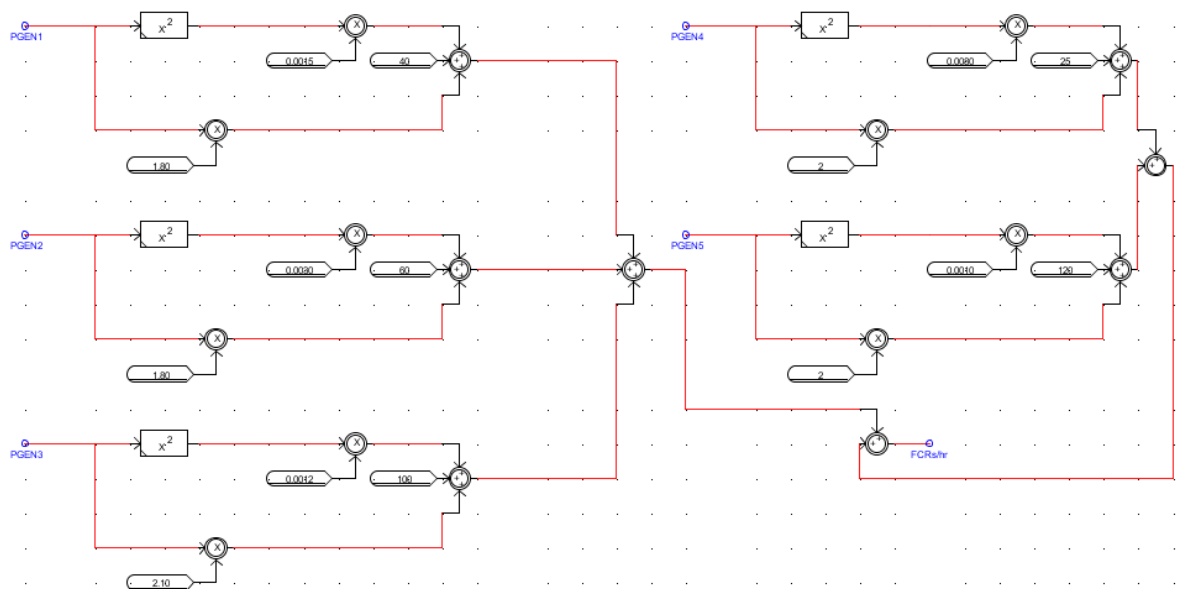


Figure 6.16: RSCAD diagram to calculate the fuel cost for the eleven bus power system

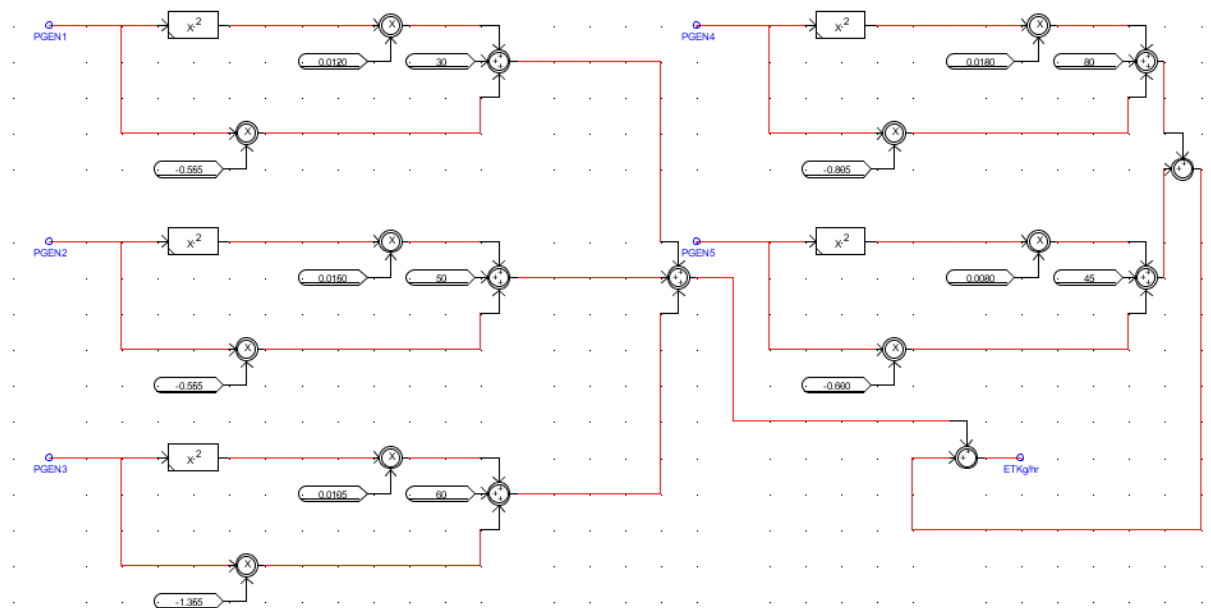


Figure 6.17: RCSAD diagram to calculate the emission value for the eleven bus power system

The economic dispatch solution for the eleven bus power system is given in Table 6.6. This solution is obtained when the power demand is varied from 380 to 435 MW's with an increment of 5 MW's. The initial power demand of 380 MW is at a fuel cost of 1212.5 Indian Rupees (INR) and an emission of 608.1 kg/hr calculated using the Lagrange's method and a fuel cost of 1214.3 INR and emission of 611 kg/hr are calculated by the Newton-Raphson method in the RSCAD environment. It is observed that the Lagrange's method provides for a reduction in fuel cost and emission in comparison to the RSCAD solution using the Newton-Raphson method.

Table 6.6a: Economic dispatch problem solution for the eleven bus power system using the LabVIEW-based data acquisition system (generator powers)

P _D in MW	Optimal generator real powers in MW					RSCAD simulation based generator real powers in MW				
	P ₁	P ₂	P ₃	P ₄	P ₅	P ₁	P ₂	P ₃	P ₄	P ₅
380	50	20	165.28	18.54	148.33	203.30	50.00	50.00	50.00	50.00
385	50	20	166.69	18.75	150.02	208.20	50.01	50.00	50.01	50.01
390	50	20	168.09	18.96	151.71	208.30	55.00	50.00	50.01	50.01
395	50	20	169.50	19.17	153.40	207.20	52.86	54.98	48.33	49.44
400	50	20	170.91	19.38	155.10	208.30	55.00	54.98	50.02	50.01
405	50	20	172.32	19.59	156.79	208.30	55.01	54.99	50.04	55.00
410	50	20	173.73	19.81	158.48	208.30	55.02	54.99	52.88	57.20

415	50	20.05	175.14	20.02	160.17	209.00	58.41	54.99	53.85	57.52
420	50	20.62	176.55	20.23	161.86	210.10	60.57	54.99	55.56	58.09
425	50	21.18	177.96	20.44	163.55	211.10	61.02	55.00	56.74	60.75
430	50	21.74	179.37	20.65	165.24	212.00	64.48	55.00	57.46	60.99
435	50	22.31	180	20.86	166.94	215.10	65.80	55.00	58.06	61.19

It is noted that the real power of the generator one (P1) in the RSCAD simulation using Newton-Raphson method provides 203.30 MW (Table 6.6a), whereas the optimal generator real power obtained by the Lagrange's method is only 50 MW. This is because the maximum loading is taking place for the generator which is connected to the slack bus in the Newton-Raphson method. This produces a variation in the fuel cost and emissions in both optimal MATLAB and RSCAD simulation results as given in Table 6.6b.

Table 6.6b: Economic dispatch problem solution for the eleven bus power system using the LabVIEW-based data acquisition system (fuel cost and emission values)

P _D in MW	P _L in MW	Fuel cost in Rs/hr		Emission in kg/hr	
		Optimal MATLAB	RSCAD simulation	Optimal MATLAB	RSCAD simulation
380	22.15	1212.5	1214.3	608.1	611.0
385	20.46	1213.2	1222.6	629.7	632.9
390	18.76	1224.1	1230.3	630.3	637.9
395	17.07	1235.0	1238.2	633.2	636.7
400	15.39	1246.0	1248.6	643.2	645.9
405	13.70	1253.9	1258.5	645.5	647.2
410	12.02	1261.9	1271.4	649.9	651
415	10.38	1269.9	1284.8	657.6	659.7
420	9.26	1279.0	1297.5	663.5	669.8
425	8.13	1288.0	1310.2	673.2	677.4
430	7.00	1297.1	1322.9	679.5	687.4
435	5.11	1304.3	1335.2	700.7	704.6

6.2.3 Discussion on the economic dispatch problem solution using the LabVIEW-based data acquisition and data transfer system

The solutions of the economic dispatch problem with the RSCAD simulation and MATLAB optimisation are very close and are given in Table 6.6b. The Lagrange's algorithm produces better values for the fuel cost and emission of pollutants as it

optimizes the dispatch problem solution according to the given constraints. The investigation on the application of the MATLAB-based data acquisition and data transfer system is described in detail in the next section.

6.3 MATLAB-based data acquisition and data transfer system using the RTDS front panel PB5 card analog output signals

This section investigates the application of the data acquisition and data transfer system based on MATLAB software. The investigations are done on the five and the eleven bus power system models. The MATLAB software is developed to capture the RTDS PB5 card analog output signals using the NI DAQ card.

6.3.1 MATLAB-based data acquisition and data transfer system using the RTDS front panel PB5 card analog output signals for the five bus power system model

A MATLAB-based data acquisition system is used to capture the real-time data of the RTDS PB5 card analog outputs through the MATLAB code given below:

```
daq.getVendors()  
daq.getDevices;  
% Create a session using the listed NI DAQ device.  
s = daq.createSession('ni');  
%Add an analog input voltage channel to the session. Choose channel '1' on the NI device.  
% Make sure your device is properly connected  
ch = s.addAnalogInputChannel('Dev5',[0 1 2 3], 'Voltage');  
% Set DAQ Parameters  
s.Rate = 10000;% how fast do you want to acquire the data  
% s.Channels.Range = [-10 10];  
s.DurationInSeconds =0.1; % acquisition total time  
% Take care of data  
[data,time] = s.startForeground
```

The MATLAB subplot, Figure 6.18 shows the captured analog signals from the RTDS front panel PB5 card. The MATLAB-based data acquisition system takes longer computational time compared to the LabVIEW-based data acquisition system. The analog output voltages from the RTDS PB5 card for the power demands P_{D1} to P_{D4} are given in Table 6.7 and the economic dispatch problem solution using the real-time power demands from Table 6.7 is given in Table 6.8.

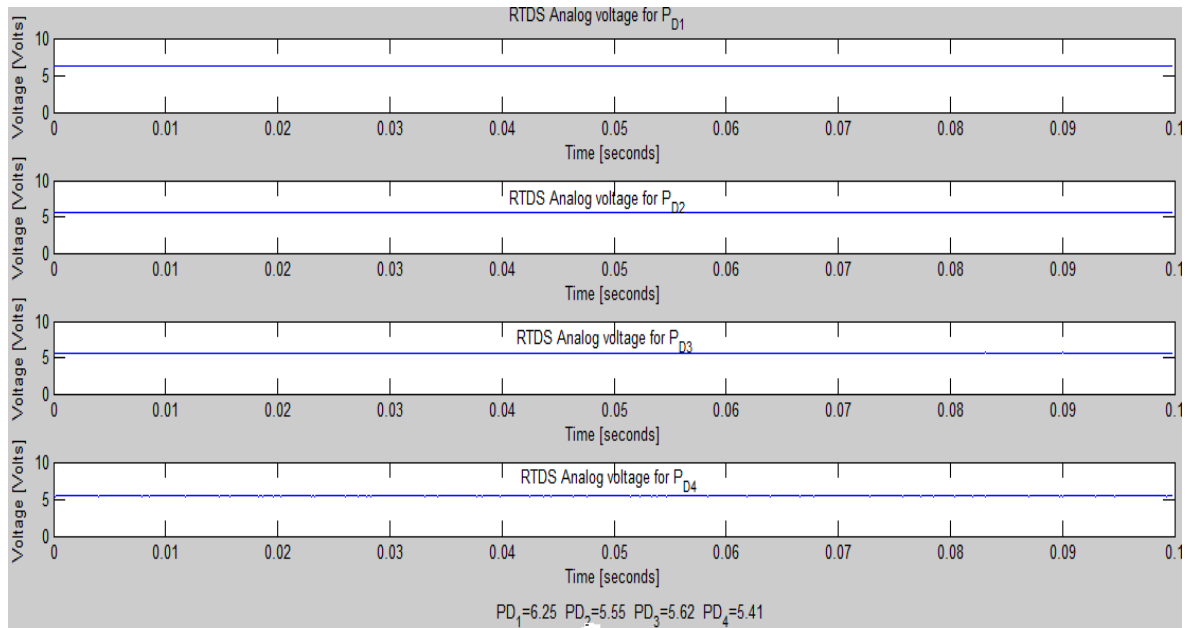


Figure 6.18: Amplitude of the analog signals captured from the RTDS PB5 card using the MATLAB-based data acquisition system for the final position of the load sliders

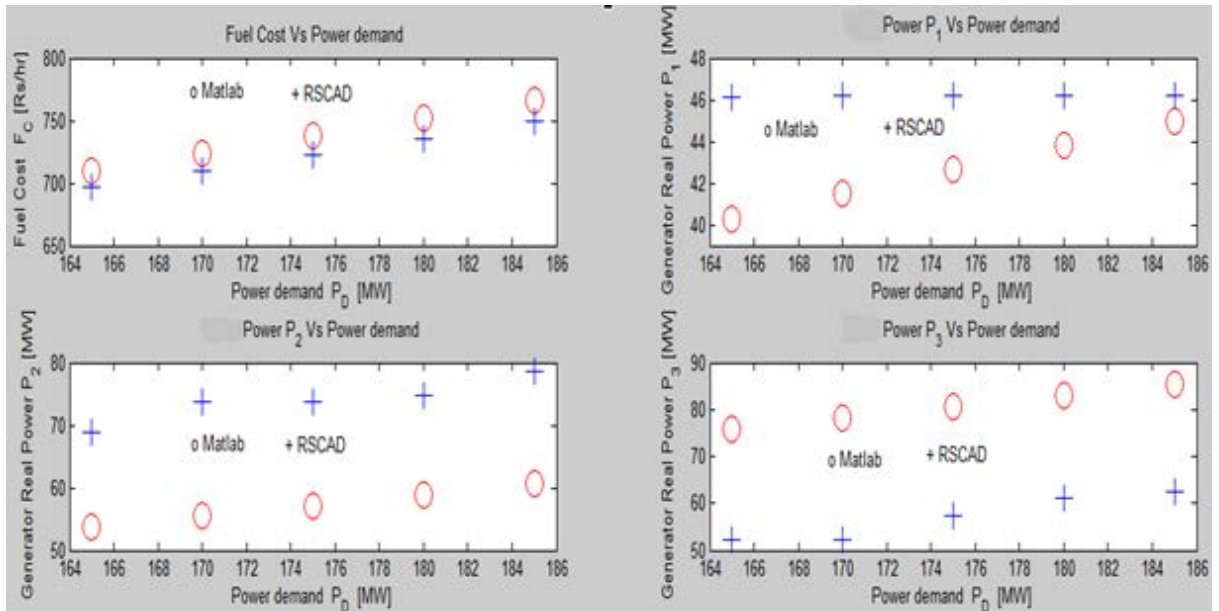
Table 6.7: Five bus system analog values from the RTDS front panel PB5 card acquired using the MATLAB-based data acquisition system

Channel #1 (Pd1)		Channel #2 (Pd2)		Channel #3 (Pd3)		Channel #4 (Pd4)	
Scaling factor = $4 \frac{MW}{V}$		Scaling factor = $9 \frac{MW}{V}$		Scaling factor = $8 \frac{MW}{V}$		Scaling factor = $15 \frac{MW}{V}$	
Analog values in Volt	Actual Values in MW	Analog values in Volt	Actual Values in MW	Analog values in Volt	Actual Values in MW	Analog values in Volt	Actual Values in MW
5.0006	20.0037	5.0070	45.0599	4.9972	39.9819	4.9998	60.0014
6.2506	25.0023	5.0070	45.0633	4.9970	39.9758	4.9996	59.9958
6.2504	25.0016	5.5588	50.0290	4.9971	39.9770	4.9997	59.9968
6.2504	25.0014	5.5587	50.0283	5.6250	45.0000	4.9978	59.9731
6.2506	25.0025	5.5592	50.0331	5.6250	45.0000	5.4131	64.9958

Table 6.8: Economic dispatch solution for the five bus system using the RTDS real-time data captured by the MATLAB-based data acquisition system (Lagrange's algorithm)

P _D in MW	Optimal generator real powers in MW			Lambda	P _L in MW	Number of iterations	Computation time in sec	Fuel cost in Rs/hr
	P ₁	P ₂	P ₃					
165.0410	40.3077	53.6596	75.9898	1.3095e+04	4.8102	701	8244.366156	709.6509
170.0381	41.4795	55.4163	78.3505	1.3522e+04	5.1040	703	9485.069563	723.4416
175.0044	42.6426	57.1720	80.7023	1.3949e+04	5.4047	705	9907.838784	737.3124
180.0067	43.8078	58.9432	83.0670	1.4380e+04	5.7156	706	11311.700633	751.4241
184.9926	44.9694	60.7209	85.4327	1.4813e+04	6.0346	708	11523.974105	765.6731

The Comparison of the fuel cost and the generator real powers between the RSCAD load flow simulation, Table 6.3 and the MATLAB optimisation solution, Table 6.8, for the five bus power system is given in Figure 6.19. The optimal fuel cost value calculated using MATLAB is less in comparison to the RSCAD solution.



Where in Figure 6.19: MATLAB means optimal solution using the Lagrange's method and RSCAD means load flow simulation in RSCAD using the Newton-Raphson method

Figure 6.19: Comparison of the fuel cost and the generator real powers between the RSCAD load flow simulation and the MATLAB optimisation solution for the five bus power system model

6.3.2 MATLAB-based data acquisition and data transfer system using the RTDS front panel PB5 card analog output signals for the eleven bus power system model

A MATLAB-based data acquisition system for the eleven bus power system is used to capture the real-time data of the RTDS PB5 card analog outputs of the initial eleven channel signals through the MATLAB code given below:

```

% 1.Create a device object - Create the analog input object AI for a ...
% National Instrument Instruments board. The installed adaptors and ...
% To find the hardware IDs
daq.getVendors()
daq.getDevices;
% 2.You should see a list of devices. Create a session using the listed NI DAQ
device.
s = daq.createSession('ni');
%3. Add an analog input voltage channel to the session. Choose channel '1' on the
NI device.
% Make sure your device is properly connected
ch = s.addAnalogInputChannel('Dev5',[0 1 2 3 4 5 6 7 16 17 18], 'Voltage');
% 4.Set DAQ Parameters
s.Rate = 10000;% how fast do you want to acquire the data

```

```

s.DurationInSeconds = 0.1; % acquisition total time
% 5. Take care of data
[data,time] = s.startForeground

```

The power demand data plots for the initial position of the sliders are given in Figure 6.20. The initial power demand values are set according to the eleven bus data. All the eleven channels are initially set to 5 Volts and the corresponding scaling factors are fixed as per the power demands.

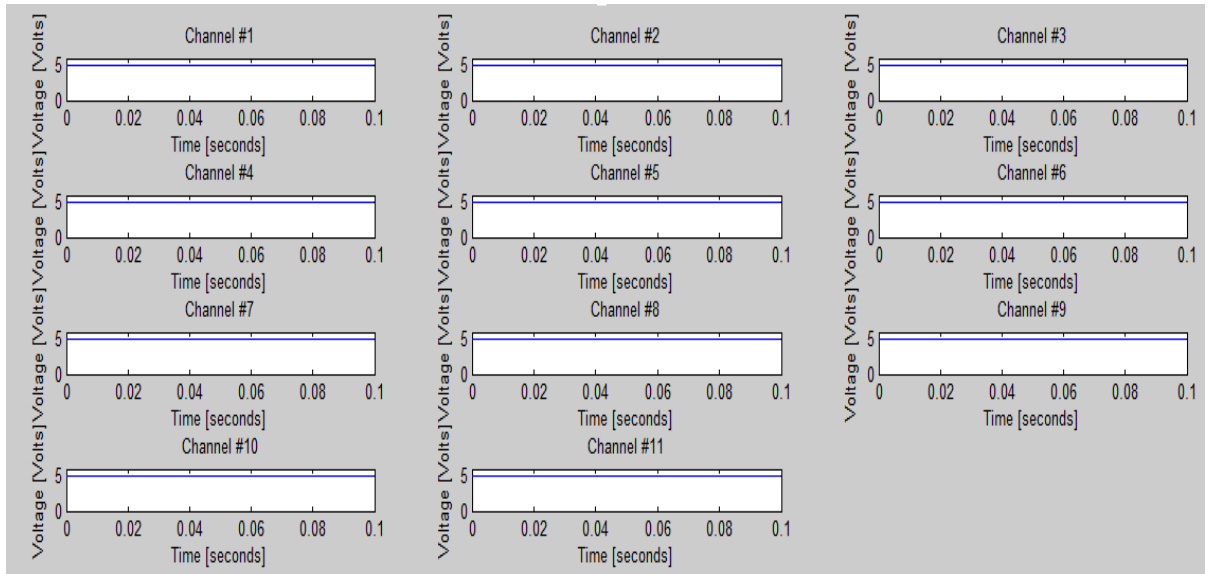


Figure 6.20: Power demand data at the analog outputs of the RTDS PB5 card

The analog voltage measurement from the RTDS PB5 card and the calculated actual values in MW for the eleven bus power system are given in Table 6.9.

Table 6.9a: Eleven bus power system analog values from the RTDS front panel PB5 card outputs and their actual values acquired using the MATLAB-based data acquisition system (Channels #1 to #6)

Channel #1 (P _{D1})		Channel #2 (P _{D2})		Channel #3 (P _{D3})		Channel #4 (P _{D4})		Channel #5 (P _{D5})		Channel #6 (P _{D6})	
Scaling factor =4 $\frac{MW}{V}$		Scaling factor =4 $\frac{MW}{V}$		Scaling factor =6 $\frac{MW}{V}$		Scaling factor =5 $\frac{MW}{V}$		Scaling factor =5 $\frac{MW}{V}$		Scaling factor =2 $\frac{MW}{V}$	
Analog values in Volt	Actual Values in MW	Analog values in Volt	Actual Values in MW	Analog values in Volt	Actual Values in MW	Analog values in Volt	Actual Values in MW	Analog values in Volt	Actual Values in MW	Analog values in Volt	Actual Values in MW
5	20	5	20	5	30	5	25	5	25	5	10
6.267	25	5	20	5	30	5	25	5	25	5	10
6.267	25	6.265	25	5	30	5	25	5	25	5	10
6.267	25	6.265	25	5.83	35	5	25	5	25	5	10
6.267	25	6.265	25	5.83	35	6.04	30	5	25	5	10
6.267	25	6.265	25	5.83	35	6.04	30	6.003	30	5	10
6.267	25	6.265	25	5.83	35	6.04	30	6.003	30	7.503	15
6.267	25	6.265	25	5.83	35	6.04	30	6.003	30	7.503	15

6.267	25	6.265	25	5.83	35	6.04	30	6.003	30	7.503	15
6.267	25	6.265	25	5.83	35	6.04	30	6.003	30	7.503	15
6.267	25	6.265	25	5.83	35	6.04	30	6.003	30	7.503	15
6.267	25	6.265	25	5.83	35	6.04	30	6.003	30	7.503	15

Table 6.9b: Eleven bus power system analog values from the RTDS front panel PB5 card outputs and their actual values acquired using the MATLAB-based data acquisition system

Channel # 7 (P _{D7})		Channel #8 (P _{D8})		Channel #9 (P _{D9})		Channel #10 (P _{D10})		Channel #11 (P _{D11})	
Scaling factor =8 $\frac{MW}{V}$		Scaling factor =9 $\frac{MW}{V}$		Scaling factor =14 $\frac{MW}{V}$		Scaling factor =5 $\frac{MW}{V}$		Scaling factor =5 $\frac{MW}{V}$	
Analog values in Volt	Actual Values in MW	Analog values in Volt	Actual Values in MW	Analog values in Volt	Actual Values in MW	Analog values in Volt	Actual Values in MW	Analog values in Volt	Actual Values in MW
5	40	5	90	5	70	5	25	5	25
5	40	5	90	5	70	5	25	5	25
5	40	5	90	5	70	5	25	5	25
5	40	5	90	5	70	5	25	5	25
5	40	5	90	5	70	5	25	5	25
5	40	5	90	5	70	5	25	5	25
5	40	5	90	5	70	5	25	5	25
5.627	45	5	90	5	70	5	25	5	25
5.627	45	5.290	95	5	70	5	25	5	25
5.627	45	5.290	95	5.371	75	5	25	5	25
5.627	45	5.290	95	5.371	75	6.012	30	5	25
5.627	45	5.290	95	5.371	75	6.012	30	6.013	30

The economic dispatch problem solution is given in Table 6.10, which uses the real-time load demands given in Table 6.9.

Table 6.10a: Economic dispatch problem optimal and load flow based solutions for the eleven bus power system using the RTDS real-time data captured by the MATLAB-based data acquisition system (generator powers)

P _D in MW	Optimal generator real powers in MW					Generator real powers in MW (RSCAD simulation)				
	P ₁	P ₂	P ₃	P ₄	P ₅	P ₁	P ₂	P ₃	P ₄	P ₅
380	50	20	165.28	18.54	148.33	203.30	50.00	50.00	50.00	50.00
385	50	20	166.69	18.75	150.02	208.20	50.01	50.00	50.01	50.01
390	50	20	168.09	18.96	151.71	208.30	55.00	50.00	50.01	50.01
395	50	20	169.50	19.17	153.40	207.20	52.86	54.98	48.33	49.44
400	50	20	170.91	19.38	155.10	208.30	55.00	54.98	50.02	50.01
405	50	20	172.32	19.59	156.79	208.30	55.01	54.99	50.04	55.00
410	50	20	173.73	19.81	158.48	208.30	55.02	54.99	52.88	57.20
415	50	20.05	175.14	20.02	160.17	209.00	58.41	54.99	53.85	57.52
420	50	20.62	176.55	20.23	161.86	210.10	60.57	54.99	55.56	58.09
425	50	21.18	177.96	20.44	163.55	211.10	61.02	55.00	56.74	60.75
430	50	21.74	179.37	20.65	165.24	212.00	64.48	55.00	57.46	60.99
435	50	22.31	180	20.86	166.94	215.10	65.80	55.00	58.06	61.19

Table 6.10b: Economic dispatch problem optimal and load flow based solutions for the eleven bus power system using the RTDS real-time data captured by the MATLAB-based data acquisition system (fuel cost and emission values)

P _D in MW	P _L in MW	Lagrange's algorithm		Fuel cost in Rs/hr		Emission in kg/hr	
		Number of iterations	Computation time in sec	Optimal MATLAB	RSCAD simulation	Optimal MATLAB	RSCAD simulation
380	22.15	960	4435.15	1212.5	1214.3	608.1	611.0
385	20.46	989	4510.23	1213.2	1222.6	629.7	632.9
390	18.76	1102	4569.16	1224.1	1230.3	630.3	637.9
395	17.07	1302	4655.10	1235.0	1238.2	633.2	636.7
400	15.39	1421	4738.49	1246.0	1248.6	643.2	645.9
405	13.70	1502	4817.30	1253.9	1258.5	645.5	647.2
410	12.02	1589	4888.94	1261.9	1271.4	649.9	651
415	10.38	1639	4972.33	1269.9	1284.8	657.6	659.7
420	9.26	1712	5056.90	1279.0	1297.5	663.5	669.8
425	8.13	1823	5122.73	1288.0	1310.2	673.2	677.4
430	7.00	1923	5234.36	1297.1	1322.9	679.5	687.4
435	5.11	1989	5305.06	1304.3	1335.2	700.7	704.6

The fuel cost for the 380 MW (Table 6.10b) total power demand is 1201 Rs/hr as calculated in (Kothari and Dhillon, 2006). The Lagrange's optimisation method gives a fuel cost of 1212.5 Rs/hr. The solution using the Newton Raphson method gives fuel cost equal to 1214.3 Rs/hr. It is observed that the economic dispatch problem solutions, obtained through using the LabVIEW and MATLAB-based methods have very close values as is given in Tables 6.6 and 6.10 respectively for the five and eleven bus power systems.

6.3.3 Discussion on the application of the MATLAB-based data acquisition and data transfer system using the RTDS front panel PB5 card analog output signals

The solutions of the economic dispatch problem obtained by the Lagrange's and Newton-Raphson methods are very similar. They are given in Tables 6.8 and 6.10 for the five and the eleven bus power systems respectively.

The economic dispatch problem determines the best way to minimize the current generator operating costs, whereas the optimal power flow determine the best way to instantaneously operate a power system by considering the impact of the transmission systems. Optimal power flow combines the power flow problem with the economic dispatch and minimizes the operating cost function with subject to both

equality and inequality constraints. It is observed that, there is a difference in power flow and economic dispatch problem solutions for the generator powers influences the fuel cost and the emission values.

The RSCAD simulation (Newton Raphson method) uses the bus voltage and the reactive power constraints in addition to the generator limits and power balance constraints, which are considered in Lagrange's method. This provides the variation in the fuel cost and emission values of the economic dispatch problem solutions as given in Tables 6.3 and 6.10b for the five and the eleven bus power systems respectively.

It is noted that the MATLAB-based system had a longer computational time when compared with the LabVIEW-based system. It can be concluded that the MATLAB-based data acquisition system is not as good for real-time data acquisition and data transfer as the LabVIEW-based system.

LabVIEW performs faster to capture the signals from the RTDS PB5 card in comparison with the MATLAB-based data acquisition system. The developed lab-scale set-up makes it possible to solve the optimal power dispatch problem in real-time and to investigate how the solution of the problem is influenced by the load changes. Such types of simulations can help in the process of planning the daily power production.

6.4 Lab-scale data acquisition and data transfer system using the RTDS GTNET card Phasor Measurement Unit (PMU) signals

This section describes the application of the Phasor Measurement Units (PMUs) for data acquisition and data transfer in order to solve the optimisation dispatch problem at the remote end. The results of this application are described. It provides a clear idea of how to transfer the RTDS GTNET card PMU real-time data from the RTDS to the remote end computer using the appropriate network protocols (IEEE C37.118-2005), and how to build a MySQL Database Management system (DMS) to store and retrieve the large volume of power system data in order to avoid delays in the solution for the economic dispatch problem.

6.4.1 GTNET card PMU-based laboratory setup to solve the economic dispatch problem

Figure 6.21a shows the block diagram schematic described in Chapter 4 for the GTNET card PMU-based data acquisition and data transfer system

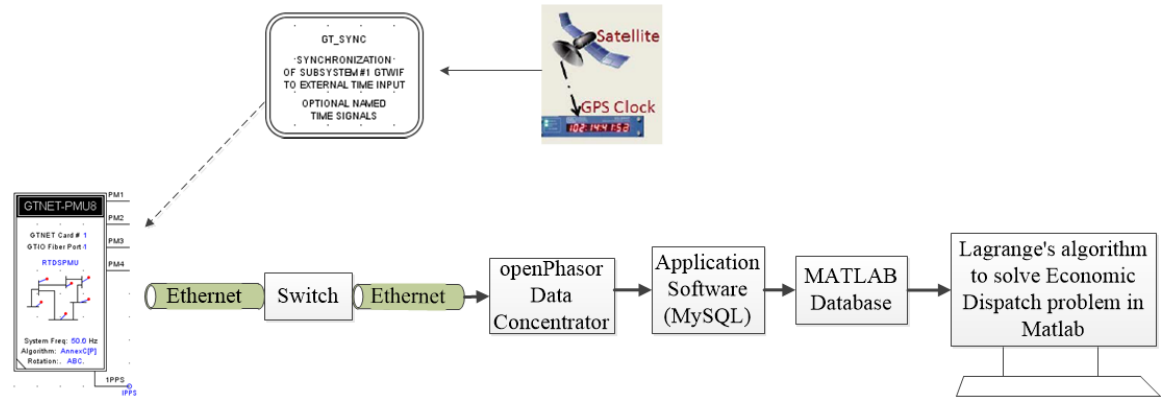


Figure 6.21a: RTDS GTNET card PMU-based laboratory setup to solve the dispatch optimisation problem in real-time

The current and voltage signals of the power demands are assigned to the GTNET card PMU software within the RSCAD environment. The idea behind the laboratory setup is to transfer the real power of the power system loads using IEEE C37.118-2205 protocol to the remote location by interfacing the OpenPDC software with the RTDS simulator via Ethernet. The GTNET card PMU used in this lab setup is from the RTDS library and is synchronized to the GPS using a SEL GPS clock and antenna.

On the remote end, a PMU connection tester and the OpenPDC software are used to capture the RTDS signals in real-time and these signals are archived in the MySQL database. Every five minutes, the data is retrieved from the MySQL database by the MATLAB-based optimisation algorithm. The Lagranges algorithm developed by (Krishnamurthy and Tzoneva, 2013) is used to solve the economic dispatch problem using the real-time data which is retrieved from the MySQL database.

6.4.2 Real-time implementation of the algorithm for solution of the dispatch problem for the PMU-based data acquisition and data transfer system

The major steps of the real-time dispatch problem solution using the PMU-based data acquisition and transfer system are: The power system model is simulated in RSCAD (RTDS) and changing of the power demand during the simulation is accomplished through changing the values of the loads in the simulated system. The

produced power demand values are measured and are sent to the GTNET card PMU analogue output signals. From these outputs, the values are captured at the remote end by the PMU connection tester and the OpenPDC, and then they are stored in the MySQL database.

The optimisation algorithm in Figure 5.5, described in Chapter 5 is executed. It reads the new values of the power demands and the optimisation problem is solved. The obtained solution is used by the operator to control the generation production. The algorithm for real-time solution of the problem is given in Figure 6.21b. This algorithm is implemented in Figure 6.21a. The thesis considers only the real-time solution of the optimisation problem based on real-time acquired and transferred data and does not solve the problem for the control of the generators. This problem can be solved by a future research project.

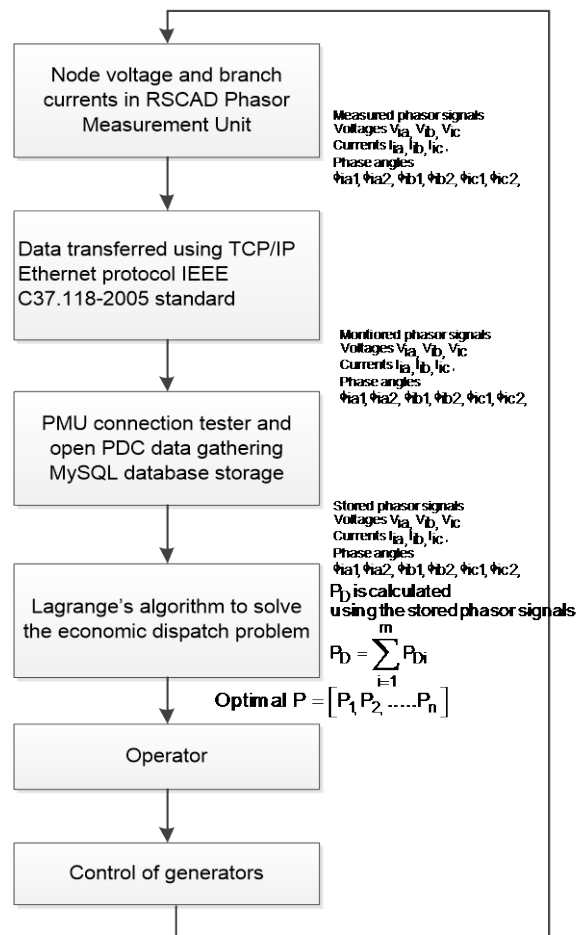


Figure 6.21b: Flow chart of the real-time solution of the dispatch problem using the GTNET card PMU-based data acquisition and transfer system

6.4.3 Implementation of the GTNET card PMU-based system for the five bus power system model

Implementation of the algorithm from Figure 6.21b is performed for the five bus model case study.

6.4.3.1 Power system model simulation and assignment of the load demand powers to the GTNET card PMU

The five bus power system model was designed and implemented within the RSCAD software as given in Figure 5.10, Chapter 5. The five bus power system has four loads components and their power demands are [20, 45, 40, 60] MWs. Currents entering into the four loads are monitored by connecting four circuit breakers to the loads as is shown in Figure 6.22. The voltage signals of the loads are observed by monitoring the bus voltages at the points where the load terminals are connected. This voltage and current signals of the load components are assigned to the GTNET card PMU within the RSCAD environment. The voltage and current phasor signals of the first two loads are assigned to be transferred to the PMU1 and PMU2 and the third and fourth loads are assigned to the PMU3 and PMU4 respectively. The monitored voltage and current signals are time-stamped by the GPS clock at the host end and are transferred to the remote end PC using the Ethernet communication IEEE C37.118-2005 standard.

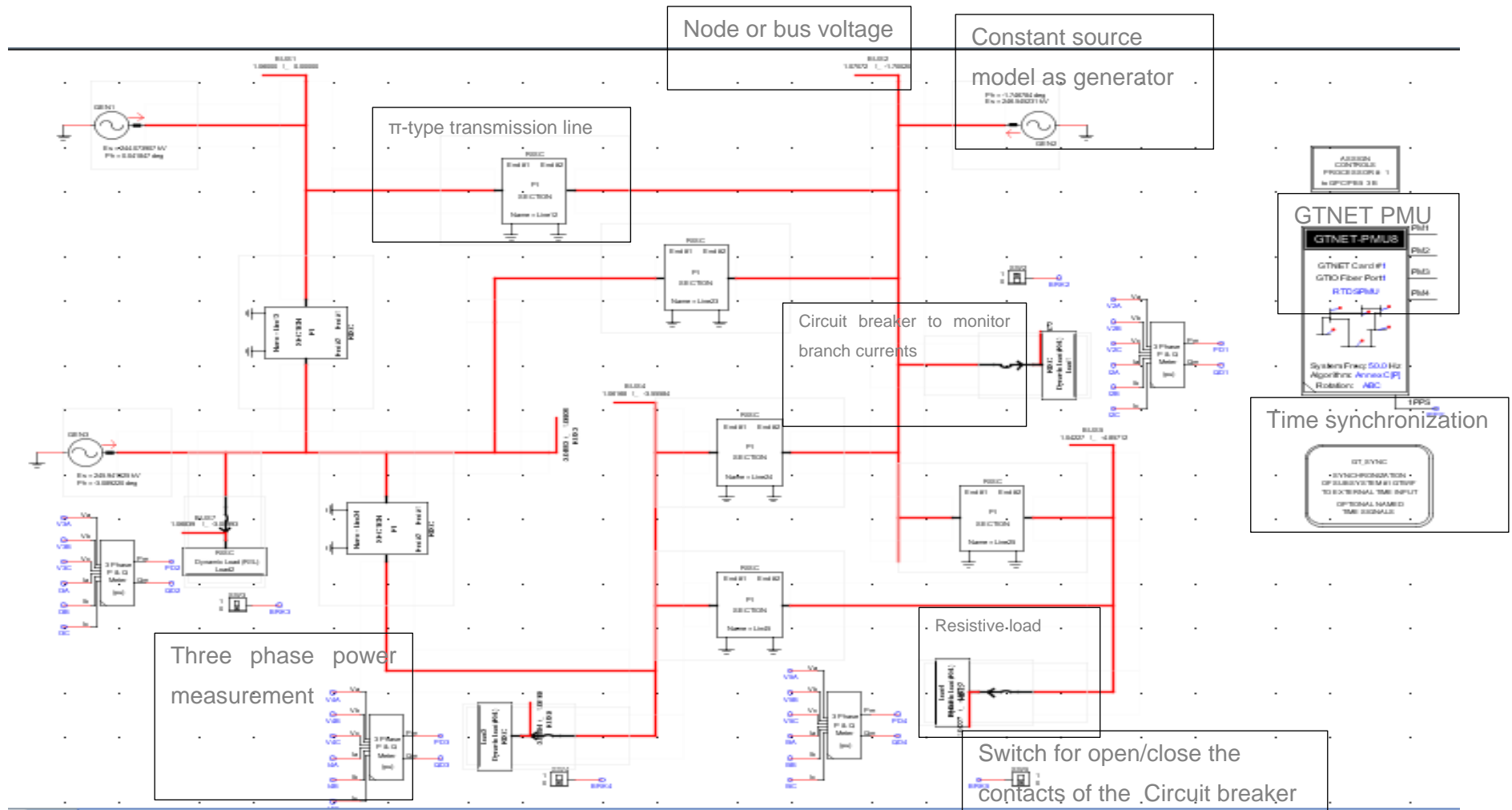


Figure 6.22: Five bus Power system network modelled in the RSCAD environment with additional components to implement data acquisition and data transfer using the GTNET card PMU signals

The RSCAD runtime window is given in Figures 6.23 and 6.24, where the three-phase voltage and current magnitudes, the phase angles, and the real power values of the individual loads (power demands) are shown.

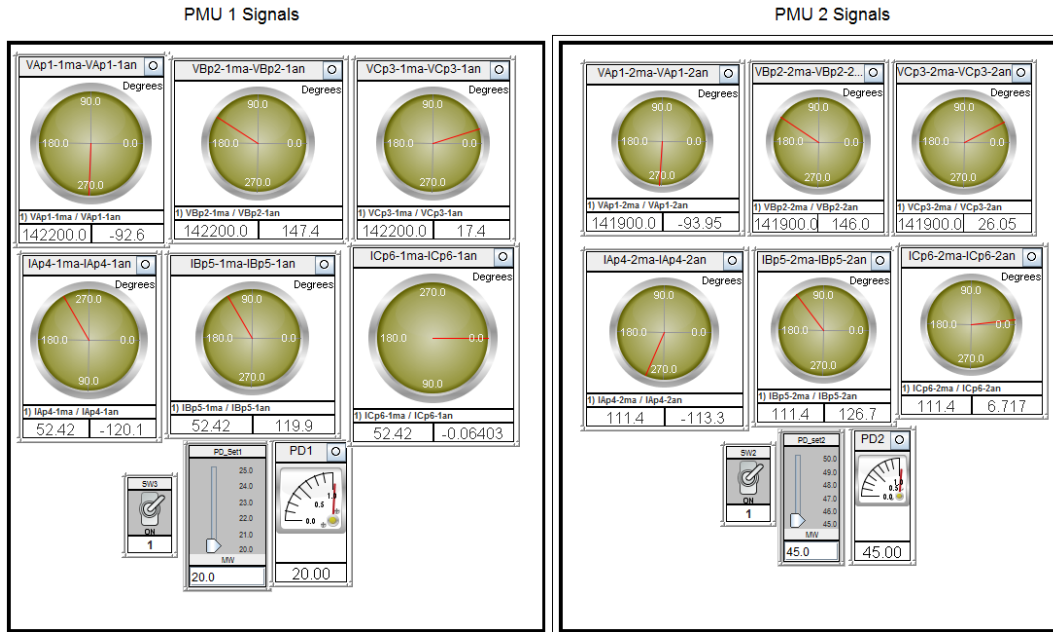


Figure 6.23: Monitoring the voltage and current magnitudes and the phase angles of the PMU 1 and PMU 2 signals in the RSCAD environment

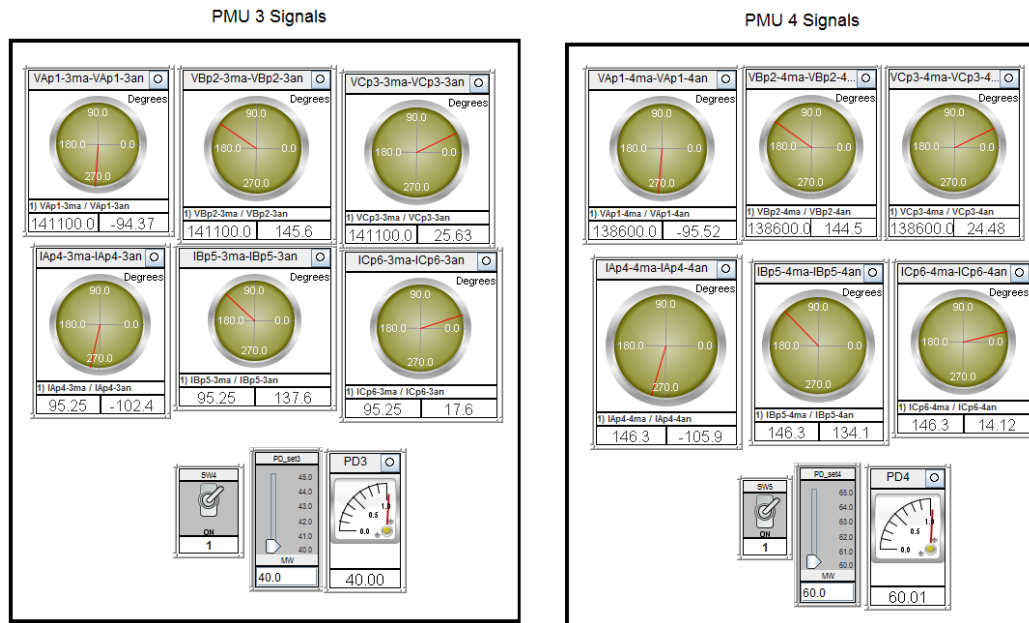


Figure 6.24: Monitoring the voltage and current magnitudes and the phase angles of the PMU 3 and PMU 4 signals in the RSCAD environment

6.4.3.2 Monitoring the RSCAD GTNET card PMU signals in the OpenPDC environment

The transferred signals are monitored in real-time in the remote end using the Open Phasor Data Concentrator (PDC) software. Figure 6.26 and 6.27 show the RSCAD GTNET signals in the OpenPDC environment, where Figure 6.26 shows the PMU 1 and PMU 2 monitored signals and Figure 6.27 shows the PMU 3 and PMU 4 monitored signals. Each signal has its own ID numbers. In Figure 6.25 the PMU 1 signal ID numbers are starting from 46 and are ending with 60. The first three phasor signal ID numbers 46 to 48 monitor the system frequency, change in frequency and the flag status respectively. The rest of the ID numbers (49 to 60) monitor the three-phase voltage and the current magnitudes and the phase angle of the load1 (P_{D1}) using the PMU1 as is given in Figure 6.26. The voltage and current phasor signals are monitored in the OpenPDC environment.

DIRECT CONNECTED		Devices Connected Directly		IEEE C37.118-2005		Time Stamp		
PMU1		Pmu1		IEEE C37.118-2005		10-29-2014 01:17:16.820	0	
47e9153f-8505-4fcd-a3c7-7e5c441c24e0	47	AEP_PMU1:DF	DFDT			10-29-2014 01:17:16.820	50	Hz
d7c11b93-ca59-4eaf-a52b-79b3af0585bf	46	AEP_PMU1:F	FREQ			10-29-2014 01:17:16.820	-92.6	Degrees
4199ac51-f55f-4347-92bc-b109f0e85cd5	50	AEP_PMU1-PA1:VH	VPHA			10-29-2014 01:17:16.820	147.4	Degrees
8a465c03-f0dd-4ab9-b244-398fb8a760a0	52	AEP_PMU1-PA2:VH	VPHA			10-29-2014 01:17:16.820	17.4	Degrees
61026a2c-9ac5-42fe-ac0e-4240bd9275f9	54	AEP_PMU1-PA3:VH	VPHA			10-29-2014 01:17:16.820	-120.064	Degrees
b7f2342d-7990-4292-bd6e-79ebc7c150b4	56	AEP_PMU1-PA4:IH	IPHA			10-29-2014 01:17:16.820	119.936	Degrees
a90932f9-085f-4cd7-aedd-0575fba73b3f	58	AEP_PMU1-PA5:IH	IPHA			10-29-2014 01:17:16.820	-0.064	Degrees
11b15f5a-20a2-4201-99af-98b4a0368bf1	60	AEP_PMU1-PA6:IH	IPHA			10-29-2014 01:17:16.820	142204.688	Volts
c962a06a-71b6-466d-b1af-88906c5a8e98	49	AEP_PMU1-PM1:V	VPHM			10-29-2014 01:17:16.820	142204.688	Volts
00c9b998-1bbe-49d9-abcc-4a29ca864124	51	AEP_PMU1-PM2:V	VPHM			10-29-2014 01:17:16.820	142204.688	Volts
c31964c3-218a-4d46-87bb-0e0b2a655919	53	AEP_PMU1-PM3:V	VPHM			10-29-2014 01:17:16.820	52.416	Amps
dc398391-2522-4a73-ab76-e5879361e516	55	AEP_PMU1-PM4:I	IPHM			10-29-2014 01:17:16.820	52.416	Amps
3238dc37-bee1-44d8-b3c2-9a4e18fcaf78	57	AEP_PMU1-PM5:I	IPHM			10-29-2014 01:17:16.820	52.416	Amps
0c88d473-ca83-4bb6-98e8-9f8005c4178b	59	AEP_PMU1-PM6:I	IPHM			10-29-2014 01:17:16.820	52.416	Amps
d4c9d5c1-69f3-4252-a288-970008ac1f7b	48	AEP_PMU1:S	FLAG			10-29-2014 01:17:16.820	0	
PMU2		Pmu2		IEEE C37.118-2005		10-29-2014 01:17:16.800	0	
ff11a8a2-f4e0-4739-8f5f-6432ebb2271c	82	AEP_PMU2:DF	DFDT			10-29-2014 01:17:16.800	50	Hz
f35ccfb1-218b-49e8-ba9e-6712dcd8da0	81	AEP_PMU2:F	FREQ			10-29-2014 01:17:16.800	-93.95	Degrees
1373328a-9101-44a8-9f21-e1324b155ca7	85	AEP_PMU2-PA1:VH	VPHA			10-29-2014 01:17:16.800	146.05	Degrees
e3f6a4a5-b5f1-4c97-9597-c475a6b14d44	87	AEP_PMU2-PA2:VH	VPHA			10-29-2014 01:17:16.800	26.05	Degrees
378cc193-23f9-4f66-a293-b347495fa2a9	89	AEP_PMU2-PA3:VH	VPHA			10-29-2014 01:17:16.800	-113.283	Degrees
3f0d1d73-c5a9-4039-b268-375f1f6cd729	91	AEP_PMU2-PA4:IH	IPHA			10-29-2014 01:17:16.800	126.717	Degrees
f4c9de87-51af-46e8-8eb2-9866d8800599	93	AEP_PMU2-PA5:IH	IPHA			10-29-2014 01:17:16.800	6.717	Degrees
d574937c-9f9b-4244-8754-c35ebd04c2fd	95	AEP_PMU2-PA6:IH	IPHA			10-29-2014 01:17:16.800	141896.266	Volts
b497c4d1-352e-4125-a196-41c7a66a05bf	84	AEP_PMU2-PM1:V	VPHM			10-29-2014 01:17:16.800	141896.266	Volts
aec009ac-152b-4f70-8936-c67a6bbf1deb	86	AEP_PMU2-PM2:V	VPHM			10-29-2014 01:17:16.800	141896.266	Volts
f3bf9e95-ef08-42d6-9176-739ceee09cde	88	AEP_PMU2-PM3:V	VPHM			10-29-2014 01:17:16.800	111.437	Amps
416782fb-f5ba-4681-84a2-70eb7c15d867	90	AEP_PMU2-PM4:I	IPHM			10-29-2014 01:17:16.800	111.437	Amps
7c9d664a-e2fc-446a-8ede-4609daf8ab70	92	AEP_PMU2-PM5:I	IPHM			10-29-2014 01:17:16.800	111.437	Amps
5b28d0dd-38c2-41d2-8ff5-7c7433a19cd5	94	AEP_PMU2-PM6:I	IPHM			10-29-2014 01:17:16.800	111.437	Amps
45163697-b10a-4cb7-8308-c6e6b37cc33	83	AEP_PMU2:S	FLAG			10-29-2014 01:17:16.800	0	

Figure 6.25: Monitoring the RSCAD GTNET card PMU 1 and PMU 2 signals in the OpenPDC environment

The abbreviation used in Figure 6.26 is described below:

- VPHM - Voltage Phasor Magnitude
- VPHA - Voltage Phasor Angle
- IPHM - Current Phasor Magnitude

- IPHA - Current Phasor Angle
- PM1 to PM4 - Phasor Magnitude of the three phase voltage and current signals respectively.
- PA 1 to PA6 - Phasor angle of the three phase voltage and current signals respectively.

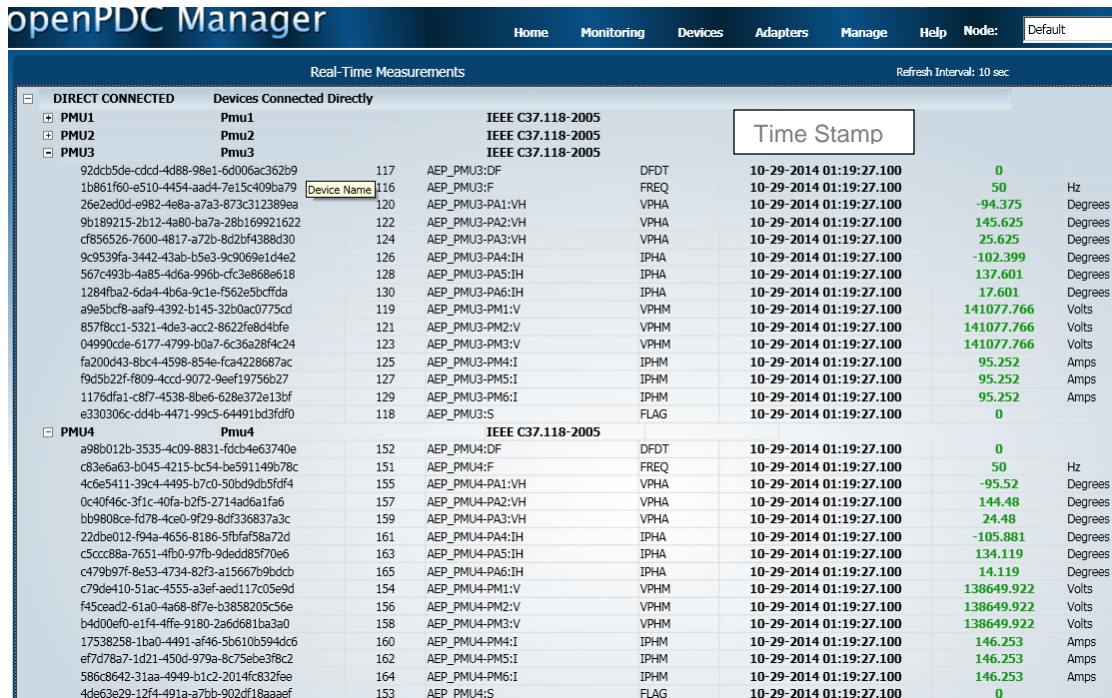


Figure 6.26: Monitoring the RSCAD GTNET card PMU 3 and PMU 4 signals in the OpenPDC environment

The OpenPDC Manager presents the data captured from the PMUs in a sequential manner. The PMU1 signals are presented first with their signal IDs. Each member (field) of the data set from a PMU has a unique ID to identify the parameter. The units for each of these parameters are given in the subsequent column.

Time-stamping of the values is also implemented in real-time; the time stamps are conveniently logged within the software and are given in Figures 6.25 and 6.26 respectively for PMU 1 to PMU 4. The detailed description of the signal ID numbers and its signal names is given in Table 6.11

Table 6.11: Signal ID Number and the name of the GTNET card PMU signals

Signal ID number	Signal Name
46	Frequency
47	Change of frequency
48	Status of flag
49	Phase A: Voltage phasor magnitude
50	Phase A: Voltage phasor angle
51	Phase B: Voltage phasor magnitude
52	Phase B: Voltage phasor angle
53	Phase C: Voltage phasor magnitude
54	Phase C: Voltage phasor angle
55	Phase A: Current phasor magnitude
56	Phase A: Current phasor angle
57	Phase B: Current phasor magnitude
58	Phase B: Current phasor angle
59	Phase C: Current phasor magnitude
60	Phase C: Current phasor angle

6.4.3.3 Storing and retrieving the RTDS GTNET card PMU real-time data to and from the MySQL database

The OpenPDC data are stored in the MySQL database situated in the remote end computer. Table 6.12 shows the signal names and acronyms used in the MySQL database. The data is read by the optimisation dispatch algorithm in the MATLAB environment at the remote end computer every 5 minutes. The SQL query is used to select the particular signal from the MySQL database. The MATLAB software developed to capture the GTNET PMU signals from the MySQL database into the MATLAB environment is given in **Appendix J**. Using these captured data the economic dispatch problem based on the Lagrange's algorithm is solved once every five minutes.

Table 6.12: MySQL archived data and their signal names

ID	Signal Name	Acronym	Suffix	Abbreviation	Source	Engineering Units
1	Current Magnitude	IPHM	PM	I	Phasor	Amps
2	Current Phase Angle	IPHA	PA	IH	Phasor	Degrees
3	Voltage Magnitude	VPHM	PM	V	Phasor	Volts
4	Voltage Phase Angle	VPHA	PA	VH	Phasor	Degrees
5	Frequency	FREQ	FQ	F	PMU	Hz
6	Frequency Delta (dF/dt)	DFDT	DF	DF	PMU	

7	Analog Value	ALOG	AV	A	PMU	
8	Status Flags	FLAG	SF	S	PMU	
9	Digital Value	DIGI	DV	D	PMU	
10	Calculated Value	CALC	CV	C	PMU	
11	Statistic	STAT	ST	P	Any	

Table 6.13 shows the PMU monitored voltage and current signals both in the RSCAD and in the MySQL environments for the initial loading condition of the power demand, $P_D = [20 \ 45 \ 40 \ 60]$ MW's respectively of the five bus power system model.

Table 6.13: PMU signal monitored in the RSCAD and MySQL environment for the initial loading condition

PMU voltage and current signals		V_a	δ_{va}	V_b	δ_{vb}	V_c	δ_{vc}	I_a	δ_{Ia}	I_b	δ_{Ib}	I_c	δ_{Ic}	P_D
PMU #1 (P_{D1})	RSCAD environment	142200	-92.6	142200	147.4	142200	17.4	52.4	-120.1	52.4	119.9	52.4	-0.06	20.0
	MySQL environment	142200	-92.6	142200	147.4	142200	17.4	52.4	-120.1	52.4	119.9	52.4	-0.06	20.0
PMU #2 (P_{D2})	RSCAD environment	141900	-93.9	141900	146.0	141900	26.5	111.4	-113.0	111.4	126.7	111.4	6.7	45.0
	MySQL environment	141900	-93.9	141900	146.0	141900	26.5	111.4	-113.0	111.4	126.7	111.4	6.7	44.7
PMU #3 (P_{D3})	RSCAD environment	141100	-94.3	141100	145.6	141100	25.6	95.2	-102.4	95.2	137.6	95.2	17.6	40.0
	MySQL environment	141100	-94.3	141100	145.6	141100	25.6	95.2	-102.4	95.2	137.6	95.2	17.6	39.7
PMU #4 (P_{D4})	RSCAD environment	138600	-95.5	138600	144.5	138600	24.4	146.3	-105.9	146.3	134.1	146.3	14.2	60.0
	MySQL environment	138600	-95.5	138600	144.5	138600	24.4	146.3	-105.9	146.3	134.1	146.3	14.2	59.7

It is observed that PMU signals monitored in the RSCAD and the MySQL environment are very close and hence it is assumed that the laboratory set-up developed is capable to transfer the RTDS power system signals from the local to the remote end without any loss of data.

The same procedure is repeated for different loading conditions in order to test the data transfer capability of the developed lab-scale system. The different loading conditions used are:

- $P_D = [20 \ 45 \ 40 \ 60]$ MW is the initial loading condition. The PMU signal for the initial loading is given in Table 6.13. The slider (P_{D1}) in the RSCAD run-time window is used to increase the load one from 20 to 25 MW. Then the power demand becomes $P_D = [25 \ 45 \ 40 \ 60]$ MW and it is called the first loading condition. Table 6.14 gives

the PMU signals monitored in both RSCAD and MySQL environment for the first loading condition.

Table 6.14: PMU signals monitored in RSCAD and MySQL environment for the first loading condition

PMU voltage and current signals		V_a	δ_{va}	V_b	δ_{vb}	V_c	δ_{vc}	I_a	δ_{Ia}	I_b	δ_{Ib}	I_c	δ_{Ic}	PD
PMU #1 (PD1)	RSCAD environment	14200	-92.6	142200	147.4	142200	17.4	63.2	-115.3	63.2	124.7	63.2	4.6	25.0
	MySQL environment	14200	-92.6	142200	147.4	142200	17.4	63.2	-115.4	63.2	124.4	63.2	4.6	25.3
PMU #2 (PD2)	RSCAD environment	141900	-93.9	141900	146.0	141900	26.5	111.4	-113.0	111.4	126.7	111.4	6.7	45.0
	MySQL environment	141900	-93.9	141900	146.0	141900	26.5	111.4	-113.5	111.4	126.6	111.4	6.5	44.7
PMU #3 (PD3)	RSCAD environment	141100	-94.3	141100.0	145.6	141100	25.6	95.2	-102.4	95.2	137.6	95.2	17.6	40.0
	MySQL environment	141100	-94.3	141100.0	145.6	141100	25.6	95.2	-102.4	95.2	137.6	95.2	17.6	39.6
PMU #4 (PD4)	RSCAD environment	138600	-95.5	138600	144.5	138600	24.4	146.3	-105.9	146.3	134.1	146.3	14.2	60.0
	MySQL environment	138600	-95.5	138600	144.5	138600	24.4	146.3	-105.9	146.3	134.1	146.3	14.2	59.7

- The slider (P_{D2}) in the RSCAD run-time window is used to increase the load two from 45 to 50 MW. Then the power demand becomes $P_D = [25 \ 50 \ 40 \ 60]$ MW and it is called the second loading condition. Table 6.15 gives the PMU signals monitored in both the RSCAD and the MySQL environment for the second loading condition.

Table 6.15: PMU signals monitored in the RSCAD and MySQL environment for the second loading condition

PMU voltage and current signals		V_a	δ_{va}	V_b	δ_{vb}	V_c	δ_{vc}	I_a	δ_{Ia}	I_b	δ_{Ib}	I_c	δ_{Ic}	PD
PMU #1 (PD1)	RSCAD environment	142200	-92.6	142200	147.4	142200	17.4	63.2	-115.3	63.2	124.7	63.2	4.6	25.0
	MySQL environment	142200	-92.6	142200	147.4	142200	17.4	63.2	-115.3	63.2	124.7	63.2	4.6	24.7
PMU #2 (PD2)	RSCAD environment	141900	-93.95	141900	146.0	141900	26.5	122.6	-115.5	122.6	128.5	122.6	8.4	50.0
	MySQL environment	141900	-93.95	141900	146.0	141900	26.5	122.6	-115.5	122.6	128.5	122.6	8.4	49.5
PMU #3 (PD3)	RSCAD environment	141100.0	-94.37	141100.0	145.6	141100.0	25.63	95.25	-102.4	95.25	137.6	95.25	17.6	40.0
	MySQL environment	141100.0	-94.37	141100.0	145.6	141100.0	25.63	95.25	-102.4	95.25	137.6	95.25	17.6	39.7
PMU #4 (PD4)	RSCAD environment	138600	-95.52	138600	144.5	138600	24.48	146.3	-105.9	146.3	134.1	146.3	14.2	60.0
	MySQL environment	138600	-95.52	138600	144.5	138600	24.48	146.3	-105.9	146.3	134.1	146.3	14.2	59.8

- The slider (P_{D3}) in the RSCAD run-time window is used to increase the load three from 40 to 45 MW. Then the power demand becomes $P_D = [25 \ 50 \ 45 \ 60]$ MW and it

is called the third loading condition. Table 6.16 gives the PMU signals monitored in both the RSCAD and the MySQL environment for the third loading condition

Table: 6.16: PMU signals monitored in the RSCAD and MySQL environment for the third loading condition

PMU voltage and current signals		V_a	δ_{va}	V_b	δ_{vb}	V_c	δ_{vc}	I_a	δ_{Ia}	I_b	δ_{Ib}	I_c	δ_{Ic}	PD
PMU #1 (PD1)	RSCAD environment	142200	-92.6	142200	147.4	142200	17.4	63.2	-115.3	63.2	124.7	63.2	4.7	25.0
	MySQL environment	142200	-92.6	142200	147.4	142200	17.4	63.2	-115.3	63.2	124.7	63.2	4.6	24.7
PMU #2 (PD2)	RSCAD environment	141900	-93.9	141900	146.0	141900	26.5	122.6	-115.5	122.6	128.5	122.6	8.4	50.0
	MySQL environment	141900	-93.9	141900	146.0	141900	26.5	122.6	-115.5	122.6	128.5	122.6	8.4	49.5
PMU #3 (PD3)	RSCAD environment	141000	-94.4	141000	145.6	141000	25.56	107.0	-101.7	107.0	138.3	107.0	18.3	45.0
	MySQL environment	141000	-94.4	141000	145.6	141000	25.56	107.0	-101.7	107.0	138.3	107.0	18.3	44.7
PMU #4 (PD4)	RSCAD environment	138600	-95.5	138600	144.5	138600	24.48	146.3	-105.9	146.3	134.1	146.3	14.1	60.0
	MySQL environment	138600	-95.5	138600	144.5	138600	24.48	146.3	-105.9	146.3	134.1	146.3	14.1	59.5

- The slider (P_{D4}) in the RSCAD run-time window is used to increase load four from 60 to 65 MW. Then the power demand becomes $P_D = [25 \ 50 \ 45 \ 65]$ MW and it is called the fourth loading condition. Table 6.17 gives the PMU signals monitored in both the RSCAD and the MySQL environment for the fourth loading condition

Table 6.17: PMU signals monitored in the RSCAD and MySQL environment for the fourth loading condition

Voltage and current signals		V_a	δ_{va}	V_b	δ_{vb}	V_c	δ_{vc}	I_a	δ_{Ia}	I_b	δ_{Ib}	I_c	δ_{Ic}	PD
PMU #1 (PD1)	RSCAD environment	142200	-92.6	142200	147.4	142200	17.4	63.2	-115.3	63.2	124.7	63.2	4.7	25.0
	MySQL environment	142200	-92.6	142200	147.4	142200	17.4	63.2	-115.3	63.2	124.7	63.2	4.6	24.750
PMU #2 (PD2)	RSCAD environment	141900	-93.9	141900	146.0	141900	26.5	122.6	-115.5	122.6	128.5	122.6	8.4	50.0
	MySQL environment	141900	-93.9	141900	146.0	141900	26.5	122.6	-115.5	122.6	128.5	122.6	8.4	49.5
PMU #3 (PD3)	RSCAD environment	141000	-94.4	141000	145.6	141000	25.56	107.0	-101.7	107.0	138.3	107.0	18.3	45.0
	MySQL environment	141000	-94.4	141000	145.6	141000	25.56	107.0	-101.7	107.0	138.3	107.0	18.3	44.7
PMU #4 (PD4)	RSCAD environment	138400	-95.7	138400	144.2	138400	24.24	158.4	-105.4	158.4	134.6	158.4	14.6	65.0
	MySQL environment	138400	-95.7	138400	144.2	138400	24.24	158.4	-105.4	158.4	134.6	158.4	14.6	64.9

The monitored PMU voltage, current, and phase angle signals are used to calculate the real power of the loads using Equation (6.1). The voltage and current data are stored in

the MySQL database; they are then read by the MATLAB-based optimisation algorithm where the real power of the load components are calculated using the data phasor signals acquired at the remote end using Equation (6.1).

$$P_D = \sum_{i=1}^m V_{ia} I_{ia} \cos(\Phi_{ia1} - \Phi_{ia2}) + V_{ib} I_{ib} \cos(\Phi_{ib1} - \Phi_{ib2}) + V_{ic} I_{ic} \cos(\Phi_{ic1} - \Phi_{ic2}) \quad (6.1)$$

Where

- P_D - Total power demand in Watts
- V_{ia}, V_{ib}, V_{ic} - Bus voltage magnitudes in volt for the i^{th} load, $i = \overline{1, m}$
- I_{ia}, I_{ib}, I_{ic} - Branch currents in Amps for the i^{th} load, $i = \overline{1, m}$
- Φ_{ia1}, Φ_{ia2} - Phase angle between the voltage and current in phase A for the i^{th} load, $i = \overline{1, m}$
- Φ_{ib1}, Φ_{ib2} - Phase angle between the voltage and current in phase B for the i^{th} load, $i = \overline{1, m}$
- Φ_{ic1}, Φ_{ic2} - Phase angle between the voltage and current in phase C for the i^{th} load, $i = \overline{1, m}$

A comparison of the measured RSCAD load power demands with the power demands calculated using the transferred GTNET card PMU signals and the OpenPDC software is given in Table 6.18.

It is observed that the signal from the RSCAD environment, conforming to the IEEE C37.118-2005 standard is successfully transferred to the remote end (MySQL database) using the GTNET card PMU-based system and the OpenPDC software, without any data loss.

On the bases of this it is proven that the proposed laboratory setup for the power system data acquisition and data transfer is operating according to the requirements. This method of data acquisition and data transfer can be used by the control centres in the monitoring and control of the power grid in order to solve the energy optimisation dispatch problem in real-time.

6.4.3.4 Solution of the dispatch problem using the RTDS GTNET card PMU-based system

The Economic dispatch solution using the RTDS GTNET card PMU data acquisition and data transfer system is given in Table 6.19. The total power demand varies from 165 to 185 MW with an increment of 5 MWs. It is observed that the fuel cost increases with the increase in the power demand. The Lagrange's method can be used to provide optimal set points for the generator power production. The load flow solution within the RSCAD software environment uses the Newton-Raphson method. By solving the power flow problem the real power of the three generators are known and are used to calculate the fuel cost of the power system which is given in Figure 6.27 for the case of $P_D=165$ MW. From Table 6.19 can be seen that the fuel cost is lower using the Lagrange's method compared to the RSCAD simulation results.

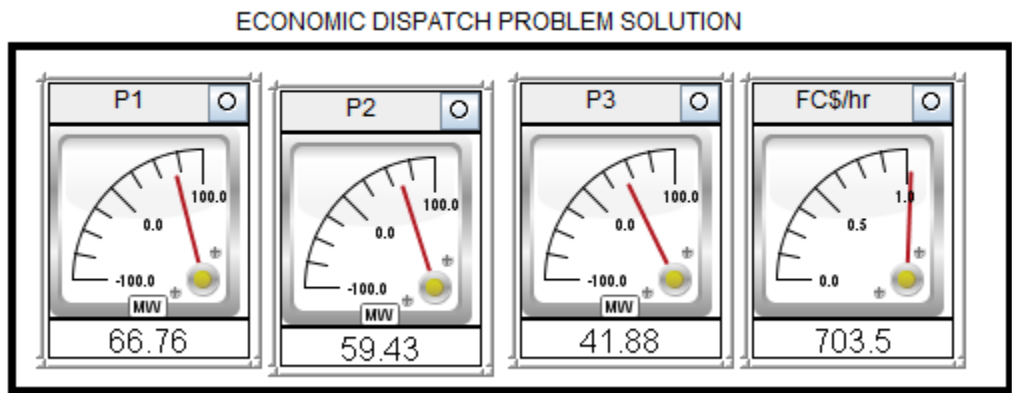


Figure 6.27: Economic dispatch problem solution in RSCAD environment for the power demand of 165 MW

Table 6.18: Comparison of the measured load power demands in the RSCAD with the power demands calculated using the GTNET card PMU signals and OpenPDC software

PMU #1 (P_{D1}) MW		PMU #2 (P_{D2}) MW		PMU #3 (P_{D3}) MW		PMU #4 (P_{D4}) MW	
RSCAD	PMU 1	RSCAD	PMU 2	RSCAD	PMU 3	RSCAD	PMU 4
20	19.84	45	44.76	40	39.91	60	59.84
25	24.84	45	44.76	40	39.91	60	59.84
25	24.84	50	49.76	40	39.91	60	59.84
25	24.84	50	49.76	45	44.91	60	59.84
25	24.84	50	49.76	45	44.91	65	64.84

Table 6.19: Economic dispatch problem solution using the GTNET card PMU signals

P _D in MW	Generator real powers in MW						P _L in MW	Lagrange's algorithm		Fuel cost in Rs/hr	
	P ₁		P ₂		P ₃			Number of iterations (optimal)	Computation time in sec (Optimal)	MATLAB (Lagrange's)	RSCAD (Newton Raphson)
	MATLAB (Optimal)	RSCAD (Simulation)	MATLAB (Optimal)	RSCAD (Simulation)	MATLAB (Optimal)	RSCAD (Simulation)					
165	55.40	46.11	55.89	68.79	59.96	52.23	6.79	520	1.029	695.5	703.5
170	56.90	51.19	57.76	69.98	61.97	52.09	7.18	523	1.022	709.7	723.35
175	58.40	56.35	59.35	68.79	63.98	52.23	7.57	525	1.107	723.6	737.27
180	59.89	61.53	61.54	68.94	66.00	52.26	7.98	527	1.19	737.8	751.35
185	61.37	66.89	63.44	68.89	68.03	52.20	8.39	529	1.63	752.2	765.58

The comparison of the solution of the dispatch problem using the developed two lab-scale systems is given in Table 6.20.

Table 6.20: Comparison of the economic dispatch problem solutions using the RTDS GTNET card PMU signals and the RTDS PB5 card front panel analog output signals

P _D in MW	Synchrophasor Technology using GTNET card PMU signals					RTDS PB5 card front panel analog output signals					
	P _L in MW	Lagrange's method		Fuel cost in Rs/hr		P _D in MW	P _L in MW	Number of iterations	Computation time in sec	Fuel cost in Rs/hr	
		Number of iterations	Computation time in sec	MATLAB	RSCAD					MATLAB	RSCAD
165	6.79	520	1.029	695.5	709.23	165	4.80	701	1.27	695.7	709.60
170	7.18	523	1.022	709.7	723.35	170	5.10	703	1.25	709.60	723.40
175	7.57	525	1.107	723.6	737.27	175	5.40	705	1.34	722.40	737.28
180	7.98	527	1.19	737.8	751.35	180	5.71	706	1.41	735.70	751.42
185	8.39	529	1.63	752.2	765.58	185	6.03	708	1.26	749.50	765.65

6.5 Discussion on the operation characteristics of the data acquisition and data transfer systems using the LabVIEW/MATLAB-based RTDS PB5 card output signals and the GTNET card PMU signals

This chapter describes the application of two methods of data acquisition and data transfer, the RTDS PB5 card front panel output signals and the RTDS GTNET card PMU signals in order to solve dispatch optimisation problems at the remote end control centre PC. The five and eleven bus Indian utility power system models are used to validate the data transfer capability of the two methods. Four different loading conditions that are used to validate the data transfer capability of the developed lab-scale systems.

The following conclusions can be done:

- The GTNET card PMU supports the IEEE C37.118-2005 standard to transfer the large complex power system network data from the local to the remote end in real-time, whereas the RTDS PB5 card front panel method is only used to transfer the real-time data between the elements at the local ends.
- The data transfer capability of the synchrophasor technology using the RTDS GTNET card PMU is very fast and accurate. The loss of data during the process of communication and signal transformations is very small.
- The comparison of the economic dispatch problem solution at both the local and remote end is done. It has been proven that the economic dispatch solution using the Lagrange's method provides accurate real power to be produced by the generators and the fuel costs are reduced when the GTNET PMU-based method is used compared to that of the PB5 card analog output.

6.6 Conclusion

This chapter investigates the capabilities of the developed data acquisition and data transfer systems based on the RTDS PB5 card analog output signals and the RTDS GTNET card PMU-based signals to provide real-time data for solution of a dispatch optimisation problem. The investigations are done for the five bus and the eleven bus power system models using different power demands. It is proven that the synchrophasor technology is an ideal solution for data acquisition and data transfer between the host and the remote PCs without any data loss. The optimized real power of the generators can be sent back to the RTDS models in RSCAD as set-points for the generators in the RSCAD simulation model. The GTNET card PMU-based data acquisition and data transfer systems creates conditions favourable for the optimisation algorithm to produce a better solution. The developed lab-scale systems will play a vital role in the future developments of a smart grid energy management system.

The following chapter provides the thesis deliverables, conclusion, and future work.

CHAPTER SEVEN

CONCLUSION, DELIVERABLES AND FUTURE RECOMMENDATIONS

7.1 Introduction

The thesis presents methods, algorithms, procedures, and the hardware and software tools which are utilized to implement a real-time data acquisition and data transfer system framework.

Two lab-scale systems for data acquisition, data transfer, and distribution using the RTDS PB5 card front panel analogue output data and the RTDS GTNET card PMU synchrophasor data are developed to investigate different possibilities for capturing the power system data from the RTDS simulation models of the power systems. The results of these applications for the case studies of the five and eleven bus power systems are presented.

This chapter describes the aim and objectives of the thesis in section 7.2. The thesis deliverables are described in section 7.3, and the application of the results is given in section 7.4. The future research direction and author's publications are given in sections 7.5 and 7.6 respectively, and the conclusion is presented in section 7.7.

7.2 Aim and objectives of the thesis

The aim of this thesis is to develop a framework which includes methods, algorithms, procedures, software and hardware tools for development and implementation of lab-scale prototypes of the power network and its data acquisition, data transfer and distribution system in order to allow the solution of the power dispatch optimisation problem in real-time using real-time data.

7.2.1 Objectives

In order to achieve the aforementioned aim, the following project objectives were proposed and have been achieved:

- To review the existing literature and investigate the communication systems, network technologies, media and protocols, and the power system application of

LabVIEW, Real-Time Digital Simulator (RTDS), and the synchrophasor technologies.

- To develop a framework which includes methods, algorithms, and procedures for implementation of two types of lab-scale data acquisition and transfer systems for application in power system monitoring and control, based on two types of data measurements: analog signals and synchrophasor signals.
- To identify suitable hardware platforms and software tools for implementation of the two lab-scale systems.
- To develop an algorithm and a procedure for capturing the RTDS PB5 card analogue output signals using the NI DAQ card in LabVIEW/MATLAB-based systems.
- To develop an algorithm and a procedure to transmit, store and retrieve the RTDS power system simulation model signals from the host PC to a remote PC using the RTDS GTNET card PMU-based synchrophasor output signals.
- To test the developed systems for two case studies of power systems.
- To apply the developed data acquisition and data transfer systems for the solution of the power dispatch optimisation problem.

7.3 Thesis deliverables

7.3.1 Investigation and a literature review of the real-time data acquisition and data transfer systems for power system applications

The review investigates the communication architectures, communication media and supporting protocols for power system applications. It investigates the use of the Real Time Digital Simulator (RTDS), a LabVIEW/MATLAB-based data acquisition, data transfer and, distribution system and the synchrophasor technologies in power engineering.

7.3.2 Development of power system models in RSCAD software environment and load flow simulation

Two models of five and eleven bus power systems are built in the RSCAD software environment and are simulated using the power flow Newton-Raphson method. The obtained load flow real powers are the signals that are to be acquired and transmitted in

order to solve the power dispatch optimisation problem. The RSCAD built models are shown in Figures D1 to D5, Appendix D.

7.3.3 Development of methods, algorithms, and procedures for lab-scale implementation of the LabVIEW/MATLAB-based data acquisition and data transfer systems using the RTDS front panel PB5 card analog output signals

The algorithm for the implementation of the data acquisition, data transfer, data storage and data retrieval systems using the RTDS PB5 card front panel analogue output signals is shown in a block diagram in Figure 4.9 and the flow diagram in Figure 4.8, in Chapter 4. The results from the simulation of the power system models are transferred from the RSCAD environment to the RTDS analog output card. The LabVIEW/MATLAB programs are developed to monitor and display the output signals from the RTDS PB5 card front panel using the NI DAQ 6343 card. The acquired data is then saved in the Microsoft Excel file format. Finally, the data retrieved from the Excel file is transferred by the developed MATLAB program which uses this data to solve the economic dispatch problem in real-time.

7.3.4 Development of software programs for the LabVIEW/MATLAB-based data acquisition, and data transfer systems using the RTDS front panel PB5 card analog output signals

1. Method One – LabVIEW-based system

- a) Software program written in the LabVIEW environment to acquire the signals from the RTDS PB5 card analog outputs through the NI DAQ card and to transfer the data to an Excel file
- b) Software program written in the MATLAB environment (M-file) to read the acquired and saved Excel file data and to use it to solve the power dispatch optimisation problem.

Two variants of these software programs are developed - for the five and the eleven bus power system models.

The software programs for the developed LabVIEW-based data acquisition and data transfer system for the five and eleven bus power system models are given in Appendices F and H respectively.

2. Method One – MATLAB-based system

A software program written in MATLAB environment to perform the following:

- To acquire the signals from the PB5 card analog outputs through the NI DAQ card.
- To save the acquired data in an Excel file.
- To read the data from the Excel file and to solve the power dispatch optimisation problem.

Two variants of this software program are developed - for the five and eleven bus power system models.

The software programs for the developed MATLAB-based data acquisition and data transfer system for the five and eleven bus power system models are given in Appendices G and I respectively.

7.3.5 Development of the method, algorithm, and procedures for the lab-scale implementation of the RTDS GTNET card PMU signal- based data acquisition and data transfer system

The voltage and current phasor signals of the RSCAD simulation models are transferred to the software based PMU (GTNET card-PMU). The measured data from the GTNET-PMU are transferred to the Phasor Data Concentrator (PDC) using Ethernet communication. At the remote end, the OpenPDC software is used to capture the RTDS signals in real-time. These signals are archived in the MySQL database. Every five minutes, the data is retrieved from the MySQL database to the MATLAB environment. The Lagrange's algorithm developed by (Krishnamurthy and Tzoneva, 2013) is used to solve the Economic Dispatch (ED) problem.

7.3.6 Development of the software program for the RTDS GTNET card PMU-based data acquisition and transfer system

Method 2: GTNET card PMU based signal system

- a) Configuration of the software PMU to acquire the signals from the GTNET card to transfer them through an Ethernet network to the PMU connection tester.

- b) Configuration of the OpenPDC to receive the acquired data at the remote end and to save it in the MySQL database.
- c) MATLAB Software program (in Appendix J), to read the data saved in the MySQL database and to use it to solve the power dispatch optimisation problem.

The developed software programs given in Appendix F to J are summarized in Table 7.1

Table 7.1: The software programs for the data acquisition and data transfer systems using the RTDS front panel PB5 card analog output signals and the RTDS GTNET card PMU output signals

Type of the data acquisition and data transfer system used to solve the economic dispatch problem	The power system model used	Algorithm	Appendix/ File names
Development of RSCAD software for simulation of the five and eleven bus power systems	Five and eleven bus power system model	Newton-Raphson	Appendix D
A LabVIEW-based data acquisition and data transfer system using the RTDS PB5 card analogue output signals	Five bus power system model	DAQ/LabVIEW	Appendix E
		Lagrange's	Appendix F: Method_One_LabVIEW_based_Five_Bus_Power_System.m
A MATLAB-based data acquisition and data transfer system using the RTDS PB5 card analogue output signals	Five bus power system model	Lagrange's	Appendix G: Method_One_MATLAB_based_Five_Bus_Power_System.m
A LabVIEW-based data acquisition and data transfer system using the RTDS PB5 card analogue output signals	Eleven bus power system model	DAQ/LabVIEW	Appendix E
		Lagrange's	Appendix H: Method_One_LabVIEW_based_Eleven_Bus_Power_System.m
A MATLAB-based data acquisition and data transfer system using the RTDS PB5 card analogue output signals	Eleven bus power system model	Lagrange's	Appendix I: Method_One_MATLAB_based_Eleven_Bus_Power_System.m
RTDS GTNET PMU-based data acquisition and data transfer system	Five bus power system model	RSCAD GTNET card PMU configuration simulation file	Appendix D
		Lagrange's	Appendix J: Method_Two_GTNET_PMU_based_Five_Bus_Power_System.m

7.4 Application of the thesis results

The developed data acquisition, data transfer, data storage and data retrieval system algorithms and software programs can be applied with small modifications to some new fields, such as:

- Optimisation of Unit-Commitment and Hydrothermal scheduling problems.

- Power grid energy management system solutions in regional or national control centers.
- Joint solution of the problems for state estimation and dispatch optimisation
- Smart grid applications.
- Solution of optimisation problems following the requirements of the IEC 61970 standard for the common information model in power systems
- Application of the new IEC 61850-90-5 standard for wide-area power system protection scheme's development.
- Power system data acquisition and data transfer systems in real-time for the educational courses and postgraduate research at universities.

7.5 Future research

Future direction for this research work could include the following:

- Testing the developed algorithms in a closed-loop manner between the Real Time Digital Simulator (RTDS) and the remote end PC using the Ethernet communication protocol IEEE C37.118-2005 in a real-time laboratory environment.
- Testing of the developed application for the larger IEEE power system models.
- Application of the developed data acquisition and data transfer systems, algorithms and programs for hydro and wind power optimisation problems and optimal capacitor placement problems on the distribution networks.

7.6 Publications

Based on the thesis outcomes, the following publications were submitted:

Deivakkannu, G., Krishnamurthy, S., Kriger, C., and Tzoneva, R. 2014. Development of a lab-scale data acquisition and data transfer system in the LabVIEW and MATLAB environment to solve the economic dispatch problem in real-time. Submitted to the International Journal of Computers, Communications and Control (IJCCC)

Deivakkannu, G., Krishnamurthy, S., Kriger, C., and Tzoneva, R. 2014. Development of a lab-scale data acquisition and data transfer system using the RTDS GTNET card PMU-based system to solve the economic dispatch problem in real-time. Submitted to the International Review of Electrical Engineering (IREE).

7.7 Conclusion

This chapter describes the aim and objectives of the thesis and addresses the thesis deliverables for the developed data acquisition and data transfer systems to solve the economic dispatch problem in real-time using the real-time data. It describes the possible application areas for the developed algorithms and software programs. The possible future research directions and the list of the author's publications are also given.

BIBLIOGRAPHY

- Adebisi, B., Treytl, A., Haidine, A., Portnoy, A., Shan, R.U., Lund, D., Pille, H. & Honary, B. 2011. IP-centric high rate narrowband PLC for smart grid applications. IEEE Communications Magazine. Volume : 49(Issue : 12): Page : 46–54.
- Adewole, A.C. and Tzoneva, R. 2014. Impact of IEC 61850-9-2 Standard-Based Process Bus on the Operating Performance of Protection IEDS: Comparative Study. In 19th IFAC World Congress. Cape Town: Page : 2245–2252.
- Afdideh, F., Shamsollahi, M.B. and Resalat, S.N. 2012. Development of a MATLAB-based toolbox for brain computer interface applications in virtual reality. In 20th Iranian Conference on Electrical Engineering (ICEE), 2012. IEEE: Page : 1579–1583.
- Apostolov, A. and Muschlitz, B. 2003. Object modeling of measuring functions in IEC 61850 based IEDs. In On IEEE Transmission and Distribution and Exposition Conference, 2003. IEEE: Page : 471–476.
- Aravinthan, V., Karimi, B., Namboodiri, V. and Jewell, W. 2011. Wireless communication for smart grid applications at distribution level—Feasibility and requirements. In IEEE Power and Energy Society General Meeting, 2011. IEEE: Page : 1–8.
- Baig, M.S., Das, S. and Rajalakshmi, P. 2013. CR Based WSN for Field Area Network in Smart Grid. In Advances in Computing, Communications and Informatics (ICACCI), 2013 International Conference on. Mysore, India: IEEE: 811–816.
- Balakrishnanan, M. 2012. Smart Energy Solutions for Home Area Networks and Grid-End Applications. : 67–72.
- Bauer, M., Plappert, W., Wang, C. and Dostert, K. 2009. Packet-oriented communication protocols for smart grid services over low-speed PLC. In IEEE International Symposium on Power Line Communications and Its Applications, 2009. IEEE: Page : 89–94.
- Behrouz, A.F. 2006. Data Communications Networking. 4th Edition. McGraw-Hill Education.
- Bhattacharyya, D. 2008. The Taxonomy of Advanced SCADA Communication Protocols. Journal of Security Engineering, Volume : 5(Issue : 6): Page : 517–525.

Biswas, S.S., Vellaithurai, C.B. and Srivastava, A.K. 2013. Development and real time implementation of a synchrophasor based fast voltage stability monitoring algorithm with consideration of load models. In IEEE on Industry Applications Society Annual Meeting, 2013. IEEE: Page : 1–9.

Branch, M. and Bradley, B. 2006. Real-time web-based system monitoring. In Conference Record of Annual Pulp and Paper Industry Technical Conference, 2006. IEEE: Page : 1–4.

Bucci, G., Ciancetta, F., Fiorucci, E., Gallo, D. and Landi, C. 2005. A low cost embedded Web service for measurements on power system. In IEEE International Conference on Virtual Environments, Human-Computer Interfaces and Measurement Systems, 2005. IEEE: Page : 6–12.

Cen, Z. and Fang, X. 2007. Procedure Analysis of IEC 870-5-101 Clock Synchronization and One of Its Improved Algorithms. In Power Engineering Society General Meeting, 2007. IEEE: Page : 1–9.

Chen, H., Bhargava, B., Habibi-Ashrafi, F., Park, J.S. and Castaneda, J. 2012. Integration of RTDS with EPG synchrophasor applications for visualization and analysis of simulation scenarios at Southern California Edison. In North American Power Symposium (NAPS), 2012. IEEE: Page : 1–5.

Chen, J. and Shen, J. 2012. Remote monitoring multi-point temperature system based on SMT16030 and DataSocket technology. In 5th International Congress on Image and Signal Processing (CISP), 2012. IEEE: Page : 1691–1694.

Cirstea, C., Cernaianu, M. and Gontean, A. 2012. An inductive system for measuring microampere currents. In IEEE 18th International Symposium for Design and Technology in Electronic Packaging (SIITME), 2012. IEEE: Page : 197–200.

Cory, L.C. 2005. LabVIEW Digital signal processing. McGraw Hill, United State.

Diakos, K., Wu, Q. and Nielsen, A.H. 2012. Phasor Measurement Unit and Phasor Data Concentrator test with Real Time Digital Simulator. In IEEE PES Asia-Pacific Power and Energy Engineering Conference 2014. Page : 1–5.

Duncan, B.K. and Bailey, B.G. 2003. Protection, metering, monitoring and control of medium voltage power systems. In IEEE Technical Conference on Industrial and Commercial Power Systems, 2003. IEEE: Page : 121–128.

Giri, J. 2011. Synchronphasor_PMU_Data_Analysis_for_Enhanced_Control_Center.

Guha, D.R. 2011. Artificial neural network based channel equalization. Master Thesis. National Institute of Technology, India.

Gungor, V.C. and Lambert, F.C. 2006. A survey on communication networks for electric system automation. Computer Networks, Volume : 50(Issue : 7): Page : 877–897.

Hasim, N., Rashid, M.Z.A., Aras, M.S.M., Kassim, A.M. and Abdullah, S.S. 2012. Development of fuzzy logic water bath temperature controller using MATLAB. In IEEE International Conference on Control System, Computing and Engineering (ICCSCE), 2012. IEEE: Page : 11–16.

Hauser, C.H. 2005. A failure to communicate: next generation communication requirements, technologies, and architecture for the electric power grid. Power and Energy Magazine, Volume : 3(Issue :2): 47–55.

Herbert, F. 2012. PAC World magazine : IEC 61850-90-5: an Overview. PAC World magazine, (March 2012).

<http://www.dnp.org>. 2011. Distributed Network Protocol.

<http://www.guru99.com>. 2012. Introduction to MySQL & MySQL workbench.

<http://www.sena.com>. 2014. Introduction_to_modbus. Technical tutorial.

<http://www.sena.com> 1 December 2014.

<http://www.toshiba-smartcommunity.com>. 2014. Smart Metering Communication System : Smart Grid : Toshiba.

<https://openpdc.codeplex.com>. 2014. The Open Source Phasor Data Concentrator.

<https://pmuconnectiontester.codeplex.com>. 2014. PMU Connection Tester.

<https://www.naspi.org>. 2014. NASPI | NASPI Home.

Huang, C.H., Su, Y.F., Su, Y.T., Su, W.H., Chen, J.J. and Zhou, W.J. 2014. Design and Application of ZigBee Wireless Techniques for an Intelligent House Lighting Control System. In International Symposium on Computer, Consumer and Control. IEEE: Page : 19–22.

Huertas, J.I., Barraza, R. and Echeverry, J.M. 2010. Wireless data transmission from inside electromagnetic fields. Journal of Microwave Power and Electromagnetic Energy, Volume : 44(Issue : 2): Page : 88–97.

Hyun, D. and Lee, Y. 2008. A Study on the Compound Communication Network over the High Voltage Power Line for Distribution Automation System. In International Conference on Information Security and Assurance. IEEE: Page : 410–414.

IEEE Guide Monitoring. 2007. IEEE Guide for Monitoring, Information Exchange, and Control of Distributed Resources Interconnected with Electric Power Systems.

IEEE Std 1646. 2004. IEEE Recommended Practice for Software Requirements Specifications. In Institute of Electrical and Electronics Engineers.

IEEE Std C37.118.2. 2011. IEEE Standard for Synchrophasor Data Transfer for Power Systems. IEEE Power & Energy Society: Page : 1–54.

Jackson, G., Annakkage, U.D., Gole, A.M., Lowe, D. and McShane, M.P. 2005. A real-time platform for teaching power system control design. In International Conference on Power System Transients. Page : 1–5.

Jiang, H. 2008. A kind of distribution power automation communication systems based on Mobitex technology. In China International Conference on Electricity Distribution, 2008. IEEE: Page : 1–3.

Jung, S., Eo, Y., Chun, Y., Kim, W., Woo, S., Sohn, S., Rho, J. and Cha, J. 2011. UWB sensor chip measurement system implementation using LabVIEW and MCU board. In International Conference on ICT Convergence (ICTC), 2011. IEEE: Page : 649–651.

Kabir, M. 2012. Network Architecture of a Modern Automotive Infotainment System. Advances in Automobile Engineering, Volume: 1(Issue: 3): Page :1–5.

Ken, M., Brunello, G., Adamiak, M., and Antonova, G. 2013. IEEE Synchrophasor Standard for Communications. PAC World magazine.

Kezunovic, M., Heydt, G.T., DeMarco, C. and Mount, T. 2009. Is teamwork the smart solution? Power and Energy Magazine, IEEE, 7(2).

Kothari, D. and Dhillon, J. 2011. Power System Optimisation. Second Edition. PHI Learning Pvt. Ltd, India.

Kruger, C., Behardien, S. and Retonda-Modiya, J.-C. 2013. A Detailed Analysis of the GOOSE Message Structure in an IEC 61850 Standard-Based Substation Automation System. International Journal of Computers, Communications & Control, Volume : 8(Issue : 5): Page : 706–721.

Krishnamurthy, S., and Tzoneva, R. 2012a. Investigation of the Methods for Single area and Multi area Optimisation of a Power System Dispatch Problem. International Review of Electrical Engineering (IREE), Praise Worthy Prize, Vol.7, No.1, Page: 3600 – 3627.

Krishnamurthy, S., and Tzoneva, R. 2012b. Multiobjective Dispatch Problem with Valve Point Effect Loading of Fuel Cost and Emission Criterion. International Journal of Computer and Electrical Engineering (IJCEE). Vol. 4, No. 5, Page: 775-784.

Krishnamurthy, S., and Tzoneva, R. 2013. Development of decomposition methods for solution of a multiarea power dispatch optimisation problem. DTech Thesis, Cape Peninsula University of Technology, South Africa.

Lee, Y.S., Kim, W.S. and Kim, S.Y. 2013. Development of a rapid control prototyping system based on MATLAB and a USB DAQ unit. In 8th IEEE Conference on Industrial Electronics and Applications (ICIEA), 2013. IEEE: Page : 161–166.

Li, Y., Cui, W., Li, D. and Zhang, R. 2011. Research based on OSI model. In International Conference on Communication Software and Networks (ICCSN), 2011. IEEE: Page : 554–557.

LIA, P. and JOSEPH, M.R. 1998. Introduction to Sampling. In Signal Processing, Harmonic Analysis, and Applications Fall 1998. Urbana: 1–24.

Lin, H., Sambamoorthy, S., Shukla, S., Thorp, J. and Mili, L. 2011. Power system and communication network co-simulation for smart grid applications. In IEEE PES Innovative Smart Grid Technologies (ISGT), 2011. IEEE: Page : 1–6.

Louie, K.W., Wang, A., Wilson, P. and Buchanan, P. 2006. Discussion on power line carrier applications. In Canadian Conference on Electrical and Computer Engineering, 2006. IEEE: Page : 655–658.

Madani, v, King, V. and Rahmatian, F. 2013. PAC World magazine : Deploying Advanced Technology - Key Success Factors and Applications. Protection, Automation and control: Page : 20–23.

Madani, V., Barich, J., Day, D., Gotesky, J., Jampala, A.K., Giri, J., Parashar, M., Rahmnatian, F., Gharpure, V., King, R. and others. 2014. Advanced EMS applications using synchrophasor systems for grid operation. In IEEE T&D Conference and Exposition, 2014. IEEE: Page : 1–5.

Mak, K.-H. and Holland, B.L. 2002. Migrating electrical power network SCADA systems to TCP/IP and Ethernet networking. Power engineering journal, Volume : 16(Issue : 6): Page : 305–311.

Mak, S. and Radford, D. 1996. Communication system requirements for implementation of a large scale demand side management and distribution automation. IEEE Transactions on Power Delivery. Volume : 11(Issue : 2): Page : 683–689.

MATLAB® DAQ. 2005. Effects of configuration interaction on intensities and phase shifts. Physical Review, Volume : 124(Issue : 6): 1866.

MATLAB®. 2014. MATLAB Programming Fundamentals. In MATLAB Programming Fundamentals. Mathworks: 77–110.

McClung, L.B. and Hill, D.J. 2010. Electrical system design techniques to improve electrical safety. In IEE Electrical Safety Workshop (ESW), 2010. IEEE: Page : 147–152.

McLaren, P.G., Kuffel, R., Wierckx, R., Giesbrecht, J. and Arendt, L. 1991. A real time digital power system simulator for testing relays. In IEEE Power Engineering Society Transmission and Distribution Conference, 1991. IEEE: Page : 370–375.

Moghe, R., Mousavi, M.J., Stoupis, J. and McGowan, J. 2009. Field investigation and analysis of incipient faults leading to a catastrophic failure in an underground distribution feeder. In Power Systems Conference and Exposition, 2009. IEEE: Page : 1–6.

Mohagheghi, S., Stoupis, J. and Wang, Z. 2009. Communication protocols and networks for power systems-current status and future trends. In International Conference on Power Systems and Exposition (PSCE), 2009. IEEE: Page : 1–9.

Nishikido, F., Moritake, T., Ito, H. and Yamaya, T. 2013. A prototype real-time dose distribution monitoring system using plastic scintillators connected to optical fiber for interventional radiology. In IEEE Nuclear Science Symposium and Medical Imaging Conference (NSS/MIC), 2013. Page : 1–3.

P.kundur, P.Paserba, G.Anderson, A.Bose and C.Canizers. 2004. Definition and Classification of Power System Stability IEEE/CIGRE Joint Task Force on Stability Terms and Definitions. IEEE Transactions on Power Systems, Volume : 19(Issue : 3): Page : 1387–1401.

Parikh, P.P., Kanabar, M.G. and Sidhu, T.S. 2010. Opportunities and challenges of wireless communication technologies for smart grid applications. In IEEE Power and Energy Society General Meeting, 2010. IEEE: Page : 1–7.

Paul, T., Kimball, J.W., Zawodniok, M., Roth, T.P. and McMillin, B. 2011. Invariants as a unified knowledge model for cyber-physical systems. In Service-Oriented Computing and Applications (SOCA), 2011 IEEE International Conference on. IEEE: Page :1–8.

Phadke, A.G. and Thorp, J. 2008. Synchronized Phasor Measurements and Their Applications. Power Electronic and power systems. Springer.

Philip, K. 2012. Applications of PMU Simulator in PDC Testing. Master Thesis. Virginia: Virginia Polytechnic Institute and State University.

Prabhaker, M. 2007. Handbook of Computer Networks: LANs, MANs, WANs, the Internet, and Global, Cellular, and Wireless Networks. John Wiley & Sons, Inc.

Qiu, B. 2002. Next generation information communication infrastructure and case studies for future power systems. DTech Thesis. Virginia Polytechnic Institute and State University, Virginia.

Rasmussen, J. and Yang, W.Q. 2008. A compact electrical capacitance tomography system. In IEEE International Workshop on Imaging Systems and Techniques, 2008. IEEE: Page : 175–180.

Retty, H., Delpont, J. and Centeno, V. 2013. Development of tests and procedures for evaluating phasor data concentrators. In IEEE Grenoble PowerTech (POWERTECH), 2013. IEEE: Page : 1–5.

Rodrigues, M., Mendes, J. and Fonseca, J. 2004. Application of a Web-based monitoring and control system in plastic rotational moulding machine. In IEEE International Conference on Industrial Technology, 2004. IEEE: Page : 819–823.

RTDS Technologies. 2014. Real Time Power System Simulation | RTDS Technologies. <http://rtds.com/index/index.html> 14 November 2014.

Russell, B.D., Benner, C.L., Cheney, R.M., Wallis, C.F., Anthony, T.L. and Muston, W.E. 2009. Reliability improvement of distribution feeders through real-time, intelligent monitoring. In IEEE Power & Energy Society General Meeting, 2009. IEEE: Page : 1–8.

Saka, F. 2001. Ethernet for the ATLAS Second Level Trigger. Master Thesis. University of London.

Shwehdi, M.H. and Khan, A.Z. 1996. A power line data communication interface using spread spectrum technology in home automation. IEEE Transactions on Power Delivery, Volume : 11(Issue : 3): Page : 1232–1237.

Sidhu, T.S. and Gangadharan, P.K. 2005. Control and automation of power system substation using IEC61850 communication. In IEEE Conference on Control Applications, 2005. IEEE: Page :1331–1336.

Singh, B., Sharma, N.K., Tiwari, A.N., Verma, K.S. and Singh, S.N. 2011. Applications of phasor measurement units (PMUs) in electric power system networks incorporated with FACTS controllers. International Journal of Engineering, Science and Technology, Volume : 3(Issue : 3): Page :64–82.

Tholomier, D., Kang, H. and Cvorovic, B. 2009. Phasor measurement units: Functionality and applications. In Power Systems Conference, 2009. PSC'09. IEEE: 1–12.

Tripathy, P. 2010. Real-time power system stability prediction using synchrophasor based wide area monitoring system. Phd Thesis. KANPUR: INDIAN INSTITUTE OF TECHNOLOGY.

US Department of Energy. 2012. Smart Grid/Department of Energy.

US Magazine. 2013. Synchrophasor Technologies and their Deployment the Recovery Act Smart Grid Program.

Wang, W., Xu, Y. and Khanna, M. 2011. A survey on the communication architectures in smart grid. *Computer Networks*, 55(15): 3604–3629.

www.selinc.com. 2014. SEL-2407® Satellite-Synchronized Clock.

Xiaoyang, T., Guodong, L., Xiaoru, W. and Shan, Z. 2005. The analysis of communication architecture and control mode of wide area power systems control. In *Autonomous Decentralized Systems*, 2005. IEEE: Page : 59–65.

Zhang, G., Sun, K., Chen, H., Carroll, R. and Liu, Y. 2011. Application of synchrophasor measurements for improving operator situational awareness. In *IEEE Power and Energy Society General Meeting*, 2011. IEEE: Page : 1–8.

Zhang, M. and Li, K. 2009. A power quality monitoring system over the Internet. In *International Conference on Information Science and Engineering (ICISE)*, 2009. IEEE: Page : 1577–1580.

APPENDICES

Appendix A: Structure of the Real-Time Digital Simulator (RTDS)

Description of the structure of the RTDS uses information from the RTDS manual. The RTDS consists of individual racks of tightly coupled digital signal processors connected to each other using a common backplane. Each rack is identical and contains the following types of cards.

- I. Processor card
- II. Workstation Interface card(WIF)
- III. Inter Rack Communication(IRC)Switch
- IV. GTNET Card (Network Interface Card)
- V. GTSYNC Synchronization Card

A1: RTDS Processor cards

The RTDS at CSEAMS lab contains two Processor Cards (PB5 cards). The PB5 Card is the processor card used to solve the equations representing the power system and control system components modelled within the RTDS. Each PB5 card contains two freescale MC7448 RISC processors, which can operate at clock speed of 1.7 GHz. These card contain these cards contain 12 loading units, which allow more components to be included on one card. Each card can handle 72 single-phase nodes or 24 three-phase nodes of the power system model cards are properly configured. PB5 cards are provided with two I/O ports and six communication ports, which will facilitate the user to communicate with PB5 cards. It also includes fiber ports which are used to connect various types of I/O cards such as GTA0 (GT Analogue Output), GTAI (GT Analogue Input), GTDO (GT Digital Output), GTDI (GT Digital Input), GTFPI (GT Front Panel Interface), GTNET (GT Network Interface Card) as shown in Figure A1. Each PB5 card consumes a maximum of 80 Watts.

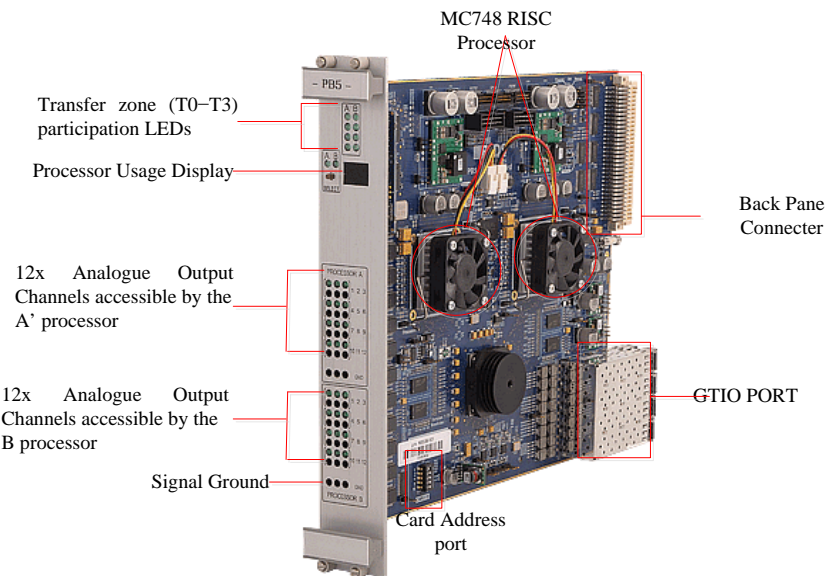


Figure A1: RTDS processor card

A2: PB5 Front Panel Analogue Output Channels

Each PB5 card includes two sets of twelve analogue output channels. The first set of twelve channels is accessible by the PB5's 'A' processor and the second set by the 'B' processor. Specifications for the analogue output channels are listed in FigureA1. The PB5's front panel DACs (Digital to Analog Converter) use DAC7802 chips for the D/A conversion, an OP470G op amp to provide the output voltage and a REF102CU precision reference for calibration. Front panel analogue outputs from the PB5 are provided for monitoring of selected signals. The analogue outputs are not optically isolated and do not include over-sampling. Use of the front panel analogue outputs is not recommended for connection to external controls or protection equipment due to the lack of optical isolation and limited dynamic range. Pin tip connectors are provided with the RTDS to permit connection of scope probes to the analogue output channels in Figure A.2.

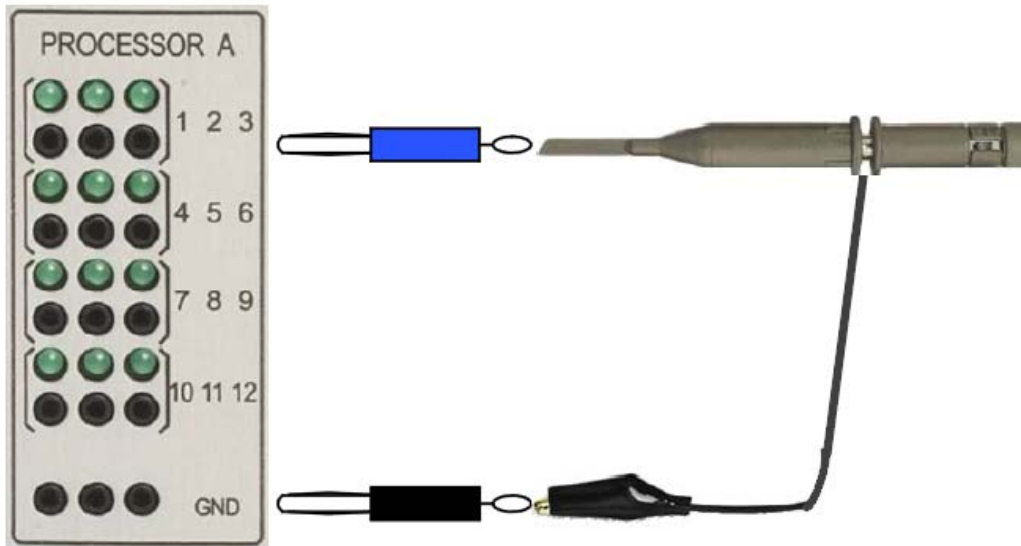


Figure A2: Pin tip connections to front panel analogue outputs

A3: Gigabit Transceiver Workstation InterFace Card (GTWIF)

The simulator has been provided with Giga Transceiver Workstation Interface (GTWIF) card to handle communication between the RTDS and the host computer. Each GTIWF contains an Ethernet transceiver assigned with its own Ethernet IP address, thus allowing connection to any standard Ethernet based local area network. The main functions of GTWIF include loading starting and stopping the power system model, time-stamp generation, rack hardware diagnostics, inter-rack synchronization along with Inter Rack Communication (IRC) card.

The communication medium used between the GTWIF and the host computer is a standard Ethernet (10/100baseT) TCP/IP based local area network.

The main functions of the GTWIF cards are.

- a. Communication between the RTDS rack and the computer workstation running the RSCAD software. Communication is over an Ethernet-based LAN.
- b. RSCAD/RunTime software communicates with the GTWIF card's real-time operating system to send and receive messages associated with plot updates and user initiated events such as change of a set-point via a Slider, Switch or other such Run-time component. The GTWIF card is also used for communication of data with the computer workstation in order to load new simulation cases, as well as, to start and stop the simulations.

- c. Synchronization of racks for multi-rack simulation cases. The GTWIF card installed in the first rack allocated for the simulation case synchronizes each time-step, and the communication intervals within the time-step. The first rack in the simulation case is designated as the master rack.
- d. Communication with other racks participating in a simulation case. Each GTWIF card uses its inter-rack communication channels to exchange data with up to six other racks while the simulation case is running.
- e. Communication of data between processors over the rack's backplane is coordinated by the GTWIF.
- f. The GTWIF performs self-tests and runs diagnostics on other cards installed in its rack. The diagnostics are automatically run at power up and may be initiated by the user. Results from the diagnostic tests are accessible from the RSCAD

Front panel components of the GTWIF are shown in Figure A3

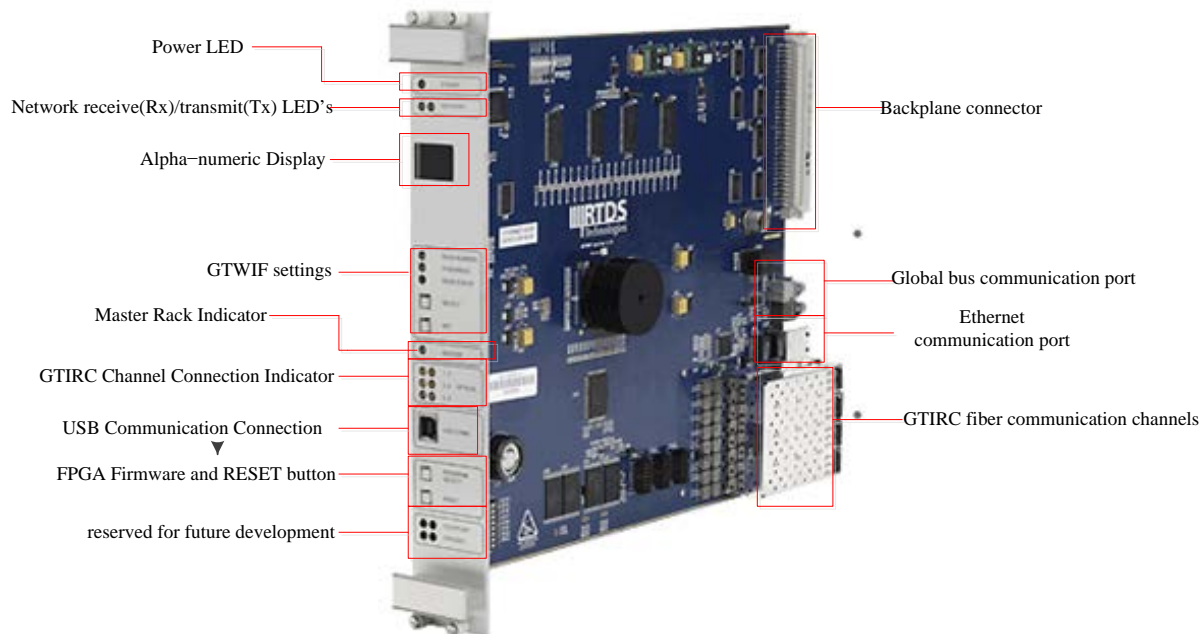


Figure A3: Typical GTWIF card

A4: Inter Rack Communication (IRC)

IRC switch stands for inter-rack communication switch and its main function is to facilitate the user to communicate among the various racks, while simulating large-scale power systems. The IRC switch is capable to communicate with as many as 60 racks simultaneously. RTDS systems equipped with GTWIF cards do not require IRC cards as

the IRC function is included as part of the GTWIF card. The six communication channels on an IRC card permit an RTDS comprised of seven racks to be fully interconnected. It is possible to include two IRC cards per rack in which case each rack is able to directly communicate with 12 others. In this case, an RTDS simulator consisting of 13 racks can be fully interconnected. It should be noted that for most power system simulation cases it is not necessary to have full and complete communication between all RTDS racks. As such, RTDS simulators consisting of a large number of racks may be used to simulate power system models, which include a large number of busses. Each IRC card consumes a maximum of 35 Watts. Figure A4 shows IRC card

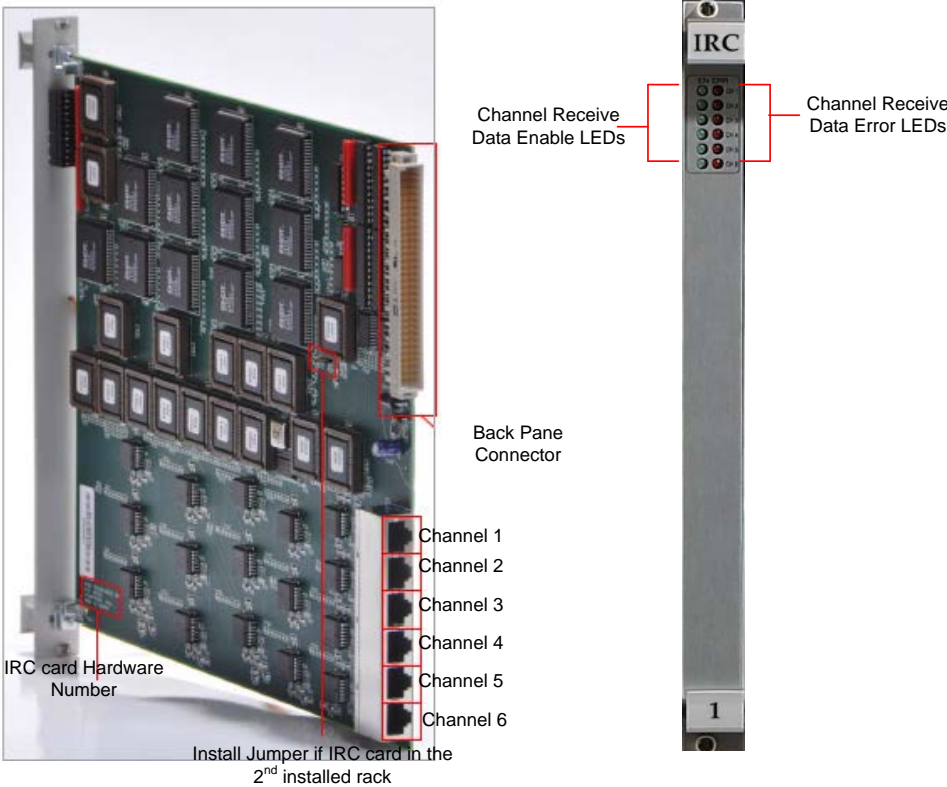


Figure A4: IRC card connector and faceplate LEDs

A5: GTNET Card (Network Interface Card)

The GTNET card is used to interface a number of external devices with the RTDS simulator using different network protocols. The following protocols are presently supported on the GTNET are

- I. GSE IEC-61850 GOOSE/GSSE
- II. SV IEC-61850-9-2(sampled values)

- III. DNP3 Distributed Network Protocol
- IV. PLAYBACK Playback of large data sets
- V. PMU IEEE C37.118 data stream output

Each supported protocol on the GTNET requires that the appropriate firmware be installed on the GTNET. Up to 4 firmware versions may be installed on a GTNET card, with only one of the firmware versions active at a given time. The GTNET card resides within the standard RTDS rack and obtains its power signals from the rack's backplane. Communication between the GPC card and the GTNET card is, however, not over the backplane, but rather using a GT port fiber cable connected between the GTNET and GPC card. Two different versions of the GTNET card are available. One version includes a 100BASE-TXRJ45 Ethernet port, the other comes equipped with a 100BASE-FX Ethernet port, and Figure A5 shows GTNET Card (100BaseTX Ethernet). Faceplate features are the same on both versions of the card in figure

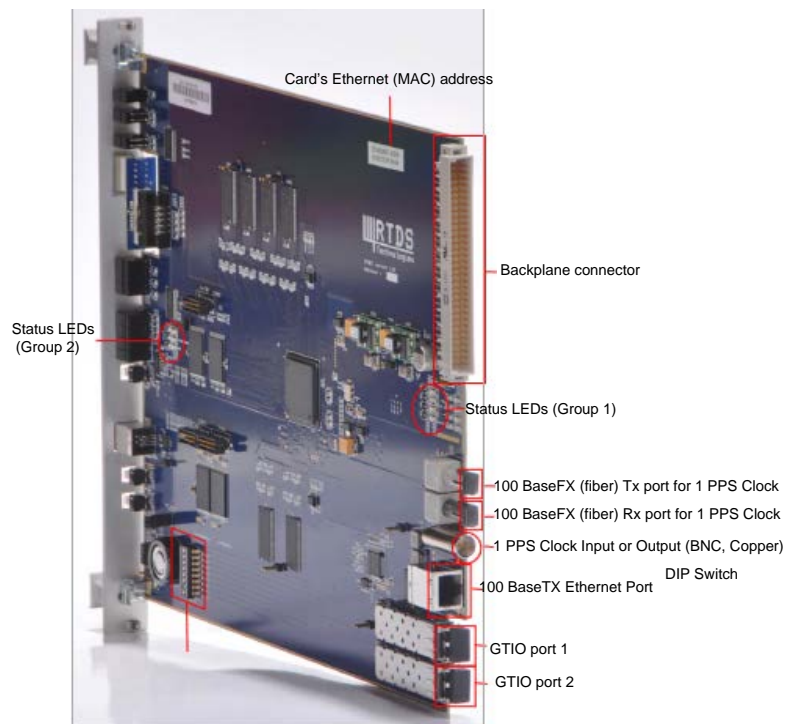


Figure A5: GTNET card (100BaseTX Ethernet)

Appendix B: Open Phasor Data Concentrator (PDC) software installation

The connection configuration of the GTNET card PMUs was tested using the PMU connection tester, the corresponding configuration and connection files for each PMU are saved on the remote Personal Computer (PC) where the OpenPDC software is installed. The saved configuration and connection files are transferred to the OpenPDC software to communicate with the PMUs running on the RSCAD software suite of RTDS. Before connecting the GTNET PMU, the saved configuration and connection files, need to be imported within the OpenPDC working environment. The following steps are used to import the RSCAD software PMU connection and configuration files to the OpenPDC software environment

Step 1: Run the configuration setup utility file from the OpenPDC software. A snippet of the configuration utility wizard shown in Figure B1:

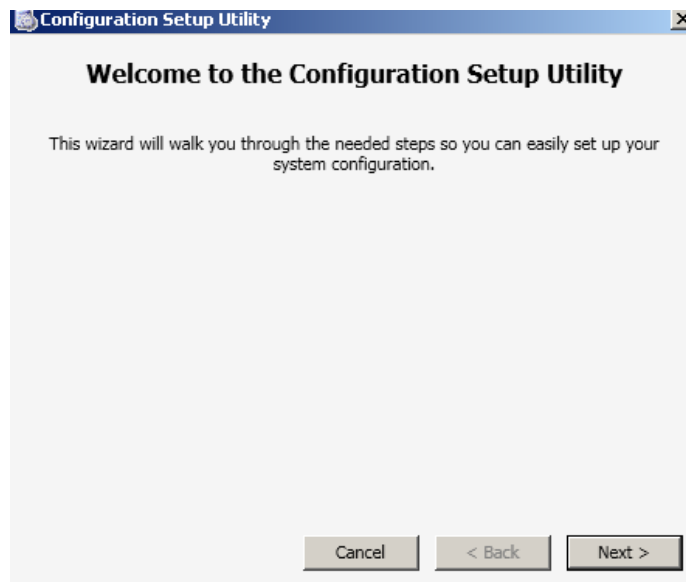


Figure B1: OpenPDC configuration setup

Step 2: Select the option for a new configuration setup in the configuration utility as shown in Figure B2:

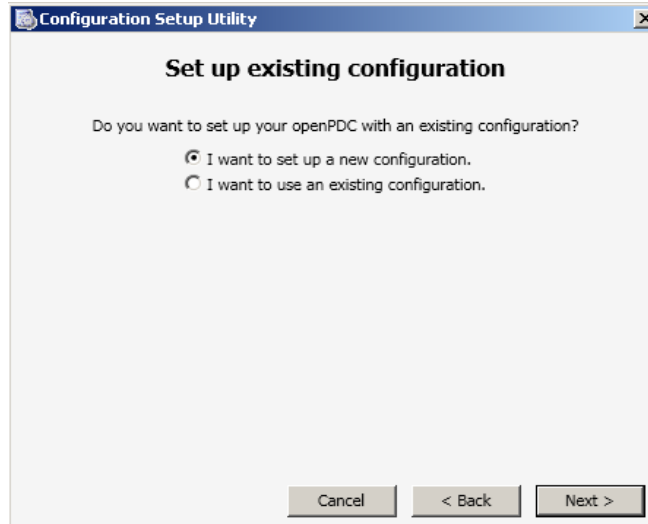


Figure B2: OpenPDC configuration setup to establish a new configuration

Step 3: The OpenPDC recommended setup configuration based on a database is shown in Figure B3

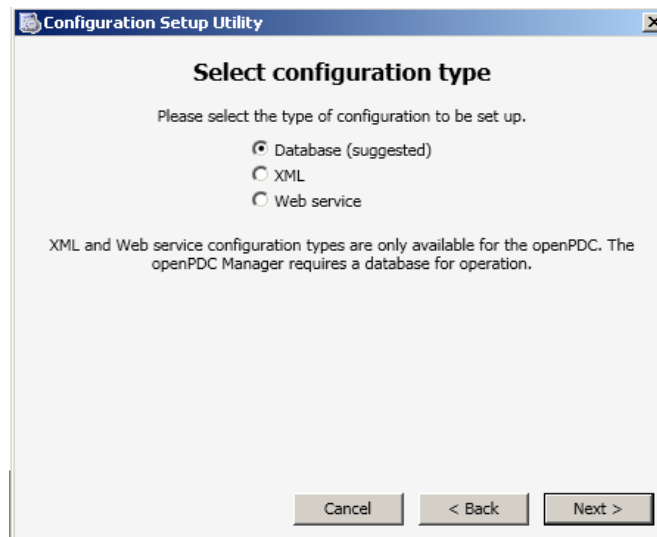


Figure B3: OpenPDC database configuration setup

Step 4: Select the type that is used in the lab-scale system. MySQL database is used as shown in Figure B4. Enable run of the initial data script that is used to create the database and run the sample data script within the OpenPDC environment.

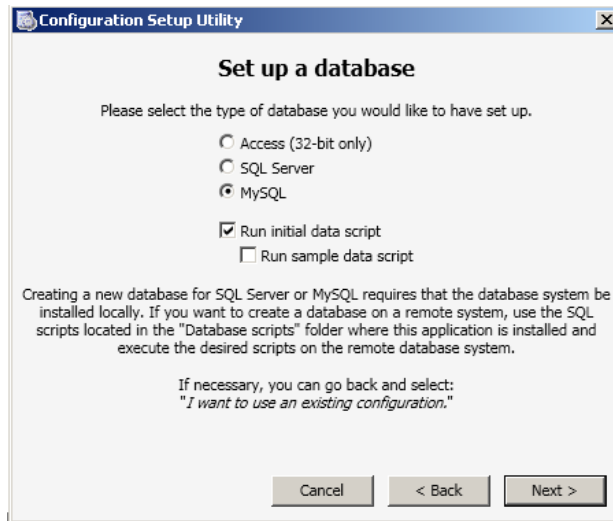


Figure B4: OpenPDC database setup

Step 5: Enter MySQL database user name and password and click on the test connection button as shown in Figure B5. The connection can be either successful or unsuccessful. If it is unsuccessful, then there is a problem with the configuration of the database and the OpenPDC will not work properly

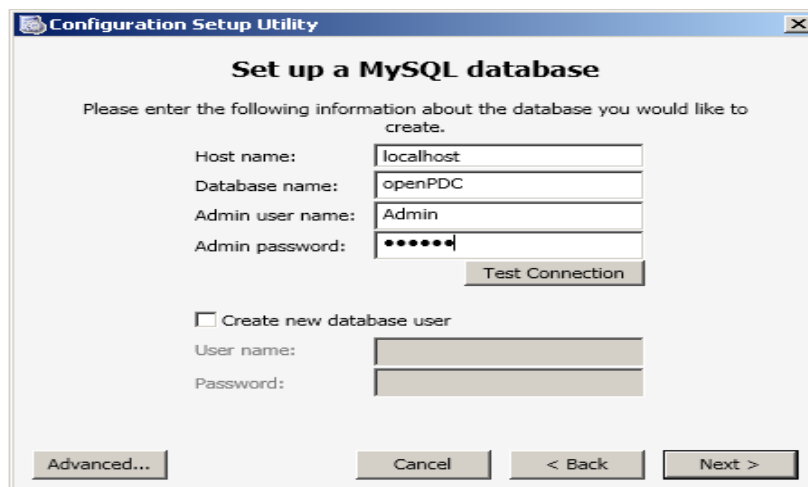


Figure B5: OpenPDC MySQL database setup

Step 6: Enter the windows authentication username and password shown in Figure B6 and click next, Figure B6

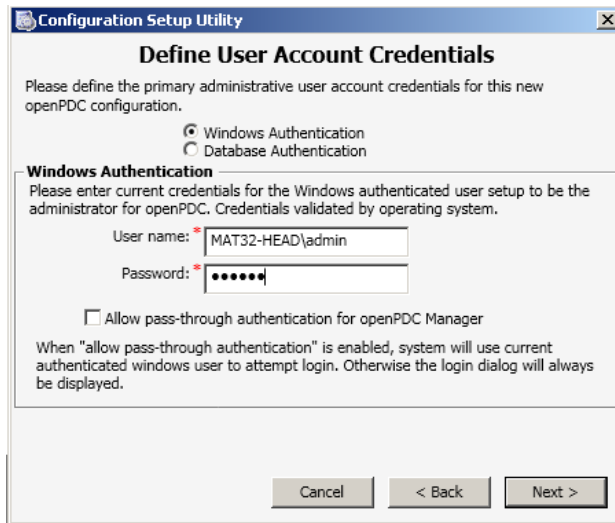


Figure B6: OpenPDC windows authentication setup

Step 7: Select the components, for which the configuration changes have to be done as shown in Figure B7: and click next:

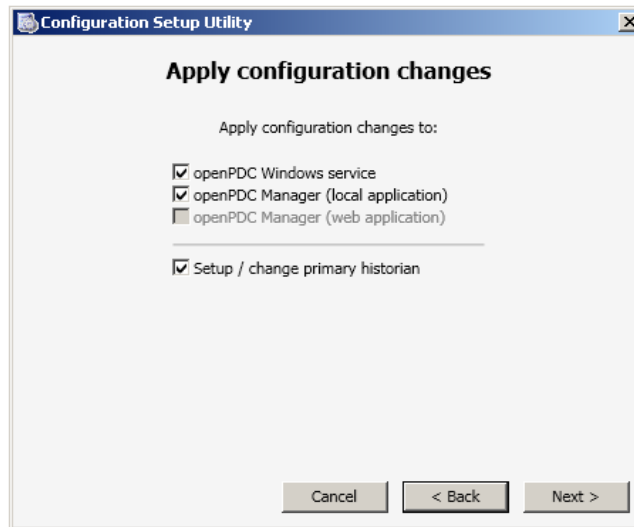


Figure B7: Change the setup of the OpenPDC configuration

Step 8: Select the primary historian In this case measured data will be saved in MySQL database. Therefore, select the archive measurement to a MySQL database and click twice and wait for the configuration to be completed as shown in Figure B8

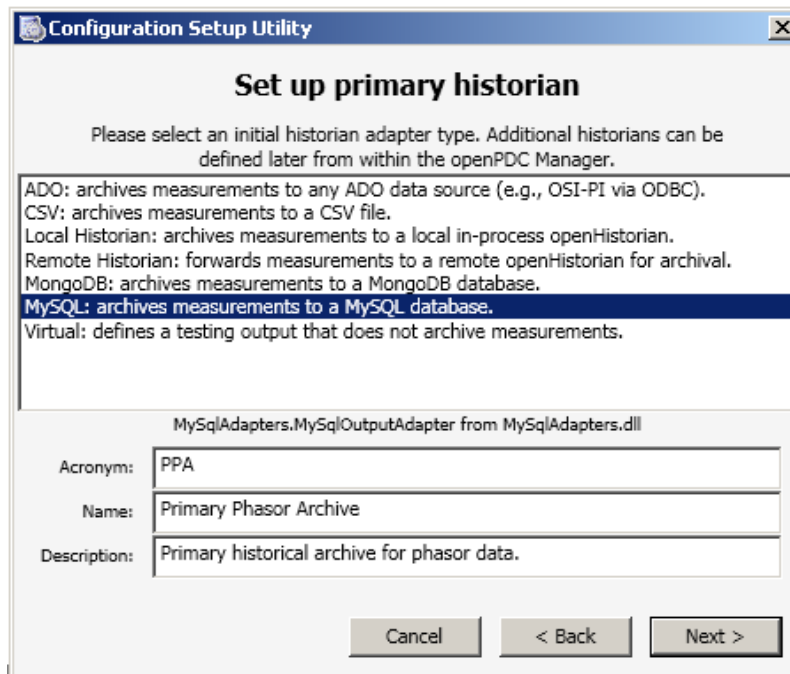


Figure B8: MySQL database for archive PMU measurement signals

Step 9: Click next after the configuration is completed and the PMU connection Tester setup will pop-up immediately.

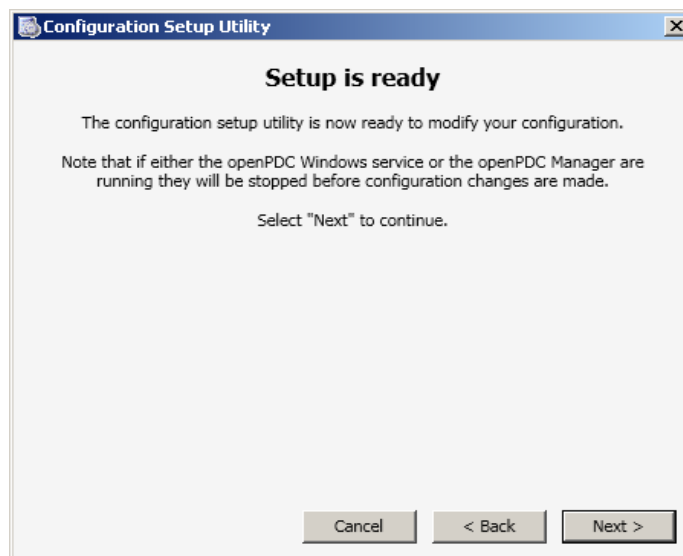


Figure B9: OpenPDC confirmation setup utility

Once the Setup within the wizard is completed, the OpenPDC software home screen appears and it gives a lot of options and menus. The home screen image is shown in Figure B10.

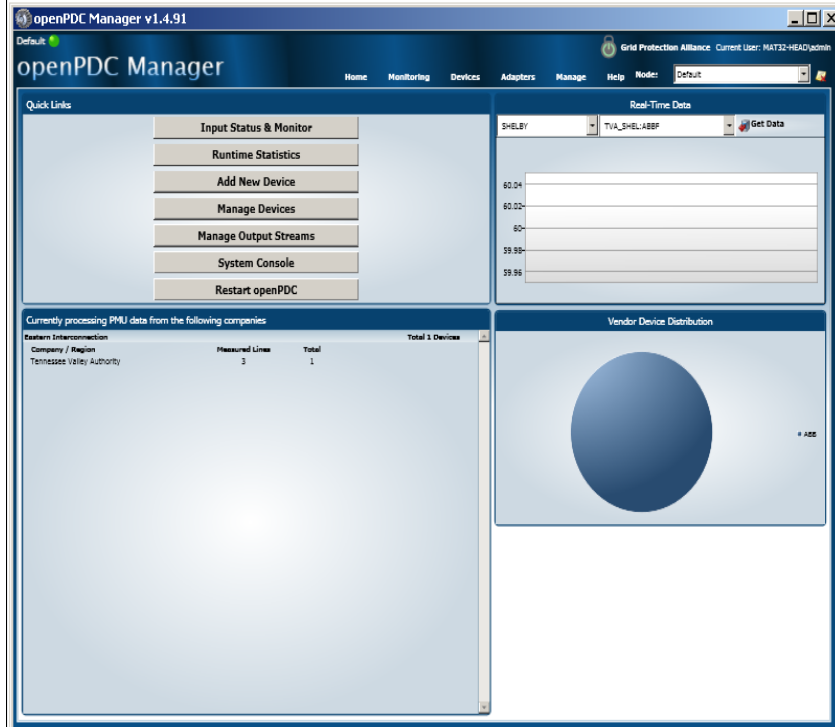


Figure B10: OpenPDC home screen window

Appendix C: MySQL Workbench Installation

The following steps must be used to install the MySQL workbench software

1. The MySQL setup-file must be run. Follow the wizard to install the MySQL software. The main window is shown in Figure C1

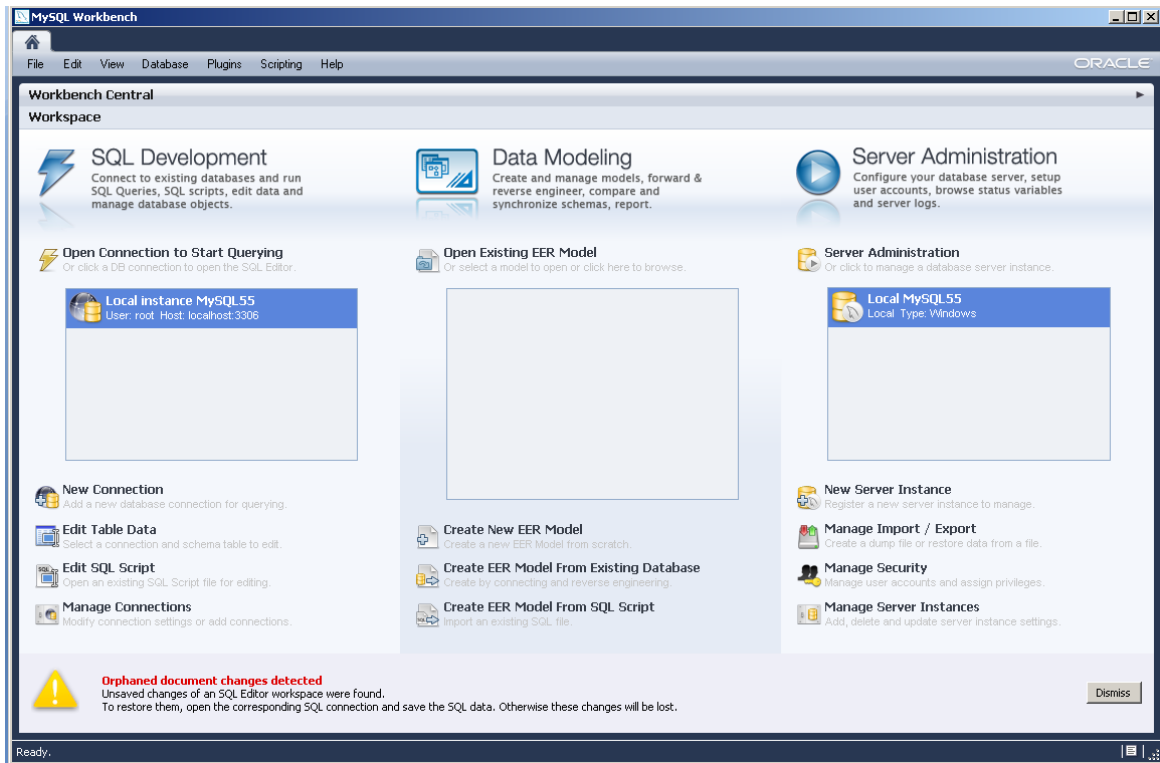


Figure C1: MySQL workbench main window

2. Open MySQL workbench software and select the database option and set-up the connection method, define the hostname, port number, username and password. The MySQL database connection setting shown in Figure C2

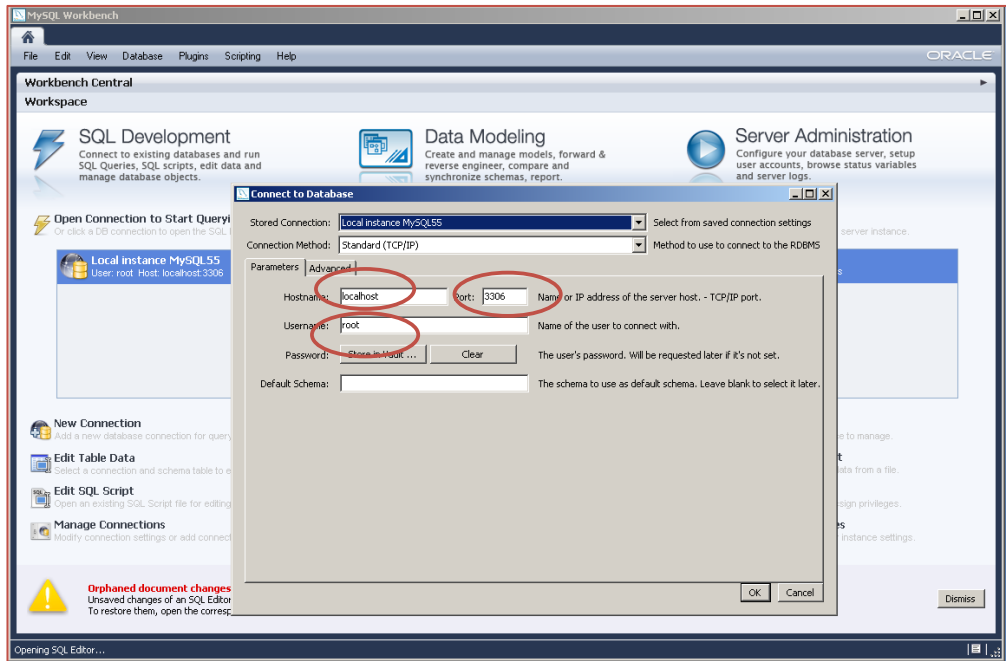


Figure C2: MySQL workbench database connection setting window

3. The username and password are provided in order to connect to the MySQL server. Then user authentication window gives the password to connect MySQL server as shown in Figure C3

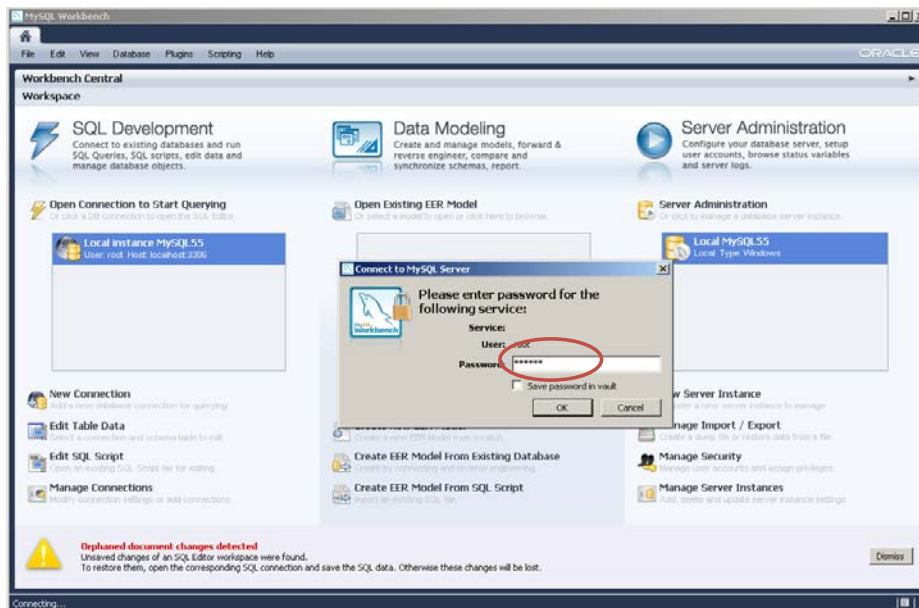


Figure C3: MySQL server authentication window

4. After the setup the MySQL workbench editor is successfully created is shown in Figure C4

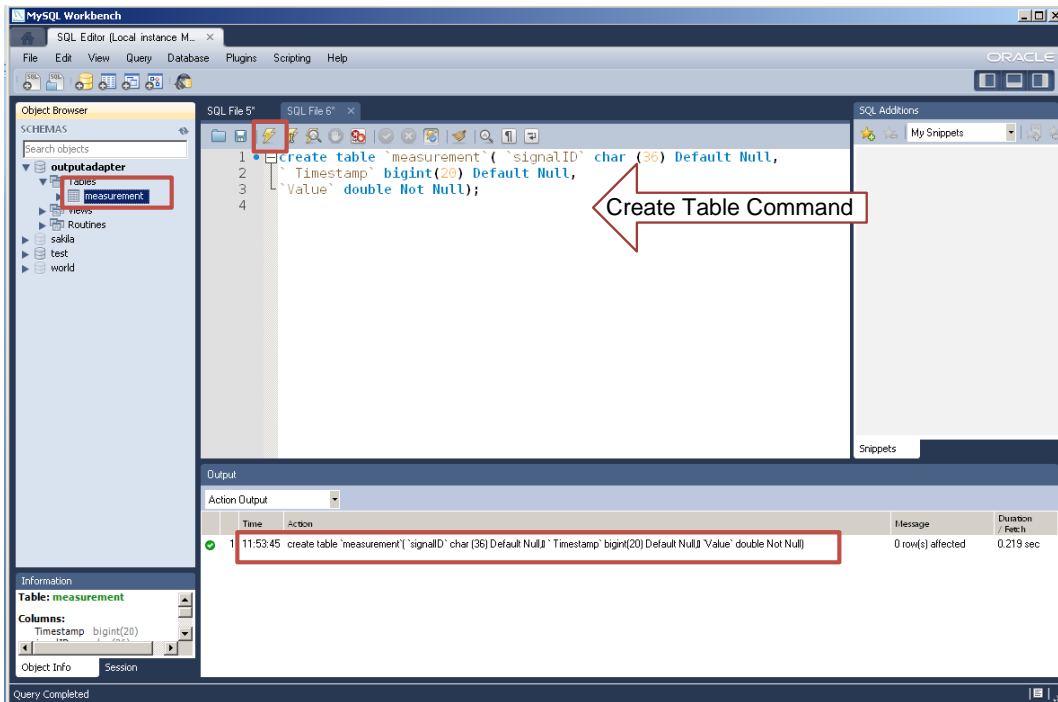


Figure C4: SQL query in MySQL workbench

Appendix D: Development of RSCAD software for simulation of the five and eleven bus power systems

This section provides the developed RSCAD software for simulation of the five and eleven bus power systems.

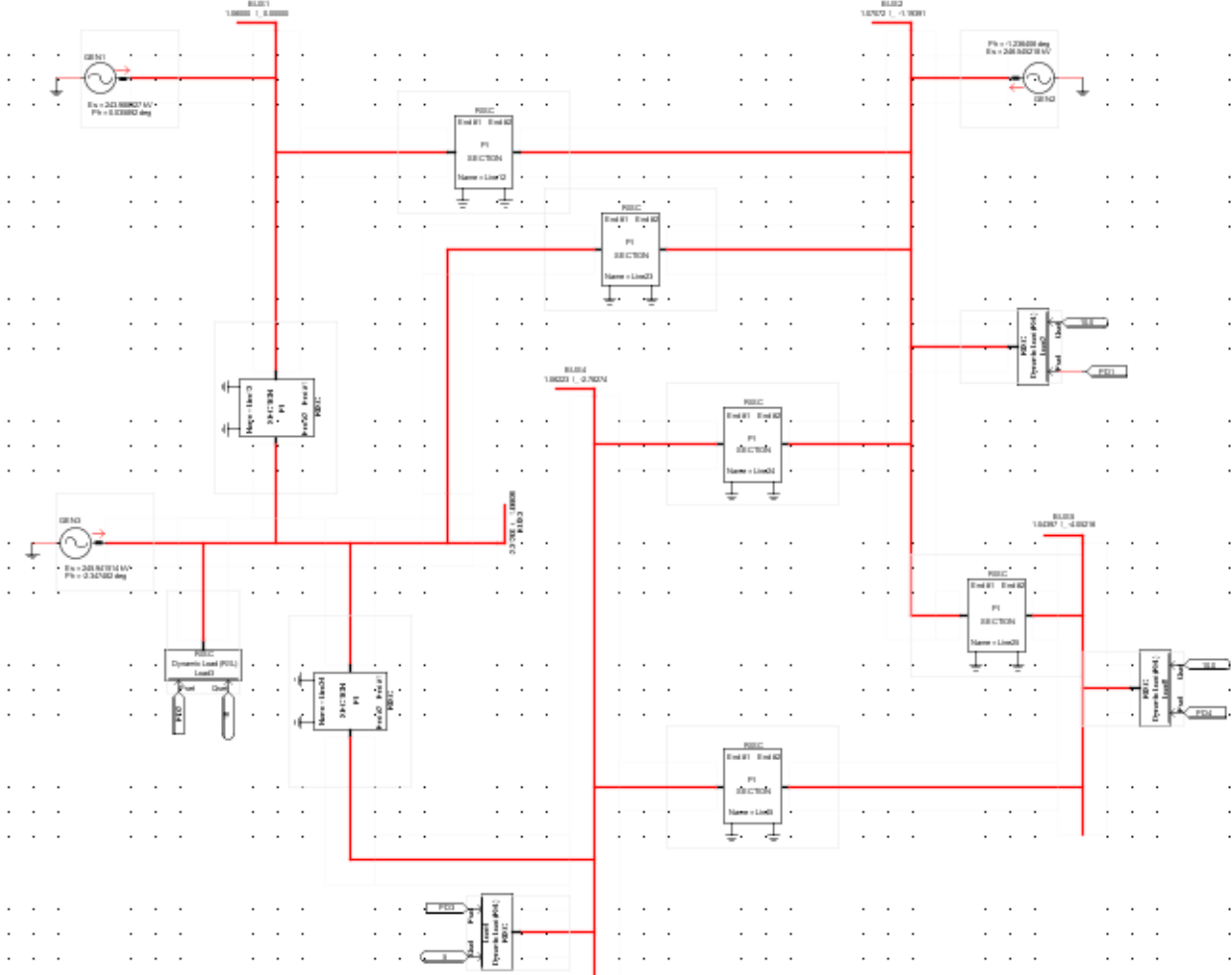


Figure D1: Five bus power system model in RSCAD environment

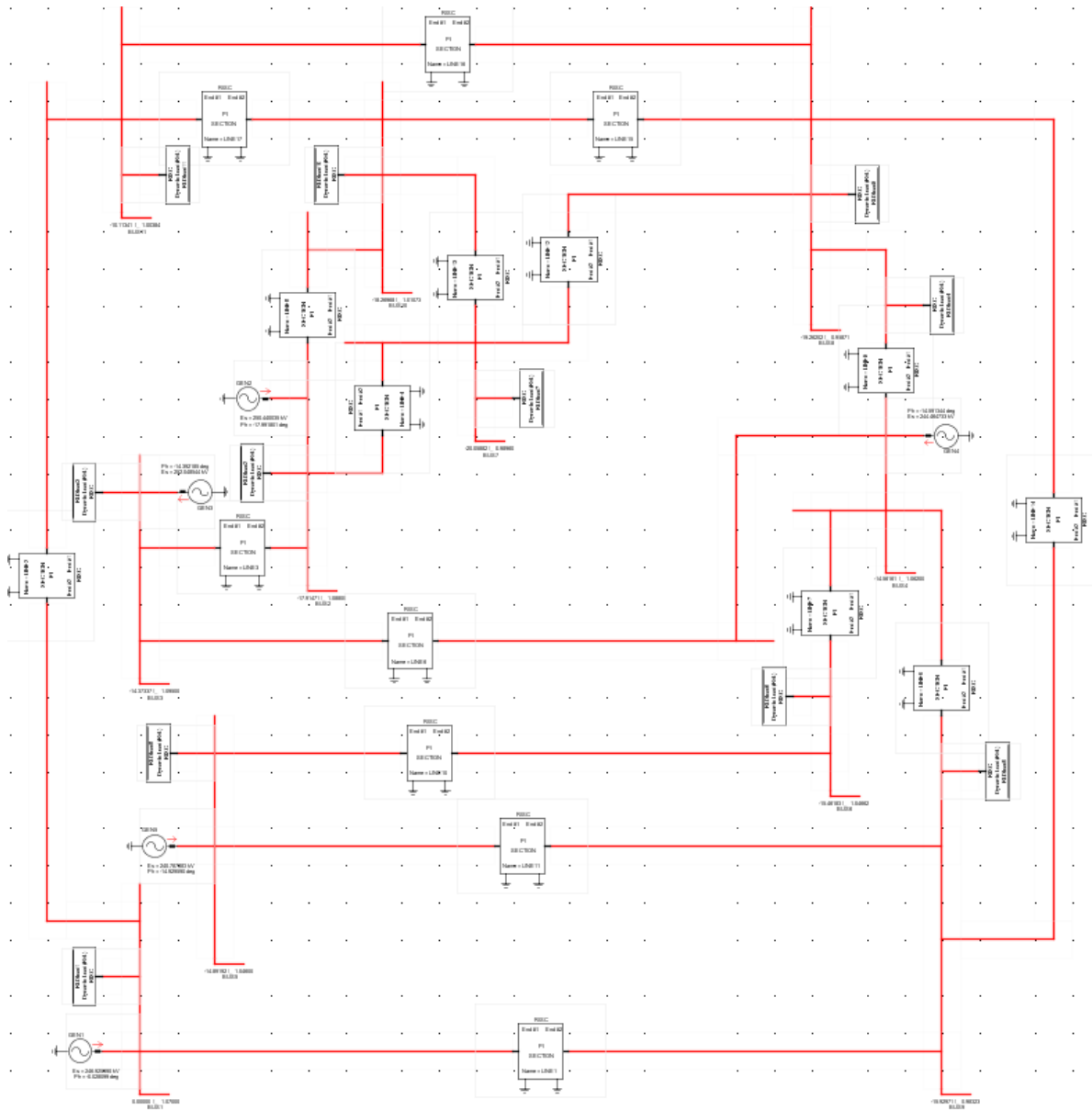


Figure D2: Eleven bus power system model in RSCAD environment

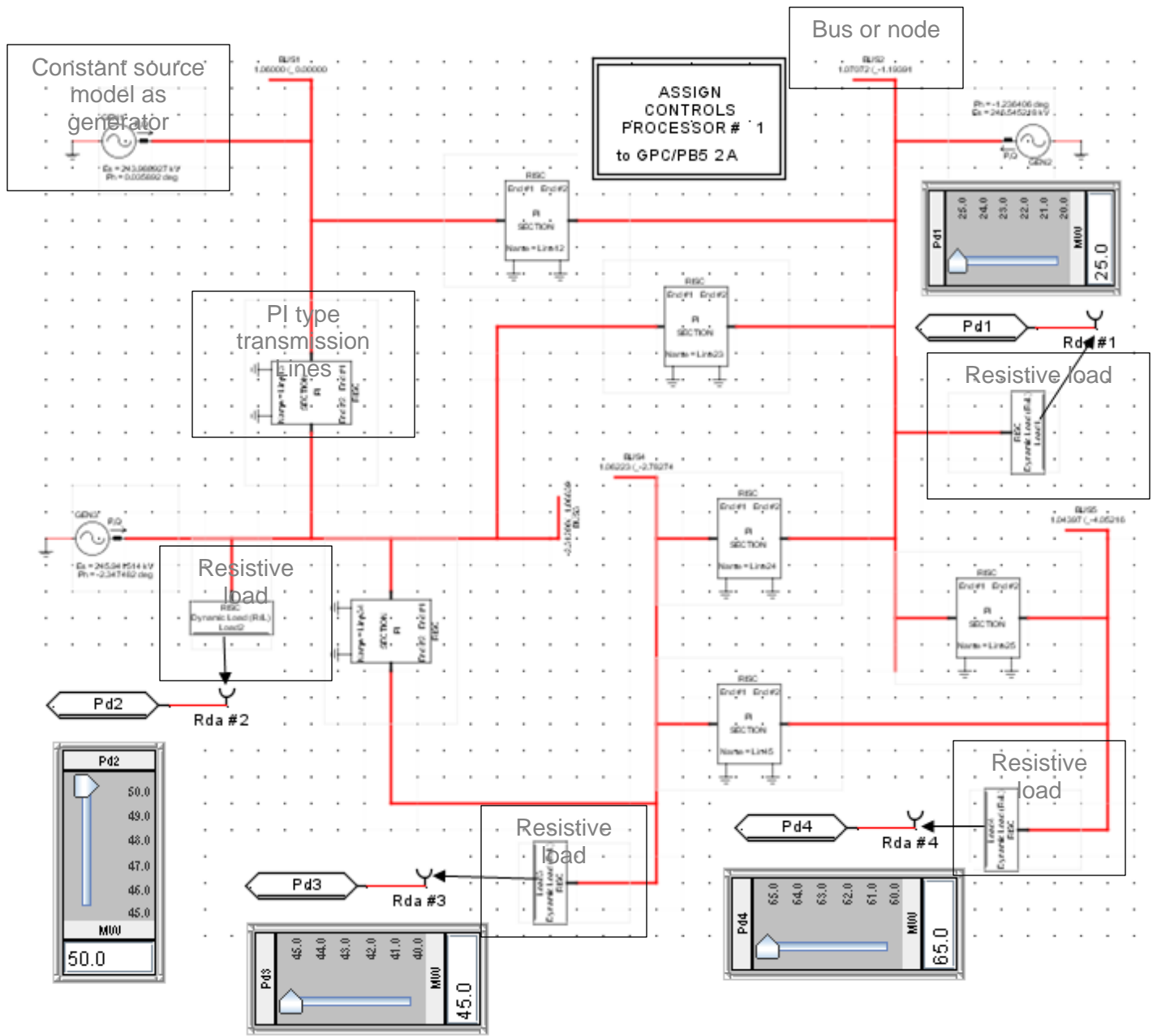


Figure D3: Five bus power system model of RSCAD environment, including the NI DAQ 6343 card input channels

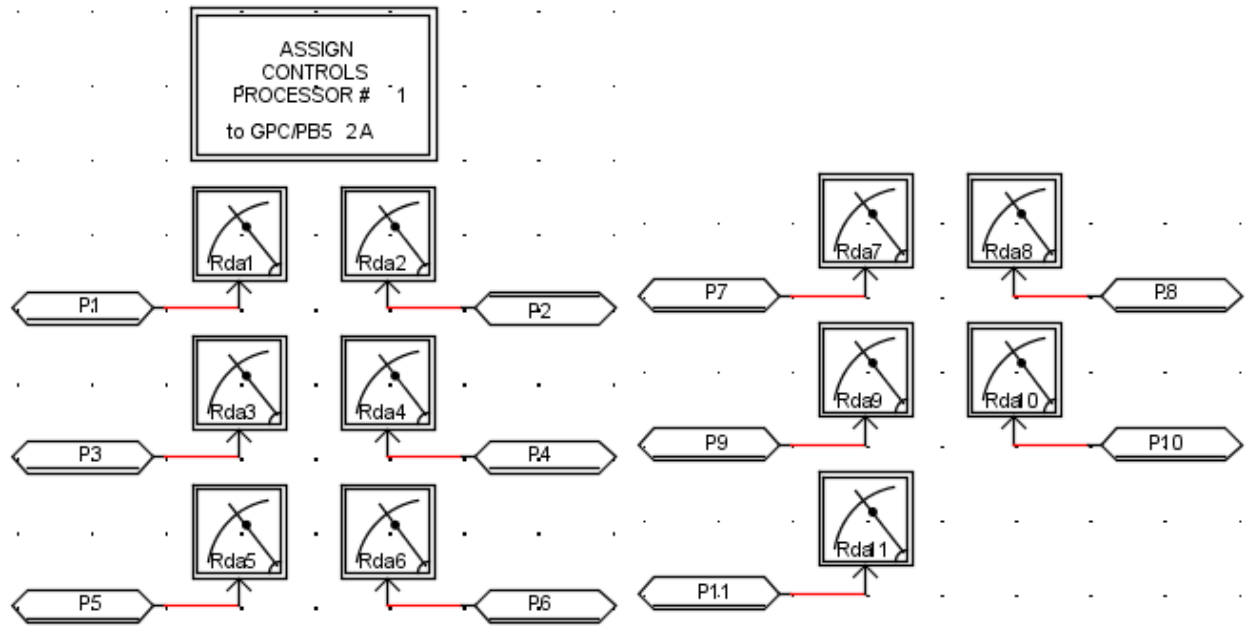


Figure D4: RCSAD diagram for the real power load signal assignment to the RTDS PB5 card for the eleven bus power system model

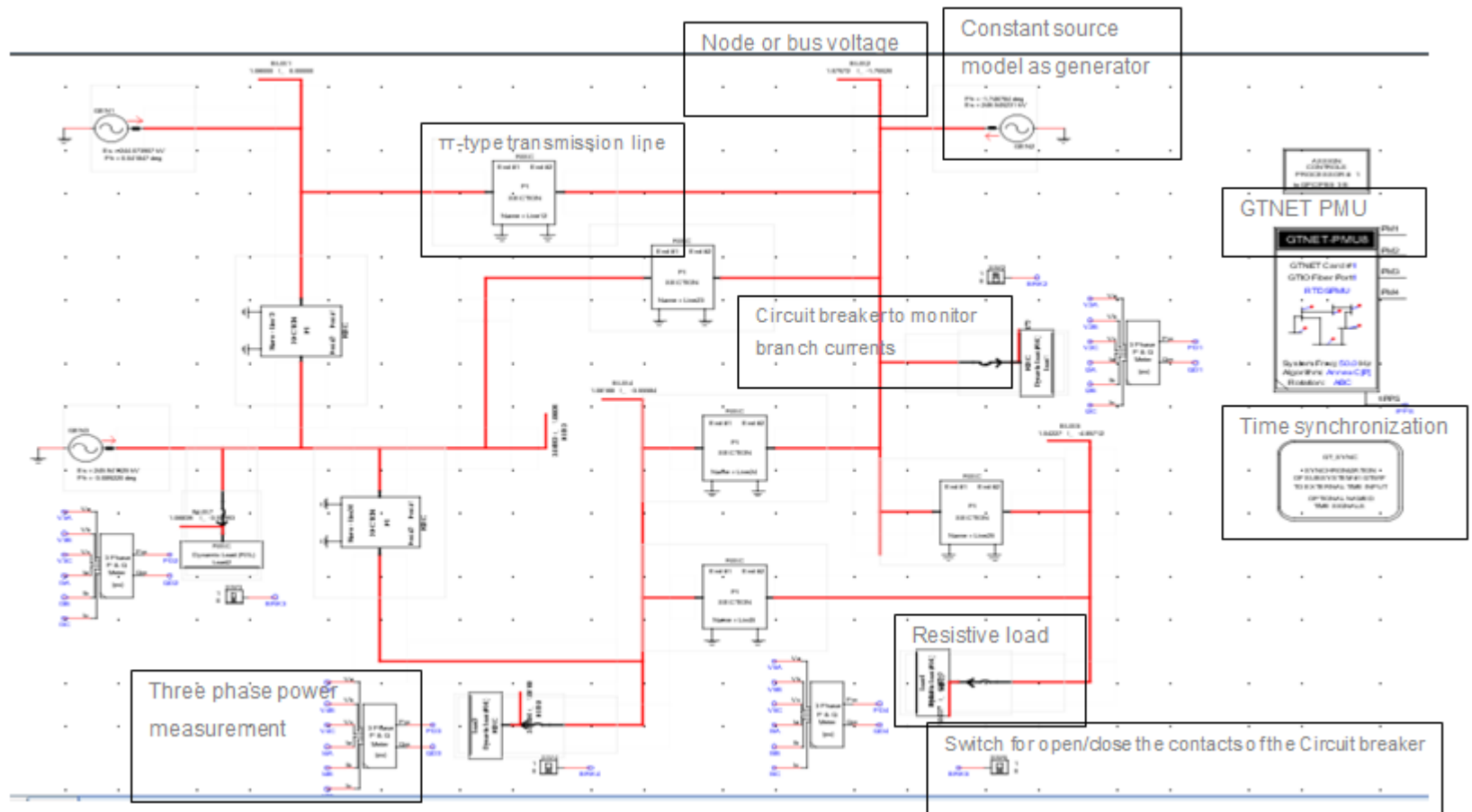


Figure D5: Five bus power system network modelled in the RSCAD environment with components to implement data acquisition and data transfer using the GTNET card PMU

Appendix E: Development of DAQ/LabVIEW software for simulation of the five and eleven bus power systems

This section provides the developed DAQ/LabVIEW software for five and eleven bus power systems.

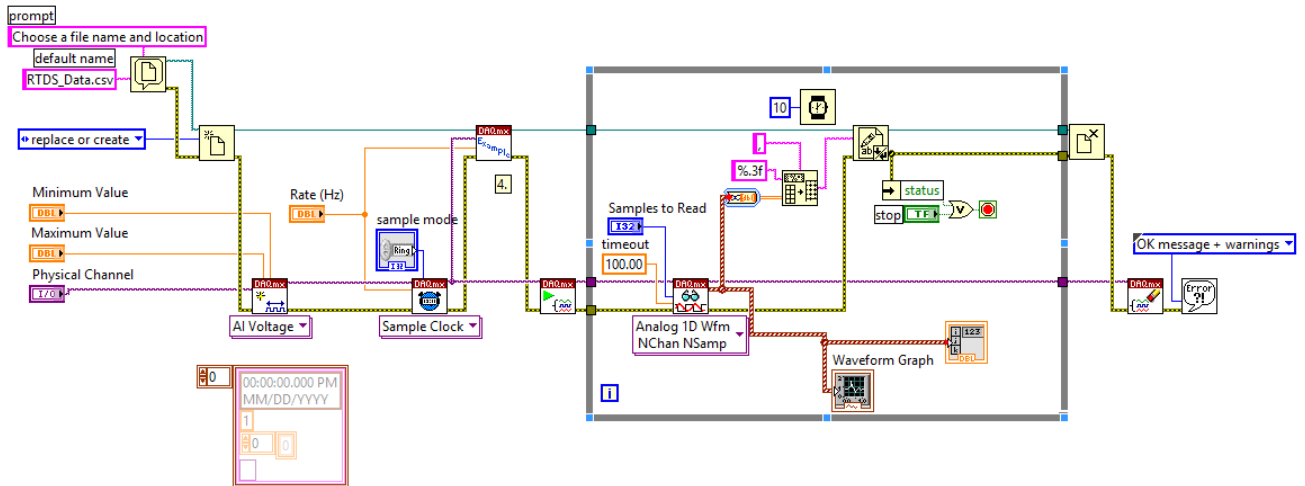


Figure E1: LabVIEW front panel diagram to connect the RTDS four channel PB5 card signals to the NI DAQ card 6343

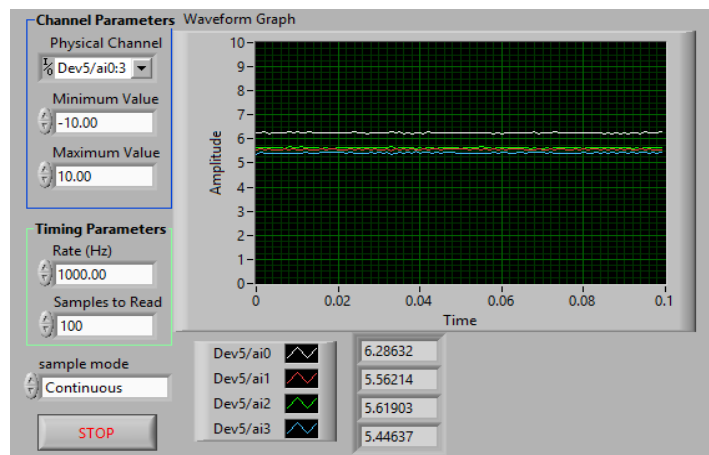


Figure E2: Front panel design of the LabVIEW data acquisition system to monitor the four analog signals coming from the RTDS PB5 card

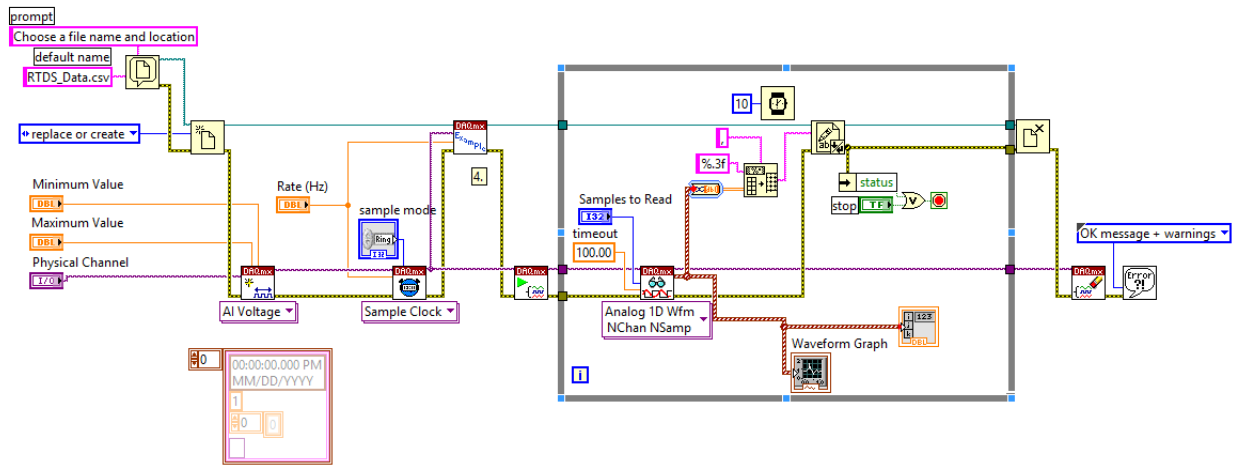


Figure E3: LabVIEW diagram to connect the RTDS eleven channel PB5 card signals to the NI DAQ 6343 card

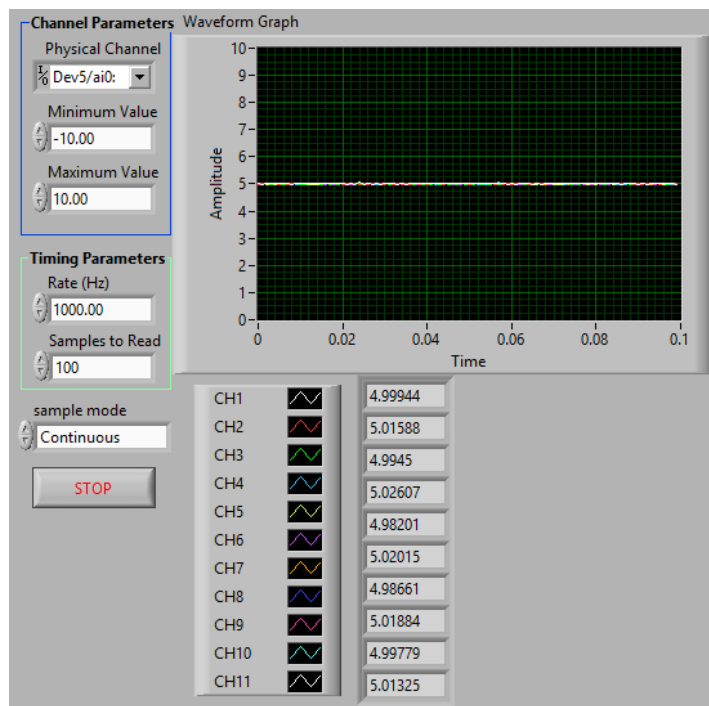


Figure E4: LabVIEW front panel waveforms which show the RTDS PB5 card captured signals for the initial load conditions of the eleven bus power system

Appendix F: Software program to read the data saved by LabVIEW in the Excel file into the MATLAB environment and using them to solve the power dispatch optimisation problem for the five bus power system

```

% M-File: Method_One_LabVIEW_based_Five_Bus_Power_System.m
% =====M-File
Description=====
% The M-File is used to read the data acquired by LabVIEW and saved in
the Excel file into the MATLAB environment and using them to solve the
power dispatch optimisation problem for the five bus power systems
clear all
clc;
tic;
%% To read the xls-file from RTDS using NI
% filename = 'myExample.xlsx';
filename = 'RTDS_Stream.csv';
A = xlsread(filename);
filename = 'RTDS_Stream.csv';
% Read data from the first worksheet into a numeric array:
%   A = xlsread('myExample.xls')
%
%   % Read a specific range of data:
%   subsetA = xlsread('myExample.xls', 1, 'B2:C3')
columnA = xlsread(filename,1,'A6:A1005');
columnB = xlsread(filename,1,'B6:B1005');
columnC = xlsread(filename,1,'C6:C1005');
columnD = xlsread(filename,1,'D6:D1005');
columnA=sum(columnA)/1000
columnB=sum(columnB)/1000
columnC=sum(columnC)/1000
columnD=sum(columnD)/1000
columnA=columnA*(20/5)
columnB=columnB*(45/5)
columnC=columnC*(40/5)
columnD=columnD*(60/5)
PD=[columnA, columnB, columnC, columnD];
figure(2); bar(PD);
axis([0 5 20 65])
title('Conversion of analog voltage into actual values for P_{D}');
xlabel('Number of P_{D} values from RTDS front panel');
ylabel('P_{D} [MW]');
PD=columnA+columnB+columnC+columnD
%optimal dispatch including losses and generator limits
% =====Economic dispatch problem including losses and generator
limits==
% =====Initial Lagrange's
variable=====
lambda= 4.0857e+04; %2.6e4; % Initial lambda
epsilon=0.1; % Tolerance value
alfa=0.1; % Inceremental deltalambda
n=3; % No of generators
m=1000; % Total number of iterations
%PD=165; % Power demand
% =====Fuel cost coefficients=====
=====
c=[60 75 70];
b=[200 150 180];
a=[140 120 80];
% =====Generator Limits =====
Pmin=[20 20 20];
%Pmax=[55 80 65];

```

```

Pmax=[200 200 200];
% =====Transmission loss
coefficients=====
B=[0.02423 0.00033 -0.00500
    0.00033 0.00469 -0.00315
    -0.00500 -0.00315 0.00868]*10^-1;
%% Lagranges algorithm starts here
for iter=1:m
iter % Print the itertaion number
% =====Calculation of generator real power
=====
E=[(diag(a)./lambda)+B];
D=0.5*((1-(b)./lambda))';
P=E\D;
%plot (P,E,'ro',P,D,'b+', 'MarkerSize', 12)
TotalP=sum(P(:, :))
%=====Generator limit checking
=====
for i=1:n
if P(i)<=Pmin(i)
P(i)=Pmin(i);
elseif P(i)>=Pmax(i);
P(i)=Pmax(i);
else P(i)=P(i);
end
end
P
%===== Calculation of Tranmission
loss=====
PL=zeros(n,n);
for i=1:n
for j=1:n
PL(i,j)=P(i)*B(i,j)*P(j);
end
end
PL=sum(PL(:, :));
PL=sum(PL(:, :));
% =====Calculation of deltalambda
=====
% deltalambda=0.0;
deltalambda=PD+PL;
for i=1:n
deltalambda=deltalambda-P(i);
end
if abs(deltalambda)<=epsilon | iter>=m
break
else lambda=lambda+deltalambda%*alfa
end
% plot(iter,lambda,'*',iter,deltalambda,'--');
% figure(3)
% plot(iter,lambda,'*');
% hold on
% figure(4)
% plot(iter,deltalambda,'*');
% hold on
end
%% Lagranges algorithm ends here
% gtext('o lambda ', 'FontSize',10)
% gtext('+ deltalambda ', 'FontSize',10)
% title (' deltalambda Vs Iteration Number ', 'FontSize',12)
% xlabel ('Itertation Number', 'FontSize',12)

```

```

% ylabel ('deltalambda','FontSize',12)
%Calculation of fuel cost, emission and CEED values
=====
P=P/100;
fuelcost=0;
for i=1:n
fuelcost=fuelcost+c(i)*P(i)^2+b(i)*P(i)+a(i);
end
%==Printing of Real power, Transmission loss, Fuel cost, Emission and
CEED=
lambda
PL
totalfuelcost=sum(fuelcost(:, :))
toc
%=====
=====

```

Appendix G: Software program for the implementation of method one: MATLAB-based data acquisition and data transfer system using PB5 card analog output signals for the five bus power system

```

% M-File: Method_One_MATLAB_based_Five_Bus_Power_System.m
%
% Description=====M-File
% The M-File is used to acquire and transfer the data from the RTDS
% PB5 card analogue output signals to the PC at the local end using the
% NI DAQ 6343 card. The transferred real-time data is used to solve the
% economic dispatch problem using the Lagrange's Algorithm
clear all
clc
%1. Create a device object - Create the analog input object AI for a
...
% National Instrument Instruments board. The installed adaptors and
...
% hardware IDs are found with daqhwinfo
daq.getVendors()
daq.getDevices;
% 2. You should see a list of devices. Create a session using the
% listed NI DAQ device.
s = daq.createSession('ni');
%3. Add an analog input voltage channel to the session. Choose channel
% '1' on the NI device.
% Make sure your device is properly connected
ch = s.addAnalogInputChannel('Dev5',[0 1 2 3], 'Voltage');
% 4.Set DAQ Parameters
s.Rate = 10000;% how fast do you want to acquire the data
% s.Channels.Range = [-10 10];
s.DurationInSeconds = 0.1; % acquisition total time
% 5. Take care of data
[data,time] = s.startForeground
plot(data)
subplot(4,1,1);plot(time, data(:,1));
%gtext('RTDS Analog voltage for P_{D1}')
xlabel('Time [seconds]');
ylabel('Voltage [Volts]');
subplot(4,1,2);plot(time, data(:,2));
%gtext('RTDS Analog voltage for P_{D2}')
xlabel('Time [seconds]');
ylabel('Voltage [Volts]');
subplot(4,1,3);plot(time, data(:,3));
%gtext('RTDS Analog voltage for P_{D3}')
xlabel('Time [seconds]');
ylabel('Voltage [Volts]');
subplot(4,1,4);plot(time, data(:,4));
%gtext('RTDS Analog voltage for P_{D4}')
xlabel('Time [seconds]');
ylabel('Voltage [Volts]');
%gtext('PD_{1}=6.25 PD_{2}=5.55 PD_{3}=5.62 PD_{4}=5.41')

%% To sum the PD values from the RTDS front panel
% PD1=data(500)
% PD2=data(1500)
% PD3=data(2500)
% PD4=data(3500)
PD1=data(:,1);
PD2=data(:,2);

```

```

PD3=data(:,3);
PD4=data(:,4);
PD1=sum(PD1)/1000
PD2=sum(PD2)/1000
PD3=sum(PD3)/1000
PD4=sum(PD4)/1000
%PD Value
PD1=PD1*(20/5)
PD2=PD2*(45/5)
PD3=PD3*(40/5)
PD4=PD4*(60/5)
PD=[PD1,PD2,PD3,PD4];
figure(2); bar(PD);
axis([0 5 20 65])
title('Conversion of analog voltage into actual values for P_{D}');
xlabel('Number of P_{D} values from RTDS front panel');
ylabel('P_{D} [MW]');
PD=PD1+PD2+PD3+PD4
%optimal dispatch including losses and generator limits
% =====Economic dispatch problem including losses and generator
limits==
% =====Initial Lagrange's variable=====
lambda= 4.0857e+04; %2.6e4; % Initial lambda
epsilon=0.1; % Tolerance value
alfa=0.1; % Inceremental deltalambda
n=3; % No of generators
m=1000; % Total number of iterations
%PD=165; % Power demand
% =====Fuel cost coefficients=====
c=[60 75 70];
b=[200 150 180];
a=[140 120 80];
% =====Generator Limits =====
Pmin=[20 20 20];
%Pmax=[55 80 65];
Pmax=[200 200 200];
% =====Transmission loss coefficients=====
B=[0.02423 0.00033 -0.00500
0.00033 0.00469 -0.00315
-0.00500 -0.00315 0.00868]*10^-1;
%% Lagranges algorithm starts here
for iter=1:m
iter % Print the iteration number
% =====Calculation of generator real power =====
E=[(diag(a)./lambda)+B];
D=0.5*((1-(b)./lambda))';
P=E\D;
%plot (P,E,'ro',P,D,'b+', 'MarkerSize', 12)
TotalP=sum(P(:,:))
%=====Generator limit checking =====
for i=1:n
if P(i)<=Pmin(i)
P(i)=Pmin(i);
elseif P(i)>=Pmax(i);
P(i)=Pmax(i);
else P(i)=P(i);
end
end
P
%===== Calculation of Transmission loss=====
PL=zeros(n,n);

```

```

for i=1:n
for j=1:n
PL(i,j)=P(i)*B(i,j)*P(j);
end
end
PL=sum(PL(:, :));
PL=sum(PL(:, :));
% =====Calculation of deltalambda =====
% deltalambda=0.0;
deltalambda=PD+PL;
for i=1:n
deltalambda=deltalambda-P(i);
end
if abs(deltalambda)<=epsilon | iter>=m
break
else lambda=lambda+deltalambda%*alfa
end
% plot(iter,lambda,'*',iter,deltalambda,'--');
% figure(3)
% plot(iter,lambda,'*');
% hold on
% figure(4)
% plot(iter,deltalambda,'*');
% hold on
End
%% Lagranges algorithm end here
% gtext('+ lambda ','FontSize',10)
% gtext('+ deltalambda ','FontSize',10)
% title (' lambda Vs Iteration Number ','FontSize',12)
% xlabel ('Iteration Number','FontSize',12)
% ylabel (' lambda','FontSize',12)
%Calculation of fuel cost, emission and CEED values =====
P=P/100;
fuelcost=0;
for i=1:n
fuelcost=fuelcost+c(i)*P(i)^2+b(i)*P(i)+a(i);
end
end
%==Printing of Real power, Transmission loss, Fuel cost, Emission and
CEED=
lambda
PL
totalfuelcost=sum(fuelcost(:, :))
toc
%=====

```


Appendix H: Software program used to read the data saved by LabVIEW in the Excel file into the MATLAB environment and using them to solve the power dispatch optimisation problem for the eleven bus power system

```

% M-File: Method_One_LabVIEW_based_Eleven_Bus_Power_System.m
% =====M-File Description=====
% The M-File is used to read the data saved by LabVIEW in the Excel
file unto MATLAB and using them to solve the power dispatch
optimisation problem for the eleven bus power system

clear all
clc;
tic;
%% To read the xls-file from RTDS using LabVIEW Front panel design
filename = 'RTDS_data.csv';
A = xlsread(filename);
filename = 'RTDS_data.csv';
% Read data from the first worksheet into a numeric array:
columnA = xlsread(filename,1,'A6:A1005');
columnB = xlsread(filename,1,'B6:B1005');
columnC = xlsread(filename,1,'C6:C1005');
columnD = xlsread(filename,1,'D6:D1005');
columnE = xlsread(filename,1,'E6:E1005');
columnF = xlsread(filename,1,'F6:F1005');
columnG = xlsread(filename,1,'G6:G1005');
columnH = xlsread(filename,1,'H6:H1005');
columnI = xlsread(filename,1,'I6:I1005');
columnJ = xlsread(filename,1,'J6:J1005');
columnK = xlsread(filename,1,'K6:K1005');
% To calculate average value for the first 1000 data read from the
first worksheet
columnA=sum(columnA)/1000
columnB=sum(columnB)/1000
columnC=sum(columnC)/1000
columnD=sum(columnD)/1000
columnE=sum(columnE)/1000
columnF=sum(columnF)/1000
columnG=sum(columnG)/1000
columnH=sum(columnH)/1000
columnI=sum(columnI)/1000
columnJ=sum(columnJ)/1000
columnK=sum(columnK)/1000
% To convert back the analog voltage read from the GPC card into the
generator real power values in MW
columnA=columnA*(20/5)
columnB=columnB*(20/5)
columnC=columnC*(30/5)
columnD=columnD*(25/5)
columnE=columnE*(25/5)
columnF=columnF*(10/5)
columnG=columnG*(40/5)
columnH=columnH*(90/5)
columnI=columnI*(70/5)
columnJ=columnJ*(25/5)
columnK=columnK*(25/5)
% Group the power demands of all the eleven loads
PD=[columnA,columnB,columnC,columnD,columnE,columnF,columnG,columnH,co
lumnI,columnJ,columnK];
figure(2); bar(PD);
axis([0 12 05 100])
% Plot the bar graph to display the real power of the loads

```

```

title('Conversion of analog voltage into actual values for P_{D}');
xlabel('Number of P_{D} values from RTDS front panel');
ylabel('P_{D} [MW]');
% Sum up all the eleven real power loads and store it in a variable
name called "PD"
PD=-
(columnA+columnB+columnC+columnD+columnE+columnF+columnG+columnH+columnI+columnJ+columnK);
%optimal dispatch including losses and generator limits
% =====Economic dispatch problem including losses and generator
limits==
% =====Initial Lagrange's variable=====
lambda=10 % Initial lambda
epsilon=0.001; % Tolerance value
alfa=0.01; % Incremental deltalambda
n=5; % No of generators
m=1000; % Total number of iterations
% =====Fuel cost coefficients=====
a=[0.0015 0.0030 0.0012 0.0080 0.0010];
b=[1.80 1.80 2.10 2.00 2.00];
c=[40 60 100 25 120];
% =====Emission coefficients=====
d=[0.0120 0.0150 0.0105 0.0180 0.00080];
e=[-0.555 -0.555 -1.355 -0.805 -0.600];
f=[30 50 60 80 45];
% =====Generator Limits =====
Pmin=[ 50 20 30 10 40];
Pmax=[300 130 180 100 250];
% =====Transmission loss coefficients=====
B=[0.02423 0.00033 -0.00500 -0.00374 -0.00339
0.00033 0.00469 -0.00315 -0.00342 -0.00132
-0.00500 -0.00315 0.00868 0.00380 -0.00390
-0.00374 -0.00342 0.00380 0.00806 -0.00298
-0.00339 -0.00132 -0.00390 -0.00298 0.01969];
for iter=1:m
iter % Print the iteration number
% =====Calculation of generator real power =====
E1=diag(2*(a));
D1=(b);
% PD=-630;
D2=[D1,PD]';
E2=[-1 -1 -1 -1 -1];
E3=[E1;E2];
E4=[-1 -1 -1 -1 0];
E5=[E3 ,E4'];
P=E5\D2 ;
P=P(1:5)
%=====Generator limit checking =====
for i=1:n
if P(i)<=Pmin(i)
P(i)=Pmin(i);
elseif P(i)>=Pmax(i);
P(i)=Pmax(i);
else P(i)=P(i);
end
end
%===== Calculation of Transmission loss=====
PL=zeros(n,n);
for i=1:n
for j=1:n
PL(i,j)=P(i)*B(i,j)*P(j);

```

```

end
end
PL=sum(PL(:, :));
PL=sum(PL(:, :));
% =====Calculation of deltalambda =====
deltalambda=0.0;
deltalambda=PD+PL;
for i=1:n
deltalambda=deltalambda-P(i);
end
deltalambda
if abs(deltalambda)<=epsilon | iter>=m
break
else lambda=lambda+deltalambda*alfa
end
end
%Calculation of fuel cost and emission values =====
fuelcost=0;
for i=1:n
fuelcost=fuelcost+a(i)*P(i)^2+b(i)*P(i)+c(i);
end
emission=0;
for i=1:n
emission=emission+d(i)*P(i)^2+e(i)*P(i)+f(i);
end
%==Printing of Real power, Transmission loss, Fuel cost and Emission
values
lambda
P
PL
totalfuelcost=sum(fuelcost(:, :))
totalemission=sum(emission(:, :))
toc
%=====

```

Appendix I: Software program for the implementation of method one: MATLAB-based data acquisition and data transfer using PB5 card analog output signals for the eleven bus power system

```

% M-File: Method_One_MATLAB_based_Eleven_Bus_Power_System.m
% =====M-File Description=====
% The M-File is used to acquire and transfer the data from the RTDS
PB5 card analogue output signals to the PC at the local end using the
NI DAQ 6343 card. The transferred real-time data is used to solve the
economic dispatch problem using the Lagrange's Algorithm

clear all
clc
%1. Create a device object - Create the analog input object AI for a
...
% National Instrument Instruments board. The installed adaptors and
...
% hardware IDs are found with daqhwinfo
daq.getVendors()
daq.getDevices;
% 2. You should see a list of devices. Create a session using the
listed NI DAQ device.
s = daq.createSession('ni');
%3. Add an analog input voltage channel to the session. Choose channel
'1' on the NI device.
% Make sure your device is properly connected
ch = s.addAnalogInputChannel('Dev5',[0 1 2 3 4 5 6 7 16 17 18],
'Voltage');
% 4.Set DAQ Parameters
s.Rate = 10000;% how fast do you want to acquire the data
% s.Channels.Range = [-10 10];
s.DurationInSeconds = 0.1; % acquisition total time
% 5. Take care of data
[data,time] = s.startForeground
plot(data);
subplot(4,3,1);plot(time, data(:,1));
%gtext('RTDS Analog voltage for P_{D1}')
xlabel('Time [seconds]');
ylabel('Voltage [Volts]');
subplot(4,3,2);plot(time, data(:,2));
%gtext('RTDS Analog voltage for P_{D2}')
xlabel('Time [seconds]');
ylabel('Voltage [Volts]');
subplot(4,3,3);plot(time, data(:,3));
%gtext('RTDS Analog voltage for P_{D3}')
xlabel('Time [seconds]');
ylabel('Voltage [Volts]');
subplot(4,3,4);plot(time, data(:,4));
%gtext('RTDS Analog voltage for P_{D4}')
xlabel('Time [seconds]');
ylabel('Voltage [Volts]');
subplot(4,3,5);plot(time, data(:,5));
%gtext('RTDS Analog voltage for P_{D5}')
xlabel('Time [seconds]');
ylabel('Voltage [Volts]');
subplot(4,3,6);plot(time, data(:,6));
%gtext('RTDS Analog voltage for P_{D6}')
xlabel('Time [seconds]');
ylabel('Voltage [Volts]');

```

```

subplot(4,3,7);plot(time, data(:,7));
%gtext('RTDS Analog voltage for P_{D7}')
xlabel('Time [seconds]');
ylabel('Voltage [Volts]');
subplot(4,3,8);plot(time, data(:,8));
%gtext('RTDS Analog voltage for P_{D8}')
xlabel('Time [seconds]');
ylabel('Voltage [Volts]');
subplot(4,3,9);plot(time, data(:,9));
%gtext('RTDS Analog voltage for P_{D9}')
xlabel('Time [seconds]');
ylabel('Voltage [Volts]');
subplot(4,3,10);plot(time, data(:,10));
%gtext('RTDS Analog voltage for P_{10}')
xlabel('Time [seconds]');
ylabel('Voltage [Volts]');
subplot(4,3,11);plot(time, data(:,11));
%gtext('RTDS Analog voltage for P_{D11}')
xlabel('Time [seconds]');
ylabel('Voltage [Volts]');
%gtext('PD_{1}=6.25 PD_{2}=5.55 PD_{3}=5.62 PD_{4}=5.41')
%% To sum the PD values from the RTDS GPC card (front panel)
PD1=data(:,1);
PD2=data(:,2);
PD3=data(:,3);
PD4=data(:,4);
PD5=data(:,5);
PD6=data(:,6);
PD7=data(:,7);
PD8=data(:,8);
PD9=data(:,9);
PD10=data(:,10);
PD11=data(:,11);
% To calculate average value for the first 1000 data read from the
first worksheet
PD1=sum(PD1)/1000;
PD2=sum(PD2)/1000;
PD3=sum(PD3)/1000;
PD4=sum(PD4)/1000;
PD5=sum(PD5)/1000;
PD6=sum(PD6)/1000;
PD7=sum(PD7)/1000;
PD8=sum(PD8)/1000;
PD9=sum(PD9)/1000;
PD10=sum(PD10)/1000;
PD11=sum(PD11)/1000;
% To convert back the analog voltage read from the GPC card into the
generator real power values in MW
PD1=PD1*(20/5);
PD2=PD2*(20/5);
PD3=PD3*(30/5);
PD4=PD4*(25/5);
PD5=PD5*(25/5);
PD6=PD6*(10/5);
PD7=PD7*(40/5);
PD8=PD8*(90/5);
PD9=PD9*(70/5);
PD10=PD10*(25/5);
PD11=PD11*(25/5);
% Group the power demands of all the eleven loads
% Plot the bar graph to display the real power of the loads

```

```

PD=[PD1,PD2,PD3,PD4,PD5,PD6,PD7,PD8,PD9,PD10,PD11];
figure(2); bar(PD);
axis([0 11 5 100])
title('Conversion of analog voltage into actual values for P_{D}');
xlabel('Number of P_{D} values from RTDS front panel');
ylabel('P_{D} [MW]');
% Sum up all the eleven real power loads and store it in a variable
name called "PD"
PD=-(PD1+PD2+PD3+PD4+PD5+PD6+PD7+PD8+PD9+PD10+PD11);
%optimal dispatch including losses and generator limits
% =====Economic dispatch problem including losses and generator
limits==
% =====Initial Lagrange's variable=====
lambda=10 % Initial lambda
epsilon=0.001; % Tolerance value
alfa=0.01; % Incremental deltalambda
n=5; % No of generators
m=1000; % Total number of iterations
% =====Fuel cost coefficients=====
a=[0.0015 0.0030 0.0012 0.0080 0.0010];
b=[1.80 1.80 2.10 2.00 2.00];
c=[40 60 100 25 120];
% =====Emission coefficients=====
d=[0.0120 0.0150 0.0105 0.0180 0.00080];
e=[-0.555 -0.555 -1.355 -0.805 -0.600];
f=[30 50 60 80 45];
% =====Generator Limits =====
% Pmin=[0.5 0.2 0.3 0.1 0.4];
% Pmax=[3.0 1.3 1.8 1.0 2.5];
Pmin=[ 50 20 30 10 40];
Pmax=[300 130 180 100 250];
% =====Transmission loss coefficients=====
B=[0.02423 0.00033 -0.00500 -0.00374 -0.00339
0.00033 0.00469 -0.00315 -0.00342 -0.00132
-0.00500 -0.00315 0.00868 0.00380 -0.00390
-0.00374 -0.00342 0.00380 0.00806 -0.00298
-0.00339 -0.00132 -0.00390 -0.00298 0.01969];
%% Lagranges algorithm starts here
for iter=1:m
iter % Print the iteration number
% =====Calculation of generator real power =====
E1=diag(2*(a));
D1=(b);
% PD=-630;
D2=[D1,PD]';
E2=[-1 -1 -1 -1 -1];
E3=[E1;E2];
E4=[-1 -1 -1 -1 -1 0];
E5=[E3 ,E4'];
P=E5\D2 ;
P=P(1:5)
%=====Generator limit checking =====
for i=1:n
if P(i)<=Pmin(i)
P(i)=Pmin(i);
elseif P(i)>=Pmax(i);
P(i)=Pmax(i);
else P(i)=P(i);
end
end
%P=P/100

```

```

%===== Calculation of Transmission loss=====
PL=zeros(n,n);
for i=1:n
for j=1:n
PL(i,j)=P(i)*B(i,j)*P(j);
end
end
PL=sum(PL(:,:));
PL=sum(PL(:,:));
% =====Calculation of deltalambda =====
deltalambda=0.0;
deltalambda=PD+PL;
for i=1:n
deltalambda=deltalambda-P(i);
end
deltalambda
if abs(deltalambda)<=epsilon | iter>=m
break
else lambda=lambda+deltalambda*alfa
end
end
%% Lagranges algorithm ends here
%Calculation of fuel cost, emission and CEED values =====
fuelcost=0;
for i=1:n
fuelcost=fuelcost+a(i)*P(i)^2+b(i)*P(i)+c(i);
end
emission=0;
for i=1:n
emission=emission+d(i)*P(i)^2+e(i)*P(i)+f(i);
end
%==Printing of Real power, Transmission loss, Fuel cost, Emission and
CEED=
lambda
P
PL
totalfuelcost=sum(fuelcost(:,:))
totalemission=sum(emission(:,:))
toc

```

Appendix J: Software program used to acquire the saved data from the MySQL database into the MATLAB environment and using them to solve the power dispatch optimisation problem

% M-File: Method_Two_GTNET_PMU_based_Five_Bus_Power_System.m

```
% =====M-File Description=====
% The M-File is used to acquire the saved data from the MySQL database
into the MATLAB environment and using them to solve the power dispatch
optimisation problem
```

```
clc ;
clear all;
% TIC and TOC functions work together to measure elapsed time.
tic; %TIC Start a stopwatch timer.

%%%%%% Add class path (if not in the class path)
p = 'C:\Program Files\MATLAB\R2011a\java\jarext\mysql-connector-java-
5.1.20-bin.jar';
if ~ismember(p,javaclasspath)
    javaaddpath(p)
end
%%%Database connection
conn =
database('outputadapter','root','litham','com.mysql.jdbc.Driver','jdbc:mysql://localhost:3306/outputadapter');
%%%%%%View the current values of all database preferences
setdbprefs('DataReturnFormat','numeric');
%%%%%%%%%%%%PMU3 %%%%%%%%%%%%%%
NN=10;
%%PMU 1 Current Magnitude%%%%%%%%%
%%%%%%%%%%%%PHASE A%%%%%%%%%%%%
Ia_PMU1 = exec(conn,'SELECT ALL Value FROM measurement WHERE signalID =
'DC398391-2522-4A73-AB76-E5879361E516''');
Ia_PMU1 = fetch(Ia_PMU1);
Ia_PMU1=Ia_PMU1.Data;
Ia_PMU1=Ia_PMU1 (1:NN,:);
%%%%%%%%%%%%PHASE B%%%%%%%%%%%%
Ib_PMU1 = exec(conn,'SELECT ALL Value FROM measurement WHERE signalID =
'3238DC37-BEE1-44D8-B3C2-9A4E18FCAFA7''');
Ib_PMU1 = fetch(Ib_PMU1);
Ib_PMU1=Ib_PMU1.Data;
Ib_PMU1=Ib_PMU1 (1:NN,:);
%%%%%%%%%%%%PHASE A%%%%%%%%%%%%
Ic_PMU1 = exec(conn,'SELECT ALL Value FROM measurement WHERE signalID =
'0C88D473-CA83-4BB6-98E8-9F8005C4178B''');
Ic_PMU1 = fetch(Ic_PMU1);
Ic_PMU1=Ic_PMU1.Data;
Ic_PMU1=Ic_PMU1 (1:NN,:);

%%%%%%%%%%%%PMU3 Current Phase Angle%%%%%%%%%
%%%%%%%%%%%%Phase A%%%%%%%%%%%%
Ia_delta_PMU1 = exec(conn,'SELECT ALL Value FROM measurement WHERE
signalID = 'B7F2342D-7990-4292-BDE6-79EBC7C150B4 ''');
Ia_delta_PMU1 = fetch(Ia_delta_PMU1);
Ia_delta_PMU1=Ia_delta_PMU1.Data;
Ia_delta_PMU1=Ia_delta_PMU1(1:NN,:);
```



```

                %%%%%%%%%PHASE B%%%%%%%%
Ib_delta_PMU1 = exec(conn,'SELECT ALL Value FROM measurement WHERE
signalID = 'A90932F9-085F-4CD7-AEDD-0575FBA73B3F''')
Ib_delta_PMU1 = fetch(Ib_delta_PMU1);
Ib_delta_PMU1=Ib_delta_PMU1.Data;
Ib_delta_PMU1=Ib_delta_PMU1(1:NN,:);

                %%%%%%%%%PHASE C %%%%%%%%%
Ic_delta_PMU1 = exec(conn,'SELECT ALL Value FROM measurement WHERE
signalID = '11B15F5A-20A2-4201-99AF-98B4A0368BF1''')
Ic_delta_PMU1 = fetch(Ic_delta_PMU1);
Ic_delta_PMU1=Ic_delta_PMU1.Data;
Ic_delta_PMU1=Ic_delta_PMU1(1:NN,:);

%%%%%%%%Voltage Magnitude(PMU3)
                %%%%%%%%%phase A %%%%%%%%%
Va_PMU1 = exec(conn,'SELECT ALL Value FROM measurement WHERE signalID =
'C962A06A-71B6-4D6D-B1AF-88906C5A8E98''')
Va_PMU1 = fetch(Va_PMU1);
Va_PMU1=Va_PMU1.Data;
Va_PMU1=Va_PMU1(1:NN,:);

                %%%%%%%%%phase B %%%%%%%%%
Vb_PMU1 = exec(conn,'SELECT ALL Value FROM measurement WHERE signalID =
'00C9B998-1BBE-49D9-ABCC-4A29CA864124 ''')
Vb_PMU1 = fetch(Vb_PMU1);
Vb_PMU1=Vb_PMU1.Data;
Vb_PMU1=Vb_PMU1(1:NN,:);

                %%%%%%%%%phase C %%%%%%%%%
Vc_PMU1 = exec(conn,'SELECT ALL Value FROM measurement WHERE signalID =
'C31964C3-218A-4D46-87BB-0E0B2A655919 ''')
Vc_PMU1 = fetch(Vc_PMU1);
Vc_PMU1=Vc_PMU1.Data;
Vc_PMU1=Vc_PMU1(1:NN,:);

%%%%%%%%PMU3 Voltage Phase Angle
                %%%%%%%%%PHASE A%%%%%%%%
Va_delta_PMU1 = exec(conn,'SELECT ALL Value FROM measurement WHERE
signalID = '4199AC51-F55F-4347-92BC-B109F0E85CD5''')
Va_delta_PMU1 = fetch(Va_delta_PMU1);
Va_delta_PMU1=Va_delta_PMU1.Data;
Va_delta_PMU1=Va_delta_PMU1(1:NN,:);

                %%%%%%%%%PHASE B %%%%%%%%%
Vb_delta_PMU1 = exec(conn,'SELECT ALL Value FROM measurement WHERE
signalID = '8A465C03-F0DD-4AB9-B244-398FB8A760A0''')
Vb_delta_PMU1 = fetch(Vb_delta_PMU1);
Vb_delta_PMU1=Vb_delta_PMU1.Data;
Vb_delta_PMU1=Vb_delta_PMU1(1:NN,:);

                %%%%%%%%%PHASE C %%%%%%%%%
Vc_delta_PMU1 = exec(conn,'SELECT ALL Value FROM measurement WHERE
signalID = '61026A2C-9AC6-42FE-AC0E-4240BD9275F9''')

```

```

Vc_delta_PMU1 = fetch(Vc_delta_PMU1);
Vc_delta_PMU1=Vc_delta_PMU1.Data;
Vc_delta_PMU1=Vc_delta_PMU1(1:NN,:);

% Arrange the PMU values with respect to voltage and current magnitudes
and %% its phase angle

PMU1=[Va_PMU1 Va_delta_PMU1 Ia_PMU1 Ia_delta_PMU1 Vb_PMU1 Vb_delta_PMU1
Ib_PMU1 Ib_delta_PMU1 Vc_PMU1 Vc_delta_PMU1 Ic_PMU1 Ic_delta_PMU1];
PMU1_store=PMU1;
%To find the length of the Real-time data captured from RTDS
length_PMU1=length(PMU1(:,1));
%To find the average PMU values which are read from the
RTDSPMU1=sum(PMU1)/length_PMU1;
Va_PMU1=PMU1(:,1);
Va_delta_PMU1=PMU1(:,2);
Ia_PMU1=PMU1(:,3);
Ia_delta_PMU1=PMU1(:,4);
Vb_PMU1=PMU1(:,5);
Vb_delta_PMU1=PMU1(:,6);
Ib_PMU1=PMU1(:,7);
Ib_delta_PMU1=PMU1(:,8);
Vc_PMU1=PMU1(:,9);
Vc_delta_PMU1=PMU1(:,10);
Ic_PMU1=PMU1(:,11);
Ic_delta_PMU1=PMU1(:,12);
% Formulae used to calculate the 3-phase power which is read from the
RTDS

PD1=(Va_PMU1.*Ia_PMU1.*(cosd(Va_delta_PMU1-
Ia_delta_PMU1)))+(Vb_PMU1.*Ib_PMU1.*(cosd(Vb_delta_PMU1-
Ib_delta_PMU1)))+(Vc_PMU1.*Ic_PMU1.*(cosd(Vc_delta_PMU1-Ic_delta_PMU1)))
PD1=sum(PD1)/length_PMU1 % AVERAGE 3-phase power

%%%%%%%%%% PMU @2 *****

%%%%%%%%%%PMU2 Current Magnitude%%%%%%%%%%
Ia_PMU2 = exec(conn,'SELECT ALL Value FROM measurement WHERE signalID =
''416782FB-F5BA-4681-84A2-70EB7C15D867''')
Ia_PMU2 = fetch(Ia_PMU2);
Ia_PMU2=Ia_PMU2.Data;
Ia_PMU2=Ia_PMU2 (1:NN,:);
%%%%%%%%%%PHASE B%%%%%%%%%%
Ib_PMU2 = exec(conn,'SELECT ALL Value FROM measurement WHERE signalID =
''7C9D664A-E2FC-446A-8EDE-4609DAF8AB70''')
Ib_PMU2 = fetch(Ib_PMU2);
Ib_PMU2=Ib_PMU2.Data;
Ib_PMU2=Ib_PMU2 (1:NN,:);
%%%%%%%%%%PHASE C%%%%%%%%%%
Ic_PMU2 = exec(conn,'SELECT ALL Value FROM measurement WHERE signalID =
''5B28D0DD-38C2-41D2-8FB5-7C7433A19CD5''')
Ic_PMU2 = fetch(Ic_PMU2);
Ic_PMU2=Ic_PMU2.Data;
Ic_PMU2=Ic_PMU2 (1:NN,:);

%%%%%%%%%%PMU2 Current Phase Angle%%%%%%%%%%

```

```

                %%% Phase A%%
Ia_delta_PMU2 = exec(conn,'SELECT ALL Value FROM measurement WHERE
signalID = ''3F0D1D73-C5A9-4039-B268-375F1F6CD729 ''')
Ia_delta_PMU2 = fetch(Ia_delta_PMU2);
Ia_delta_PMU2=Ia_delta_PMU2.Data;
Ia_delta_PMU2=Ia_delta_PMU2(1:NN,:);

                %%%PHASE B%%
Ib_delta_PMU2 = exec(conn,'SELECT ALL Value FROM measurement WHERE
signalID = ''F4C9DEA7-51AF-46E8-8EB2-9866D8800599''')
Ib_delta_PMU2 = fetch(Ib_delta_PMU2);
Ib_delta_PMU2=Ib_delta_PMU2.Data;
Ib_delta_PMU2=Ib_delta_PMU2(1:NN,:);

                %%%PHASE C %%
Ic_delta_PMU2 = exec(conn,'SELECT ALL Value FROM measurement WHERE
signalID = ''D574937C-9F9B-4244-8754-C35EBD04C2FD''')
Ic_delta_PMU2 = fetch(Ic_delta_PMU2);
Ic_delta_PMU2=Ic_delta_PMU2.Data;
Ic_delta_PMU2=Ic_delta_PMU2(1:NN,:);

%%Voltage Magnitude(PMU3)
    %%%phase A %%
Va_PMU2 = exec(conn,'SELECT ALL Value FROM measurement WHERE signalID =
''B497C4D1-352E-4125-A196-41C7A66A05BF ''')
Va_PMU2= fetch(Va_PMU2);
Va_PMU2=Va_PMU2.Data;
Va_PMU2=Va_PMU2(1:NN,:);

    %%%phase B %%
Vb_PMU2 = exec(conn,'SELECT ALL Value FROM measurement WHERE signalID =
''AEC009AC-152B-4F70-8936-C67A6BBF1DEB ''')
Vb_PMU2 = fetch(Vb_PMU2);
Vb_PMU2=Vb_PMU2.Data;
Vb_PMU2=Vb_PMU2(1:NN,:);

    %%%phase C %%
Vc_PMU2 = exec(conn,'SELECT ALL Value FROM measurement WHERE signalID =
''F3BF9E95-EF08-42D6-9176-739CEEE09CDE ''')
Vc_PMU2 = fetch(Vc_PMU2);
Vc_PMU2=Vc_PMU2.Data;
Vc_PMU2=Vc_PMU2(1:NN,:);

%%PMU3 Voltage Phase Angle
    %%%PHASE A%%
Va_delta_PMU2 = exec(conn,'SELECT ALL Value FROM measurement WHERE
signalID = ''1373328A-9101-44A8-9F21-E1324B155CA7''')
Va_delta_PMU2 = fetch(Va_delta_PMU2);
Va_delta_PMU2=Va_delta_PMU2.Data;
Va_delta_PMU2=Va_delta_PMU2(1:NN,:);

    %%%PHASE B %%
Vb_delta_PMU2 = exec(conn,'SELECT ALL Value FROM measurement WHERE
signalID = ''E3F6A4A5-B5F1-4C97-9597-C475A6B14D44''')
Vb_delta_PMU2 = fetch(Vb_delta_PMU2);

```

```

Vb_delta_PMU2=Vb_delta_PMU2.Data;
Vb_delta_PMU2=Vb_delta_PMU2(1:NN,:);

%%%%%%%%%%%%%%%%%%%%%%%%%%%%%%%%%%%%%%%%%%%%%%%%%%%%%%%%%%%%%%%%%%%%%%%%PHASE C %%%%%%%%%%%%%%%%%%%%%%%%%%%%%%%%%%%%%%%%%%%%%%%%%%%%%%%%%%%%%%%%%%%%%%%%%
Vc_delta_PMU2 = exec(conn,'SELECT ALL Value FROM measurement WHERE
signalID = ''378CC193-23F9-4FE6-A293-B347495FA2A9''');
Vc_delta_PMU2 = fetch(Vc_delta_PMU2);
Vc_delta_PMU2=Vc_delta_PMU2.Data;
Vc_delta_PMU2=Vc_delta_PMU2(1:NN,:);

% Arrange the PMU values with respect to voltage and current magnitudes
and %% its phase angle
PMU2=[Va_PMU2 Va_delta_PMU2 Ia_PMU2 Ia_delta_PMU2 Vb_PMU2 Vb_delta_PMU2
Ib_PMU2 Ib_delta_PMU2 Vc_PMU2 Vc_delta_PMU2 Ic_PMU2 Ic_delta_PMU2];
PMU2_store=PMU2;
%To find the length of the Real-time data captured from RTDS
length_PMU2=length(PMU2(:,1));
%To find the average PMU values which are read from the
RTDSPMU1=sum(PMU3)/length_PMU1;
Va_PMU2=PMU2(:,1);
Va_delta_PMU2=PMU2(:,2);
Ia_PMU2=PMU2(:,3);
Ia_delta_PMU2=PMU2(:,4);
Vb_PMU2=PMU2(:,5);
Vb_delta_PMU2=PMU2(:,6);
Ib_PMU2=PMU2(:,7);
Ib_delta_PMU2=PMU2(:,8);
Vc_PMU2=PMU2(:,9);
Vc_delta_PMU2=PMU2(:,10);
Ic_PMU2=PMU2(:,11);
Ic_delta_PMU2=PMU2(:,12);
% Formulae used to calculate the 3-phase power which is read from the
RTDS

PD2=(Va_PMU2.*Ia_PMU2.*(cosd(Va_delta_PMU2-
Ia_delta_PMU2)))+(Vb_PMU2.*Ib_PMU2.*(cosd(Vb_delta_PMU2-
Ib_delta_PMU2)))+(Vc_PMU2.*Ic_PMU2.*(cosd(Vc_delta_PMU2-Ic_delta_PMU2)))
PD2=sum(PD2)/length_PMU2 % Aaverage 3-phase power

%%% PMU3 Current Magnitude%%%%%%%%%%%%%%%%%%%%%%%%%%%%%%%%%%%%%%%%%%%%%%%%%%%%%%%%%%%%%%%%%%%%%%%%
%%%%%%%%%%%%%%%%%%%%%%%%%%%%%%%%%%%%%%%%%%%%%%%%%%%%%%%%%%%%%%%%%%%%%%%%PHASE A%%%%%%%%%%%%%%%%%%%%%%%%%%%%%%%%%%%%%%%%%%%%%%%%%%%%%%%%%%%%%%%%%%%%%%%%
Ia_PMU3 = exec(conn,'SELECT ALL Value FROM measurement WHERE signalID =
''FA200D43-8BC4-4598-854E-FCA4228687AC''');
Ia_PMU3 = fetch(Ia_PMU3);
Ia_PMU3=Ia_PMU3.Data;
Ia_PMU3=Ia_PMU3 (1:NN,:);
%%%%%%%%%%%%%%%%%%%%%%%%%%%%%%%%%%%%%%%%%%%%%%%%%%%%%%%%%%%%%%%%%%%%%%%%PHASE B%%%%%%%%%%%%%%%%%%%%%%%%%%%%%%%%%%%%%%%%%%%%%%%%%%%%%%%%%%%%%%%%%%%%%%%%
Ib_PMU3 = exec(conn,'SELECT ALL Value FROM measurement WHERE signalID =
''F9D5B22F-F809-4CCD-9072-9EEF19756B27''');
Ib_PMU3 = fetch(Ib_PMU3);
Ib_PMU3=Ib_PMU3.Data;
Ib_PMU3=Ib_PMU3 (1:NN,:);
%%%%%%%%%%%%%%%%%%%%%%%%%%%%%%%%%%%%%%%%%%%%%%%%%%%%%%%%%%%%%%%%%%%%%%%%PHASE A%%%%%%%%%%%%%%%%%%%%%%%%%%%%%%%%%%%%%%%%%%%%%%%%%%%%%%%%%%%%%%%%%%%%%%%%
Ic_PMU3 = exec(conn,'SELECT ALL Value FROM measurement WHERE signalID =
''1176DFA1-C8F7-4538-8BE6-628E372E13BF''');
Ic_PMU3 = fetch(Ic_PMU3);

```

```

Ic_PMU3=Ic_PMU3.Data;
Ic_PMU3=Ic_PMU3 (1:NN, :);

%%%%%%%%%%%%%%%%%%%%%%%%%%%%%%%%%%%%%%%%%%%%%%%%%%%%%%%%%%%%%%%%%%%%%%%%%
                    %%% Phase A%%%%%%%%%%%%%%%%%%%%%%%%%%%%%%%%%%%%%%%%%%%%%%%%%%%%%%%%%%%%%%%%%%%%%%%%%
Ia_delta_PMU3 = exec(conn, 'SELECT ALL Value FROM measurement WHERE
signalID = ''9C9539FA-3442-43AB-B5E3-9C9069E1D4E2 ''')
Ia_delta_PMU3 = fetch(Ia_delta_PMU3);
Ia_delta_PMU3=Ia_delta_PMU3.Data;
Ia_delta_PMU3=Ia_delta_PMU3(1:NN, :);

                    %%%%%%%%%PHASE B%%%%%%%%%%%%%%%%%%%%%%%%%%%%%%%%%%%%%%%%%%%%%%%%%%%%%%%%%%%%%%%%%%%%%%%%%
Ib_delta_PMU3 = exec(conn, 'SELECT ALL Value FROM measurement WHERE
signalID = ''567C493B-4A85-4D6A-996B-CFC3E868E618''')
Ib_delta_PMU3 = fetch(Ib_delta_PMU3);
Ib_delta_PMU3=Ib_delta_PMU3.Data;
Ib_delta_PMU3=Ib_delta_PMU3(1:NN, :);

                    %%%%%%%%%PHASE C %%%%%%%%%%%%%%%%%%%%%%%%%%%%%%%%%%%%%%%%%%%%%%%%%%%%%%%%%%%%%%%%%%%%%%%%%%
Ic_delta_PMU3 = exec(conn, 'SELECT ALL Value FROM measurement WHERE
signalID = ''1284FBA2-6DA4-4B6A-9C1E-F562E5BCFFDA''')
Ic_delta_PMU3 = fetch(Ic_delta_PMU3);
Ic_delta_PMU3=Ic_delta_PMU3.Data;
Ic_delta_PMU3=Ic_delta_PMU3(1:NN, :);

%%%%%%%%%%%%%%%%%%%%%%%%%%%%%%%%%%%%%%%%%%%%%%%%%%%%%%%%%%%%%%%%%%%%%%%%%
                    %%%%%%%%%Voltage Magnitude(PMU3)
                    %%%%%%%%%%phase A %%%%%%%%%%%%%%%%%%%%%%%%%%%%%%%%%%%%%%%%%%%%%%%%%%%%%%%%%%%%%%%%%%%%%%%%%%
Va_PMU3 = exec(conn, 'SELECT ALL Value FROM measurement WHERE signalID =
''A9E5BCF8-AAF9-4392-B145-32B0AC0775CD ''')
Va_PMU3 = fetch(Va_PMU3);
Va_PMU3=Va_PMU3.Data;
Va_PMU3=Va_PMU3(1:NN, :);

                    %%%%%%%%%%phase B %%%%%%%%%%%%%%%%%%%%%%%%%%%%%%%%%%%%%%%%%%%%%%%%%%%%%%%%%%%%%%%%%%%%%%%%%%
Vb_PMU3 = exec(conn, 'SELECT ALL Value FROM measurement WHERE signalID =
''857F8CC1-5321-4DE3-ACC2-8622FE8D4BFE ''')
Vb_PMU3 = fetch(Vb_PMU3);
Vb_PMU3=Vb_PMU3.Data;
Vb_PMU3=Vb_PMU3(1:NN, :);

                    %%%%%%%%%%phase C %%%%%%%%%%%%%%%%%%%%%%%%%%%%%%%%%%%%%%%%%%%%%%%%%%%%%%%%%%%%%%%%%%%%%%%%%%
Vc_PMU3 = exec(conn, 'SELECT ALL Value FROM measurement WHERE signalID =
''04990CDE-6177-4799-B0A7-6C36A28F4C24 ''')
Vc_PMU3 = fetch(Vc_PMU3);
Vc_PMU3=Vc_PMU3.Data;
Vc_PMU3=Vc_PMU3(1:NN, :);

%%%%%%%%%%%%%%%%%%%%%%%%%%%%%%%%%%%%%%%%%%%%%%%%%%%%%%%%%%%%%%%%%%%%%%%%%
                    %%%%%%%%%PMU3 Voltage Phase Angle
                    %%%%%%%%%%PHASE A%%%%%%%%%%%%%%%%%%%%%%%%%%%%%%%%%%%%%%%%%%%%%%%%%%%%%%%%%%%%%%%%%%%%%%%%%
Va_delta_PMU3 = exec(conn, 'SELECT ALL Value FROM measurement WHERE
signalID = ''26E2ED0D-E982-4E8A-A7A3-873C312389EA''')
Va_delta_PMU3 = fetch(Va_delta_PMU3);
Va_delta_PMU3=Va_delta_PMU3.Data;
Va_delta_PMU3=Va_delta_PMU3(1:NN, :);

```

```

%%%%%%%%%%%%%%%%%%%%%%%%%%%%%%%%%%%%%%%%%%%%%%%%%%%%%%%%%%%%%%%%%%%%%%%%PHASE B %%%%%%%%%%%%%%%%%%%%%%%%%%%%%%%%%%%%%%%%%%%%%%%%%%%%%%%%%%%%%%%%%%%%%%%%%
Vb_delta_PMU3 = exec(conn,'SELECT ALL Value FROM measurement WHERE
signalID = ''9B189215-2B12-4A80-BA7A-28B169921622''')
Vb_delta_PMU3 = fetch(Vb_delta_PMU3);
Vb_delta_PMU3=Vb_delta_PMU3.Data;
Vb_delta_PMU3=Vb_delta_PMU3(1:NN,:);

%%%%%%%%%%%%%%%%%%%%%%%%%%%%%%%%%%%%%%%%%%%%%%%%%%%%%%%%%%%%%%%%%%%%%%%%PHASE C %%%%%%%%%%%%%%%%%%%%%%%%%%%%%%%%%%%%%%%%%%%%%%%%%%%%%%%%%%%%%%%%%%%%%%%%%
Vc_delta_PMU3 = exec(conn,'SELECT ALL Value FROM measurement WHERE
signalID = ''CF856526-7600-4817-A72B-8D2BF4388D30''')
Vc_delta_PMU3 = fetch(Vc_delta_PMU3);
Vc_delta_PMU3=Vc_delta_PMU3.Data;
Vc_delta_PMU3=Vc_delta_PMU3(1:NN,:);

% Arrange the PMU values with respect to voltage and current magnitudes
and %% its phase angle
PMU3=[Va_PMU3 Va_delta_PMU3 Ia_PMU3 Ia_delta_PMU3 Vb_PMU3 Vb_delta_PMU3
Ib_PMU3 Ib_delta_PMU3 Vc_PMU3 Vc_delta_PMU3 Ic_PMU3 Ic_delta_PMU3];
PMU3_store=PMU3;
%To find the length of the Real-time data captured from RTDS
length_PMU3=length(PMU3(:,1));
%To find the average PMU values which are read from the
RTDSPMU1=sum(PMU3)/length_PMU1;
Va_PMU3=PMU3(:,1);
Va_delta_PMU3=PMU3(:,2);
Ia_PMU3=PMU3(:,3);
Ia_delta_PMU3=PMU3(:,4);
Vb_PMU3=PMU3(:,5);
Vb_delta_PMU3=PMU3(:,6);
Ib_PMU3=PMU3(:,7);
Ib_delta_PMU3=PMU3(:,8);
Vc_PMU1=PMU3(:,9);
Vc_delta_PMU3=PMU3(:,10);
Ic_PMU3=PMU3(:,11);
Ic_delta_PMU3=PMU3(:,12);
% Formulae used to calculate the 3-phase power which is read from the
RTDS

PD3=(Va_PMU3.*Ia_PMU3.*(cosd(Va_delta_PMU3-
Ia_delta_PMU3)))+(Vb_PMU3.*Ib_PMU3.*(cosd(Vb_delta_PMU3-
Ib_delta_PMU3)))+(Vc_PMU3.*Ic_PMU3.*(cosd(Vc_delta_PMU3-Ic_delta_PMU3)))
PD3=sum(PD3)/length_PMU3 % Aaverage 3-phase power

%% PMU4 Current Magnitude%%%%%%%%%%%%%%%%%%%%%%%%%%%%%%%%%%%%%%%%%%%%%%%%%%%%%%%%%%%%%%%%%%%%%%%%
%%%%%%%%%%%%%%%%%%%%%%%%%%%%%%%%%%%%%%%%%%%%%%%%%%%%%%%%%%%%%%%%%%%%%%%%PHASE A%%%%%%%%%%%%%%%%%%%%%%%%%%%%%%%%%%%%%%%%%%%%%%%%%%%%%%%%%%%%%%%%%%%%%%%%
Ia_PMU4 = exec(conn,'SELECT ALL Value FROM measurement WHERE signalID =
''17538258-1BA0-4491-AF46-5B610B594DC6''')
Ia_PMU4 = fetch(Ia_PMU4);
Ia_PMU4=Ia_PMU4.Data;
Ia_PMU4=Ia_PMU4 (1:NN,:);
%%%%%%%%%%%%%%%%%%%%%%%%%%%%%%%%%%%%%%%%%%%%%%%%%%%%%%%%%%%%%%%%%%%%%%%%PHASE B%%%%%%%%%%%%%%%%%%%%%%%%%%%%%%%%%%%%%%%%%%%%%%%%%%%%%%%%%%%%%%%%%%%%%%%%
Ib_PMU4 = exec(conn,'SELECT ALL Value FROM measurement WHERE signalID =
''EF7D78A7-1D21-450D-979A-8C75EBE3F8C2''')
Ib_PMU4 = fetch(Ib_PMU4);
Ib_PMU4=Ib_PMU4.Data;
Ib_PMU4=Ib_PMU4 (1:NN,:);

```

```

        %%%%%%%%%PHASE A%%%%%%%%
Ic_PMU4 = exec(conn,'SELECT ALL Value FROM measurement WHERE signalID =
''586C8642-31AA-4949-B1C2-2014FC832FEE''')
Ic_PMU4 = fetch(Ic_PMU4);
Ic_PMU4=Ic_PMU4.Data;
Ic_PMU4=Ic_PMU4 (1:NN,:);

%%%%%%%%PMU4 Current Phase Angle%%%%%%%%
        %%% Phase A%%%%%%%%
Ia_delta_PMU4 = exec(conn,'SELECT ALL Value FROM measurement WHERE
signalID = ''22DBE012-F94A-4656-8186-5FBFAF58A72D ''')
Ia_delta_PMU4 = fetch(Ia_delta_PMU4);
Ia_delta_PMU4=Ia_delta_PMU4.Data;
Ia_delta_PMU4=Ia_delta_PMU4(1:NN,:);

        %%%%%%%%%PHASE B%%%%%%%%
Ib_delta_PMU4 = exec(conn,'SELECT ALL Value FROM measurement WHERE
signalID = ''C5CCC88A-7651-4FB0-97FB-9DEDD85F70E6''')
Ib_delta_PMU4 = fetch(Ib_delta_PMU4);
Ib_delta_PMU4=Ib_delta_PMU4.Data;
Ib_delta_PMU4=Ib_delta_PMU4(1:NN,:);

        %%%%%%%%%PHASE C %%%%%%%%%
Ic_delta_PMU4 = exec(conn,'SELECT ALL Value FROM measurement WHERE
signalID = ''C479B97F-8E53-4734-82F3-A15667B9BDCB''')
Ic_delta_PMU4 = fetch(Ic_delta_PMU4);
Ic_delta_PMU4=Ic_delta_PMU4.Data;
Ic_delta_PMU4=Ic_delta_PMU4(1:NN,:);

%%%%%%%%Voltage Magnitude(PMU3)
        %%%phase A %%%%%%%%%
Va_PMU4 = exec(conn,'SELECT ALL Value FROM measurement WHERE signalID =
''B4D00EF0-E1F4-4FFE-9180-2A6D681BA3A0 ''')
Va_PMU4 = fetch(Va_PMU4);
Va_PMU4=Va_PMU4.Data;
Va_PMU4=Va_PMU4(1:NN,:);

        %%%phase B %%%%%%%%%
Vb_PMU4 = exec(conn,'SELECT ALL Value FROM measurement WHERE signalID =
''C79DE410-51AC-4555-A3EF-AED117C05E9D''')
Vb_PMU4 = fetch(Vb_PMU4);
Vb_PMU4=Vb_PMU4.Data;
Vb_PMU4=Vb_PMU4(1:NN,:);

        %%%phase C %%%%%%%%%
Vc_PMU4 = exec(conn,'SELECT ALL Value FROM measurement WHERE signalID =
''F45CEAD2-61A0-4A68-8F7E-B3858205C56E''')
Vc_PMU4 = fetch(Vc_PMU4);
Vc_PMU4=Vc_PMU4.Data;
Vc_PMU4=Vc_PMU4(1:NN,:);

%%%%%%%%PMU3 Voltage Phase Angle
        %%%%%%%%%PHASE A%%%%%%%%
Va_delta_PMU4 = exec(conn,'SELECT ALL Value FROM measurement WHERE
signalID = ''0C40F46C-3F1C-40FA-B2F5-2714AD6A1FA6''')

```

```

Va_delta_PMU4 = fetch(Va_delta_PMU4);
Va_delta_PMU4=Va_delta_PMU4.Data;
Va_delta_PMU4=Va_delta_PMU4(1:NN,:);

%%%%%%%%%%%%%%PHASE B %%%%%%%%%%%%%%%
Vb_delta_PMU4 = exec(conn,'SELECT ALL Value FROM measurement WHERE
signalID = ''BB9808CE-FD78-4CE0-9F29-8DF336837A3C''');
Vb_delta_PMU4 = fetch(Vb_delta_PMU4);
Vb_delta_PMU4=Vb_delta_PMU4.Data;
Vb_delta_PMU4=Vb_delta_PMU4(1:NN,:);

%%%%%%%%%%%%%%PHASE C %%%%%%%%%%%%%%%
Vc_delta_PMU4 = exec(conn,'SELECT ALL Value FROM measurement WHERE
signalID = ''4C6E5411-39C4-4495-B7C0-50BD9DB5FDF4''');
Vc_delta_PMU4 = fetch(Vc_delta_PMU4);
Vc_delta_PMU4=Vc_delta_PMU4.Data;
Vc_delta_PMU4=Vc_delta_PMU4(1:NN,:);

% Arrange the PMU values with respect to voltage and current magnitudes
and %% its phase angle
PMU4=[Va_PMU4 Va_delta_PMU4 Ia_PMU4 Ia_delta_PMU4 Vb_PMU4 Vb_delta_PMU4
Ib_PMU4 Ib_delta_PMU4 Vc_PMU4 Vc_delta_PMU4 Ic_PMU4 Ic_delta_PMU4];
PMU4_store=PMU4;
%To find the length of the Real-time data captured from RTDS
length_PMU4=length(PMU4(:,1));
%To find the average PMU values which are read from the
RTDSPMU1=sum(PMU3)/length_PMU1;
Va_PMU4=PMU4(:,1);
Va_delta_PMU4=PMU4(:,2);
Ia_PMU4=PMU4(:,3);
Ia_delta_PMU4=PMU4(:,4);
Vb_PMU4=PMU4(:,5);
Vb_delta_PMU4=PMU4(:,6);
Ib_PMU4=PMU4(:,7);
Ib_delta_PMU4=PMU4(:,8);
Vc_PMU4=PMU4(:,9);
Vc_delta_PMU4=PMU4(:,10);
Ic_PMU4=PMU4(:,11);
Ic_delta_PMU4=PMU4(:,12);
% Formulae used to calculate the 3-phase power which is read from the
RTDS

PD4=(Va_PMU4.*Ia_PMU4.*(cosd(Va_delta_PMU4-
Ia_delta_PMU4)))+(Vb_PMU4.*Ib_PMU4.*(cosd(Vb_delta_PMU4-
Ib_delta_PMU4)))+(Vc_PMU4.*Ic_PMU4.*(cosd(Vc_delta_PMU4-Ic_delta_PMU4)))
PD4=sum(PD4)/length_PMU4 % Aaverage 3-phase power

%optimal dispatch including losses and generator limits
% =====Economic dispatch problem including losses and generator limits
% =====Initial Lagrange's variable=====
lambda= 4.0857e+04; %2.6e4; % Initial lambda
epsilon=0.1; % Tolerance value
alfa=0.1; % Inceremental deltalambda
n=3; % No of generators
m=1000; % Total number of iterations

```



```

PD=(PD1+PD2+PD3+PD4)/10^6      % Power demand calculated using the PMU
which is generated by the RTDS in Real-Time
%PD=165;                        % Power demand
% =====Fuel cost coefficients=====
c=[60 75 70];
b=[200 150 180];
a=[140 120 80];
% =====Generator Limits =====
Pmin=[20 20 20];
%Pmax=[55 80 65];
Pmax=[200 200 200];
% =====Transmission loss coefficients=====
B=[0.02423 0.00033 -0.00500
    0.00033 0.00469 -0.00315
    -0.00500 -0.00315 0.00868]*10^-1;
%% Lagranges algorithm is starts here
for iter=1:m
iter % Print the itertaion number
% =====Calculation of generator real power =====
E=[(diag(c)./lambda)+B];
D=0.5*((1-(b)./lambda))';
P=E\D;
%plot (P,E,'ro',P,D,'b+', 'MarkerSize', 12)
TotalP=sum(P(:, :))
%=====Generator limit checking =====
for i=1:n
if P(i)<=Pmin(i)
P(i)=Pmin(i);
elseif P(i)>=Pmax(i);
P(i)=Pmax(i);
else P(i)=P(i);
end
end
P
%===== Calculation of Transmission loss=====
PL=zeros(n,n);
for i=1:n
for j=1:n
PL(i,j)=P(i)*B(i,j)*P(j);
end
end
PL=sum(PL(:, :));
PL=sum(PL(:, :));
% =====Calculation of deltalambda =====
% deltalambda=0.0;
deltalambda=PD+PL;
for i=1:n
deltalambda=deltalambda-P(i);
end
if abs(deltalambda)<=epsilon | iter>=m
break
else lambda=lambda+deltalambda%*alfa
end
% plot(iter,lambda,'*',iter,deltalambda,'--');
% figure(3)
% plot(iter,lambda,'*');
% hold on

```

```

% figure(4)
% plot(iter,deltalambda,'*');
% hold on
end
%% Lagranges algorithm is ends here

fuelcost=0;
emissioncost=0;
CEED=0;
P=P/100;
for i=1:n
    fuelcost=fuelcost+c(i)*P(i)^2+b(i)*P(i)+a(i); % Equation (3.1)
    % emissioncost=emissioncost+d(i)*P(i)^2+e(i)*P(i)+f(i); % Equation
    (3.5)
    % CEED=
    CEED+a(i)*P(i)^2+b(i)*P(i)+c(i)+h(i)*(d(i)*P(i)^2+e(i)*P(i)+f(i)); %
    Equation (3.6)
end
%==== Printing of Real power, Transmission loss, Fuel cost, Emission and
CEED====
lambda
P
PL
totalfuelcost=sum(fuelcost(:, :))
% totalemissioncost=sum(emissioncost(:, :))
% CEED=sum(CEED(:, :))
toc; %TOC Stop a stopwatch timer.
%=====

```